

INFORMATION TO USERS

This manuscript has been reproduced from the microfilm master. UMI films the text directly from the original or copy submitted. Thus, some thesis and dissertation copies are in typewriter face, while others may be from any type of computer printer.

The quality of this reproduction is dependent upon the quality of the copy submitted. Broken or indistinct print, colored or poor quality illustrations and photographs, print bleedthrough, substandard margins, and improper alignment can adversely affect reproduction.

In the unlikely event that the author did not send UMI a complete manuscript and there are missing pages, these will be noted. Also, if unauthorized copyright material had to be removed, a note will indicate the deletion.

Oversize materials (e.g., maps, drawings, charts) are reproduced by sectioning the original, beginning at the upper left-hand corner and continuing from left to right in equal sections with small overlaps. Each original is also photographed in one exposure and is included in reduced form at the back of the book.

Photographs included in the original manuscript have been reproduced xerographically in this copy. Higher quality 6" x 9" black and white photographic prints are available for any photographs or illustrations appearing in this copy for an additional charge. Contact UMI directly to order.

UMI

A Bell & Howell Information Company
300 North Zeeb Road, Ann Arbor MI 48106-1346 USA
313/761-4700 800/521-0600

**EXPERIMENTAL AND THEORETICAL STUDIES OF THE
PHOTOSYSTEM II REACTION CENTER: IMPLICATIONS FOR
BICARBONATE BINDING AND FUNCTION**

BY

JIN XIONG

B.S., Zhongshan University, 1984
M.S., Eastern Illinois University, 1988
M.S., Bowling Green State University, 1991

THESIS

Submitted in partial fulfillment of the requirements
for the degree of Doctor of Philosophy in Biology
in the Graduate College of the
University of Illinois at Urbana-Champaign, 1996

Urbana, Illinois

UMI Number: 9712487

**Copyright 1997 by
Xiong, Jin**

All rights reserved.

**UMI Microform 9712487
Copyright 1997, by UMI Company. All rights reserved.**

**This microform edition is protected against unauthorized
copying under Title 17, United States Code.**

UMI
300 North Zeeb Road
Ann Arbor, MI 48103

UNIVERSITY OF ILLINOIS AT URBANA-CHAMPAIGN

THE GRADUATE COLLEGE

OCTOBER 1996

WE HEREBY RECOMMEND THAT THE THESIS BY

JIN XIONG

ENTITLED EXPERIMENTAL AND THEORETICAL STUDIES OF THE PHOTOSYSTEM II
REACTION CENTER: IMPLICATIONS FOR BICARBONATE BINDING AND FUNCTION

BE ACCEPTED IN PARTIAL FULFILLMENT OF THE REQUIREMENTS FOR

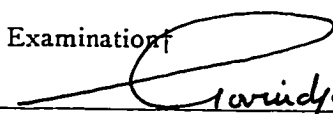
THE DEGREE OF DOCTOR OF PHILOSOPHY IN BIOLOGY

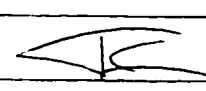


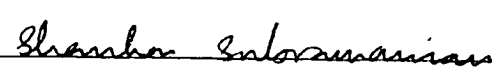

Director of Thesis Research

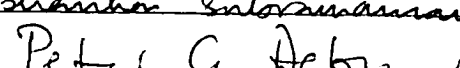
Head of Department

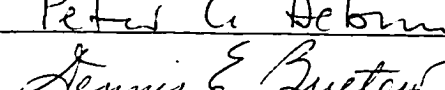
Committee on Final Examination†


Chairperson ..

 H. Marsh

 Shambhu Subramanian

 Peter A. Debnar

 Dennis E. Queten

† Required for doctor's degree but not for master's.

EXPERIMENTAL AND THEORETICAL STUDIES OF THE PHOTOSYSTEM II REACTION CENTER: IMPLICATIONS FOR BICARBONATE BINDING AND FUNCTION

Jin Xiong, Ph.D.
Department of Biology
University of Illinois at Urbana-Champaign, 1996
Govindjee, Adviser

To investigate the role of arginine residues in bicarbonate binding in the photosystem II (PSII) reaction center, arginines 257 and 269 of the D1 polypeptide (D1-R257 and D1-R269) near the putative bicarbonate binding sites, the non-heme iron and the Q_B binding niche, were mutated in a unicellular green alga *Chlamydomonas reinhardtii*. The effects of mutations on bicarbonate binding and on other aspects of PSII photochemistry were investigated.

D1-R269 was mutated into a glycine. The mutant was shown to be unable to grow photoautotrophically and to have significant modifications on both the donor and acceptor sides of PSII, which includes a substantial reduction of the electron transfer kinetics from Q_A^- to the plastoquinone pool, a significantly increased minimal fluorescence level (F_0) interpreted by a decrease in the excitation energy transfer from antennae to the PSII reaction center, a loss of the two-electron gate functioning, a reduction in 77 K PSII chlorophyll *a* fluorescence emission bands (F685 and F695) suggesting a possible destabilization of the PSII complex, a significantly modified Q_B niche, substantially reduced Ty_{D^+}/Q_A^- and Q_A^- Fe^{2+} EPR signals, the absence of the $S_2Q_A^-$ and $S_2Q_B^-$ thermoluminescence bands in the mutant, the absence of the tetranuclear Mn cluster, and a 4 fold less sensitivity to the bicarbonate-reversible formate inhibition for the electron transfer from Q_A^- to the plastoquinone pool. However, the formate/bicarbonate binding site still appears to exist, suggesting that D1-R269 plays some role in the binding niche of bicarbonate but is of more importance for the general structure and function of PSII.

D1-R257 was mutated into a glutamate and a methionine. The mutants are able to grow photosynthetically, but at a slower rate compared to the wild type. Inhibition of the

PSII reaction in the two mutants appears to be mainly on the acceptor side. The mutants show a significantly elevated F_0 level, a reduction of 77 K fluorescence emission bands (F685 and F695), a reduction of PSII electron transfer, particularly, from Q_A^- to the plastoquinone pool. Although the binding affinity to the herbicide DCMU in the mutants appears to be unaltered, their sensitivity to the bicarbonate-reversible formate inhibition is drastically reduced. Further, the two mutants are poorly inhibited by arginine-specific reagents (phenylglyoxal and 2,3-butanedione) which inhibit the electron transfer in the wild type with a reversal by the addition of bicarbonate. The evidence implicates the near absence of bicarbonate binding in these two mutants and the essentiality of D1-R257 for the *in vivo* binding of bicarbonate/formate.

To obtain a more detailed understanding of the mechanism of bicarbonate-mediated PSII electron transfer as well as the structure of the PSII reaction center, three dimensional models of the PSII reaction center of *C. reinhardtii* and the cyanobacterium *Synechocystis* sp. PCC 6803 were generated. The models were constructed partly based on the significant homology with the anoxygenic purple bacterial photosynthetic reaction centers for which high resolution X-ray crystal structures are available, and partly based on existing experimental evidence. The model for *Synechocystis* 6803 includes D1, D2 and most of the cofactors associated with the two proteins. The model for *C. reinhardtii* includes D1, D2, cytochrome b559 as well as a complete set of cofactors. The availability of the three dimensional models of the PSII reaction center leads to the proposal for a catalytic mechanism of bicarbonate-mediated Q_B protonation and a transport channel for bicarbonate and water molecules in the PSII reaction center.

ACKNOWLEDGMENTS

I express my sincere appreciation to my adviser, Dr. Govindjee, for his continuous support, guidance, encouragement, and constructive criticisms which made this thesis possible. His dedication and enthusiasm for photosynthesis research and for science in general will always be an inspiration to me. I am very grateful to Dr. John Whitmarsh, chairman of my committee, for his invaluable support during my graduate career at Illinois. I would also like thank Dr. Shankar Subramaniam for his support and guidance in my computer modeling work. Sincere thanks are extended to Drs. Dennis Buetow and Peter Debrunner for serving on my committee. Collaborations with Drs. Richard Sayre, Ronald Hutchison, Antony Crofts, Jun Minagawa and David Kramer are also sincerely appreciated. I would also like to thank all my friends and colleagues in the Department of Plant Biology for their friendships and support over the years. The research in this thesis was supported by an NSF grant (91-16838), and a University of Illinois Research Board grant given to Dr. Govindjee, and a graduate fellowship from the Integrative Photosynthesis Research Training Grant (NSF/USDA/DOE, DOE 92ER20095) awarded to me.

TABLE OF CONTENTS

LIST OF TABLES	xi
LIST OF FIGURES	xii
LIST OF ABBREVIATIONS.....	xvii
CHAPTER I. INTRODUCTION.....	1
A. Overview of Structure and Function of Photosystem II	1
B. Overview of Bicarbonate Effect in PSII.....	8
C. Objective of This Thesis.....	11
D. References.....	11
CHAPTER II. CONSTRUCTION AND CHARACTERIZATION	
OF A PUTATIVE BICARBONATE BINDING SITE MUTANT	
(ARGININE-269-GLYCINE) OF <i>CHLAMYDOMONAS</i>	
<i>REINHARDTII</i>.....	19
A. Introduction	19
B. Materials and Methods.....	21
1. <i>Mutagenesis of psbA gene and screening for homoplasmic</i>	
<i>mutant</i>	21
2. <i>Growth conditions of C. reinhardtii</i>	23
3. <i>Chlorophyll and growth determination</i>	24
4. <i>Thylakoid preparation</i>	24
5. <i>Western blot analysis</i>	25
6. <i>Steady state of oxygen evolution</i>	25
7. <i>Manganese determination</i>	25
8. <i>EPR analysis</i>	25
9. <i>Thermoluminescence</i>	26

10. Chlorophyll a fluorescence induction kinetics and measurements of F_0	26
11. Flash induced chlorophyll a fluorescence changes.....	27
12. Bicarbonate depletion and recovery treatments	28
13. Low temperature fluorescence spectra.....	28
14. Herbicide binding assay.....	29
C. Results.....	29
1. Construction and isolation of D1-R269G mutant	29
2. D1 protein stability in the D1-R269G mutant.....	33
3. Inhibition to PSII electron transfer: steady state oxygen evolution and manganese determination.....	36
4. EPR analysis of PSII stable charge separation	41
5. Thermoluminescence	44
6. Inhibition to PSII electron transfer: Chl a changes after flashes.....	47
7. Chlorophyll a fluorescence induction.....	50
8. F_0	54
9. Functioning of the two-electron gate.....	57
10. Bicarbonate depletion and recovery.....	58
11. EPR analysis of the fine structure of the coordination of the non-heme iron	65
12. Low temperature fluorescence emission spectra.....	66
13. Herbicide binding assay.....	69
D. Discussion.....	74
E. References.....	80

CHAPTER III. CONSTRUCTION AND CHARACTERIZATION OF BICARBONATE/FORMATE BINDING SITE MUTANTS ON ARGININE-257 IN THE PHOTOSYSTEM II D1 PROTEIN OF <i>CHLAMYDOMONAS REINHARDTII</i>	88
A. Introduction	88
B. Materials and Methods.....	91
1. <i>Site-directed mutagenesis</i>	91
2. <i>Growth of C. reinhardtii cells</i>	94
3. <i>Chlorophyll a fluorescence induction kinetics and measurements of F_0</i>	95
4. <i>Bicarbonate depletion and recovery treatments</i>	96
5. <i>Low temperature fluorescence spectra</i>	96
6. <i>Flash induced chlorophyll a fluorescence decay</i>	96
7. <i>Steady-state oxygen evolution</i>	97
8. <i>Treatment of arginine specific reagents</i>	98
C. Results.....	98
1. <i>Site-directed mutagenesis of psbA and mutant confirmation</i>	98
2. <i>Growth characteristics</i>	99
3. <i>Chlorophyll a fluorescence induction</i>	104
4. <i>F_0</i>	108
5. <i>Low temperature fluorescence emission spectra</i>	111
6. <i>Characterization of kinetics of $Q_A \rightarrow Q_B$ and DCMU binding</i>	114
7. <i>Effects of bicarbonate depletion on the kinetics of $Q_A \rightarrow Q_B$ electron transfer</i>	117
8. <i>Bicarbonate-reversible formate inhibition of the PSII electron transfer</i>	125

9. <i>Inhibition of PSII electron transfer by arginine specific reagents and recovery of inhibition by bicarbonate</i>	127
D. Discussion.....	129
E. References.....	133
CHAPTER IV. MODELING OF THE D1/D2 PROTEINS AND COFACTORS OF THE PHOTOSYSTEM II REACTION CENTER: IMPLICATIONS FOR HERBICIDE AND BICARBONATE BINDING	141
A. Introduction	141
B. Materials and Methods.....	145
C. Results and Discussion	149
1. <i>Sequence alignment and sequence-specific loop modeling</i>	149
2. <i>General topology and evaluation of the model</i>	154
3. <i>General description of important cofactors</i>	164
4. <i>Chlorophyll P680</i>	164
5. <i>Accessory chlorophylls</i>	170
6. <i>Pheophytins</i>	171
7. <i>β-Carotene</i>	174
8. <i>Donors to P680⁺</i>	174
9. <i>Plastoquinone Q_A and its binding niche</i>	177
10. <i>Plastoquinone Q_B and its binding niche</i>	179
11. <i>Herbicide DCMU binding</i>	180
12. <i>Non-heme iron and the liganding histidines and bicarbonate</i>	183
13. <i>Bicarbonate in the Q_B niche</i>	190
14. <i>Bicarbonate/water transport in PSII</i>	197
D. References.....	204

CHAPTER V. A KNOWLEDGE-BASED THREE DIMENSIONAL

MODEL OF D1-D2-CYTOCHROME B559 OF

CHLAMYDOMONAS REINHARDTII	222
A. Introduction.....	222
B. Materials and Methods.....	224
C. Results.....	227
1. <i>Sequence alignment, loop building and model evaluation</i>	227
2. <i>General description of the model</i>	232
3. <i>Chlorophylls</i>	233
4. <i>Donors to P680⁺</i>	239
5. <i>β-Carotenes</i>	240
6. <i>Cytochrome b559 and the heme binding region</i>	241
D. Discussion	246
E. References	258
VITA	267

LIST OF TABLES

Table 2.1.	D1 protein content in D1-R269G and wild type cell and thylakoid membrane fractions isolated from dark or light grown cells.	39
Table 2.2.	Photosynthetic oxygen evolution, photosystem II artificial donor oxidation and manganese content of isolated membrane fractions from dark and dark plus 20 min dim light grown cells	40
Table 3.1.	Steady-state oxygen evolution of the mixotrophically grown wild type and D1-R257E, M mutant cells.....	126
Table 3.2.	Steady-state oxygen evolution measurements of mixotrophically grown wild type and D1-R257E, M mutant cells treated with arginine-specific reagents phenylglyoxal and 2,3-butanedione and subsequently with bicarbonate.....	128
Table 4.1.	Search results by the BLAST prgram through the Brookhaven Protein Data Bank for the unconserved loop sequences of <i>Synechocystis</i> sp. PCC 6803 D1 and D2 proteins.....	155
Table 5.1.	BLAST search results. Search results by the BLAST program through the Brookhaven Protein Data Bank for the non-conserved loop or terminal sequences of <i>Chlamydomonas reinhardtii</i> D1, D2 and cytochrome b559 (Cyt b559) proteins.....	230
Table 5.2.	Comparison of modeling results of the binding niches of PSII cofactors from several existing models of the PSII reaction center.	249

LIST OF FIGURES

Figure 1.1.	Schematic diagram of the four major protein complexes on thylakoid membrane catalyzing the photosynthetic electron transfer from water to NADP ⁺ through PSII, cytochrome b ₆ /f complex and PSI.....	2
Figure 2.1.	Verification of mutations on mutagenized plasmid <i>psbA</i> DNA of <i>Chlamydomonas reinhardtii</i>	31
Figure 2.2.	Genetic verification of the R269G/V307 mutant in <i>Chlamydomonas reinhardtii</i>	34
Figure 2.3.	Western blot analysis of the D1 protein levels in wild type and R269G cells, thylakoids and PSII particles isolated from cells grown in the dark or light.....	37
Figure 2.4.	Photo-accumulation of the Tyr _D ⁺ EPR signal in PSII particles isolated from dark grown, wild type (top) and R269G (bottom) cells.....	42
Figure 2.5.	Thermoluminescence of wild type <i>C. reinhardtii</i> and D1-R269G mutant thylakoid ([Chl] is ~1 mg/ml) in the presence and absence of DCMU (10 µM)	45
Figure 2.6.	Flash-induced chlorophyll <i>a</i> fluorescence yield kinetics of the dark-grown wild type and the dark-grown D1-R269G mutant of <i>Chlamydomonas reinhardtii</i> , treated with or without DCMU (10 µM), or with DCMU (10 µM) and NH ₂ OH (5 mM), or with DCMU (10 µM) and hydroquinone (HQ, 5 mM).	48
Figure 2.7.	Chlorophyll <i>a</i> fluorescence transients (as a function of time of illumination) of the dark-grown <i>Chlamydomonas reinhardtii</i> wild type and D1-R269G in the absence and the presence of	

	10 μ M DCMU measured with a PAM-2000 fluorometer	51
Figure 2.8.	Measurements of minimal (baseline) fluorescence F_0 at low light intensities.	55
Figure 2.9.	Flash oscillation pattern for the variable chlorophyll <i>a</i> fluorescence of the dark-grown wild type and D1-R269G cells of <i>Chlamydomonas reinhardtii</i> measured at 200 μ s after an actinic flash.	59
Figure 2.10.	Flash-induced chlorophyll <i>a</i> fluorescence decay kinetics of the dark-grown <i>Chlamydomonas reinhardtii</i> wild type.....	61
Figure 2.11.	Effect of bicarbonate depletion and recovery of the wild type and the mutant.....	63
Figure 2.12.	The formate enhanced Q_A^- Fe^{+2} EPR signal in PSII particles isolated from dark grown wild type and R269G cells.....	67
Figure 2.13.	The 77 K chlorophyll <i>a</i> fluorescence emission spectra of the cells of the dark-grown <i>Chlamydomonas reinhardtii</i> wild type and the D1-R269G mutant.....	70
Figure 2.14.	Double reciprocal plot for the ^{14}C -terbutryn binding to the thylakoids of the dark-grown wild type and the D1-R269G mutant of <i>C. reinhardtii</i>	72
Figure 2.15.	A partial three dimensional model of the PSII reaction center according to the author (Chapter IV)	78
Figure 3.1.	Engineered plasmid vector (pBA157) containing the intronless <i>psbA</i> gene and the spectinomycin resistance gene (<i>Spec^r</i> , <i>aadA</i> gene from <i>E. coli</i>) (see Minagawa and Crofts 1994).....	92
Figure 3.2.	Analyses confirming the presence of the introduced D1-R257E, M mutations.....	100

Figure 3.3.	Photosynthetic growth determination of the wild type and D1-R257E, M mutants.....	102
Figure 3.4.	Chlorophyll <i>a</i> fluorescence transients (as a function of time of illumination) of the mixotrophically-grown wild type and D1-R257E, M mutants in the absence and the presence of 10 μ M DCMU and in the presence of formate, and formate plus bicarbonate measured with a PAM-2000 fluorimeter.....	105
Figure 3.5.	Measurements of minimal (baseline) fluorescence F_0 at low light intensities.....	109
Figure 3.6.	The 77 K chlorophyll <i>a</i> fluorescence emission spectra of the <i>C. reinhardtii</i> wild type and the D1-R257E, M mutant cells.....	112
Figure 3.7.	Flash-induced chlorophyll <i>a</i> fluorescence decay kinetics of the wild type and the D1-R257E, M mutant cells, treated with or without 1 μ M DCMU.	115
Figure 3.8.	Determination of DCMU binding in the wild type and the D1-R257E, M mutants using normalized variable fluorescence yield (F_v/F_0) as a function of DCMU concentration.	118
Figure 3.9.	Chlorophyll <i>a</i> fluorescence decay kinetics of the wild type and D1-R257E, M mutants without formate (control) or treated with formate (25 mM).....	120
Figure 3.10.	Effect of formate inhibition at various concentrations and pHs for the wild type and the mutants.....	123
Figure 4.1.	Sequence alignment of the D1 protein of <i>Synechocystis</i> sp. PCC 6803 with the L subunit of photosynthetic bacterial reaction center of <i>Rhodobacter sphaeroides</i> (SL) and <i>Rhodopseudomonas viridis</i> (VL).	150

Figure 4.2.	Sequence alignment of D2 protein of <i>Synechocystis</i> sp. PCC 6803 with the M subunit of the photosynthetic bacterial reaction center of <i>Rhodobacter sphaeroides</i> (SM) and <i>Rhodopseudomonas viridis</i> (VM).....	152
Figure 4.3.	The ribbon drawing diagram of the modeled three dimensional structure of the PSII reaction center including cofactors.	156
Figure 4.4.	The secondary structure profile of the modeled D1 protein.....	159
Figure 4.5.	The secondary structure profile of the modeled D2 protein.....	161
Figure 4.6.	Various possible models for the structures of P680 chlorophylls.....	167
Figure 4.7.	Herbicide DCMU modeled in the Q _B binding niche according to its binding pattern determined in the crystal structure of a mutant <i>Rps. viridis</i> reaction center.....	181
Figure 4.8.	The non-heme iron of the modeled PSII reaction center shown to be coordinated by four histidines, D1-H215, D1-H272, D2-H214, D2-H268, and a bicarbonate (HCO ₃ ⁻).	185
Figure 4.9.	Amino acid residues that are experimentally implicated in the bicarbonate stabilization, binding and functioning in the acceptor side of the PSII reaction center.....	191
Figure 4.10.	Modeling of the second bicarbonate anion in the PSII reaction center and proposed mechanism for the bicarbonate mediated Q _B protonation.....	195
Figure 4.11	Schematic diagram of the water transport channel in the bacterial reaction center (Ermler et al. 1994) and a hypothesis for a similar transport channel for water and bicarbonate in the PSII reaction center.	201
Figure 5.1.	Sequence alignment of the D1 protein of <i>C. reinhardtii</i> with the L subunit of the photosynthetic bacterial reaction center of	

	<i>Rhodobacter sphaeroides</i> (SL) and <i>Rhodopseudomonas viridis</i> (VL).	228
Figure 5.2.	The ribbon drawing diagram of the modeled three dimensional structure of the <i>C. reinhardtii</i> PSII reaction center including the cofactors.	234
Figure 5.3.	The modeled conformation of six chlorophylls in the <i>C. reinhardtii</i> PSII reaction center.....	237
Figure 5.4.	Two β -carotenes were modeled in the <i>C. reinhardtii</i> PSII reaction center, one on the D1 side and the other on the D2 side.....	242
Figure 5.5.	The binding niche for the heme in cytochrome b559.	247
Figure 5.6.	The water transport channel in the bacterial reaction center (Ermler et al. 1994) and a hypothesis for a similar transport channel for water and bicarbonate in the PSII reaction center of <i>C. reinhardtii</i>	256

LIST OF ABBREVIATIONS

ABNR	Adopted Basis Newton Raphson energy minimization approach.
ADP	adenosine diphosphate.
ATP	adenosine triphosphate.
BLAST	basic local alignment search tool.
bp	base pair.
Chl	Chlorophyll.
DBMB	2,5-dibromo-3-methyl-6-isopropyl- <i>p</i> -benzoquinone.
DCBQ	2,6-dichloro- <i>p</i> -benzoquinone.
DCMU	3-(3,4-dichlorophenyl)-1,1-dimethylurea.
DCPIP	2,6-dichlorophenolindophenol.
EDTA	ethylenediaminetetraacetic acid.
EPR	electron paramagnetic resonance.
F ₀	initial level of chlorophyll fluorescence.
FUDR	5-fluoro deoxyuridine.
F _v	variable level of chlorophyll fluorescence.
HEPES	N-(2-hydroxyethyl)piperazine-N'-(2-ethane sulfonic acid).
LHCII	light harvesting complex II.
MES	2-(N-morpholino) ethane sulfonic acid.
NADP or NADPH	oxidized or reduced form of nicotinamide adenine dinucleotide phosphate.
P680	the primary electron donor of photosystem II.
PCC	Pasteur culture collection.
PCR	polymerase chain reaction.
PDF	Probability Density Functions method.
PSII	photosystem II.

Q _A	the primary plastoquinone electron acceptor of photosystem II.
Q _B	the secondary plastoquinone electron acceptor of photosystem II.
QH ₂	plastoquinol.
rms	root mean square deviation.
SCR	structurally conserved region.
TAP	Tris-acetate-phosphate culture medium.
Tyr _D	redox active tyrosine 160 of the D2 protein of photosystem II.

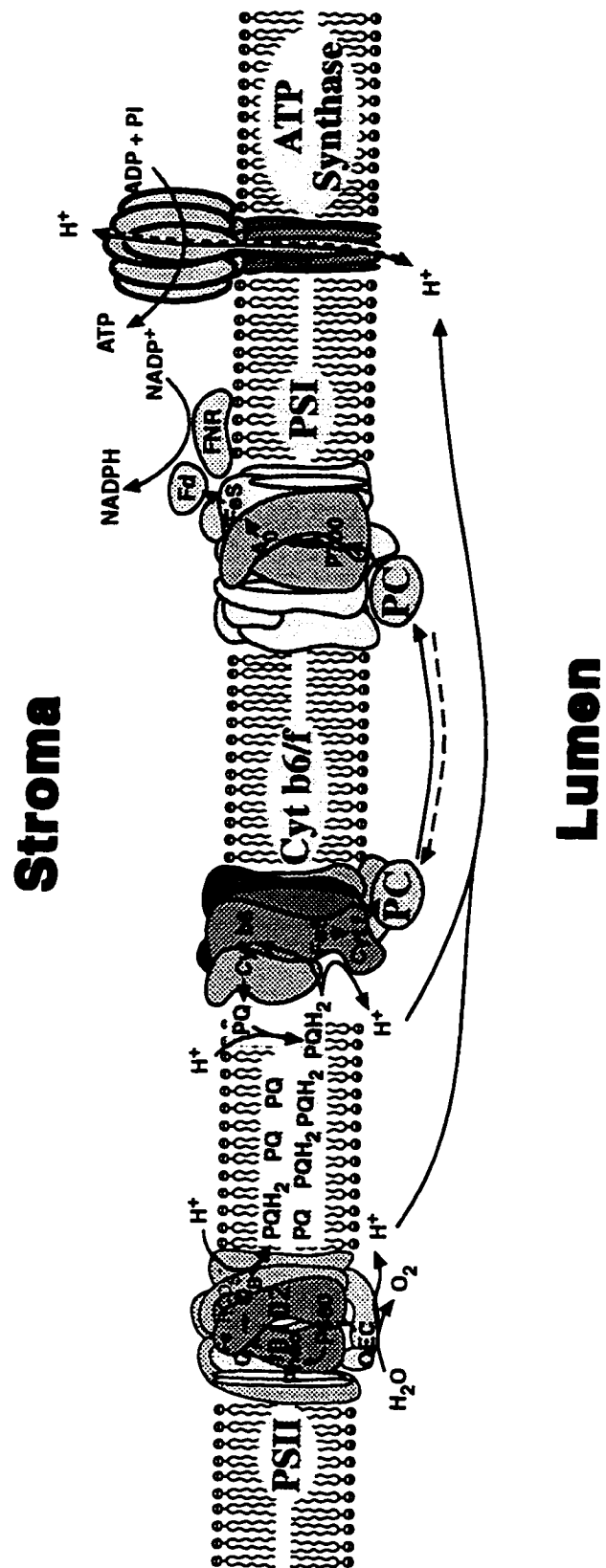
CHAPTER I. INTRODUCTION

A. Overview of Structure and Function of Photosystem II

Photosynthesis is the process by which living organisms convert light energy into biochemical energy. Oxygenic photosynthesis is a unique process in plants, algae and cyanobacteria, in which oxygen is produced by the oxidation of water molecules. This process is coupled by a light-driven electron transfer against a redox potential gradient (for review, see Whitmarsh and Govindjee 1995). The end result of this light-dependent process is the conversion of harvested photo-energy into chemical energy in the forms of NADPH and ATP. This light-dependent photochemical reaction occurs on the membrane sacs termed thylakoids where four major protein complexes involved in the reaction are located. These protein complexes are photosystem II (PSII), cytochrome b_6f complex, photosystem I (PSI) and ATP synthase (Fig. 1.1). Upon receiving photons, the chlorophyll molecules located within the reaction centers of PSI and PSII are simultaneously excited to high energy levels and perform charge separations, after which a course of electron transfer from water to NADP^+ is initiated via cytochrome b_6f complex. During the electron transfer process, oxygen is produced and a proton motive force is generated across the thylakoid membranes, which is utilized for converting ATP from ADP and phosphate by the function of ATP synthase.

The focus of this thesis research is the structure and function of PSII which is responsible for the oxygen evolution. The primary photochemical reactions in PSII occur within its reaction center which is composed of D1, D2, cytochrome b_{559} , PsbI and PsbW polypeptides (for reviews, see Whitmarsh and Govindjee 1995; Diner and Babcock 1996; for a recent paper on PsbW, see Lorkovic et al. 1995). The core of the PSII reaction center is composed of D1 and D2 polypeptides (32 kD and 34 kD, respectively) which form a

Figure 1.1. Schematic diagram of the four major protein complexes on thylakoid membrane catalyzing the photosynthetic electron transfer from water to NADP^+ through PSII, cytochrome b_6/f complex and PSI. ATP synthase catalyzes the reaction of forming ATP using the proton gradient produced across the thylakoid membrane. Certain important polypeptide constituents of the four protein complexes are shown. Fd, ferredoxin; FNR, ferredoxin-NADP reductase; OEC, oxygen evolving complex; PC, plastocyanin; PQ, plastoquinone.



protein assembly that embeds all the cofactors for the PSII charge separation and electron transfer. These cofactors include chlorophyll P680, accessory chlorophylls, pheophytins, plastoquinones, β -carotenes, the non-heme iron, and a tetra-manganese cluster. Cytochrome b559 is a small membrane polypeptide closely associated with the D1/D2 assembly and has two subunits, α and β (9 kD and 4 kD). It is believed to be involved in the assembly of PSII and in the photoprotection of PSII (see review of Whitmarsh and Pakrasi 1996). The physiological role of the small polypeptides psbI and psbW is still unclear at present.

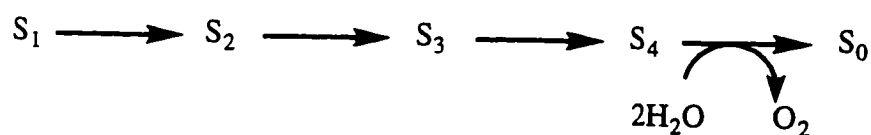
The photochemical reactions in PSII rely on with the absorption of light by various antenna pigments (*e.g.* chlorophylls, carotenoids, or phycobilins in cyanobacteria) that are surrounding the PSII reaction center. After absorbing the light energy, these pigments are excited to a high energy singlet state within femtoseconds. The energy at the excited state can be efficiently transferred, in the form of excitons, to a nearby pigment and ultimately to a monomer or dimer of specialized chlorophyll *a* molecules known as P680 in the reaction center (see review in Whitmarsh and Govindjee 1995).

The light energy reaching the PSII reaction center excites the P680 chlorophyll to the singlet state. Within 3 ps, charge separation occurs between the P680 and a nearby pheophytin (Pheo) when the excited singlet state P680 gives off an electron to Pheo, forming a $P680^+$ and a $Pheo^-$. Rapid oxidation of $Pheo^-$ (~200 ps) occurs when the negative charge on $Pheo^-$ reduces a nearby plastoquinone molecule known as Q_A , the primary plastoquinone, forming Pheo and Q_A^- . Within a half life of 20-200 ns, the $P680^+$ is reduced by a redox-active tyrosine residue known as Z (or Y_Z). Q_A^- is oxidized within 100-200 μ s by a nearby plastoquinone known as Q_B , forming Q_B^- . Q_B^- has a long lifetime and its negative charge is thought to be stabilized by a protonated protein environment. Z^+ is reduced in about 600 μ s by a water-oxidizing complex containing four manganese ions. The electron transfer events from water to $P680^+$ are referred to as the donor side events and those from $P680^*$ to the plastoquinone pool as the acceptor side events. As will be

mentioned in detail in Chapter IV, there are in fact two redox active tyrosine residues, Z and D. Z is the fast electron donor to P680⁺ and is tyrosine 161 on the D1 protein. D is a slow electron donor and is tyrosine 160 on the D2 protein.

When a second charge separation occurs, a similar electron transfer scheme is repeated. However, on the second round, Q_B is fully reduced and becomes protonated, forming Q_BH₂ which is a plastoquinol molecule. Q_BH₂ has low affinity in the Q_B site and readily diffuses out of the site. Another oxidized plastoquinone molecule will diffuse into the empty site from the membrane-associated plastoquinone pool. On the donor side, the second P680 turnover causes the water-oxidizing complex to accumulate one more positive charge after the reduction of Z⁺. Water molecules are only oxidized to produce oxygen after two additional charge separations (for details, see reviews by Debus 1992; Klein et al. 1993; Renger 1993). The net result of the four charge separation events is the oxidation of two water molecules and the formation of two plastoquinols with the release of one oxygen molecule.

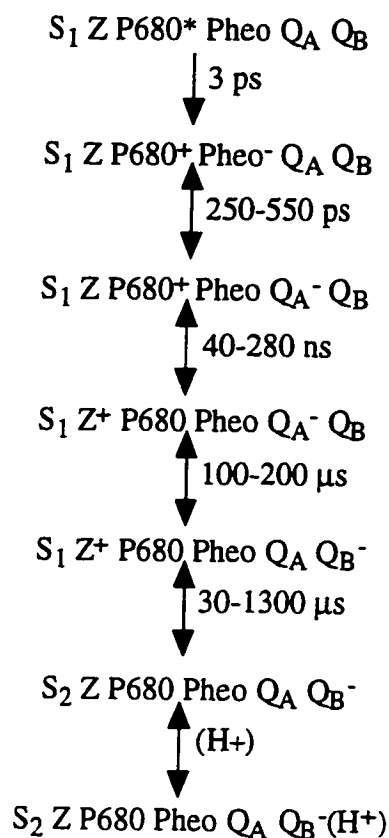
The accumulation of four oxidizing equivalents corresponding to the removal of four electrons from water by the water-oxidizing complex is the consecutive action of five different oxidation states, termed S₀, S₁, S₂, S₃, and S₄. In the dark-adapted samples, the S₁ state predominates and the oxidation of water is believed to occur through the sequential oxidation of the S-states up to S₄. The S₄ state is believed to be a transient intermediate that spontaneously reverts to the S₀ state. During this step, oxygen is released, as shown below:



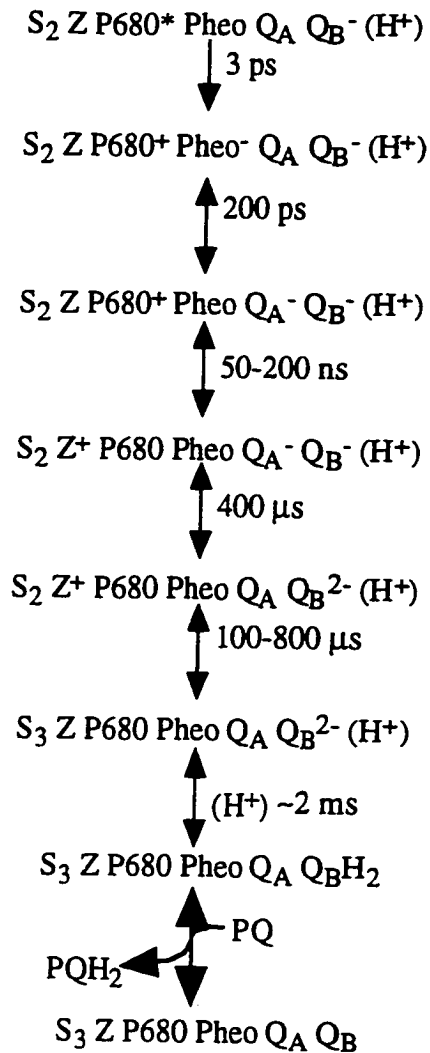
The most reduced state S₀ is converted by a one-electron oxidation to the dark-stable state S₁. This S-state model was originally formulated by B. Kok and co-workers to explain the phenomenon of the period four oscillation of oxygen evolution by chloroplasts in response

to a series of light flashes (Kok et al. 1970; Forbush et al. 1971). It is now considered that four Mn ions, arranged on a multinuclear cluster, are responsible for the transitions of the S states, accumulating at least three or maybe all four oxidizing equivalents. There are certain pieces of evidence to suggest that a histidine residue may accumulate one oxidizing equivalent (see review by Debus 1992).

The above PSII reactions following the excitation of the P680 can be summarized as follows:



Q_B^- in the above scheme can be stabilized by the protonated protein neighborhood for a long lifetime. After another photo-excitation, the reaction continues:



On the PSII acceptor side, as mentioned above, Q_A which is a one electron carrier delivers the electron to Q_B (or Q_B^-), whereas Q_B is a two electron carrier requiring to be reduced twice by Q_A^- . The two-step reduction of Q_B is the concept known as the "two electron gate" (Crofts and Wraight 1983) first discovered by Velthuys and Ames (1974) and Bouges-Bocquet (1973).

PSII herbicides (such as atrazine, DCMU, etc.) inhibit the electron transfer and kill photosynthetic organisms by displacing Q_B from its binding site (Wraight 1981; Velthuys 1981). The identification of the herbicide binding within PSII was achieved by photoaffinity labeling in which herbicides belonging to the category of organic azides are

capable of being split off nitrogen under illumination forming a reactive dehydroazepine intermediate which is capable of covalent binding (see review in Oettmeier 1992). If the azide is radioactively labeled, its binding protein also becomes radioactive and can be easily identified. In this way, the herbicide binding protein was identified to be the D1 protein.

There is a non-heme iron known to be located between Q_A and Q_B . It is shown to interact with both Q_A^- and Q_B^- magnetically (see review in Diner et al. 1991). Although this iron is not a redox-active intermediate in the electron transport under physiological conditions, its presence is crucial for maintaining the normal PSII electron transfer process (see Vermaas et al. 1994).

The high resolution crystal structure of the PSII reaction center is not available to date. However, significant sequence and functional homology is known to exist between the D1 and D2 polypeptides and the L and M subunits of the reaction centers of purple non-sulfur bacteria (Trebst 1986; Michel and Deisenhofer 1988), for which high resolution X-ray crystallographic structures are available. The significant homology information has guided researchers to construct reasonable three dimensional models in order to obtain more accurate structural understanding on the PSII reaction center (see *e.g.* Ruffle et al. 1992; Svensson et al. 1996). A detailed three dimensional computer modeling on the PSII reaction center of *Synechocystis* sp. PCC 6803 and *Chlamydomonas reinhardtii* was conducted by the author and will be presented in Chapters IV and V.

B. Overview of Bicarbonate Effect in PSII

The electron transfer in PSII, both in the acceptor and the donor sides, is known to be inhibited by the depletion of bicarbonate anions. The inhibition can be fully recovered by the readdition of bicarbonate. This is the so-called "bicarbonate effect" (see reviews in Govindjee and van Rensen 1993; Govindjee 1993; for a recent paper on the donor side

effect, see Klimov et al. 1995). Formate, azide, nitrite and nitric oxide are all able to produce the bicarbonate-depletion effects. Studies suggested that the site of action for the bicarbonate anions in the acceptor side is located between Q_A and the plastoquinone pool (Wydrzynski and Govindjee 1975; Govindjee et al. 1976; Jursinic et al. 1976; Khanna et al. 1977; Siggel et al. 1977). Further studies on the formate inhibitory effect on the PSII electron transfer was shown to be at the Q_A^- to Q_B^- step, whereas the electron transfer from Q_A^- to Q_B is much less inhibited, suggesting that the formate inhibition may be primarily in the Q_B protonation step (Eaton-Rye and Govindjee 1988a, b; Blubaugh and Govindjee 1988a; Xu et al. 1991).

Bicarbonate was also shown to be involved in liganding with the non-heme iron. EPR experiments (Diner and Petrouleas 1990) showed that NO is able to displace bicarbonate on the non-heme iron and this replacement is reversed by the addition of bicarbonate. A Fourier transform infrared difference spectroscopy study using ^{13}C -labeled bicarbonate further indicated that bicarbonate is a bidentate ligand of the non-heme iron in PSII (Hienerwadel and Berthomieu, 1995).

Binding of bicarbonate in PSII was confirmed by the release of $\text{CO}_2/\text{HCO}_3^-$ upon formate treatment (Govindjee et al. 1991; Govindjee et al. 1996). Though Jursinic and Stemler (1992) failed to detect the release of CO_2 upon the addition of formate, Stemler (1977) measured the binding of $\text{H}^{14}\text{CO}_3^-$ to isolated thylakoids and determined that there were two pools for HCO_3^- , a high affinity pool and a low affinity pool. The normal PSII electron flow depends on the presence of the high affinity pool.

Since bicarbonate is negatively charged, it is expected that the binding in PSII would be electrostatic in nature and therefore positively charged amino acid residues in D1 and D2 are likely to participate in bicarbonate binding. Only a few positively charged D1 and D2 residues are found near the putative non-heme iron based on previous homology studies (see Govindjee and van Rensen 1993). These positively charged residues includes D1-R269, D2-R233, D1-R251, D2-K264, and D2-R265. Site-directed mutagenesis have

shown that mutants of D2-R233 and D1-R251 were able to increase the PSII susceptibility to formate inhibition by 10 fold (Cao et al. 1991). The role of two arginines was suggested to function in stabilizing the bicarbonate binding *in vivo*. However, the mutations in the above two residues did not abolish the formate/bicarbonate binding capabilities. Site-directed mutations on D2-K264 showed that the mutants have a reduced rate of the electron flow from $Q_A \rightarrow Q_B$ and are very resistant to formate and NO treatment (unpublished data, cited in Diner et al. 1991). In addition, the D2-K264 mutants require much higher levels of bicarbonate to increase the electron transfer of $Q_A \rightarrow Q_B$, suggesting that the residue is involved in the binding of bicarbonate. Mutations at a nearby residue D2-R265 also showed similar effects, though to a lesser extent. As these residues are considered to be close to the non-heme iron, they are considered to play a role in stabilizing the bicarbonate liganded with the iron.

In addition to liganding to the iron, many experiments have suggested that bicarbonate may also function in promoting the protonation of Q_B^- or Q_B^{2-} (Eaton-Rye and Govindjee 1988a, b; van Rensen et al. 1988; Xu et al. 1991). Kinetic studies by Blubaugh and Govindjee (1988b) also suggested the possibility of two high affinity bicarbonate binding sites in the PSII reaction center. This second binding site is likely to exist in the Q_B niche and is thought to be related to the protonation of plastoquinone. Characterization of a number of Q_B mutants which are also herbicide resistant have implicated the Q_B binding niche to be involved for the bicarbonate functioning in PSII (Govindjee et al. 1990; Govindjee et al. 1992; Cao et al. 1992; Strasser et al. 1992; Mäenpää et al. 1995; Srivastava et al. 1995; Vernotte et al. 1995). The tested residues involved are: D1-F211, D1-V219, D1-E242, D1-E243, D1-E244, D1-A251, D1-F255, D1-G256, D1-S264, D1-N266, D1-L275.

A hypothesis on the bicarbonate function was formulated by Blubaugh and Govindjee (1988b), in which bicarbonate is suggested to be associated with certain histidine and arginine residues and to play a role in the protonation of Q_B . It was proposed

that the bicarbonate may hydrogen-bond to a histidine residue and be stabilized by an arginine residue. Upon the formation of Q_B^- , bicarbonate donates a proton to the histidine which eventually uses it to stabilize Q_B . Thus bicarbonate forms a part of the proton-relay mechanism.

C. Objective of This Thesis

As mentioned above, bicarbonate binding in the PSII reaction center is likely to involve residues near the putative Q_B and the non-heme iron sites, and basic residues are strongly implicated in the binding. Such residues in this region, based on early sequence analyses (see Govindjee and van Rensen 1993), include D1-R257 and D1-R269. To investigate the involvement of these two arginine residues in bicarbonate binding *in vivo*, site-directed mutagenesis will be carried out on these two residues using a unicellular green alga *Chlamydomonas reinhardtii*. In addition, more detailed structural analysis of the PSII reaction center will be conducted by constructing three dimensional models of the PSII reaction center. With the availability of the three dimensional models, bicarbonate binding and its mode of action in PSII reaction center will be analyzed in a more accurate way. The study is expected to provide an integrated understanding of the interactions between the D1 protein and bicarbonate and of the mechanism of plastoquinone reduction in PSII.

D. References

- Blubaugh, D.J. and Govindjee. (1998a) Kinetics of the bicarbonate effect and the number of bicarbonate-binding sites in thylakoid membranes. *Biochim. Biophys. Acta* 936: 208-214.

- Blubaugh, D.J. and Govindjee. (1988b) The molecular mechanism of the bicarbonate effect at the plastoquinone reductase site of photosynthesis. *Photosynth. Res.* 19: 85-128.
- Bouges-Bocquet, B. (1973) Electron transfer between the two photosystems in spinach chloroplasts. *Biochim. Biophys. Acta* 314: 250-256.
- Cao, J., Vermaas, W.F.J. and Govindjee. (1991) Arginine residues in the D2 polypeptide may stabilize bicarbonate binding photosystem II of *Synechocystis* sp. PCC 6803. *Biochim. Biophys. Acta* 1059: 171-180.
- Cao, J., Ohad, N., Hirschberg, J., Xiong, J. and Govindjee. (1992) Binding affinity of bicarbonate and formate in herbicide-resistance D1 mutants of *Synechococcus* sp. PCC 7942. *Photosyn. Res.* 34: 397-408.
- Crofts, A.R. and Wraight, C. (1983) The electrochemical domain of photosynthesis. *Biochim. Biophys. Acta* 726: 149-185.
- Debus, R.J. (1992) The manganese and calcium ions of photosynthetic oxygen evolution. *Biochim. Biophys. Acta* 1102: 269-352.
- Diner, B.A. and Petrouleas, V. (1990) Formation by NO of nitrosyl adducts of redox components of the photosystem II reaction center. II. Evidence that $\text{HCO}_3^-/\text{CO}_2$ binds to the acceptor-side non-heme iron. *Biochim. Biophys. Acta* 1015: 141-149.
- Diner, B.A. and Babcock, G.T. (1996) Structure, dynamics, and energy conversion efficiency in photosystem II. In: Ort, D.R. and Yocum, C.F. (eds) *Oxygenic Photosynthesis: The light Reactions*. (in press) Kluwer Academic Publishers, Dordrecht.

- Diner, B.A., Petrouleas, V. and Wendoloski, J.J. (1991) The iron-quinone electron-acceptor complex of photosystem II. *Physiol. Plant.* 81: 423-436.
- Eaton-Rye, J.J. and Govindjee. (1988a) Electron transfer through the quinone acceptor complex of photosystem II in bicarbonate-depleted spinach thylakoid membranes as a function of actinic flash number and frequency. *Biochim. Biophys. Acta* 935: 237-247.
- Eaton-Rye, J.J. and Govindjee. (1988b) Electron transfer through the quinone acceptor complex of photosystem II after one or two actinic flashes in bicarbonate-depleted spinach thylakoid membranes. *Biochim. Biophys. Acta* 935: 248-257.
- Forbush, B., Kok, B. and McGloin, M.P. (1971) Cooperation of charges in photosynthetic O₂ evolution--II. Dumping of flash yield oscillation, deactivation. *Photochem. Photobiol.* 14: 307-475.
- Govindjee. (1993) Bicarbonate-reversible inhibition of plastoquinone reductase in photosystem II. *Z. Naturforsch.* 48c: 251-258.
- Govindjee and van Rensen, J.J.S. (1993) Photosystem II reaction center and bicarbonate. In: Deisenhofer, J. and Norris, J. (eds), *The Photosynthetic Reaction Center*, Vol. I, pp. 357-389, Academic Press, Inc., San Diego.
- Govindjee, Pulles, M.P.J., Govindjee, R., Van Gorkom, H. and Duysens, L.N.M. (1976) Inhibition of the reoxidation of the secondary electron acceptor of photosystem II by bicarbonate depletion. *Biochim. Biophys. Acta* 449: 602-605.
- Govindjee, Vernotte, C., Peteri, B., Astier, C. and Etienne, A.-L. (1990) Differential sensitivity of bicarbonate-reversible formate effects on herbicide resistant mutants of *Synechocystis* 6714. *FEBS Lett.* 267: 273-276.

- Govindjee, Weger, H.G., Turpin, D.H., Van Rensen, J.J.S., de Vos, O.J. and Snel, J.F.H. (1991) Formate releases carbon dioxide/bicarbonate from thylakoid membranes, measurements by mass spectroscopy and infrared gas analyzer. *Naturwissenschaften* 78: 168-170.
- Govindjee, Eggenberg P, Pfister K and Govindjee. (1992) Chlorophyll *a* fluorescence decay in herbicide-resistant D1 mutants of *Chlamydomonas reinhardtii* and the formate effect. *Biochim Biophys Acta* 1101: 353-358.
- Govindjee, Xu, C., Schansker, G., and van Rensen, J.J.S. (1996) Chloroacetates as inhibitors of photosystem II: effects on electron acceptor side. *J. Photochem. Photobiol.* (in press)
- Hienerwadel, R. and Berthomieu, C. (1995) Bicarbonate binding to the non-heme iron of photosystem II investigated by Fourier transform infrared difference spectroscopy and ¹³C-labeled bicarbonate. *Biochemistry* 34: 16288-16297.
- Jursinic, P.A. and Stemler, A. (1992) High rates of photosystem II electron flow occur in maize thylakoids when the high-affinity binding site for bicarbonate is empty of all monovalent anions or has bicarbonate bound. *Biochim. Biophys. Acta* 1098: 359-367.
- Jursinic, P., Warden, J. and Govindjee. (1976) A major site of bicarbonate effect in system II reaction; evidence for EPR signal II_{vf}, fast fluorescence yield charges and delayed light emission. *Biochim. Biophys. Acta* 440: 322-330.
- Khanna, R., Govindjee and Wydrzynski, T. (1977) Site of bicarbonate effect in Hill reaction: evidence from the use of artificial electron acceptors and donors. *Biochim. Biophys. Acta* 462: 208-214.

- Klein, M.P., Sauer, K. and Yachandra, V.K. (1993) Perspectives on the structure of the photosynthetic oxygen evolving manganese complex and its relation to the Kok cycle. *Photosyn. Res.* 38: 265-277.
- Klimov, V.V., Allakhverdiev, S.I., Feyziev, Y.M. and Baranov, S.V. (1995) Bicarbonate requirement for the donor side of photosystem II. *FEBS Lett.* 363: 251-255.
- Kok, B., Forbush, B. and McGloin, M.P. (1970) Cooperation of charges in photosynthetic O₂ evolution--I. A linear four step mechanism. *Photochem. Photobiol.* 11: 457-475.
- Lorkovic, Z.J., Schröder W.P., Pakrasi, H.B., Irrgang, K.-D., Herrmann, R.G. and Oelmüller, R. (1995) Molecular characterization of PsbW, a nuclear-encoded component of the photosystem II reaction center complex in spinach. *Proc. Natl. Acad. Sci. USA* 92: 8930-8934.
- Mäenpää, P., Miranda, T., Tyystjärvi, E., Tyystjärvi, T., Govindjee, Ducruet, J.-M., Etienne, A.-L. and Kirilovsky, D. (1995) A mutation in the D-de loop of D₁ modifies the stability of the S₂Q_A⁻ and S₂Q_B⁻ states in photosystem II. *Plant Physiol.* 107: 187-197.
- Michel, H. and Deisenhofer, J. (1988) Relevance of the photosynthetic reaction center from purple bacteria to the structure of photosystem II. *Biochemistry* 27: 1-7.
- Oettmeier, W. (1992) Herbicides of photosystem II. In: Barber, J. ed., *The Photosystems: Structure, Function and Molecular Biology*. pp. 349-407, Elsevier Science Publishers, Amsterdam.
- Renger, G. 1993. Water cleavage by solar radiation--an inspiring challenge of photosynthesis research. *Photosyn. Res.* 38: 229-247.

- Ruffle, S.V., Donnelly, D., Blundell, T.L. and Nugent, J.H.A. (1992) A three-dimensional model of the photosystem II reaction centre of *Pisum sativum*. *Photosyn. Res.* 34: 287-300.
- Siggel, U., Khanna, R., Renger, G. and Govindjee. (1977) Investigation of the absorption changes of the plastoquinone system in broken chloroplasts: the effect of bicarbonate depletion. *Biochim. Biophys. Acta* 462: 196-207.
- Srivastava, A., Strasser, R.J. and Govindjee. (1995) Polyphasic rise of chlorophyll *a* fluorescence in herbicide-resistant D1 mutants of *Chlamydomonas reinhardtii*. *Photosyn Res* 43: 131-141.
- Stemler, A. (1977) The binding of bicarbonate ions to washed chloroplast grana. *Biochim. Biophys. Acta* 460: 511-522.
- Stemler, A. and Jursinic, P. (1992) Oxidation-reduction potential dependence of formate binding to photosystem II in maize thylakoids. *Biochim. Biophys. Acta* 1183: 269-280.
- Strasser, R.J., Eggenberg, P., Pfister, K. and Govindjee. (1992) An equilibrium model for electron transfer in photosystem II acceptor complex: An application to *Chlamydomonas reinhardtii* cells of D1 mutants and those treated with formate. *Arch. Sci. Gen.* 45: 207-224.
- Svensson B, Etchebest C, Tuffery P, van Kan P, Smith J and Styring S (1996) A model for the photosystem II reaction centre core including the structure of the primary donor P680. *Biochemistry* (in press)
- Trebst, A. (1986) The topology of the plastoquinone and herbicide binding peptides of photosystem II—a model. *Z. Naturforsch.* 41c: 240-245.

- van Rensen, J.J.S., Tonk, W.J.M. and de Bruijn, S.M. (1988) Involvement of bicarbonate in the protonation of the secondary quinone electron acceptor of photosystem II via the non-heme iron of the quinone-iron acceptor complex. *FEBS Lett* 226: 347-351.
- Velthuys, B.R. (1981) Electron dependent competition between plastoquinone and inhibitors for binding to photosystem II. *FEBS Lett.* 126: 277-281.
- Velthuys, B.R. and Ames, J. (1974) The effect of dithionite on fluorescence and luminescence of chloroplasts. *Biochim. Biophys. Acta* 325: 126-137.
- Vermaas, W.F.J., Vass, I., Eggers, B. and Styring, S. (1994) Mutation of a putative ligand to the non-heme iron in photosystem II: Implications for Q_A reactivity, electron transfer, and herbicide binding. *Biochim. Biophys. Acta* 1184: 263-272.
- Vernotte, C., Briantais, J.-M., Astier, C. and Govindjee (1995) Differential effects of formate in single and double mutants of D1 in *Synechocystis* sp. PCC 6714. *Biochim. Biophys. Acta* 1229: 296-301.
- Whitmarsh, J. and Govindjee. (1995) Photosynthesis. In: *Encyclopedia of Applied Physics*, 13: 513-532.
- Whitmarsh, J. and Pakrasi, H.B. (1996) Form and function of cytochrome b559. In: Ort, D.R. and Yocum, C.F. (eds.) *Oxygenic Photosynthesis: The Light Reactions*, Kluwer Academic Publishers, Dordrecht. (in press)
- Wraight, C.A. (1981) Oxidation-reduction physical chemistry of the acceptor quinone complex in bacterial photosynthetic reaction centers: evidence for a new model of herbicide activity. *Isr. J. Chem.* 21: 348-354.

- Wydrzynski, T. and Govindjee. (1975) A new site of bicarbonate effect in photosystem II of photosynthesis: evidence from chlorophyll fluorescence transients in spinach chloroplasts. *Biochim. Biophys. Acta* 387: 403-408.
- Xiong, J., Hutchison, R., Sayre R. and Govindjee. (1995) Characterization of a site-directed mutant (D1-arginine 269-glycine) of *Chlamydomonas reinhardtii*. In: Mathis, P. (ed.), *Photosynthesis: from Light to Biosphere*, Vol. I, pp. 575-578. Kluwer Publishers, Dordrecht.
- Xu, C., Taoka, S., Crofts, A.R., and Govindjee. (1991) Kinetic characteristics of formate/formic acid binding at the plastoquinone reductase site in spinach thylakoids. *Biochim. Biophys. Acta* 1098: 32-40.

CHAPTER II. CONSTRUCTION AND CHARACTERIZATION OF A PUTATIVE BICARBONATE BINDING SITE MUTANT (ARGININE-269-GLYCINE) OF *CHLAMYDOMONAS REINHARDTII*

A. Introduction

Electron transfer in photosystem II (PSII) has been shown by numerous studies to be regulated by bicarbonate anions in higher plants, algae and cyanobacteria (see Chapter I). Although there are studies showing a donor side effect of bicarbonate (El-Shintinawy et al. 1990; El-Shintinawy and Govindjee 1990; Klimov et al. 1995; Wincencjusz et al. 1996), depletion of bicarbonate causes a significant inhibition on the electron transfer on the acceptor side of PSII, particularly on the Q_A^- to Q_B^- step (Blubaugh and Govindjee 1988a; Diner et al. 1991; Govindjee and van Rensen 1993; Govindjee 1993).

The non-heme iron in PSII is likely to be coordinated by four histidine residues (located on the stromal side of transmembrane spans D and E of the D1 and D2 proteins) as in the bacterial reaction center. However, amino acid residue M-E232 (*Rhodospseudomonas viridis*) which provides the fifth and sixth ligands to the iron lacks its amino acid homologue in PSII. Michel and Deisenhofer (1988) and van Rensen et al. (1988) proposed that bicarbonate could serve as a functional homologue of M-E232, providing the fifth and sixth ligands to the non-heme iron in PSII. A close association of bicarbonate with the non-heme iron in PSII was supported from EPR spectroscopic studies (Vermaas and Rutherford 1984; Petrouleas and Diner 1990). A recent Fourier transform infrared difference spectroscopy study using ^{13}C -labeled bicarbonate has confirmed that bicarbonate is a bidentate ligand of the non-heme iron in PSII like M-E232 (Hienerwadel and Berthomier 1995). However, this suggested equivalence of E232 on the M subunit and bicarbonate has its limitations since site-directed mutagenesis of M-E232 to several amino acid residues (R,

V, A, Q, etc.) in bacterial reaction centers did not modify the Q_A^- to Q_B (or to Q_B^-) electron flow (Wang et al. 1992).

Since anionic bicarbonate may be the active species functioning in the PSII reaction center (Blubaugh and Govindjee 1986), it is expected that the binding would be electrostatic in nature and therefore positively charged amino acid residues are likely to participate in bicarbonate binding. Only a few positively charged D1 and D2 residues are found near the putative non-heme iron based on homology studies (see Govindjee and van Rensen 1993). Further, experimental evidence has suggested bicarbonate to aid in the protonation of Q_B^{2-} (Blubaugh and Govindjee 1988a; Eaton-Rye and Govindjee 1988a; Xu et al. 1991; Govindjee and van Rensen 1993), implicating the involvement of D1 protein in bicarbonate binding.

Sequence analysis of the D1 protein indicated that D1-R269 residue was the only basic residue near the putative non-heme iron site (see Govindjee and van Rensen 1993). This residue is thought to be located on the stromal side of the putative transmembrane helix E and may be separated from D1-H272, one of the four putative non-heme iron ligands, by approximately 3/4 of a helical turn (according to a three dimensional model of the PSII reaction center by the author, see Chapter IV). Thus, a hypothesis that a close interaction between the arginine and the iron-liganding bicarbonate may exist has emerged. This hypothesis is partially supported by the analogy found in the x-ray crystal structure of human lactoferrin which has a (bi)carbonate binding to an iron at the active site (Anderson et al. 1989). In this protein, the (bi)carbonate is stabilized by hydrogen bonding interactions with an arginine and several other adjacent amino acid residues. An x-ray crystal structure of hemoglobin and myoglobin with a formate (a bicarbonate analog) bound to the heme iron also indicates the involvement of an arginine residue interacting with the formate (Aime et al. 1996). Thus, it is possible that a similar binding motif may exist in the HCO_3^-/Fe site of the PSII reaction center.

To investigate whether D1-R269 is a bicarbonate liganding residue, a site-directed mutant in the unicellular green alga *Chlamydomonas reinhardtii* has been generated and characterized to test whether the D1-R269 residue binds bicarbonate. Residue R269 has been replaced with a non-conservative residue, glycine (D1-R269G). To understand the full implication of this mutation, the resultant mutant was characterized on the structure and function of both the donor and acceptor sides of PSII. In this chapter, I will describe the construction, structural and functional properties of this mutant.

The characterization shows that the mutant (1) has lowered stability of D1, (2) is unable to assemble the tetramanganese cluster in the PSII donor side, (3) has a significant inhibition on the electron transfer either for the full chain or for $Q_A \rightarrow Q_B$, (4) loses the two electron gate functioning, (5) has a block in the excitation energy transfer to the PSII reaction center, (6) has a significant reduction in herbicide binding affinity, (7) lacks the thermoluminescence bands due to $S_2Q_A^-$ and $S_2Q_B^-$ recombination, and (8) has a significant reduction in the bicarbonate/formate effect on the acceptor side. Though the data show that the bicarbonate binding may still exist in the PSII reaction center, the importance of R269 residue in the structure and function of PSII has been clearly demonstrated.

B. Materials and Methods

1. Mutagenesis of psbA gene and screening for homoplasmic mutant

The plasmid (pWT) which contains exons 4 and 5 of the *psbA* gene (3.0 kb) cloned onto a phagemid vector pBS(+) (Roffey et al. 1991) was used for site-directed mutagenesis of the D1 protein. The site-directed mutagenesis on the R269 located on the exon 5 of *psbA* DNA was based on Kunkel et al. (1987) and Eggenberger et al. (1990). Arginine 269 was changed into a non-conservative residue glycine in an attempt to create a deletion-like mutation. A silent mutation on valine 307 was made, introducing a new *Sal* I restriction

site, which was designed to facilitate the subsequent screening of the mutant DNA from *C. reinhardtii* transformants. Two separate oligonucleotides were used to create a glycine substitution at residue R269 (GAAGTGTAATGAACCAGAGTTGTTGAA converts a CGT to a GGT codon) and a silent and diagnostic Sal I restriction endonuclease recognition site at residue V307 (ACCTTGAGTCGACTACTGATGGTT converts a GTA codon to a GTC codon). The resulting plasmid (pR269G/V301) was sequenced using a Sequenase 2.0 kit (U.S. Biochemicals, Cleveland, OH) to confirm the presence of the mutations.

Plasmid pR269G/V301 and plasmid p228, containing the chloroplast 16S rRNA gene conferring spectinomycin resistance (Harris et al. 1989), were co-transformed into wild type cells using a helium particle inflow gun with 1 micron tungsten particles (Roffey et al. 1994a). *C. reinhardtii* cells were grown in the presence of 0.5 mM FUDR for 2 days (~8 generations) in the dark to reduce the chloroplast DNA copy number prior to being shot (Roffey et al. 1991). Cells transformed with plasmid p228 were selected on TAP plates containing 85 µg/ml spectinomycin to identify chloroplast DNA transformants. Spectinomycin resistant colonies were visible after two to three weeks.

To isolate the p228-pR269G/V301 chloroplast DNA co-transformants, spectinomycin resistant colonies (transformed with p228) were screened for the presence of the diagnostic restriction endonuclease recognition site introduced into the *psbA* gene with plasmid pR269G/V301. Single colony isolates were transferred to 3 ml of TAP containing 85 µg/ml spectinomycin and grown for 1 week and an aliquot (100 µl) of the cell suspension was plated on TAP plates (containing 100 µg/ml spectinomycin) to begin the secondary screen for chloroplast transformants. Total DNA was isolated from 1.5 ml of the liquid culture. The cells were concentrated by centrifugation, frozen in liquid nitrogen, and the DNA extracted using an S&S Elu-Quik DNA purification kit (chromosomal DNA isolation protocol). The isolated DNA was then subjected to PCR amplification of the *psbA* region spanning the entire exon 5. The 5' oligonucleotide (GGTTACTTTGGTCGTCTA) used for the PCR amplification corresponds to amino acid residues G253 - L258 in the D1

protein, and the 3' oligonucleotide (GAAGTTGTCAGCGTTACG) corresponds to amino acid residues R344-F339. These primers generate a 260 bp fragment which includes the R269G mutation site plus the diagnostic Sal I restriction site located at residue V307. Digestion of the PCR product with Sal I generates two diagnostic 160 and 100 bp fragments assuming complete exchange of the donor (transforming) with the recipient (chloroplast) DNA.

Using this PCR screening procedure, heteroplasmic mutant colonies were identified which contained wild type and mutant PCR products. Single colony isolates from the secondary screen were then subjected to a second round of screening by analysis of the PCR products digested with Sal I in order to isolate homoplasmic R269G mutant strains. In order to confirm that the mutants were homoplasmic, chloroplast DNA was isolated from putative homoplasmic mutants and wild type strains (Roffey et al. 1991), digested with Sal I, and probed on Southern blots using radiolabelled pWT DNA according to the Genescreen (DuPont, Wilmington, DE) protocol. DNA sequence analysis of the mutagenized region of the chloroplast DNA from homoplasmic isolates was carried out according to the U. S. Biochemicals cycle sequencing kit using the aforementioned PCR primers. It is important to note that the sequence of the transformed DNA fragment showed no other mutation except R269G and the silent V307.

2. *Growth conditions of C. reinhardtii*

Wild type (CC-2137 or CC-125) and mutant *C. reinhardtii* cultures were grown at 25°C in Tris-Acetate-Phosphate (TAP) medium (see Harris 1989) under continuous low light (8-12 $\mu\text{mol photon}\cdot\text{m}^{-2}\cdot\text{sec}^{-1}$) exposure, continuous darkness, or continuous darkness plus 20 min low light exposure (Roffey et al. 1991; 1994a; Kramer et al. 1994). Cultures were inoculated from a starter culture at 1/100 volume and harvested 4 days later in log phase at a cell density of $\sim 6 \times 10^6$ cells·ml⁻¹. The wild type strain was maintained in

TAP agar plates with 100 µg/ml ampicillin and the mutant strain was maintained in TAP plates with 200 µg/ml spectinomycin and 100 µg/ml ampicillin.

3. Chlorophyll and growth determination

Chlorophyll concentration was determined by suspending the cells in 80% acetone at 40°C for 20 min. The samples were centrifuged at $14,000 \times g$ for 1 min, and the resulting pellet was discarded. The absorbance of the supernatant was measured at 663.6 nm and 646.6 nm using a commercial spectrophotometer (Shimadzu UV160U, Shimadzu Co., Kyoto, Japan). Chlorophyll concentrations were calculated according to the equations of Porra et al. (1989). The growth rate of the wild type and the mutant was determined by measuring the optical density of the cells in original culture media at 750 nm. In the heterotrophic growth condition, both the wild type and the mutant had near identical growth rate (22 hr.).

4. Thylakoid preparation

The thylakoid preparation was according to Shim et al. (1990) with slight modifications. The late log-phase cells were centrifuged at $2,000 \times g$ for 4 min. at 4°C. The pellet was washed twice with a buffer containing 350 mM sucrose, 20 mM HEPES (pH 7.5), 2.0 mM $MgCl_2$. The cells were resuspended with the above buffer to ~0.5 mg Chl/ml and passed through a French press once at 14,000 lbs/in². The broken cells were centrifuged at $100,000 \times g$ for 20 min. at 4°C. The pellet was resuspended in a buffer containing 400 mM sucrose, 20 mM HEPES (pH 7.5), 5.0 mM $MgCl_2$, 5.0 mM EDTA, 1.0 mg/ml bovine serum albumin, and 20 % (v/v) glycerol. It was further homogenized with a tissue grinder and briefly centrifuged ($1,000 \times g$, 10 s.) to remove the unbroken cells. The supernatant containing the thylakoids was concentrated to ~1 mg Chl/ml and frozen quickly, in 1.5 ml microcentrifuge tubes, at 77 K.

5. Western blot analysis

D1 protein levels (per unit Chl) were determined by western blot analysis (according to the Immuno-blot assay kit procedures, Bio-Rad, Richmond, CA) using an antibody directed against the C-terminus of the D1 protein (see, e.g., Roffey et al. 1994a).

6. Steady state of oxygen evolution

Photosynthetic oxygen evolution was measured using a Hansatech CB1 electrode with thylakoids (5 μg Chl/ml) suspended in 0.3 M sucrose, 20 mM HEPES (pH 7.5), 1 mM MgCl_2 , 20 mM methylamine, 2 mM $\text{K}_3\text{Fe}(\text{CN})_6$ and 200 μM of one of three different electron acceptors: DCBQ, DMBQ, or PBQ. DCPIP photoreduction was measured spectrophotometrically at 600 nm with thylakoids having a Chl concentration of 5.0 $\mu\text{g}/\text{ml}$ in 0.3 M sucrose, 20 mM HEPES (pH 7.5), 1 mM MgCl_2 , and 25 μM DCPIP containing either 1 mM DPC or 5 mM NH_2OH as artificial electron donors.

7. Manganese determination

Elemental analysis of the manganese content of EDTA washed PSII particles was completed at the Ohio State University REAL labs using PSII particles containing 1 mg Chl (Roffey et al. 1994a).

8. EPR analysis

Electron paramagnetic resonance (EPR) studies were performed in collaboration with Dr. C. Russ Hille using a Bruker ESP-300. The following instrument settings were used for the $\text{Q}_\text{A}^- \text{Fe}^{+2}$ measurements: modulation amplitude, 28 G; temperature, 5 K; microwave power, 32 mW. PSII particles having a Chl concentration of 5 mg/ml were illuminated at $1,000 \mu\text{E}\cdot\text{m}^{-2}\cdot\text{sec}^{-1}$ in the presence of 100 mM formate for 10 min at 77 K. Each sample was scanned 15 times. For measurement of the Tyr_D^+ signal, dark adapted samples were scanned at 150 K, warmed to room temperature, illuminated for 1 min., and

scanned again at 150 K in the dark. Instrument settings were as described in Roffey et al. (1991).

9. Thermoluminescence

Thermoluminescence, that probes both the donor and acceptor sides of PSII (see reviews by Inoue 1996; Vass and Govindjee 1996), was measured as described by Kramer et al. (1994). Thylakoid samples (~1 mg Chl/ml, pH 7.6) were isolated from the heterotrophically grown cells that were briefly adapted by light (20 min., 70 $\mu\text{E}/\text{m}^2\cdot\text{s}$ white light). The measurement was done by illuminating one saturating flash in the presence and absence of 10 μM DCMU. The thermoluminescence curves were recorded from -55 to +55°C at a heating rate of 1°C/s.

10. Chlorophyll *a* fluorescence induction kinetics and measurements of F_0

The Chl *a* fluorescence induction of cell or thylakoid samples was measured with a commercial pulse-modulated fluorometer (Walz PAM-2000, Effeltrich, Germany). Actinic and measuring beams were provided by the built-in red-light-emitting diodes. The intensity of the measuring light was 0.7 $\mu\text{E}/\text{m}^2\cdot\text{s}$ and the intensity of the actinic light was 470 $\mu\text{E}/\text{m}^2\cdot\text{s}$. Before the measurements, the cells were resuspended in TAP medium, and the thylakoids in a buffer containing 20 mM HEPES (pH 7.0), 100 mM sorbitol, 10 mM KCl, 10 mM MgCl_2 , 0.1 mM NH_4Cl . Chl concentration of the samples was 5 $\mu\text{g}/\text{ml}$. All samples were prepared in the presence of weak (< 0.3 $\mu\text{E}/\text{m}^2\cdot\text{s}$) background green light; and the measurements were done after the samples were dark-adapted for 5 min. When a light treatment of cells was needed, the dark-grown cells were illuminated with 70 $\mu\text{E}/\text{m}^2\cdot\text{s}$ white light for 1 h in the TAP medium while being stirred and bubbled with air.

In view of the fact that conclusions regarding the photochemical activity are obtained from a knowledge of the variable fluorescence (F_v) whose value is dependent upon the precise value of F_0 (see Govindjee 1995), special efforts were made to measure

the true F_0 . F_0 is the yield of fluorescence when $[Q_A]$ is maximal, i.e., when the yield of photochemistry is maximal; it reflects the antenna fluorescence that is obtained in competition with excitation energy transfer to the reaction center. This is achieved only at very low light intensities so that the quantum yield of true F_0 (i.e. F_0/I , where I is intensity of excitation) must be independent of I . Further, the addition of herbicide DCMU in darkness is not expected to increase the value of true F_0 since DCMU is not expected to affect the excitation energy transfer process. Thus, F_0 was measured as a function of light intensities in the low range (0.01-0.45 $\mu\text{E}/\text{m}^2\cdot\text{s}$) with and without the presence of 10 μM DCMU to prove that the true F_0 was indeed being measured. This was done using a different pulse-modulated fluorometer (Walz PAM-103, Effeltrich, Germany). Light intensity was varied with Oriel neutral density filters.

11. Flash induced chlorophyll a fluorescence changes

The kinetics of Chl *a* fluorescence changes in darkness after single-turnover actinic flashes were measured with a laboratory-made multiframe fluorometer (Kramer et al. 1990). All sample manipulations were done in the dark with weak background green light ($< 0.3 \mu\text{E}/\text{m}^2\cdot\text{s}$). Measurements were made with cells suspended in the TAP medium, or with thylakoids suspended in the buffer and conditions described above. Chlorophyll concentration of the measured samples was 5 $\mu\text{g}/\text{ml}$. When necessary, the cells and thylakoids were treated with 5 mM NH_2OH , or 5 mM hydroquinone, and/or 10 μM DCMU in total darkness. Treatment of cells with 100 μM *p*-benzoquinone for measuring the binary oscillation pattern was also done with samples dark-adapted for 5 min.

Chl fluorescence changes with time after the flashes were deconvoluted into three exponential components with the KaleidoGraph™ program. The fitting equation used was: $F_v/F_0 = A_1 \exp(t/\tau_1) + A_2 \exp(t/\tau_2) + A_3 \exp(t/\tau_3)$, where "A" represents the amplitude and " τ " the lifetime of the components. It is assumed here (see Govindjee et al. 1996) that the fast component (A_1, τ_1) in sub-ms range reflects the kinetics of direct reoxidation of Q_A^-

by Q_B (or by Q_B^-); the intermediate component (A_2 , τ_2) in ms range reflects the $[Q_A^-]$ equilibrium, partially controlled by the movement of plastoquinone to PSII without bound Q_B ; and the slow component (A_3 , τ_3) in seconds range reflects both the back-reaction between Q_A^- and the S states and between Q_B^- and the S-states.

12. Bicarbonate depletion and recovery treatments

Bicarbonate depletion of cells by formate was carried out with a formate treatment procedure described in El-Shintinawy et al. (1990) with modifications. The harvested dark-grown cells were resuspended to 100 $\mu\text{g Chl/ml}$ in a buffer containing 100 mM HEPES (pH 5.8), 40 mM NaCl, and 5 mM MgCl_2 . The resuspended samples were treated with various concentrations of sodium formate for 5 min. under gentle vacuum, after which they were diluted to 5 $\mu\text{g Chl/ml}$ in the same buffer at pH 6.5. The samples were immediately used for the Chl fluorescence yield measurements. Sodium bicarbonate (10 mM) was added to the formate-treated samples to reverse the formate inhibition. The control samples were subject to similar treatments except without formate and bicarbonate in the buffers.

13. Low temperature fluorescence spectra

Measurements of the low temperature fluorescence emission spectra of the heterotrophically grown cells and the thylakoids isolated from these cells were performed at 77 K in TAP medium containing 20% glycerol (for cells) or in the thylakoid buffer (for thylakoids) as described in section 2.4 with the addition of 20% glycerol. Chlorophyll concentration was 30 $\mu\text{g/ml}$. Measurements were made using a Perkin Elmer LS-5 fluorescence spectrophotometer (Perkin Elmer Ltd., Oak Brook, IL) which was equipped with a red-sensitive photomultiplier (R928, Hamamatsu Corp., Shizuoka-ken, Japan). The samples were placed in a Dewar flask with an optical clear region through which the fluorescence was excited and measured. The samples were frozen in liquid nitrogen prior to measurement. The excitation wavelength was set at 435 nm and the monochromator

bandwidth 10 nm for excitation and 3 nm for emission. The fluorescence emission was collected from the front surface of the sample. The obtained emission spectra were corrected for the wavelength dependence of the photomultiplier sensitivity, but not the monochromator. The emission spectra for different samples were normalized at the 715-nm band.

14. Herbicide binding assay

The herbicide ^{14}C -terbutryn binding assay was done according to Vermaas et al. (1990). Thylakoid samples (25 μg Chl/ml) were incubated with various concentrations of ^{14}C -terbutryn (24 $\mu\text{Ci}/\text{mg}$, kindly provided by Dr. Donald Ort), known to bind at the Q_B site, in the thylakoid buffer described above (section 2.4) at 25°C in darkness for 15 min. with occasional shaking. The thylakoids were then centrifuged for 10 min. at 14,000 \times g, and the supernatant was mixed with a scintillation cocktail (Scintiverse II, Fisher Scientific, Fair Lawn, NJ). The radioactivity of the liquid mixture was counted in a scintillation counter (LS1701, Beckman Instruments, Fullerton, CA) to 1% error. To eliminate the contribution of the unspecific binding, the samples were measured in the presence and the absence of another herbicide, atrazine (20 μM), that also binds at the Q_B site. The specific binding was obtained by subtracting the atrazine-replaceable terbutryn binding from the total terbutryn binding.

C. Results

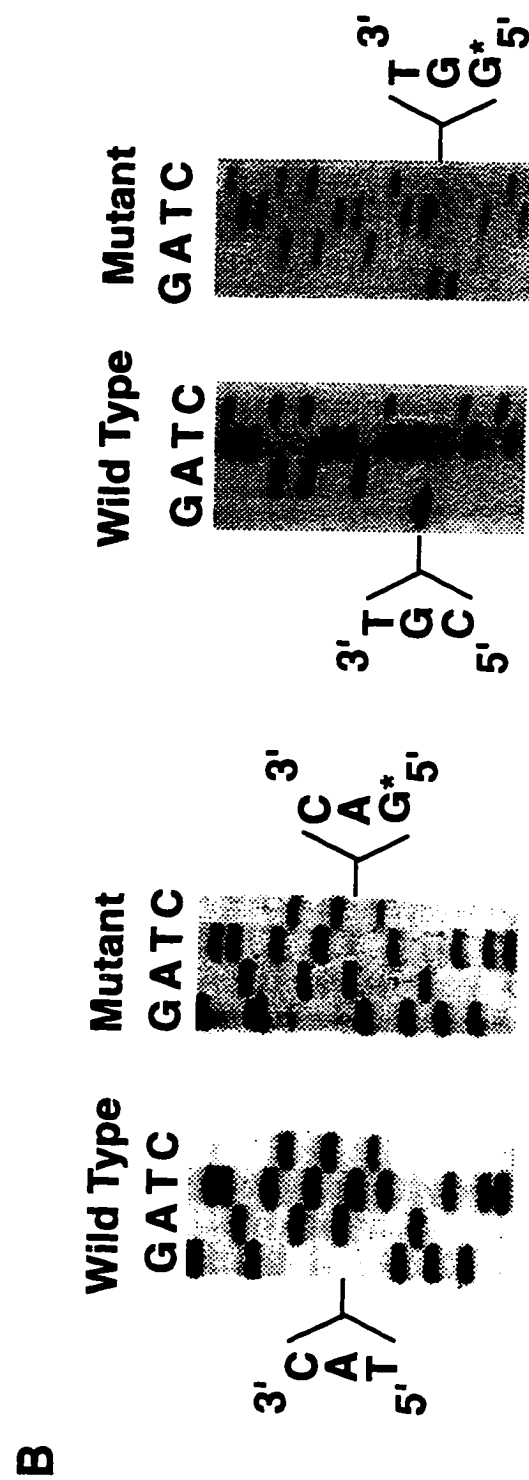
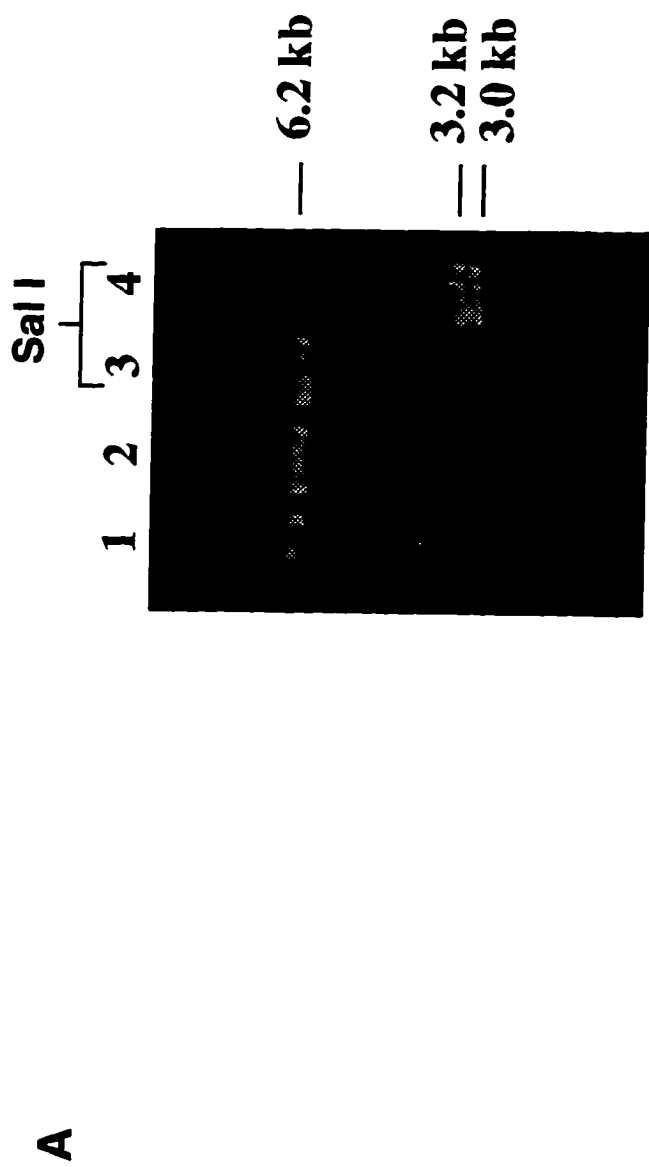
1. Construction and isolation of D1-R269G mutant

Using the conventional site-directed mutagenesis method (see Kunkel et al. 1987), R269 was mutated into a glycine on the pWT plasmid. While it is preferable to directly tag the introduced site directed mutation with a unique diagnostic restriction endonuclease

recognition sequence, this was not possible with the R269G mutant. Therefore, the silent mutation which introduced the diagnostic Sal I restriction endonuclease recognition site was created at residue V307. Fig. 2.1A shows the mutated plasmid was treated by Sal I producing 3.0 and 3.2 kb fragments (lane 4, lanes 1-3 are controls). The wild type plasmid and the one DNA containing the mutations was sequenced, the introduced mutations were confirmed on the mutant DNA (Fig. 2.1B).

The mutagenized plasmid DNA (pR269G/V301), along with another plasmid DNA p228 containing spectinomycin resistance gene, was transformed into wild type *C. reinhardtii* cells. Approximately 200 spectinomycin resistant colonies were obtained from the initial chloroplast DNA transformation attempt. This number corresponds to a chloroplast transformation frequency of 10^{-6} /cell. No spectinomycin resistant colonies were recovered from a mock (without DNA) transformation of *C. reinhardtii* cells. Forty of the spectinomycin resistant colonies were then screened for the presence of the R269G/V307 *psbA* mutation. DNA was amplified from a region of the *psbA* gene encoding the R269G and V307 silent mutations (Sal I recognition site) followed by digestion with the diagnostic restriction endonuclease Sal I. Figure 2.2 shows the pattern of DNA restriction fragments generated by digestion of the *psbA* PCR products with Sal I. PCR products containing the diagnostic Sal I site are cut into a 160 bp and a 100 bp fragment unlike wild type DNA. As indicated in the figure, most of the spectinomycin resistant colonies had a wild type Sal I restriction fragment pattern (i.e. undigested); however, two isolates (Lanes 2 and 9) contained both undigested DNA (wild type) and the 160 and 100 bp Sal I fragments diagnostic for the transforming *psbA* gene fragment. The presence of both the wild type and mutant DNA restriction patterns indicated that the cells were heteroplasmic for the R269G/V307 mutation. Segregation of the mutant and wild type genomes was subsequently achieved by streaking the heteroplasmic colonies (Fig. 2.2A, Lanes 2 and 9) to obtain single colony isolates. During cell division the mutant and wild type genomes segregate giving rise to homoplasmic colonies. Subsequent analysis (Sal I

Figure 2.1. Verification of mutations on mutagenized plasmid *psbA* DNA of *Chlamydomonas reinhardtii*. (A) An agarose gel was stained with ethidium bromide demonstrating the introduced V307 mutation that creates a new Sal I site. Lane 1, wild type pWT plasmid with Sal I treatment (6.2 kb); Lane 2, mutated pWT plasmid without Sal I treatment (6.2 kb); Lane 3, wild type pWT plasmid with Sal I treatment (6.2 kb); Lane 4, mutated pWT plasmid with Sal I treatment (3.2 kb and 3.0 kb). (B) (left) Autoradiogram of a sequencing gel demonstrating the introduced silent V307 mutation. The antisense strand sequence is shown, in which the valine antisense codon TAC is changed into glycine antisense codon GAC. (Right) Autoradiogram of a sequencing gel demonstrating the introduced R269G mutation. The sense strand sequence is shown, in which the arginine codon CGT is changed into glycine codon GGT.

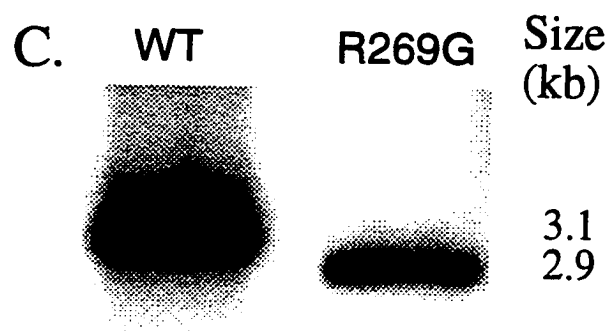


digestion of the *psbA* PCR product) of the PCR products from the secondary screen indicated that most colonies had > 95% mutant DNA (Fig. 2.2B). In order to confirm that the colonies were homoplasmic for the mutation, Southern blot analyses were carried out using Sal I digested chloroplast DNA (4 µg, or approx. 10^6 *psbA* copies). As shown in Figure 2C, one of the colonies obtained from the secondary screen had no apparent copies of the wild-type DNA, i.e. it was homoplasmic for the V307 mutation (Fig. 2.2C). DNA sequence analysis of the *psbA* gene from this isolate indicated that both the V307 and R269G mutations were present and that it was homoplasmic (data not shown). Furthermore, independent homoplasmic R269G transformants were also unable to grow photosynthetically indicating that it is unlikely that a second site mutation resulted in obligate heterotrophic growth.

2. D1 Protein stability in the D1-R269G mutant

After obtaining the homoplasmic mutant, it is important to determine whether the D1-R269G mutation affected the stability of the PSII complex. One measure of the stability of the PSII complex is the D1 protein content per unit chlorophyll (see Roffey et al. 1994a). Using western blots, the D1 content of cells, isolated thylakoids and PSII enriched particles from dark and continuous low light grown the wild type and R269G mutant cells were compared. Sub-saturating amounts of the D1 protein, i.e. samples with < 10 µg Chl/lane, were used for the western blot analysis in order to obtain a linear response from the antigen detection system. As shown in Figure 2.3 and Table 2.1, the D1 protein levels in R269G mutant cells were higher than wild type cells regardless of whether they were grown in the dark (13% > than wild type) or continuous low light (60% > wild type). It is noted that the D1 protein content of whole cells includes D1 protein present in intact as well as partially assembled PSII complexes (see Roffey et al. 1994a). In contrast to whole cells, the D1 protein content of thylakoids and PSII particles prepared from dark grown R269G cells was less than that of dark grown wild type. The D1 protein content of thylakoids and

Figure 2.2. Genetic verification of the R269G/V307 mutant in *Chlamydomonas reinhardtii*. Panel A shows the Sal I digested PCR products amplified from the *psbA* region spanning the V307 and R269G mutations. Lanes 1 -12 are Sal I digested PCR products obtained from separate spectinomycin resistant colonies. Mut and WT correspond to the Sal I digested PCR products amplified from plasmids pR269G/V307 and pWT respectively. Panel B shows the Sal I digested PCR products obtained from single colony isolates derived from colony 2. Panel C is a Southern blot analysis of chloroplast DNA isolated from colony 12 (panel B) digested with Sal I and probed with pWT. The smaller band migrating at 2.9 kb represents the expected size for the R269G/V307 mutant.



PSII particles isolated from dark grown R269G cells was 17% and 12% respectively, less than wild type (dark grown) membrane fractions (Fig. 2.3, Table 2.1). These results suggest that the D1 protein in the R269G membranes is less stable than in the membranes of wild type. The R269G D1 protein content was further reduced in mutant thylakoids relative to wild type when the cells were grown in continuous low light. The D1 protein content of thylakoids and PSII particles isolated from light grown R269G cells was 62% and 60% of the corresponding wild type fractions. These results suggest that the R269G mutant D1 protein is more susceptible to light-dependent (photoinhibitory) turnover than wild type. Interestingly, detergent treatments associated with preparation of R269G PSII particles did not decrease the R269G D1 protein relative to wild type PSII particles.

3. Inhibition to PSII electron transfer: steady state oxygen evolution and manganese determination

In order to determine what effects the R269G mutation had on photosynthetic electron transport, oxygen evolution was measured in the presence of various PSII (Q_B site) electron acceptors. As shown in Table 2.2, the D1-R269G mutant was unable to evolve oxygen regardless of the PSII acceptors used (DMBQ, DCBQ or PBQ). The absence of oxygen evolution could be due to inhibition anywhere between electron donation by water to electron acceptance by the artificial acceptors.

In order to determine if the inability to evolve oxygen was due to a donor side effect, the manganese content of the wild type and R269G PSII particles were measured. Since the R269G PSII complex was shown to be sensitive to photoinhibition, the cells were grown in the dark followed by a brief (20 min) exposure to low light to facilitate assembly of the water oxidizing complex with minimal photoinhibitory damage. Cells were also grown in complete darkness for comparison. As expected, the manganese content of PSII particles isolated from dark grown plus dim light exposed wild type cells was 4.2 Mn/250 Chl while the manganese content of totally dark grown wild type cells was < 1

Figure 2.3. Western blot analysis of the D1 protein levels in wild type and R269G cells, thylakoids and PSII particles isolated from cells grown in the dark or light. Lane 1, wild type; Lane 2, R269G. 10 µg of total chlorophyll was loaded for each lane.

Table 2.1. D1 protein content in D1-R269G and wild type cell and thylakoid membrane fractions isolated from dark or light grown cells. D1 protein levels are expressed as a percentage of wild type amount for each treatment and membrane fraction type. Values were determined by densitometry of western blots (Figure 2.3) and are the average of two measurements. The values varied by no more than 10% of the total.

Fraction	Low Light Grown	Dark Grown
	% wild type	
Whole Cells	160	113
Thylakoids	62	83
PSII Particles	60	88

Table 2.2. Photosynthetic oxygen evolution, photosystem II artificial donor oxidation and manganese content of isolated membrane fractions from dark and dark plus 20 min dim light grown cells. Values are the average of three separate measurements for electron transfer assays and two separate measurements for Mn determinations. See materials and Methods for details.

Strain	Growth Conditions	Oxygen Evolution ^a	<u>DCPIP Reduction</u> ^b		Mn/250 Chl ^c
			DPC (1 mM)	NH ₂ OH (5 mM)	
μmol/mg Chl/hr					
Wild Type	Plus Light*	265 ± 49	34 ± 4	43 ± 4	4.1± 0.2
Wild Type	Dark	ND	ND	ND	<1.0
D1-R269G	Plus Light	0	0	0	<1.0
D1-R269G	Dark	0	0	0	<1.0

^a DMBQ used as an acceptor with wild type thylakoids. Neither DCBQ, DMBQ or PBQ supported oxygen evolution in D1-R269G thylakoids.

^b Rates were determined with isolated thylakoids

^c Measurements were made with PSII particles.

ND, not determined

* Dark plus 20 min dim (12 μE/m²·s⁻¹) white light grown cells.

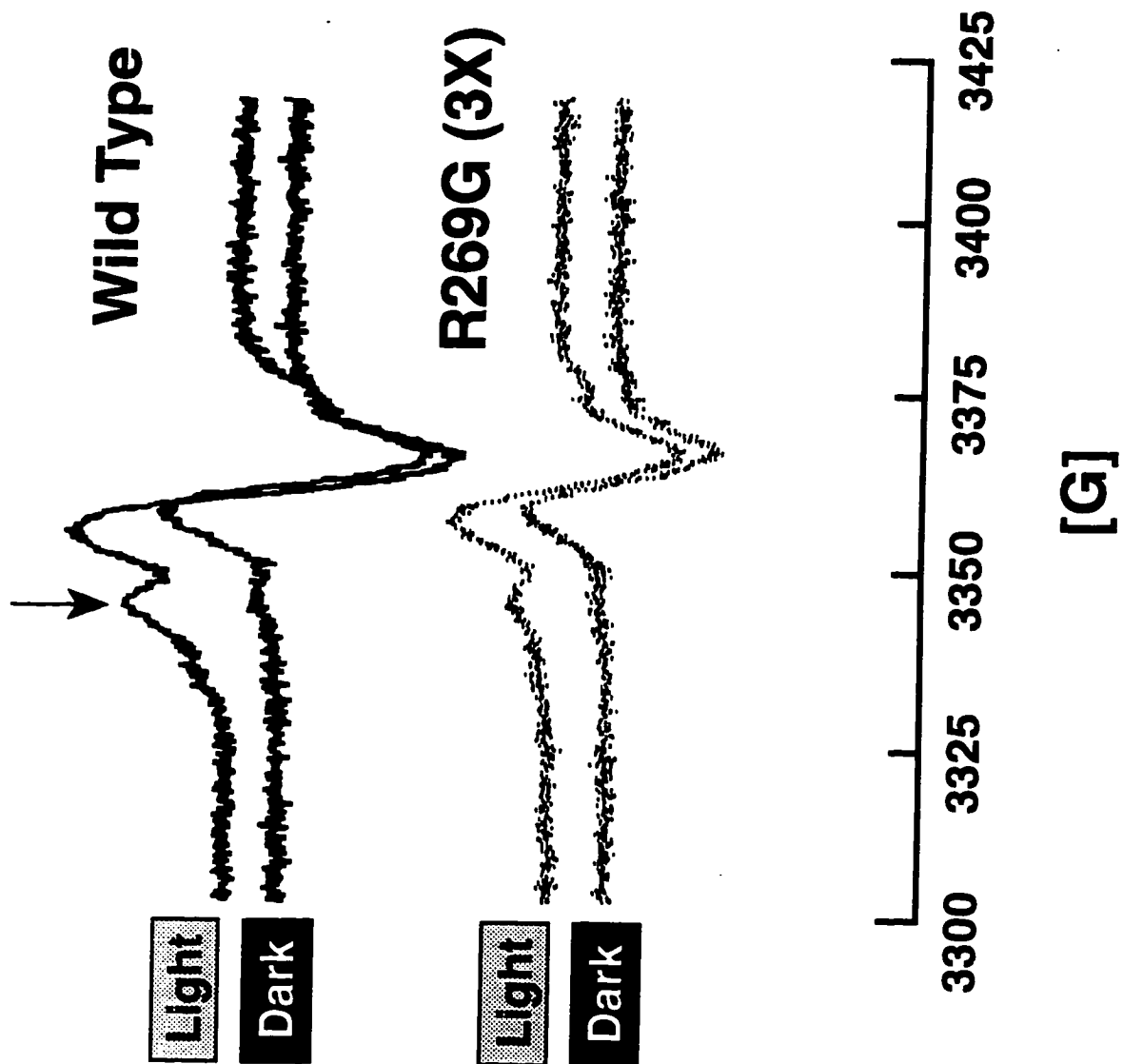
Mn/250 Chl (Table 2.2). The latter value is indicative of the light requirement for assembly of the functional manganese complex (Radmer and Cheniae 1977). In contrast to the dim light exposed wild type cells, the manganese content of dim light exposed R269G cells was < 1 Mn/250 Chl. These results indicate that the R269G mutant was unable to assemble or stabilize a tetra-manganese, water oxidizing complex.

The inability to form a manganese water oxidizing complex could be due to structural perturbations on the lumenal (donor) side of the complex or result from a disruption in electron transfer which would prevent photoligation of the manganese complex (Radmer and Cheniae 1977). One measure of the ability to transfer electrons in PSII is the light dependent reduction of DCPIP using artificial PSII electron donors which circumvent the water oxidizing complex (see Roffey et al. 1994a). As shown in Table 2.2, the R269G mutant was unable to reduce DCPIP using either DPC or hydroxylamine as a PSII donor. These results indicate several possible reasons for the lesion on the donor side as well as the acceptor side of PSII. Either the R269G mutant is unable to carry out a light dependent charge separation, unable to oxidize artificial donors, or unable to reduce DCPIP. As will be shown in a later section, a significant block in electron transfer from Q_A^- to Q_B (or Q_B^-) was also observed for the mutant. Thus a block on both the electron acceptor and donor sides of PSII has occurred as a consequence of the R269G mutation.

4. EPR analysis of PSII stable charge separation

In order to determine whether the R269G mutant could accumulate a stable charge separated state (Tyr_D^+/Q_A^-), the formation of the dark stable radical Tyr_D^+ was measured in PSII particles from dark grown cells. Due to its long half life, Tyr_D^+ accumulates in illuminated non-oxygen evolving PSII particles which are unable to oxidize water (Barry and Babcock, 1987). Tyr_Z signal amplitudes were not measured due to the sensitivity of Tyr_Z to photoinhibitory damage (Roffey et al. 1994b). As shown in Fig. 2.4, the extent of Tyr_D^+ accumulation in D1-R269G PSII particles (isolated from dark grown cells) was

Figure 2.4. Photo-accumulation of the TyrD^+ EPR signal in PSII particles isolated from dark grown, wild type (top) and R269G (bottom) cells. The symmetrical signal centered around $g = 2.0$ is attributed to contamination from P700 (28). The arrow indicates the location of the downfield hyperfine signal attributed to TyrD .



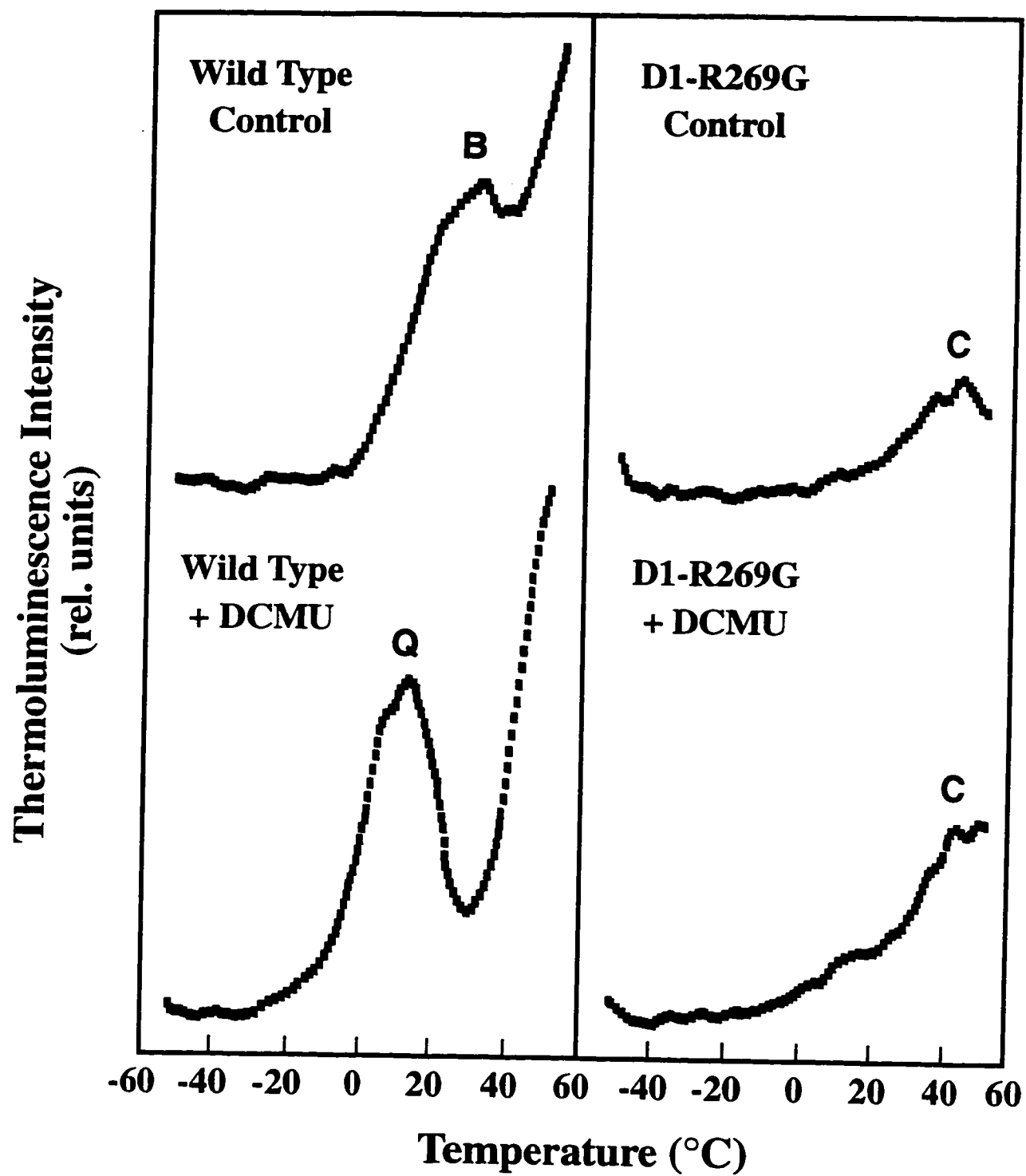
approximately one third that of wild type. These results indicate that at least some portion of the mutant reaction centers were capable of accumulating Tyr_D^+ , but not all. The inability to accumulate wild type levels of Tyr_D^+ could result from either: 1) a reduced ability to form the charge separated state $\text{P680}^+/\text{Q}_A^-$; 2) a reduced ability of P680^+ to oxidize Tyr_D ; or 3) an increased back reaction from $\text{Q}_A^- \rightarrow \text{P680}^+$.

5. Thermoluminescence

Since thermoluminescence (see Inoue, 1996; Vass and Govindjee 1996) measures the recombination of charges between S_2 and Q_A^- (the D or the Q band) and between S_2 (or S_3) and Q_B^- (the B band), it can be used to check if the mutant is blocked in the S-state transition.

Figure 2.5 shows that the wild type thylakoids have the normal B band (a broad band in the 30-35°C region). Upon treatment with DCMU (10 μM), the B band is abolished, and the Q band (a broad band at 15°C) appears due to inhibition of electron transfer from $\text{Q}_A \rightarrow \text{Q}_B$ enabling stabilization of Q_A^- . The mutant, however, lacks both the B and Q bands confirming that it is unable to store charges on the S-states. However, a difference thermoluminescence curve (for DCMU-treated minus untreated mutant thylakoids) showed a slight negative band in the B band region, and a slight positive band in the Q band region, but it was within the noise level of the measurements. A high temperature band that includes a "C" band, suggested to arise from recombination of Y_D^+ and Q_A^- (Johnson et al. 1994), is however, present. A good part of the high temperature band, observed here, was unrelated to photosynthesis (data not shown); but this does not affect the clear conclusions noted above. Thermoluminescence results confirm the defective nature of the mutant on the donor side of its PSII.

Figure 2.5. Thermoluminescence of wild type *C. reinhardtii* and D1-R269G mutant thylakoid ([Chl] is ~1 mg/ml) in the presence and absence of DCMU (10 μ M). The samples were measured after one saturating, single-turnover, flash at 25°C for control and 10°C for the DCMU treatment. The heating rate was 1°C/s. Data obtained by David Kramer.



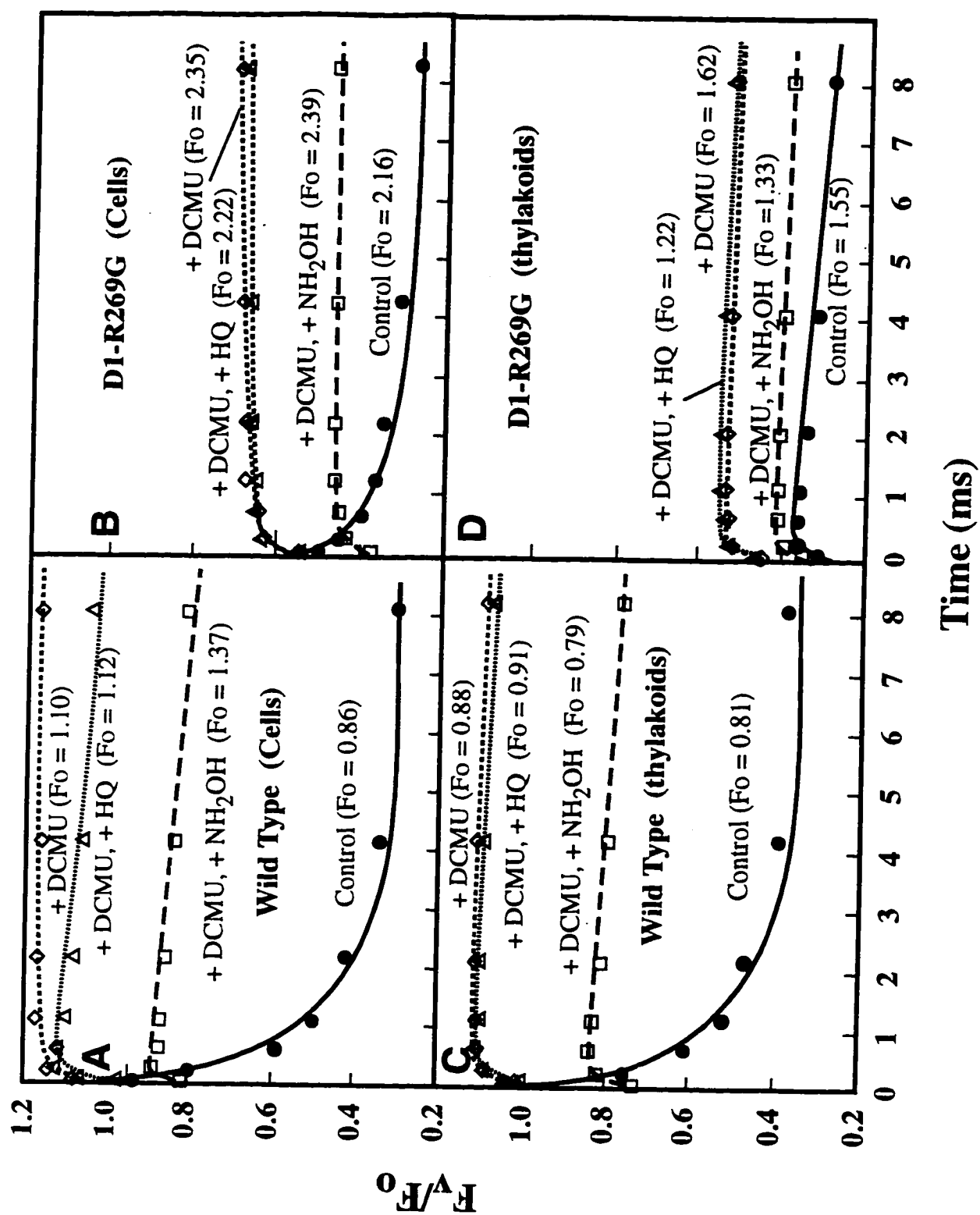
6. Inhibition to PSII electron transfer: Chl *a* changes after flashes

To locate the effect of the mutation on the electron transfer on the acceptor side of PSII, I measured Chl *a* fluorescence changes on the microsecond time scale after a series of single turnover flashes. The kinetics of these changes correspond mainly to the electron transfer from Q_A^- to Q_B or Q_B^- (see Eaton-Rye and Govindjee 1988a; b); however, the fluorescence yield at F_m and in the sub-ms range also include effects of changes in electron flow on the donor side of PSII, i.e. changes in $[P680^+]$, a quencher of Chl fluorescence (Butler 1972). A slowed equilibrium between $S_n \rightleftharpoons Z \rightleftharpoons P680$ results in lowering of F_m and a rise phase of fluorescence (see Kramer et al. 1990; Shinkarev and Govindjee 1993). Figure 2.6 shows Chl *a* fluorescence yield changes for the dark-grown, non-oxygen evolving cells and thylakoids in the presence and absence of DCMU (10 μ M) and of hydroxylamine (NH_2OH , 5 mM) and hydroquinone (5 mM), donors to $P680^+$.

I will first discuss the donor side effects. The mutant cells and thylakoids show (Figs. 2.6A with 2.6B) a significant reduction in the ratio F_v/F_o . Further, the mutant thylakoids have even lowered F_v/F_o level compared to not only the wild type thylakoids, but also the mutant cells. These results are related not only to the inactive PSII in the mutant, but to inhibitions on the donor side of PSII.

The addition of both 5 mM NH_2OH and 10 μ M DCMU is unable to restore the maximum level of F_v/F_o in the mutant sample (cells or thylakoids) to that of the wild type level. NH_2OH (5 mM) is usually expected to be an electron donor to $P680^+$. It should inhibit the normal donor side function and outcompete the charge recombination process from Q_A^- to $P680^+$ (see Metz et al. 1989; Roffey et al. 1994a). However, NH_2OH was shown to be a poor donor in D1-Y160 mutant (Metz et al. 1989) and, thus, lack of recovery of F_v/F_o cannot be taken to mean that there are no donor side effects. The addition of hydroquinone (5 mM), a better electron donor to $P680^+$, results in variable fluorescence level equivalent to the DCMU treatment without added donors. The consistent lower level

Figure 2.6. Flash-induced chlorophyll *a* fluorescence yield kinetics of the dark-grown wild type and the dark-grown D1-R269G mutant of *Chlamydomonas reinhardtii*, treated with or without DCMU (10 μ M), or with DCMU (10 μ M) and NH_2OH (5 mM), or with DCMU (10 μ M) and hydroquinone (HQ, 5 mM). The kinetic measurements were done with 5 μ g Chl/ml samples. Only the second-flash kinetic traces are shown. (A) Kinetics of fluorescence change from the wild type cells. (B) Kinetics of fluorescence change from the D1-R269G mutant cells. Data show a lowered yield of photochemistry (calculated from F_v/F_m) and a slowed rate of electron flow from QA^- to the plastoquinone pool in the mutant. (C) Kinetics of fluorescence change from the wild type thylakoids. (D) Kinetics of fluorescence change from the D1-R269G thylakoids. Note the slowed decay kinetics and the lowered F_v/F_m in the mutant samples suggesting an inhibition on the PSII acceptor side and the presence of high proportion of inactive PSII reaction centers. The addition of NH_2OH or hydroquinone is unable to restore the chlorophyll *a* fluorescence level in the mutant (cells or thylakoids) to the wild type level.



of variable fluorescence in the D1-R269G mutant indicates that the functional PSII_s may be much lower than that in the wild type.

I now discuss the acceptor side effects. The rate of decay kinetics of Chl *a* fluorescence is significantly slower in the mutant than in the wild type. The lifetime of the first component (τ_1) in the first flash which is indicative of the rate of Q_A^- to Q_B transfer is 90 μ s in the wild type cells versus 1.6 ms in the mutant; τ_1 of the second flash is 120 μ s in the wild type versus 2.0 ms in the mutant. Thus, there is ~17 fold decrease in the rate constant of electron transfer from Q_A^- to the plastoquinone pool. The decay rate for the mutant thylakoid samples was even slower (~50 fold) compared to that of the wild type, consistent with other lines of evidence that the mutant PSII has much less structural stability in the thylakoid preparations (Figs. 2.6C and 2.6D). The addition of high concentration (10 μ M) of DCMU inhibits the electron transfer in both the wild type and the mutant cells and thylakoids.

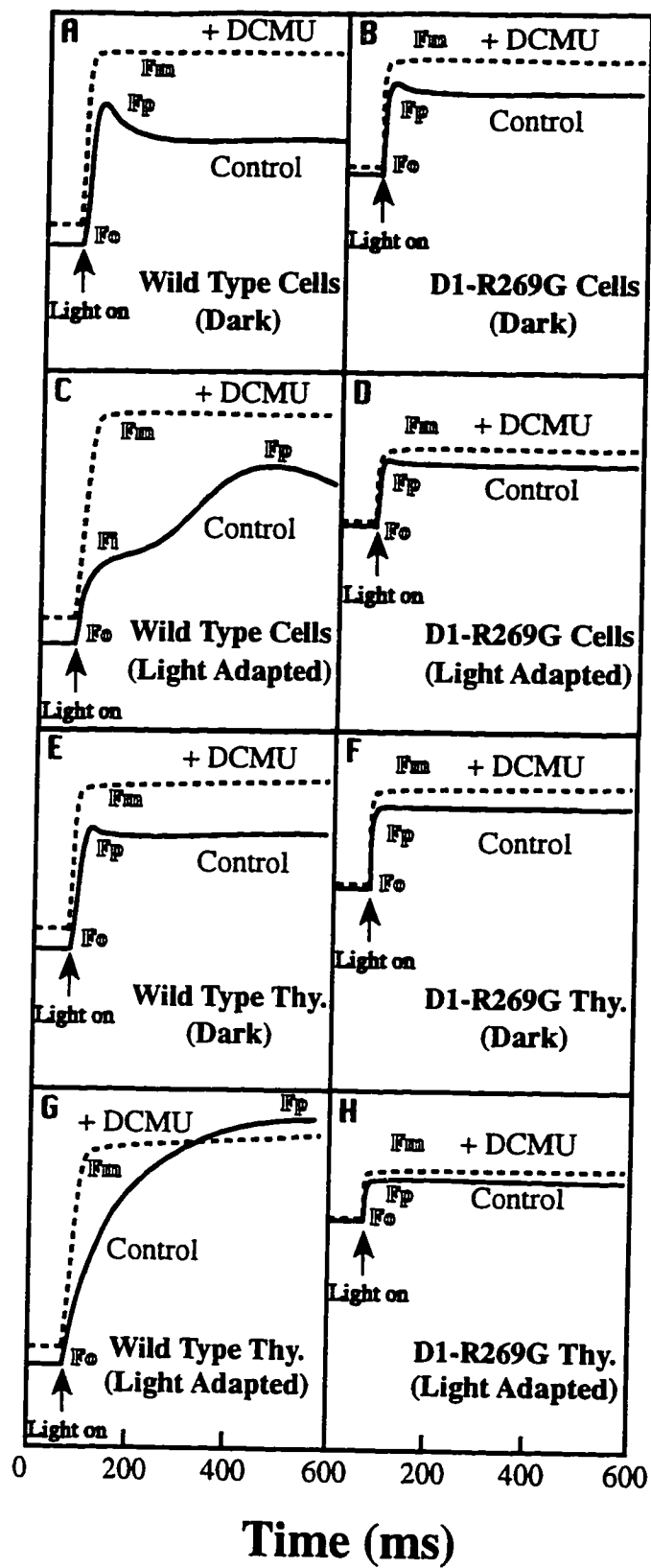
In addition to the slowing of the electron transfer from Q_A^- to the plastoquinone pool, Fig. 2.6 also shows dramatically increased measured F_0 in the mutant cells and thylakoids relative to the wild type, the cause for this will be discussed in a later section.

7. Chlorophyll a fluorescence induction

To obtain information on the electron transfer reactions on the PSII acceptor side in D1-R269G mutant, chlorophyll fluorescence induction (up to 0.6 s) (see Papageorgiou 1975; Briantais et al. 1986) was measured in the dark-grown wild type and mutant cells and thylakoids with a pulse-modulated fluorometer. The induction kinetics of Chl *a* fluorescence of these samples were measured in the absence and the presence of the herbicide DCMU, known to block electron flow by displacing Q_B and are shown in Fig. 2.7. Figures. 2.7A and 2.7B show the fluorescence induction kinetics of the dark-grown cells. The rise kinetics of the fluorescence reflects the net balance between the rate of reduction of Q_A and reoxidation of Q_A^- , whereas the area over the curve reflects the size of

Figure 2.7. Chlorophyll *a* fluorescence transients (as a function of time of illumination) of the dark-grown *Chlamydomonas reinhardtii* wild type and D1-R269G in the absence and the presence of 10 μM DCMU measured with a PAM-2000 fluorometer. The full scale is 200 mv. (A) The transient of the wild type cells. (B) The transient of the mutant cells. (C) The transient of the light-adapted wild type cells (treated with 70 $\mu\text{E}/\text{cm}^2\text{s}$ white light for 1 hr). Note the transformation of the kinetics from the dark phase to the light phase indicated by the shift of F_p . (D) The transient of the light-treated (70 $\mu\text{E}/\text{m}^2\text{s}$) mutant cells. Note the absence of the kinetic transformation and a more elevated F_0 and a decreased F_v , suggesting a possible photo-damage to the mutant PSII. (E) The transient of the wild type thylakoid isolated from the dark-grown cells. (F) The transient of the mutant thylakoid isolated from the dark-grown cells. (G) The transient of the wild type thylakoids isolated from the light-adapted cells. Note the F_v is basically unchanged compared with the cells. (H) The transient of the mutant thylakoids isolated from the light-adapted cells. Note the even lowered F_v in this sample. In all measurements, the [Chl] of the samples is 5 $\mu\text{g}/\text{ml}$, and the actinic illumination is 470 $\mu\text{E}/\text{m}^2\text{s}$.

Chlorophyll Fluorescence (rel. units)



the plastoquinone pool present. The addition of DCMU blocks the electron transfer beyond Q_A , and thus Chl a fluorescence rapidly reaches the maximum level (F_m). The difference between F_m and the minimal fluorescence level, F_0 , is the maximal variable fluorescence (F_v) which is related to photochemistry of PSII (Φ_p) as follows: $\Phi_p \equiv \frac{F_m - F_0}{F_m} = \frac{F_v}{F_m}$ (see review in Govindjee 1995). Figures. 2.7A and 2.7B show the results of dark-grown wild type and D1-R269G cells. Since F_m is approximately the same in the two cases, a 50% reduction in F_v means that the mutant has lowered photochemistry. If this is assumed to reflect charge separation in PSII ($Z\ P680^* Q_A \rightarrow Z^+ P680 Q_A^-$), then it can be concluded that the mutant has lowered yield of charge separation. This conclusion is totally dependent upon the measured F_0 being true F_0 , as is shown later in Fig. 2.7. The simplest interpretation is that the D1-R269G mutant has decreased number of active PSII/Chl. The shape of the transient in both the wild type and the mutant shows that dark-adapted cells are not normal, as is well known (see, e.g., Cheniae and Martin 1973): the water oxidation machinery is not functional and one observes, perhaps, only one turnover of PSII following slow oxidation of Q_A^- .

Figures. 2.7C and 2.7D show the Chl a fluorescence induction transient of light adapted cells (dark grown cells exposed to 1 hr of $70\ \mu\text{E}/\text{m}^2\cdot\text{s}$ white light). The light treatment causes the wild type kinetics to display a slower rise phase and a normal fluorescence transient (see Strasser et al. 1995). F_p is shifted to a longer time (400 ms versus 25 ms after actinic light illumination) since both the donor and acceptor sides of PSII are now functional: the F_0 to F_p rise now reflects the filling up of the plastoquinone pool with electrons from the donor side of PSII. This phenomenon of photoadaptation which is a slower rise of transient kinetic curve to F_p due to the recovery of the PSII donor side was observed in *C. reinhardtii* by Guenther et al. (1990). However, this transition is not observed in the R269G mutant, indicating that the mutation has inhibited the necessary photoadaptation process. It was shown earlier that the Mn centers for the donor side functions are missing in the mutant. Further, after a light treatment, the F_v of the mutant

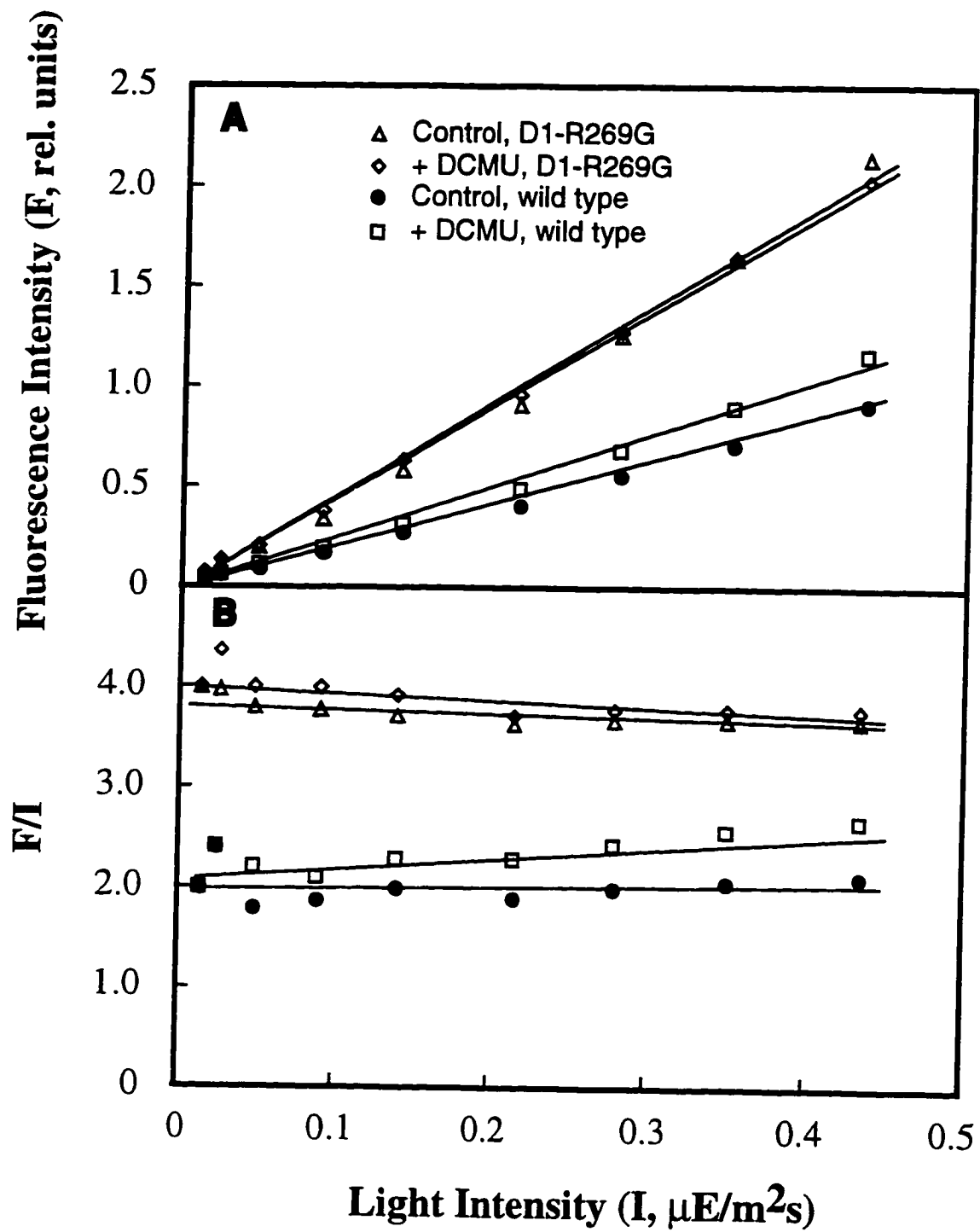
cells becomes further reduced (only 35% of that of the wild type), and F_v/F_m reflecting photochemistry is reduced by 60%. This significant lowering of the F_v after light treatment indicates an increased susceptibility of the mutant PSII to photoinhibition, confirming conclusions on the D1 stability presented earlier.

Figures. 2.7E and 2.7F are the fluorescence transient of the thylakoids isolated from the dark-grown cells. The F_v of the mutant thylakoids is ~60% of the wild type level. After the light treatment of the cells, the F_v of the isolated mutant thylakoids is reduced to only ~20% of the wild type level (Figs. 2.7G and 2.7H), indicating that the combination of the steps involved in biochemical preparations and the light treatment may cause further lesions to the mutant PSII. Fluorescence transient in wild type cells now displays a normal sigmoidal rise due to filling up of the plastoquinone pool.

8. F_o

D1-R269G mutant samples have a consistently elevated F_o compared to that of the wild type. As F_o is the minimal level of chlorophyll fluorescence originating from antenna, in competition with energy transfer to the PSII reaction center, an increase in F_o may indicate a decreased excitation energy transfer to the active PSII reaction center, possibly due to the disconnection between antennae and the reaction center II. A second possibility is the existence of inactive PSII (Lavergne and Briantais 1996) incompetent in trapping excitons arriving from antennae, which then can return to antennae and fluoresce. A third possibility is an increase in the absorption cross section of the antennae/PSII reaction (see, e.g., Munday and Govindjee 1969; Eaton-Rye and Govindjee 1988b). The data do not allow me to distinguish between these possibilities. However, as shown in Fig. 2.8, the wild type (cells or thylakoids) displays a small increase of F_o when measured in the presence of DCMU which blocks the electron transfer beyond Q_A^- ; this may indicate that the measured F_o level may not be true F_o . This slight increase in measured F_o in the presence of DCMU is thought to be due to the small actinic effect of the measuring beam of

Figure 2.8. Measurements of minimal (baseline) fluorescence F_0 at low light intensities. (A) Baseline chlorophyll *a* fluorescence (F_0), as a function of light intensities in the low intensity of range, in the presence and the absence of 10 μ M DCMU. Measurements of the heterotrophically grown wild type and D1-R269G mutant cells were made as in Materials and Methods. (B) The quantum yield of F_0 , or the ratio of fluorescence to the light intensity of the measuring beam, basically does not change with the light intensities indicating that the measured F_0 is the true F_0 . It is further confirmed by the absence of any significant effect of DCMU.



the fluorometer. This effect may be especially prominent when the process of Q_A reoxidation is blocked. As is shown in a later section, the Q_B binding niche of the mutant PSII is drastically modified, blocking the electron transfer from Q_A to the plastoquinone pool. Thus, the measured F_0 required further investigation according to the rationale given under Materials and Methods.

Independent measurement of F_0 for the wild type and mutant cells at very low light intensities of the measuring beam indicate that F_0 intensity is a linear function of light intensities (I) (Fig. 2.8A). The quantum yield (F_0/I) remains constant as it should for true F_0 which should be independent of photochemistry (Fig. 2.8B). Further, addition of DCMU did not cause significant increases in the measured F_0 levels, as it should since all $[Q_A]$ remains essentially unchanged. Mutant F_0 was consistently double that in the wild type (~200%). Thus, F_0 of the mutant is indeed higher than the wild type, and F_v is, therefore, indeed reduced in the mutant.

9. Functioning of the two-electron gate

PSII variable Chl *a* fluorescence is controlled by the redox state of the primary plastoquinone, Q_A , a one electron carrier, which is oxidized by Q_B (or Q_B^-), a two electron carrier ("the two electron gate", see Velthuys and Ames, 1974; Bouges-Bocquet 1973). As the electron flow from Q_A^- to Q_B is faster than Q_A^- to Q_B^- , it is reflected in a period two oscillation pattern in the Chl *a* fluorescence decays (see Bowes and Crofts 1980). To test the functioning of the two electron gate in the mutant, I pretreated the dark-grown wild type and the D1-R269G cells with *p*-benzoquinone (100 μ M) and NH_2OH (5 mM), and illuminated the samples with a series of single turnover flashes. In this assay, the flash frequency was 0.67 Hz, and the variable fluorescence values at 200 μ s are shown. NH_2OH was added to eliminate most of the period 4 oscillations due to the donor side activities and to serve as an electron donor since the mutant cells were unable to oxidize water (see above). An obvious binary oscillation pattern of the chlorophyll variable

fluorescence is observed for the wild type (Fig. 2.9). In the mutant sample, however, this typical period two oscillation pattern was eliminated suggesting a defective two-electron gate mechanism caused by the mutation. The data indicate that the PSII acceptor side reactions are drastically modified due to the R269G mutation.

10. Bicarbonate depletion and recovery

Since the initial hypothesis is that D1-R269 may be involved in bicarbonate binding, I also determined the effect of bicarbonate-reversible formate inhibition on the Q_A^- to Q_B (or Q_B^-) electron transfer in PSII. Flash-induced Chl fluorescence decay kinetics of the dark-grown wild type and the D1-R269G cells with or without formate or formate plus bicarbonate after the second flash are shown in Fig. 2.10. Similar kinetic traces for the decay after the first flash is not shown. In view of the fact that in intact cells, ratio of Q_B to Q_B^- in darkness is close to 1 (Xu et al. 1990), Q_A^- to Q_B and Q_A^- to Q_B^- reactions are not easily separable. The addition of a sub-optimal concentration of formate (25 mM, pH 6.5) significantly slows down the electron flow from Q_A^- to Q_B (or Q_B^-) in the wild type sample. The kinetics of Q_A^- to the Q_B^- is shown in Fig. 2.10A. The formate inhibition is fully reversed by the addition of bicarbonate (10 mM). The Q_A^- to Q_B (or Q_B^-) reaction in the mutant samples also appear to be inhibited by the presence of formate. Addition of bicarbonate readily reverses this effect (Fig. 2.10B). It is now established that formate has additional significant effects on the donor side (El-Shintinawy and Govindjee 1990; Klimov et al. 1995; Wincencjusz et al. 1996); the insets in Fig. 2.10 show that formate causes decrease in F_v/F_o at $< 250 \mu s$ before an increase can be observed. This confirms the dual effect of bicarbonate-reversible formate effect in thylakoids of both wild type and D1-R269G cells.

A more quantitative assay of the formate inhibition and bicarbonate recovery for both the wild type and the mutant samples is shown in Fig. 2.11. The dark-grown cells were treated with various concentrations of formate in the absence or presence of

Figure 2.9. Flash oscillation pattern for the variable chlorophyll *a* fluorescence of the dark-grown wild type and D1-R269G cells of *Chlamydomonas reinhardtii* measured at 200 μ s after an actinic flash. The samples were treated with *p*-benzoquinone (100 μ M) to convert Q_B^- to Q_B , and NH_2OH (5 mM) to block S-state transitions, if any, prior to measurement. The [Chl] of the samples is 5 μ g/ml, the flash frequency during the measurement was 0.67 Hz. The data indicate a loss of the period two oscillation pattern in the mutant.

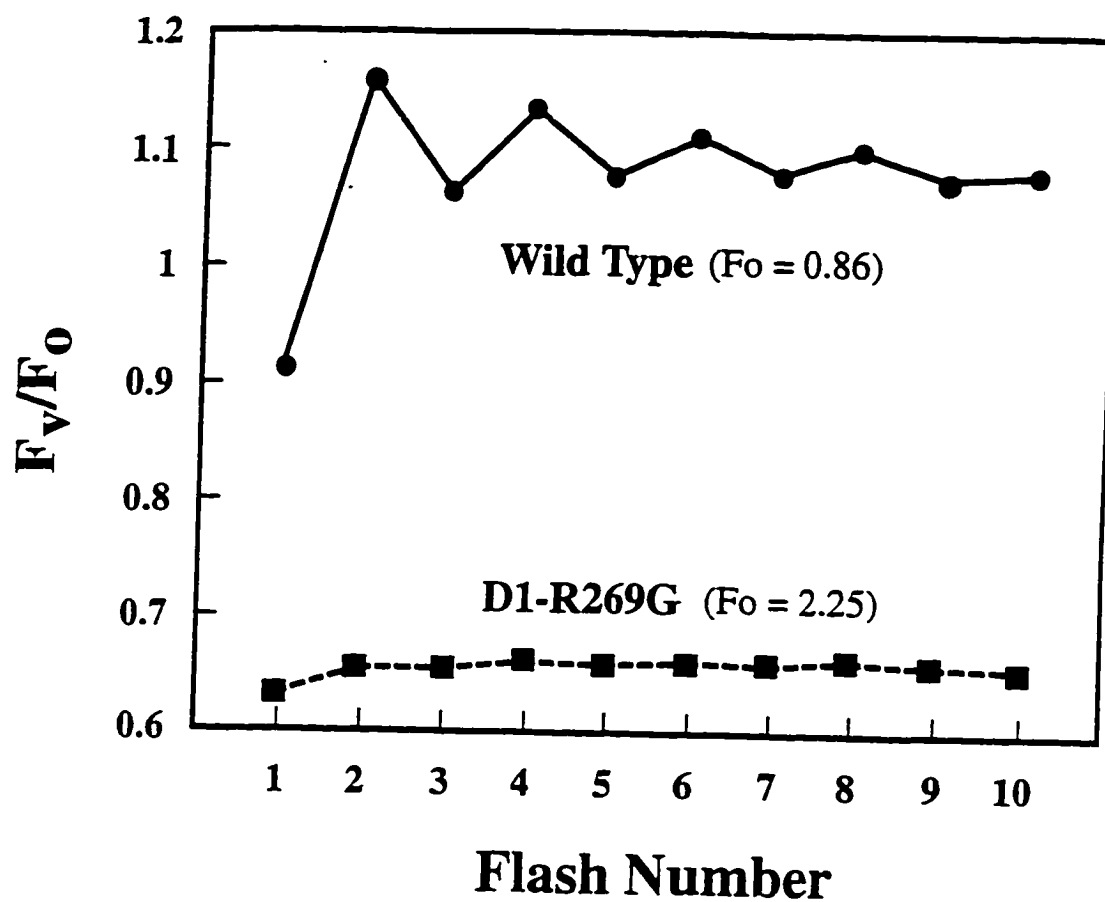


Figure 2.10. Flash-induced chlorophyll *a* fluorescence decay kinetics of the dark-grown *Chlamydomonas reinhardtii* wild type (A) and the D1-R269G (B) cells treated with (□) or without (●) sodium formate (25 mM, pH 6.5) and with a subsequent addition of sodium bicarbonate (10 mM) (◇). Insets show data plotted on an expanded time scale up to 2 ms. Formate treatment was according to El-Shintinawy et al. (1990). Kinetic measurements were done with 5 µg Chl/ml samples. Only the second flash kinetic traces are shown.

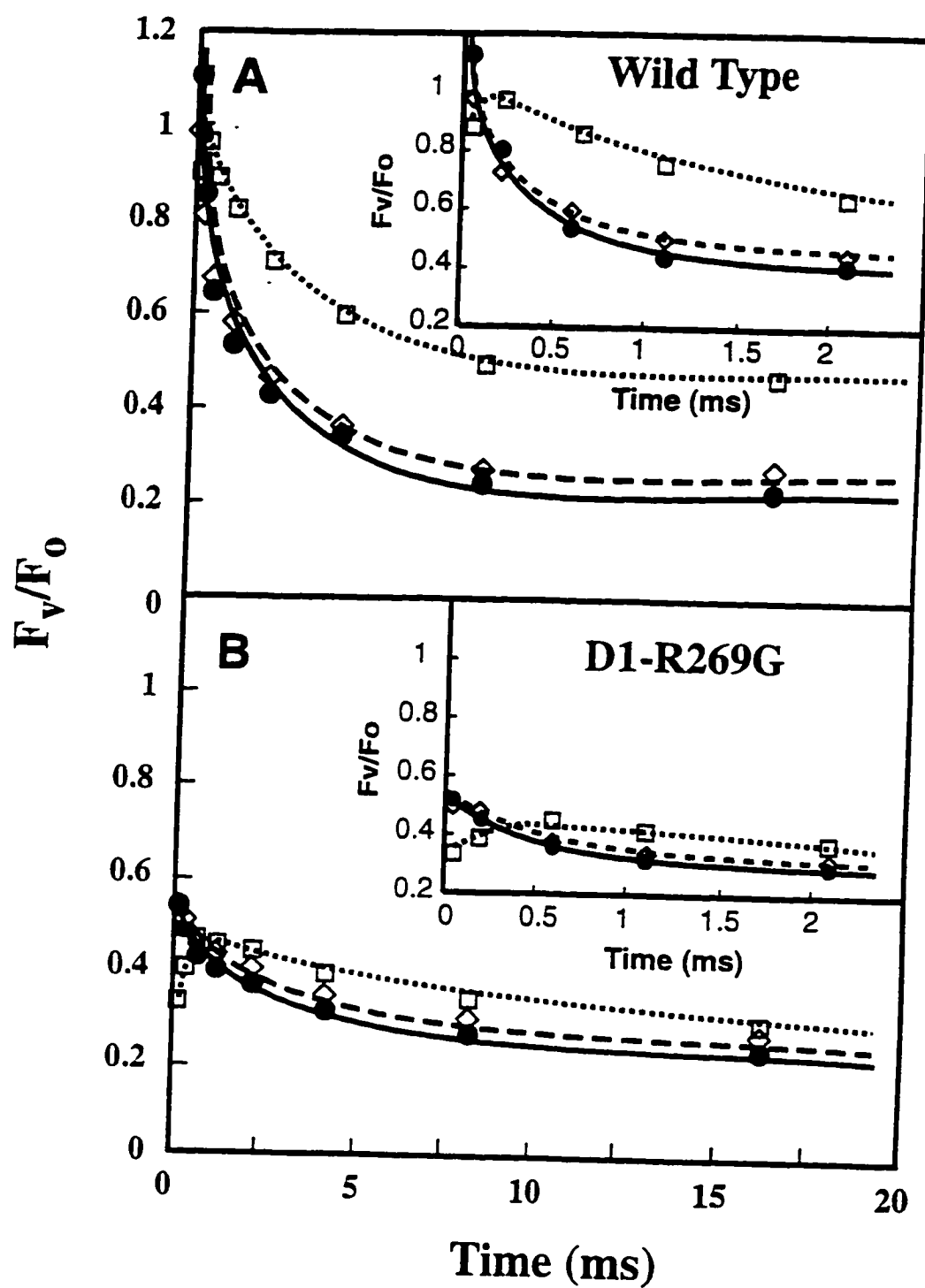
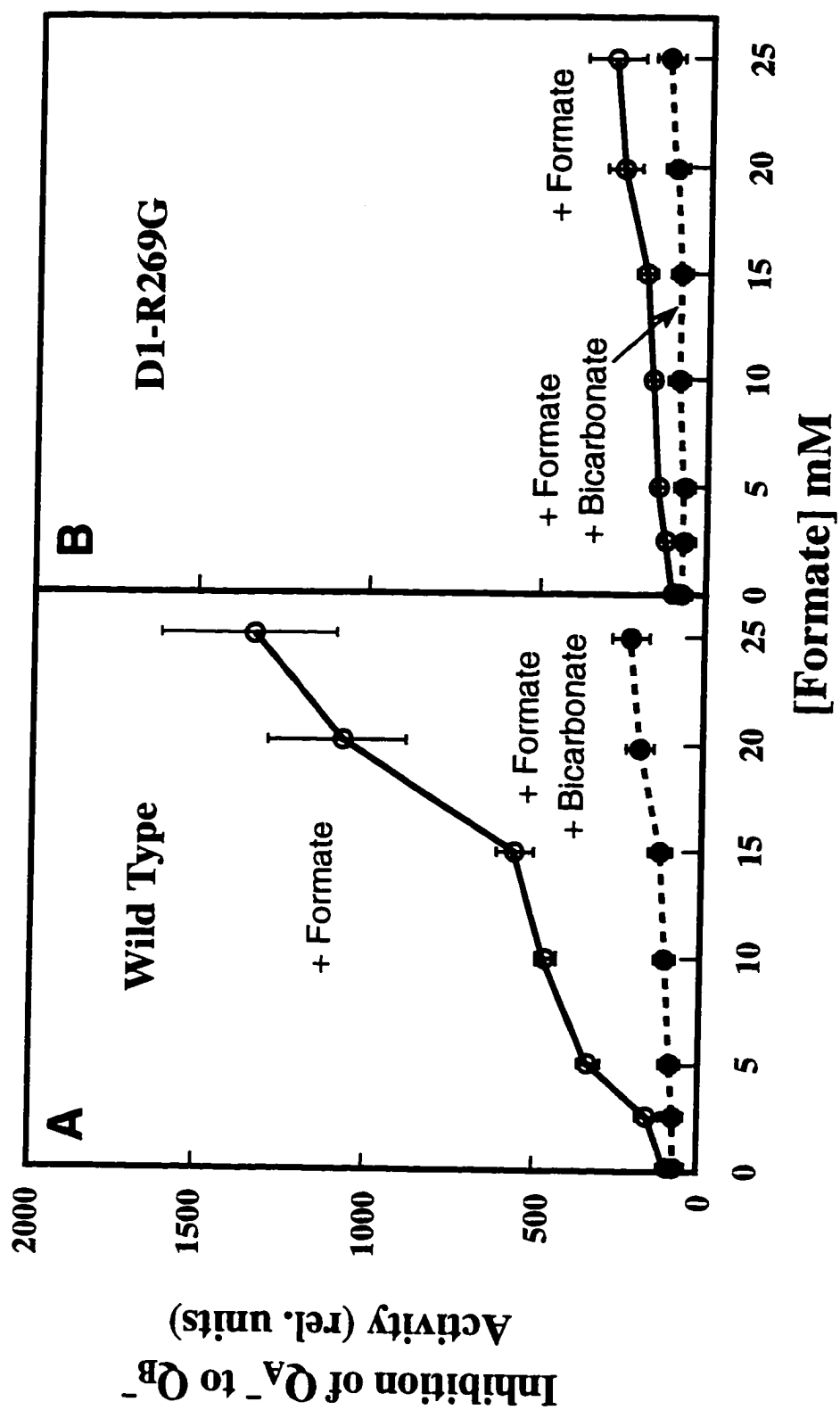


Figure 2.1.1. Effect of bicarbonate depletion and recovery of the wild type and the mutant. (A) Dark-grown *Chlamydomonas reinhardtii* wild type cells treated with various concentrations of formate (pH 6.5) in the absence or the presence of bicarbonate (10 mM) and assayed for fluorescence decay after the second actinic flash. Formate treatment and bicarbonate recovery was according to El-Shintinawy et al. (1990). The resulting Chl fluorescence decay curves were deconvoluted into three exponential components. The life time of the first component (τ_1) of the decay curve after the second flash, corresponding to the kinetics of QA^- to QB^- , is depicted as a function of formate concentrations when the τ_1 of the control is assumed to be 100. (B) The same treatment and analysis for the D1-R269G mutant. The mutant is shown to be ~5 times less sensitive to formate inhibition than the wild type.



bicarbonate and assayed for Chl *a* fluorescence decay as above. The resulting decay curves were deconvoluted with three exponential components (see Crofts et al. 1993; Govindjee et al. 1996). The fast decay component represents the kinetics of Q_A^- to Q_B (or Q_B^-) electron transfer. Thus, I plotted the normalized lifetime of the first component (τ_1) as a function of formate concentration with the τ_1 of the control (without formate treatment) as 100 in arbitrary units. For the second flash, the τ_1 of the wild type in the control is 120 μ s and that of the mutant is 2.0 ms. As shown in Fig. 2.10, at increasing formate concentrations, the τ_1 of the wild type increases up to 1.6 ms at the highest concentration (25 mM) corresponding to an ~13 fold increase. A similar increase for the first flash τ_1 was observed (data not shown). However, τ_1 of mutant sample only increases from 2.0 ms (control) to 5.5 ms (25 mM formate) corresponding to an ~2.5 fold increase. The addition of bicarbonate is able to fully recover the inhibition for both the mutant and the wild type. Thus, there is a 5 fold difference in the sensitivity to formate suggesting that D1-R269 must play some role in the binding niche of bicarbonate. However, it is noted that since the maximum τ_1 for the wild type cells in 25 mM formate treatment is 1.6 ms, whereas the τ_1 of the mutant without formate treatment is 2.0 ms, it may be possible that any formate effect may be obscured by the intrinsic effect of the mutation on τ_1 .

11. EPR analysis of the fine structure of the coordination of the non-heme iron

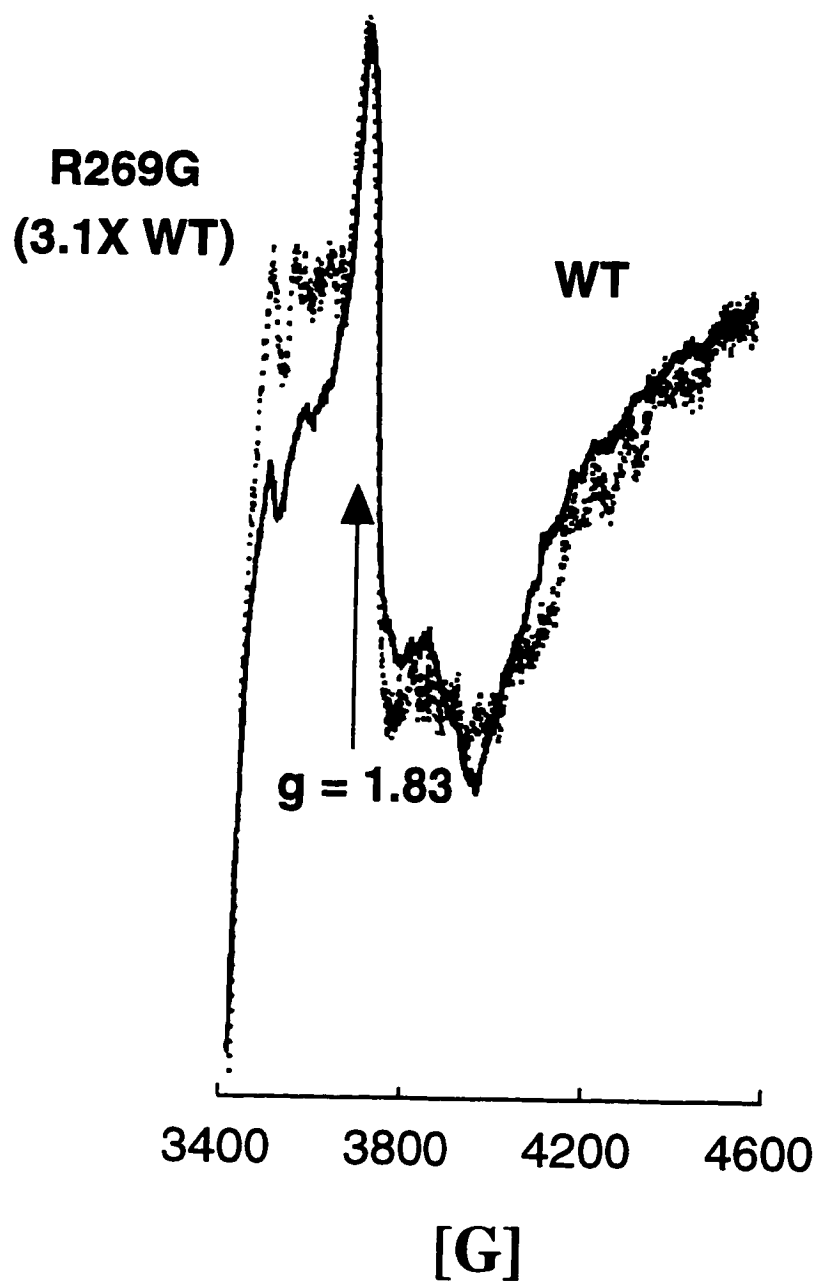
In order to further probe the effect of the mutation on bicarbonate binding, the accumulation and hyperfine structure of the formate enhanced Q_A^- Fe⁺² EPR signal at $g = 1.82$ which is a probe of the bicarbonate-Fe ligand (Vermaas and Rutherford 1984; Petrouleas and Diner 1990; Petrouleas et al. 1994) was measured. This signal can be trapped during illumination at 77 K and is greatly enhanced by formate pre-treatment. The formate enhancement is due to the displacement of bicarbonate from its binding site which inhibits Q_A^- to Q_B (or Q_B^-) electron transfer. In addition to the extent of formation of the Q_A^- Fe⁺² signal, information on the coordination environment of the non-heme iron can be

obtained from the g value and the line width of the $Q_A^- Fe^{+2}$ EPR signal. As shown in Figure 2.12, wild type PSII particles exhibit a typical formate (100 mM) enhanced $Q_A^- Fe^{+2}$ EPR signal at $g = 1.82$. Similarly, a $Q_A^- Fe^{+2}$ EPR signal was generated from illuminated R269G PSII particles; however, the yield of the signal was reduced by 68% relative to wild type. In fact, in the absence of formate it was not possible to detect the $Q_A^- Fe^{+2}$ EPR signal (unlike wild type) in R269G PSII particles. These results suggest that the bicarbonate-iron coordination is significantly perturbed by the mutation. However, it is noted that the line shape and g value of the $Q_A^- Fe^{+2}$ EPR signal were similar to wild type suggesting the existence of the bicarbonate binding at the non-heme iron. Furthermore, the formate enhanced $Q_A^- Fe^{+2}$ EPR signal is reduced to the same extent as the Tyr_D^+ signal, supporting the above notion that the perturbation of the bicarbonate/formate binding at the non-heme iron is due to an indirect cause.

12. Low temperature fluorescence emission spectra

Based on the above measurements that indicate a significantly lowered quantum yield of photochemistry (indicating a lowered yield of stable charge separation) and elevated F_0 (indicating a lowered net excitation energy transfer from antennae to the PSII reaction center), it is reasonable to conclude that the D1-R269G mutation has altered the structure and function of the PSII complex. This conclusion is fully consistent with the above EPR measurement on Tyr_D^+ and $Q_A^- Fe^{+2}$. To investigate possible physical changes in the PSII complexes, low temperature (77 K) fluorescence emission spectra was used as an indirect means to probe the state of PSII. At 77 K, PSII has two distinct emission bands at 685 nm (F685) and 695 nm (F695). F685 is thought to originate mostly from the CP43 polypeptide and F695 from CP47 polypeptide (see Nakatani et al. 1984; Govindjee and Satoh 1986; Dekker et al. 1995). Haag et al. (1993) suggest that the intensity of these two bands, especially F695, correlates well with the level of the PSII core proteins and can be used as an indicator for the concentration of PSII. Thus, whether there are inactive or active

Figure 2.12. The formate enhanced $Q_A^- Fe^{+2}$ EPR signal in PSII particles isolated from dark grown wild type and R269G cells. Solid line, wild type; dotted line, R269G mutant.



PSII reaction centers would influence the F685 and F695 fluorescence intensities. However, I also realize that the intensities of F685 and F695 must also be influenced by the efficiency of excitation energy transfer from peripheral antenna chlorophylls to core antennae and from the core antennae to the PSII reaction center.

The fluorescence emission spectra of the wild type and mutant cells and thylakoids were measured upon excitation by 435 nm light (absorption mainly by Chl *a*). The intensities of the emission bands of the obtained spectra (Fig. 2.13) were further deconvoluted into three individual peaks (data not shown) for F685, F695, and F716 (for PSI). Assuming that no changes occur in PSI, analysis shows that both F685 and F695 bands of the mutant cells and thylakoids show a reduction of 20-30% compared to the wild type. However, the F695 band appears to be reduced to a slightly greater extent than F685. The ratio of F695/F685 in the mutant cells was reduced by 36%, and in the mutant thylakoids by 22% compared to the wild type. This result may indicate a differential reduction in these PSII antenna complexes *provided* the mutation had not caused changes in excitation energy transfer among these complexes and the PSII reaction center. Since it was assumed that there were no changes in the CP43 and CP47 genes, this reduction could be partly attributed to the changes in the assembly or stability of the D1/D2 complexes to which the antenna proteins are associated, and partly to the changes in the excitation energy transfer to and away from the PSII reaction center.

13. Herbicide binding assay

To test possible structural changes in the Q_B binding niche caused by the R269G mutation, a radioactive herbicide binding assay was performed. The herbicide ¹⁴C-terbutryn binding was measured with the thylakoids of the wild type and D1-R269G according to Vermaas et al. (1990). A double reciprocal plot for the ¹⁴C-terbutryn binding is shown in Fig. 2.14. The data indicate that the mutant thylakoids have a significantly lowered ¹⁴C-terbutryn binding affinity compared to the wild type. The binding constants

Figure 2.13. (A) The 77 K chlorophyll *a* fluorescence emission spectra of the cells of the dark-grown *Chlamydomonas reinhardtii* wild type and the D1-R269G mutant. The emission spectra of the samples (30 µg Chl/ml with 20% glycerol) were measured with a front-surface optics with an excitation at 435 nm and were corrected for the wavelength dependence of the sensitivity of the photodetector and normalized to the 715-nm peak. (B) The 77 K chlorophyll *a* fluorescence emission spectrum of the thylakoids (pH 7.0) of the dark-grown *Chlamydomonas reinhardtii* wild type and the D1-R269G mutant. The measurements were made just as in (A) above. Both F685 (from CP43) and F695 (from CP47) bands were lowered in the mutant with respect to F715 band. Further, data indicate a differential reduction of these two emission peaks for the D1-R269G mutant cells and thylakoids.

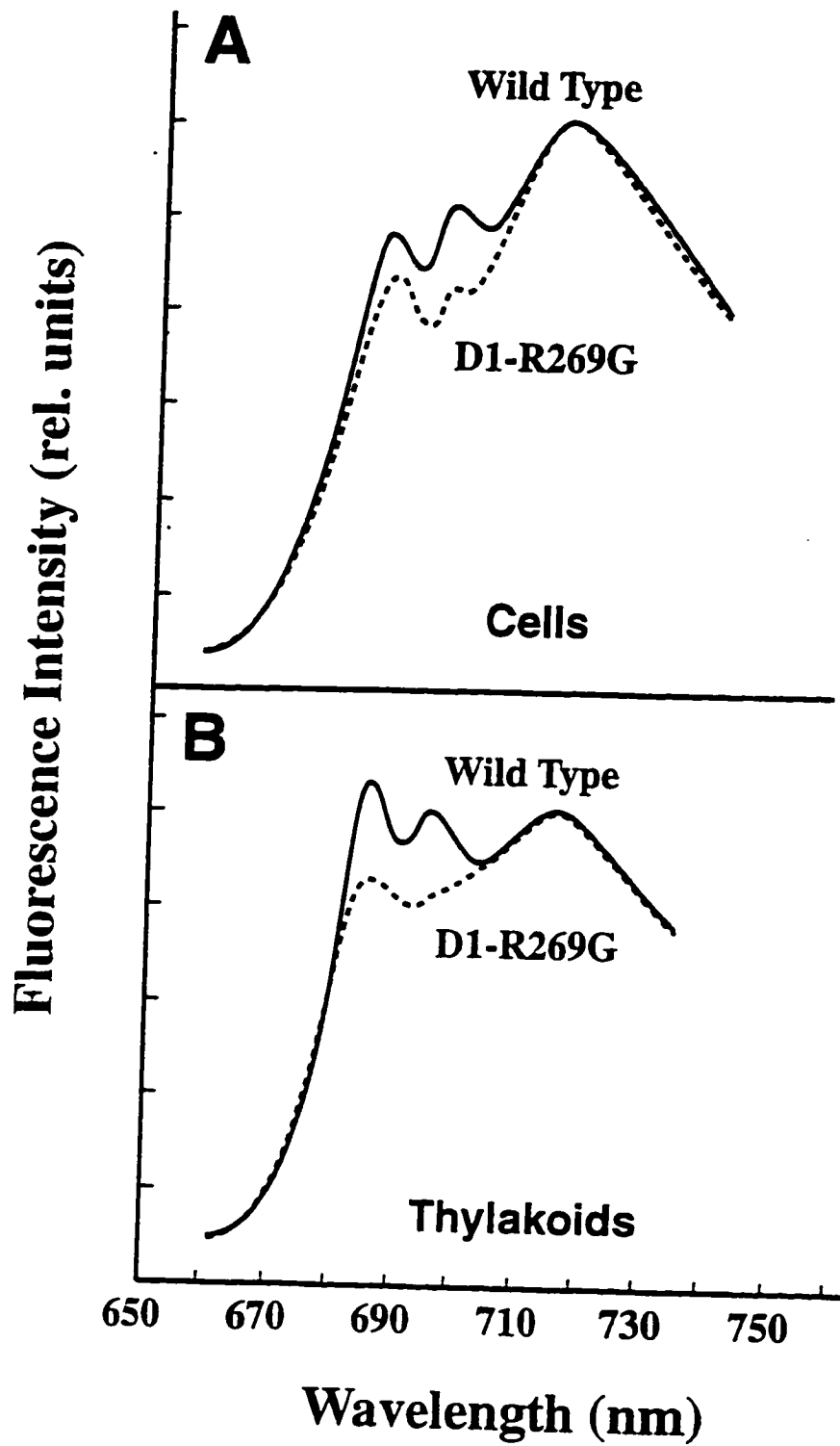
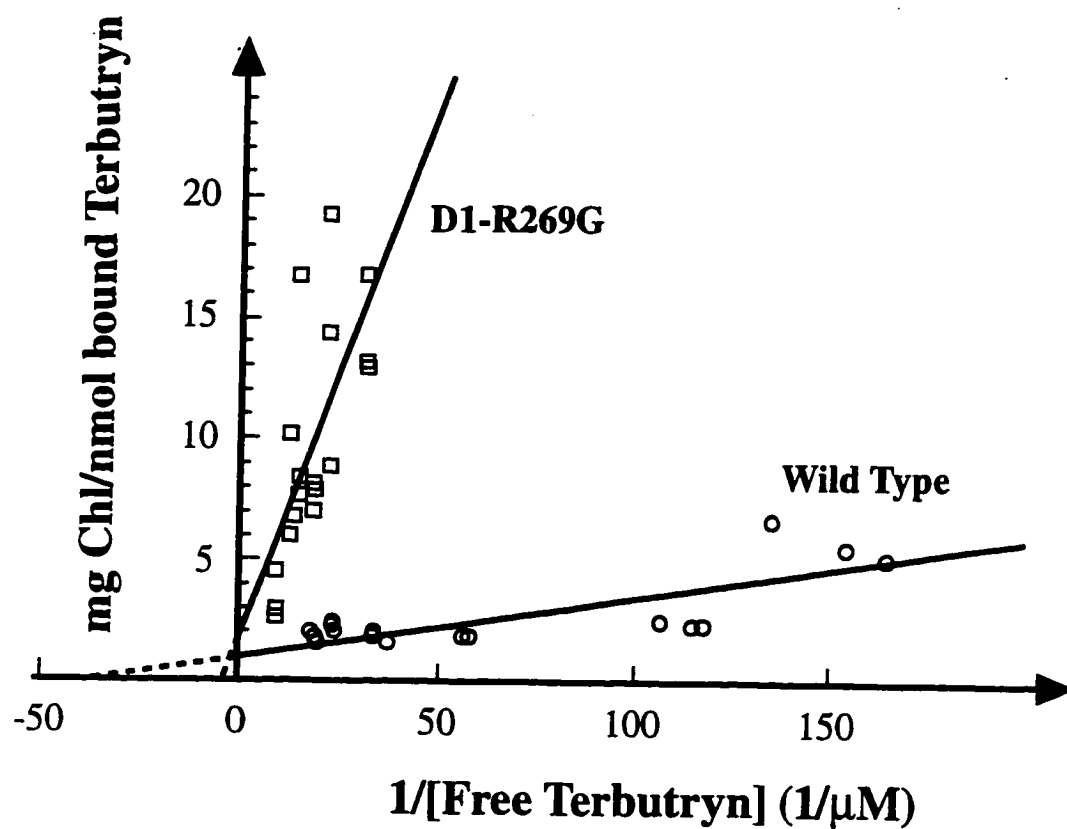


Figure 2.14. Double reciprocal plot for the ^{14}C -terbutryn binding to the thylakoids of the dark-grown wild type and the D1-R269G mutant of *C. reinhardtii*. Terbutryn specific binding was obtained by subtracting the atrazine-replaceable terbutryn binding from the total terbutryn binding according to Vermaas et al. (1990). The reactions were performed as in Materials and Methods. The calculated terbutryn binding site for the wild type is $28.9 (\pm 11.1)$ nM and that of the mutant is $223.3 (\pm 71.1)$ nM.



for the wild type is $28.9 (\pm 11.1)$ nM, and for the mutant is $223.3 (\pm 71.1)$ nM, about 8 fold effect. This suggests a drastically altered Q_B binding niche in the mutant. A variability is observed among thylakoid samples, especially with time of storage, and a difference of up to 30 fold with the wild type was observed in certain trials. The relative number of the PSII reaction centers on a chlorophyll basis for the wild type in the experiment in Fig. 2.14 is $1087 (\pm 415)$ Chl/PSII, and that for the mutant is $2185 (\pm 2975)$ Chl/PSII. It is not possible to quantitatively differentiate between the sizes of the PSII unit of the wild type and the mutant due to such errors, even though the average Chl/PSII value of the mutant may suggest a lowered PSII number per unit chlorophyll. The notion that the PSII stability is affected in the mutant is supported from other assays such as the 77 K fluorescence emission spectra (Fig. 2.13), fluorescence kinetics measurements (Fig. 2.6) as well as the western blot and EPR analyses (Figs. 2.3-2.4).

D. Discussion

The site-directed mutagenesis study that alters D1-R269 to D1-R269G shows that the mutation leads to a reduced level of stable charge separation, a higher susceptibility to photoinhibitory damage, significant inhibition on the electron transfer process as well as the disruption on the structure of both the donor side and the acceptor side of the PSII reaction center. Although the results do not substantiate D1-R269 as the site of bicarbonate binding, the mutation may indirectly perturb the bicarbonate and formate effect *in vivo*.

The important conclusion of this study is that the D1-R269G mutation alters the acceptor as well as the donor side electron transfer processes in PSII and destabilizes the PSII complex. This is intriguing since the R269G residue is predicted to be located at the stromal end of transmembrane span E. Glycine residues are frequently found at the end of transmembrane spanning domains. Due to the free rotation permitted around the alpha

carbon, the regular alpha helical structure of the transmembrane spanning domain can be broken (Aurora et al. 1994). This may lead to a shortening of the transmembrane span and/or disrupt interactions between transmembrane spans leading to structural perturbations on the luminal or donor side of the complex.

It is noteworthy that luminal side mutations (e.g. D1-H190F), as well as treatments which extract manganese from PSII, slow acceptor (Q_A^- to Q_B) side electron transfer processes (Roffey et al. 1994a). These observations suggest that structural perturbations of extrinsic domains at the margins of transmembrane spans can be transduced from one side of the membrane protein to the other altering charge transfer processes. The perturbations do not, however, prevent assembly of the PSII complex. It is apparent that only a fraction of the mutant PSII centers are capable of forming a stabilized charge separated state.

My recently constructed three dimensional PSII reaction center model (Chapter IV) suggests that D1-R269 is not a direct binding residue for bicarbonate at the non-heme iron site. The geometric position of D1-R269 is modeled 8-11 Å from bicarbonate or the iron, which does not support direct interaction. D1-R269 is located near the N-terminal region of the transmembrane α -helix E of D1. According to the model, D1-R269 is separated from D1-H272, one of the non-heme iron ligands, by nearly 3/4 of a helical turn (~5 Å). This close vicinity to D1-H272, which is located approximately equally in between Q_A and Q_B , may help explain a structural perturbation of D1-R269G mutation on the functionality of the iron and the liganding of bicarbonate and formate (Figs. 2.10-2.12).

In addition to D1-R269, several other positively charged residues on the D2 protein of cyanobacteria near the non-heme iron have also been investigated for involvement in bicarbonate/formate effect (Cao et al. 1991; Diner et al. 1991; Govindjee 1993). D2-R233 and D2-R251 have been shown to increase the PSII susceptibility to formate inhibition of full chain electron transfer by 10 fold relative to the wild type and are suggested to function in stabilizing bicarbonate binding *in vivo* (Cao et al. 1991). However, a mutation on D2-R139 (D1-R139H) showed no effect on bicarbonate-reversible formate inhibition

(Govindjee 1993). Thus, there is clearly a specificity here. D2-K264 was suggested to be a strong candidate for bicarbonate binding at the non-heme iron site, as its site-directed mutants were considerably slow in electron transfer from Q_A^- to Q_B compared to the wild type, and are very resistant to formate and NO treatment (see Diner et al. 1991). This mutant required much higher bicarbonate concentration than the wild type to accelerate Q_A/Q_B electron transfer, suggesting that the residue may be intimately involved in binding of bicarbonate. Mutations at a nearby residue D2-R265 also showed similar effects, though to a lesser extent.

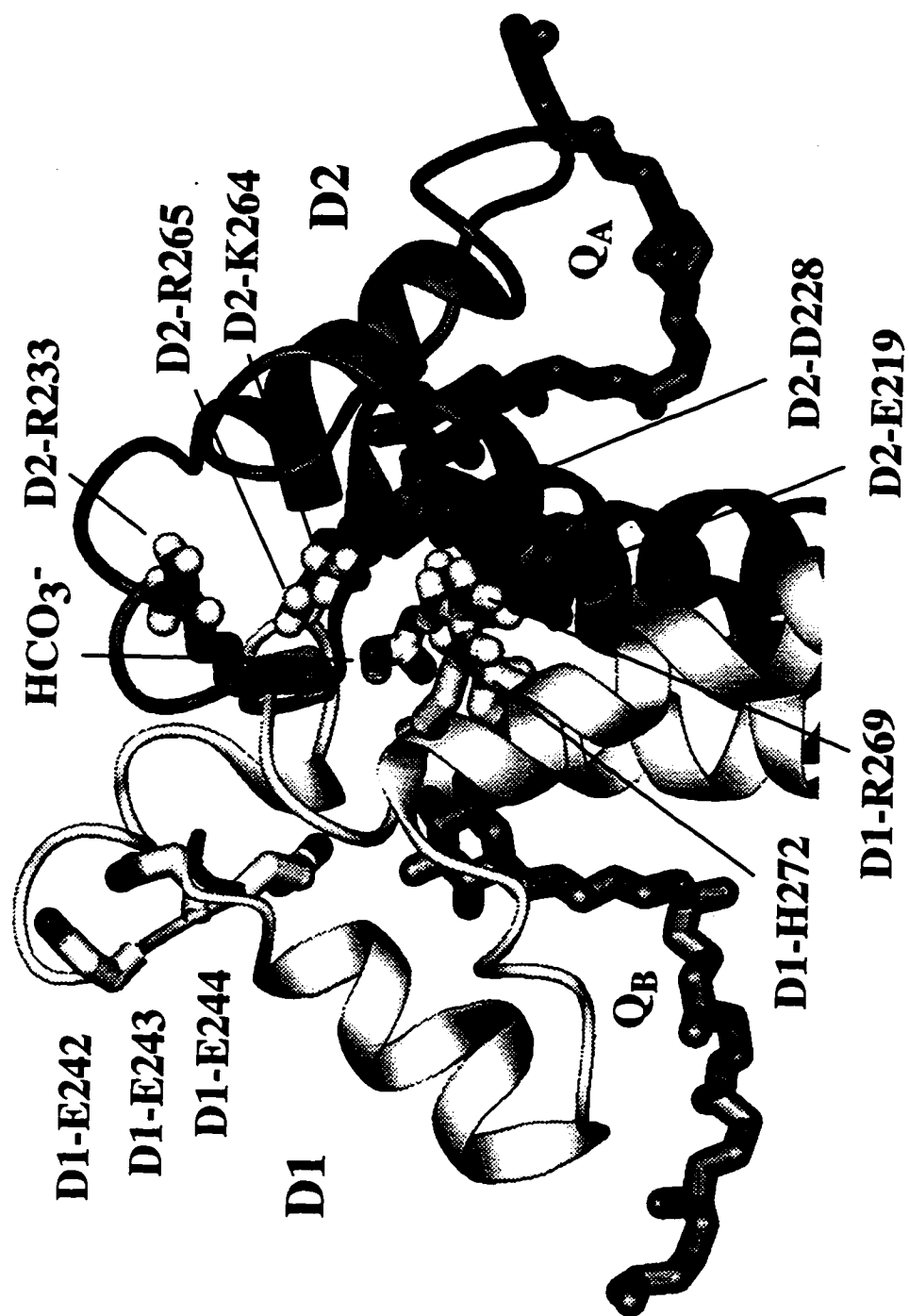
In addition to liganding to the iron, bicarbonate may also function in promoting the protonation of Q_B^{2-} (see Blubaugh and Govindjee 1988a; Govindjee and van Rensen 1993). Kinetic studies by Blubaugh and Govindjee (1988b) suggested the possibility of two tight bicarbonate binding sites in PSII. One of these binding sites may well be at the non-heme iron site, while the other may be related to the protonation of plastoquinone and thus likely to be near the Q_B site in the D1 protein. Mäenpää et al. (1995) demonstrated that a strain of *Synechocystis* 6803 with deletion of residues D1-E242 to D1-E244 near the Q_B site exhibits a seven fold higher resistance to formate inhibition than the wild type. The site-directed mutagenesis experiments on D1-R257 of *C. reinhardtii* have indicated that this residue is intimately involved in affecting the bicarbonate/formate functionality in the Q_B protonation step (see Chapter III).

In the three dimensional model of the PSII reaction center (Chapter IV), I propose a channel for transporting bicarbonate anions and water molecules to the non-heme iron and Q_B in the PSII reaction center, based on the analogy with a water transport channel in the bacterial reaction center (Ermler et al. 1994). This channel or a large binding niche involves a series of charged residues of the D1 and D2 proteins, including D1-R269. Substitution on D1-R269 is thus expected to cause perturbations on bicarbonate functionality, which is supported by the data in Figs. 2.10-2.12.

The model indicates that D1-R269 may also be involved in D1/D2 interaction. The correct assembly and stability of the D1/D2 complex of the PSII reaction center rely partly on the interactions of the contact residues located on the transmembrane spans. As shown in Fig. 2.15, D1-R269 may be a contact residue located in the interface of D1 and D2 polypeptides and may provide interactions important for maintaining the conformation of D1 and D2 polypeptides. The model shows that D1-R269 may have electrostatic or hydrogen bonding interactions with certain D2 residues, such as D2-E219 and D2-D228 (Fig. 2.15). The glycine mutation may thus abolish such interactions affecting the stability of the PSII reaction center, resulting in a series of primary and secondary effects such as lowered charge separation, slowed PSII electron transfer, decreased binding of Q_B /herbicide, perturbed bicarbonate/formate functioning at the non-heme iron and/or Q_B site, etc. Therefore, it may be interesting to test this hypothesis by mutagenizing the D2-E220 or D2-D228 residue and see whether a similar structural instability effect on PSII may exist in these mutants.

Since D1-R269 is considered to be located on the acceptor side, the transduction of the mutational effect from the acceptor side to the donor side can be understood by D1-R269 being a contact residue affecting the assembly the PSII reaction center thus altering the structure and function of the donor side (Table 2). Similar transduction of mutational effects between the donor side and acceptor side has previously been observed. Etienne and Kirilovsky (1993) and Constant et al. (1996) showed that several herbicide-resistant mutations at the Q_B site affect the S states functions during oxygen evolution. Similar effects have previously been observed for mutants lacking the PSII 43 kD chlorophyll binding protein and in site-directed mutants of the D1 protein (de Vitry et al. 1989; Hutchison and Sayre 1995). Carpenter et al. (1993) have observed that the S_2 and S_3 states (on the D1/D2) are affected by changes in CP-43 protein, and Kless et al. (1993) have shown that alterations in the Q_A region of the D2 protein affects DCMU affinity in the D1 protein.

Figure 2.15. A partial three dimensional model of the PSII reaction center according to the author (Chapter IV). Shown are certain residues from the membrane helix D to helix E of both D1 and D2 proteins in their secondary structure representation. The D1-R269 residue is shown to be one of the contact residues located in the interface of D1 and D2 polypeptides and is also close to the putative non-heme iron and the liganding bicarbonate. The D1-R269G mutation is thought to abolish the putative interaction between the D1-R269 and several D2 residues, such as D2-E219 and D2-D228, affecting the non-heme iron and the Q_B sites, and even the stability of the PSII reaction center. Several other residues demonstrated in literature to be important for bicarbonate binding and function are also labeled.



Data presented in this chapter are based on the published and to be published work of the author and his collaborators (Xiong et al. 1996b; Hutchison et al. 1996).

E. References

- Aime, S., Fasano, M., Paoletti, S., Cutruzzolà, F., Desideri, A., Bolognesi, M., Rizzi, M. and Ascenzi, P. (1996) Structural determinants of fluoride and formate binding to hemoglobin and myoglobin: Crystallographic and ^1H -NMR relaxometric study. *Biophys. J.* 70: 482-488.
- Anderson, B.F., Baker, H.M., Norris, G.E., Rice, D.W. and Baker, E.N. (1989) Structure of human transferrin: Crystallographic structure analysis and refinement at 2.8 Å resolution. *J. Mol. Biol.* 209: 711-734.
- Aurora, R., Srinivasan R. and Rose, G.D. (1994) Rules for α -helix termination by glycine. *Science* 264: 1126-1130.
- Barry, B.A. and Babcock, G.T. (1987) *Proc. Natl. Acad. Sci. USA* 84: 7099-7103.
- Blubaugh, D. and Govindjee. (1986) Bicarbonate, not CO_2 , is the species required for the stimulation of Photosystem II electron transport. *Biochim. Biophys. Acta* 848: 147-151.
- Blubaugh, D.J. and Govindjee. (1988a) The molecular mechanism of the bicarbonate effect at the plastoquinone reductase site of photosynthesis. *Photosynth. Res.* 19: 85-128.
- Blubaugh, D.J. and Govindjee. (1998b) Kinetics of the bicarbonate effect and the number of bicarbonate-binding sites in thylakoid membranes. *Biochim. Biophys. Acta* 936: 208-214.
- Bouges-Bocquet, B. (1973) Electron transfer between the two photosystems in spinach chloroplasts. *Biochim. Biophys. Acta* 314: 250-256.

- Bowes, J. and Crofts, A.R. (1980) Binary oscillations in the rate of reoxidation of the primary acceptor of photosystem II. *Biochim. Biophys. Acta* 590: 373-384.
- Briantais, J.-M., Vernotte, C., Krause, G.H. and Weis, E. (1986) Chlorophyll *a* fluorescence of higher plants: Chloroplasts and leaves. In: Govindjee, Ames, J. and Fork, D.C. (eds.) *Light Emission by Plants and Bacteria* pp. 539-583. Academic Press, Orlando.
- Butler, W.L. (1972) On the primary nature of fluorescence yield changes associated with photosynthesis. *Proc. Natl. Acad. Sci. USA* 69: 3420-3422.
- Cao, J., Vermaas, W.F.J. and Govindjee. (1991) Arginine residues in the D2 polypeptide may stabilize bicarbonate binding photosystem II of *Synechocystis* sp. PCC 6803. *Biochim. Biophys. Acta* 1059: 171-180.
- Carpenter, S.D., Ohad, I. and Vermaas, W.F.J. (1993) Analysis of chimeric spinach/cyanobacterial CP43 mutants of *Synechocystis* sp. PCC 6803: The chlorophyll binding protein CP43 affects the water-splitting system of photosystem II. *Biochim. Biophys. Acta* 1144: 204-212.
- Cheniae, G.M. and Martin, I.F. (1973) Absence of oxygen-evolving capacity in dark-grown *Chlorella*: the photoactivation of oxygen-evolving centers. *Photochem. Photobiol.* 17, 441-459.
- Constant, S., Perewoska, I., Nedbal, L., Miranda, T., Etienne, A.-L. and Kirilovsky, D. (1996) A new phenotype for a herbicide resistant mutant of *Synechocystis* 6714 with a high sensitivity to photoinhibition. *Plant Sci.* 115: 165-174.
- Crofts, A.R., Baroli, I., Kramer, D. and Taoka. (1993) Kinetics of electron transfer in Q_A and Q_B in wild type and herbicide-resistant mutants of *Chlamydomonas reinhardtii*. *Z. Naturforsch.* 48c: 259-266.
- Dekker, J.P., Hassoldt, A., Petterson, A., van Roon, H., Groot, M.L. and van Grondelle, R. (1995) On the nature of the F695 and F685 emission of photosystem

- II. In: Mathis, P. (ed.) Photosynthesis: from Light to Biosphere, Vol. I, pp. 53-56. Kluwer, Dordrecht.
- de Vitry C., Olive, J., Drapier, D., Recouvreur, M. and Wollman F.-A. (1989) Posttranslational events leading to the assembly of photosystem II protein complex: A study using photosynthesis mutants from *Chlamydomonas reinhardtii*. J. Cell Biol. 109: 991-1006.
- Diner, B.A., Petrouleas, V. and Wendoloski, J.J. (1991) The iron-quinone electron-acceptor complex of photosystem II. Physiol. Plant. 81: 423-436.
- Eaton-Rye, J.J. and Govindjee. (1988a) Electron transfer through the quinone acceptor complex of photosystem II in bicarbonate-depleted spinach thylakoid membranes as a function of actinic flash number and frequency. Biochim. Biophys. Acta 935: 237-247.
- Eaton-Rye, J.J. and Govindjee. (1988b) Electron transfer through the quinone acceptor complex of photosystem II after one or two actinic flashes in bicarbonate-depleted spinach thylakoid membranes. Biochim. Biophys. Acta 935: 248-257.
- Eggenberger, A.L., De Ciechi, P. and Pakrasi, H. (1990) Multiple replacement mutagenesis of the *psbEFIJ* operon of *Synechocystis* PCC 6803. In: Baltscheffsky, M. (ed.) Current Research in Photosynthesis, vol. I, pp. 363-366. Kluwer Academic Publishers, Dordrecht.
- El-Shintinawy, F. and Govindjee. (1990) Bicarbonate effect in leaf discs from spinach. Photosyn. Res. 24: 189-200.
- El-Shintinawy, F., Xu, C. and Govindjee. (1990) A dual bicarbonate-reversible formate effect in *Chlamydomonas* cells. J. Plant. Physiol. 136: 421-428.
- Ermler, U., Fritsch, G., Buchanan, S.K. and Michel, H. (1994) Structure of the photosynthetic reaction centre from *Rhodobacter sphaeroides* at 2.65 Å resolution: Cofactors and protein-cofactor interactions. Structure 2: 925-936.

- Etienne, A.-L. and Kirilovsky, D. (1993) The primary structure of D1 near the Q_B pocket influences oxygen evolution. *Photosyn. Res.* 38: 387-394.
- Govindjee. (1993) Bicarbonate-reversible inhibition of plastoquinone reductase in photosystem II. *Z. Naturforsch.* 48c: 251-258.
- Govindjee. (1995) Sixty-three years since Kautsky: Chlorophyll *a* fluorescence. *Aust. J. Plant Physiol.* 22: 131-160.
- Govindjee and Satoh, K. (1986) Fluorescence properties of chlorophyll *b*- and chlorophyll *c*- containing algae. In: Govindjee, Ames, J., and Fork, D.C. (eds.) *Light Emission by Plants and Bacteria*, pp. 497-537. Academic Press, Orlando.
- Govindjee and van Rensen, J.J.S. (1993) Photosystem II reaction center and bicarbonate. In: Deisenhofer, J. and Norris, J. (eds.), *The Photosynthetic Reaction Center*, Vol. I, pp. 357-389, Academic Press, Inc., San Diego.
- Govindjee, Xu, C., Schansker, G., and van Rensen, J.J.S. (1996) Chloroacetates as inhibitors of photosystem II: Effects on electron acceptor side. *J. Photochem. Photobiol.* (in press)
- Guenther, J.E., Nemson, J.A., and Melis, A. (1990) Development of photosystem II in dark grown *Chlamydomonas reinhardtii*. A light-dependent conversion of PS II_β, Q_B-nonreducing centers to the PS II_α, Q_B-reducing form. *Photosyn Res.* 24: 35-46.
- Haag, E., Eaton-Rye, J.J., Renger, G., and Vermaas, W.F.J. (1993) Functionally important domains of the large hydrophilic loop of CP47 as probed by oligonucleotide directed mutagenesis in *Synechocystis* sp. PCC 6803. *Biochemistry* 32: 4444-4454.
- Harris, E.H. (1989) In: *The Chlamydomonas Sourcebook, A Comprehensive Guide to Biology and Laboratory Use*. pp. 25-31. Academic Press, San Diego.

- Hienerwadel, R. and Berthomieu, C. (1995) Bicarbonate binding to the non-heme iron of photosystem II investigated by Fourier transform infrared difference spectroscopy and ^{13}C -labeled bicarbonate. *Biochemistry* 34: 16288-16297.
- Hutchison, R.H. and Sayre, R.T. (1995) Site-specific mutagenesis at histidine 118 of the photosystem II D1 protein of *Chlamydomonas reinhardtii*. In: Mathis, P. (ed.) *Photosynthesis: from Light to Biosphere*. vol. I, pp. 471-474. Kluwer Academic Publishers, Dordrecht.
- Hutchison, R.S., Xiong, J., Sayre, R.T. and Govindjee. Construction and characterization of a D1 mutant (arginine-269-glycine) of *Chlamydomonas reinhardtii* *Biochim. Biophys. Acta* (in press)
- Inoue, Y. (1996) Photosynthetic thermoluminescence as a simple probe of photosystem II electron transport. In: Ames, J. and Hoff, A. (eds.) *Biophysical Techniques in Photosynthesis*. pp. 93-107. Kluwer Academic Publishers, Dordrecht.
- Johnson, G.N., Boussac, A. and Rutherford, A.W. (1994) The origin of 40-50°C thermoluminescence bands in photosystem II. *Biochim. Biophys. Acta* 1184, 85-92.
- Kless, H., Oren-Shamir, M., Ohad, I., Edelman, M. and Vermaas, W.F.J. (1993) Protein modifications of the D2 protein of photosystem II affect properties of Q_B /herbicide binding environment. *Z. Naturforsch.* 48c: 185-190.
- Klimov, V.V., Allakhverdiev, S.I., Feyziev, Y.M. and Baranov, S.V. (1995) Bicarbonate requirement for the donor side of photosystem II. *FEBS Lett.* 363: 251-255.
- Kramer, D.M., Robinson, H.R. and Crofts, A.R. (1990) A portable multi-flash fluorimeter for measurements of donor and acceptor reactions of photosystem 2 in leaves of intact plants under field conditions. *Photosynth. Res.* 26: 181-193.
- Kunkel, T.A., Roberts, J.D. and Zakour, R.A. (1987) Rapid and efficient site-specific mutagenesis without phenotypic selection. *Methods. Enzymol.* 154: 367-382.

- Lavergne, J. and Briantais, J.-M. (1996) In: Ort, D.R. and Yocum, C. (eds.) *Oxygenic Photosynthesis: The Light Reactions*. Kluwer Academic Publishers, Dordrecht. (in press)
- Mäenpää, P., Miranda, T., Tyystjärvi, E., Tyystjärvi, T., Govindjee, Ducruet, J.-M., Etienne, A.-L. and Kirilovsky, D. (1995) A mutation in the D-de loop of D₁ modifies the stability of the S₂Q_A⁻ and S₂Q_B⁻ states in photosystem II. *Plant Physiol.* 107: 187-197.
- Metz, J.G., Nixon, P.J., Rogner, M., Brudvig, G.W. and Diner, B.A. (1989) Directed alteration of the D1 polypeptide of photosystem II: Evidence that tyrosine-161 is the redox component, Z, connecting the oxygen-evolving complex to the primary electron donor, P680. *Biochemistry* 28: 6960-6969.
- Michel, H. and Deisenhofer, J. (1988) Relevance of the photosynthetic reaction center from purple bacteria to the structure of photosystem II. *Biochemistry* 27: 1-7.
- Munday, J.C.M. Jr. and Govindjee. (1969) Light-induced changes in the fluorescence yield of chlorophyll *a* in vivo. IV. The effect of preillumination on the fluorescence transient of *Chlorella pyrenoidosa*. *Biophys. J.* 9: 22-35.
- Nakatani, H.Y., Ke, B., Dolan, E., and Arntzen, C.J. (1984) Identity of the photosystem II reaction center polypeptide. *Biochim. Biophys. Acta* 765: 347-352.
- Papageorgiou, G. (1975) Chlorophyll fluorescence: an intrinsic probe of photosynthesis. In: Govindjee, (ed.) *Bioenergetics of Photosynthesis* pp. 319-371. Academic Press, New York.
- Petrouleas, V. and Diner, B. (1990) Formation of NO of nitrosyl adducts of redox components of the photosystem II reaction center. I. NO binds to the acceptor-side non-heme iron. *Biochim. Biophys. Acta* 1015: 131-140.
- Petrouleas, V., Deligiannakis, Y. and Diner, B.A. (1994) Binding of carboxylate anions at the non-heme Fe(II) of PS II .2. Competition with bicarbonate and effects on the Q_a/Q_b electron transfer rate. *Biochim. Biophys. Acta* 1188: 271-277.

- Porra, R.J., Thompson, W.A. and Kriedemann, P.E. (1989) Determination of accurate extinction coefficients and simultaneous equations for assaying chlorophylls *a* and *b* extracted with four different solvents: verification of the concentration of chlorophyll standards by atomic absorption spectroscopy. *Biochim. Biophys. Acta* 975: 384-394.
- Radmer, R. and Cheniae, G.M. (1977) In: Barber, J. (ed.) Mechanisms of oxygen evolution. In: Topics in Photosynthesis. vol. 2, pp. 303-348, Elsevier Science Publishers, Amsterdam.
- Roffey, R.A., Golbeck, J.H., Hille, C.R. and Sayre, R.T. (1991) Photosynthetic electron transport in genetically altered photosystem II reaction centers of chloroplasts. *Proc. Natl. Acad. Sci. USA* 88: 9122-9126.
- Roffey, R.A., Kramer, D.M., Govindjee and Sayre, R.T. (1994a) Lumenal side histidine mutations in the D1 protein of photosystem II affect donor side electron transfer in *Chlamydomonas reinhardtii*. *Biochim Biophys Acta* 1185: 257-270.
- Roffey, R.A., van Wijk, K.J., Sayre, R.T. and Styring, S. (1994) Spectroscopic characterization of tyrosine-Z in histidine 190 mutants of the D1 protein in photosystem II (PSII) in *Chlamydomonas reinhardtii* -implications for the structural model of the donor side of PSII. *J. Biol. Chem.* 269: 5115-5121.
- Shinkarev, V.P. and Govindjee. (1993) Insight into the relationship of chlorophyll *a* fluorescence yield to the concentration of its natural quenchers in oxygenic photosynthesis. *Proc. Natl. Acad. Sci. USA* 90: 7466-7469.
- Strasser, R.J., Srivastava, A. and Govindjee. (1995) Polyphasic chlorophyll *a* fluorescence transient in plants and cyanobacteria. *Photochem. Photobiol.* 61: 32-42.
- van Rensen, J.J.S., Tonk, W.J.M. and de Bruijn, S.M. (1988) Involvement of bicarbonate in the protonation of the secondary quinone electron acceptor of

- photosystem II via the non-heme iron of the quinone-iron acceptor complex. FEBS Lett. 226: 347-351.
- Vass, I. and Govindjee. (1996) Thermoluminescence of photosynthetic apparatus. Photosyn. Res. (in press)
- Velthuys, B.R. and Ames, J. (1974) The effect of dithionite on fluorescence and luminescence of chloroplasts. Biochim. Biophys. Acta 325: 126-137.
- Vermaas, W.F.J. and Rutherford, A.W. (1984) EPR measurements on the effects of bicarbonate and triazine resistance on the acceptor side of photosystem II. FEBS Lett. 175: 243-248.
- Vermaas, W., Charité, J. and Shen, G. (1990) Glu-69 of the D2 protein in photosystem II is a potential ligand to Mn involved in photosynthetic oxygen evolution. Biochemistry 29: 5325-5332.
- Wang, X., Cao, J., Maroti, P., Stolz, H.U., Finkbeiner, U., Lauterwasser, C., Zinth, W., Oesterhelt, D., Govindjee and Wraight, C.A. (1992) Is bicarbonate in photosystem II the equivalent of the glutamate ligand to the iron atom in bacterial reaction center? Biochim Biophys Acta 1100: 1-8.
- Wincencjusz, H., Allakverdiev, S.I., Klimov, V.V. and van Gorkom, H.J. (1996) Bicarbonate-reversible formate inhibition at the donor side of photosystem II. Biochim. Biophys. Acta 1273: 1-3.
- Xiong, J., Hutchison, R.S., Sayre, R.T. and Govindjee. (1996) Plastoquinone reductase function of a photosystem II D1 mutant (arginine-269-glycine) of *Chlamydomonas reinhardtii*: Chlorophyll *a* fluorescence and herbicide binding. submitted to Biochim. Biophys. Acta
- Xu, C., Rogers, S.M.D., Goldstein, C., Widholm, J.M. and Govindjee (1989) Fluorescence characteristics of photoautotrophic soybean cells. Photosynth. Res. 21: 93-106.

CHAPTER III. CONSTRUCTION AND CHARACTERIZATION OF BICARBONATE/FORMATE BINDING SITE MUTANTS ON ARGININE-257 IN THE PHOTOSYSTEM II D1 PROTEIN OF *CHLAMYDOMONAS REINHARDTII*

A. Introduction

Electron transfer of photosystem II (PSII) has been shown by numerous studies to be regulated by bicarbonate anions in higher plants, algae and cyanobacteria (see reviews Blubaugh and Govindjee 1988a, Diner et al. 1991; Govindjee and van Rensen 1993). Although there exists a donor side effect by bicarbonate (see *e.g.* Klimov et al. 1995), depletion of bicarbonate causes significant inhibition of the electron transfer on the acceptor side of PSII, particularly, from Q_A^- to Q_B^- (see Eaton-Rye and Govindjee 1988a, b; Xu et al. 1991). According to a suggestion of Michel and Deisenhofer (1988), bicarbonate may be a functional homologue of the amino acid residue E232 of the M subunit of the *Rhodospseudomonas viridis* reaction center, and may play an important role in liganding to the non-heme iron in PSII. It may provide the fifth and/or the sixth ligand to the non-heme iron. A close association of bicarbonate with the non-heme iron in PSII was verified by EPR spectroscopic studies (Vermaas and Rutherford 1984; Petrouleas and Diner 1990) as well as by a Fourier transform infrared difference spectroscopy study (Hienerwadel and Berthomieu 1995). In addition to liganding to the iron, many experiments have suggested that bicarbonate may also function in promoting the protonation of Q_B^- or Q_B^{2-} (Eaton-Rye and Govindjee 1988a, b; van Rensen et al. 1988; Xu et al. 1991). Kinetic studies by Blubaugh and Govindjee (1988b) suggested the possibility of two high affinity bicarbonate binding sites in the PSII reaction center. This second binding site is likely to exist in the Q_B niche and is considered to be related to the protonation of plastoquinone. Characterization of a number of Q_B mutants which are also herbicide resistant have implicated the Q_B

binding niche to be involved for the bicarbonate functioning in PSII (Govindjee et al. 1990; Cao et al. 1992; Govindjee et al. 1992; Mäenpää et al. 1995; Srivastava et al. 1995; Vernotte et al. 1995).

Since anionic bicarbonate may well be the active species functioning in the PSII reaction center (Blubaugh and Govindjee 1986), it is expected that the binding would be electrostatic in nature and therefore positively charged amino acid residues are likely to participate in bicarbonate binding. Only two positively charged D1 residues, D1-R257 and D1-R269, are found near the putative Q_B and the non-heme iron site based on sequence homology analysis (see Govindjee and van Rensen 1993). To investigate whether these two residues are involved in the bicarbonate binding and functioning *in vivo*, site-directed mutagenesis was carried out on these two residues using a unicellular green alga *Chlamydomonas reinhardtii* as the model system. The study of a site-directed mutant on D1-R269 (D1-R269G) reveals that this residue is important for the structure and function of the PSII complex on both the donor and acceptor sides of PSII (see Chapter II). However, the non-conservative mutation did not abolish the *in vivo* bicarbonate/formate binding and functionality. The current chapter focuses on the role of D1-R257 residue and its relation to the bicarbonate effect. Sequence analysis of the D1 protein indicates that D1-R257 is closer to the Q_B niche making it a more likely residue to be involved in Q_B protonation. This residue is thought to be located on the stromal side between the putative transmembrane helices D and E of D1 and may be located within or close to the D1-*de* helix (according to three dimensional models of the PSII reaction center, for details see Chapter III).

The association of arginines with bi(carbonate) or its analogue has been shown in many protein systems. The x-ray crystal structure of human lactoferrin has a (bi)carbonate at the active site binding to an iron while being stabilized by hydrogen bonding interactions with an arginine and several other adjacent amino acid residues Anderson et al. (1989). A high resolution X-ray structure of a similar protein duck ovotransferrin also shows a

bicarbonate anion bound to an arginine residue (Lindley et al. 1993). Another example is found in the x-ray crystal structure of a formate derivative of hemoglobin and myoglobin in which a formate (a bicarbonate analog) is bound to the heme iron and directly interacts with an arginine (Aime et al. 1996). Site-directed mutagenesis studies of Yano et al. (1995) in phosphoenolpyruvate carboxylase of *Escherichia coli* also clearly indicated an arginine residue participating in bicarbonate binding. Thus, it is possible that a similar binding motif may exist in the Q_B site of the PSII reaction center.

In this chapter, I describe the construction and characterization of two site-directed mutants of D1-R257 using a newly developed D1 mutagenesis system in the unicellular green alga *Chlamydomonas reinhardtii* (Minagawa and Crofts 1994). The arginyl residue was mutated into a glutamate and a methionine, which have similar sizes in sidechains but different electrostatic properties. The characterization of these two mutants indicates that (1) there is ~30% reduction in the rate of photoautotrophic growth; (2) mutational effects on the PSII appear to be located on the acceptor side only; (3) the mutants have a significantly elevated F₀ level (~40-50%) suggesting a net decrease in the excitation energy transfer from the antenna to the PSII reaction center or an increased [Q_A⁻] in the dark; (4) there is ~10% reduction in F685 and F695 bands in the low temperature fluorescence emission spectra suggesting a change in the PSII antenna complex which may be caused by the destabilization of the mutant PSII; (5) DCMU binding in the mutants appears to be essentially the same as in the wild type; (6) the rate of electron transfer from Q_A⁻ to the plastoquinone pool as well as the full chain electron transfer was reduced by ~40-50%; (7) the mutants have a very low sensitivity to the bicarbonate-reversible formate inhibition: there is an 8 fold increase in apparent formate dissociation constant; (8) the full chain electron transfer of the two mutants are poorly inhibited by arginine-specific reagents which strongly inhibits the electron transfer of the wild type, the inhibition of which can be reversed by bicarbonate. The evidence strongly implicates the absence of bicarbonate binding in these two mutants.

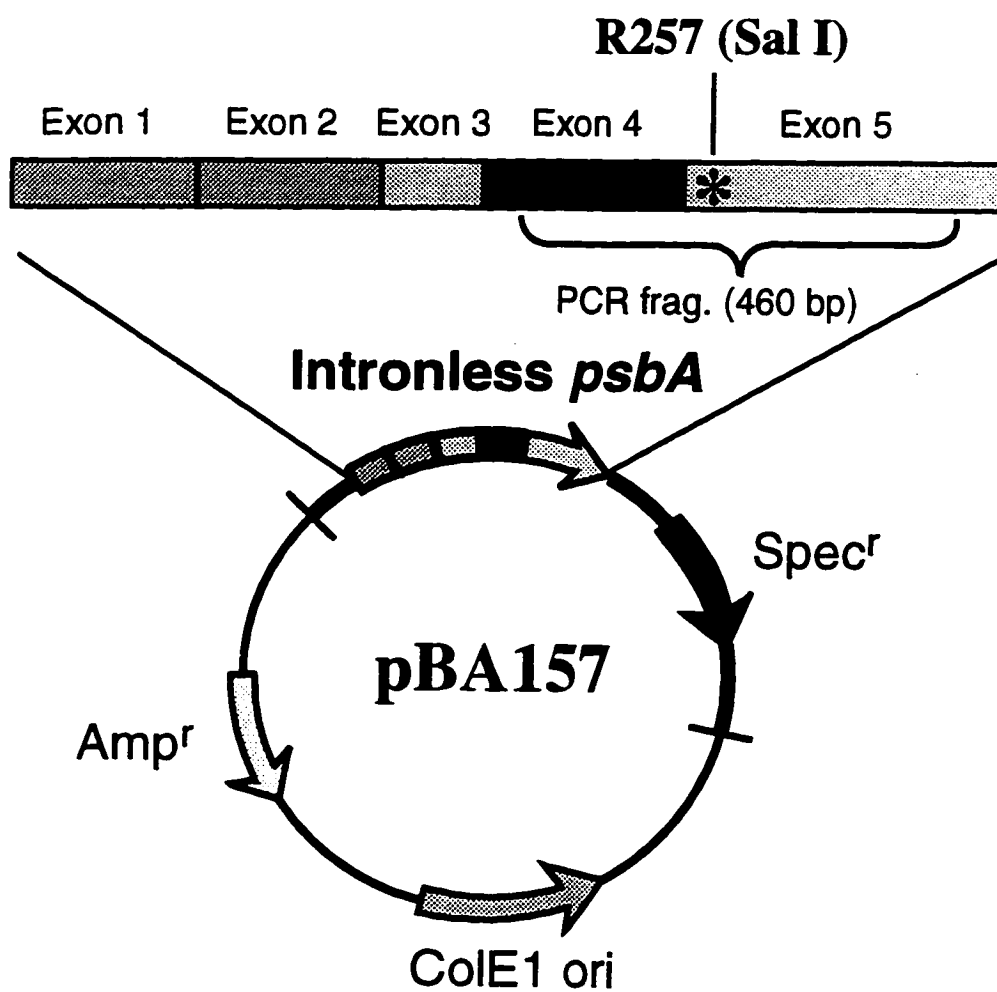
B. Materials and Methods

1. Site-directed mutagenesis

Site-directed mutagenesis of *C. reinhardtii* D1 gene (*psbA*) was carried out using an engineered plasmid vector (pBA157) containing the entire *psbA* gene without all the introns (Minagawa and Crofts 1994) (Fig. 3.1). In addition, a gene conferring the spectinomycin resistance (*Spec^r*) was cloned downstream of the intron-free *psbA* gene on the vector. Codon for D1-R257 is located on the exon 5 of *psbA* and contains a *Sal* I restriction site. Site-directed mutagenesis on D1-R257 using PCR was essentially done as described by Minagawa and Crofts (1994). The D1-R257E mutation was made using a synthetic oligonucleotide primer that alters the arginine-257 codon CGA to GAA (antisense sequence: TTGGAAGATTAGTTCACCAAAGTAACC). The D1-R257M mutation was made with a primer (antisense sequence: TTGGAAGATTAGCATACCAAAGTAACC) changing CGA to ATG. The mutagenized plasmid was purified using the Magic Minipreps™ DNA purification system (Promega Co., Madison, WI). The mutations were confirmed by automated DNA sequencing performed at the Genetics Facility of University of Illinois at Urbana-Champaign, using the primer: TTAATCCGTGAAACAACCTGAA (for residues 223-229).

Mutagenized plasmid DNA was used to transform a *psbA* deletion *C. reinhardtii* strain (ac-u-ε). Transformation was performed using a laboratory-built helium particle inflow gun which bombarded DNA-coated tungsten particles (M-17, Bio-Rad Laboratories, Hercules, CA) into *C. reinhardtii* cells. The cells were then plated on Tris-Acetate-Phosphate (TAP) medium (see Harris 1989) containing 100 µg/ml spectinomycin and incubated at 22°C under dim light conditions. Two weeks after the bombardment, numerous colonies were obtained on the spectinomycin TAP plates. As the engineered construct contains the intron-free *psbA* and the *Spec^r* genes in tandem and the

Figure 3.1. Engineered plasmid vector (pBA157) containing the intronless *psbA* gene and the spectinomycin resistance gene (*Spec^r*, *aadA* gene from *E. coli*) (see Minagawa and Crofts 1994). D1-R257, the site of mutagenesis, located at the Exon 5, contains a *Sal* I restriction site. The relative position of the PCR product (460 bp) of the chloroplast DNA after transformation is also shown on the plasmid map.



transformation was done with a *psbA* deletion host strain, the isolated colonies on the spectinomycin-containing plates are thus presumably homoplasmic for the newly introduced *psbA* gene. For experimental details, see Minagawa and Crofts (1994).

Chloroplast DNA of the transformants was isolated for further sequence confirmation. The putative mutant and intron-free wild type cells were grown in liquid TAP without spectinomycin and were harvested in the late logarithmic phase (O.D. ~0.65, $\sim 6 \times 10^6$ cells/ml). Harvested cells were concentrated to ~1 mg Chl/ml. Chlorophyll concentration was calculated according to the equations used in Porra et al. (1989). For isolating the DNA, cells were disrupted for 3 min. by a minibead beater in a tube containing an extraction buffer (0.1 LiCl, 100 mM Tris-HCl (pH 8.0), 10 mM EDTA, 1% SDS) and phenol:chloroform (1:1). Extracted DNA was further purified with phenol:chloroform (1:1) and precipitated with sodium acetate:ethanol (1:25). The DNA was resuspended in 150 μ l of water, of which 1 μ l was used for PCR amplification for the fragment from residues 186 to 339 using Taq polymerase (Gibco BRL, Gaithersburg, MD) and the primers CCAAGCAGAACACAACATCC and GAAGTTGTGAGCGTTACG. The amplified DNA fragment (460 bp) was subjected to restriction digests and automated DNA sequencing analyses.

2. Growth of *C. reinhardtii* cells

C. reinhardtii wild type (with intronless *psbA*) and the confirmed mutant cells were grown at 22°C in a liquid TAP medium under $\sim 10 \mu\text{E}/\text{m}^2\cdot\text{s}$ white light illumination. The intronless wild type and mutant strains were maintained in TAP agar plates with 200 $\mu\text{g}/\text{ml}$ spectinomycin and 100 $\mu\text{g}/\text{ml}$ ampicillin to prevent bacterial contamination. For the liquid culture, the cells were grown in TAP in the absence of spectinomycin. The cell culture reaching the late logarithmic phase (O.D. ~0.65, $\sim 6 \times 10^6$ cells/ml) was harvested and used for the subsequent measurements. In order to determine the photosynthetic growth rate, the wild type and mutant cells were grown in a liquid HS (high salt, see Harris 1989) medium

bubbled with 5% CO₂ and illuminated with 70 $\mu\text{E}/\text{m}^2\text{s}$ white light with constant shaking. The inocula used were obtained from mature TAP-grown algal cultures which were washed twice with the HS medium. They were used to inoculate a flask of HS medium to reach an optical density of 0.04. The growth rate was determined by measuring the optical density of the cells in original culture media at 750 nm at 12 hr. intervals using a commercial spectrophotometer (Shimadzu UV160U, Shimadzu Co., Kyoto, Japan). Similar measurements were also done for the heterotrophically grown cultures when all the cells were kept in the dark constantly.

3. Chlorophyll a fluorescence induction kinetics and measurements of F_0

Chl *a* fluorescence induction (transient) of the wild type and mutant cells was measured with a commercial pulse-modulated fluorimeter (Walz PAM-2000, Effeltrich, Germany). Actinic and measuring beams were provided by the built-in red-light-emitting diodes. The intensity of the measuring light was 0.7 $\mu\text{E}/\text{m}^2\text{s}$ and the intensity of the actinic light was 470 $\mu\text{E}/\text{m}^2\text{s}$. Before the measurements, the cells were resuspended in TAP medium with a Chl concentration of 5 $\mu\text{g}/\text{ml}$. All sample manipulations were done in the presence of a weak ($< 0.3 \mu\text{E}/\text{m}^2\text{s}$) background green light. The fluorescence transient measurements were done in the presence or absence of DCMU (10 μM) with samples dark-adapted for 5 min while being stirred.

In view of the fact that conclusions regarding the photochemical activity are obtained from a knowledge of the variable fluorescence (F_v) whose value is dependent upon the precise value of F_0 (see review by Govindjee 1995), special efforts were made to measure the true F_0 . This was done separately using a different pulse-modulated fluorimeter (Walz PAM-103, Effeltrich, Germany). F_0 measurement at various low light intensities in the presence and absence of DCMU (10 μM) was done as described by in Chapter II.

4. Bicarbonate depletion and recovery treatments

Bicarbonate depletion of cells by formate was carried out with a formate treatment procedure as described in El-Shintinawy et al. (1990) with modifications (see, Chapter II). Samples were treated with sodium formate at various concentrations and pHs as indicated. To remove the formate inhibition, these samples were incubated with 10 mM sodium bicarbonate for 10 min.

5. Low temperature fluorescence spectra

Low temperature (77 K) Chl *a* fluorescence emission spectra of the wild type and mutant cells suspended in TAP medium containing 20% glycerol were measured as described in detail in Chapter II. Chlorophyll concentration was 30 µg/ml. Front surface fluorescence measurements were made using a Perkin Elmer LS-5 fluorescence spectrophotometer (Perkin Elmer Ltd., Oak Brook, IL). For details, see Chapter II. The obtained emission spectra were corrected for the wavelength dependence of the photomultiplier sensitivity, but not the monochromator. The emission spectra for different samples were normalized at the 715-nm band.

*6. Flash induced chlorophyll *a* fluorescence decay*

Chlorophyll *a* fluorescence decay in darkness after single-turnover actinic flashes were measured with a laboratory-made multiflash fluorimeter (Kramer et al. 1990). All sample manipulations were done in the dark with a weak background green light (< 0.3 µE/m²·s). Measurements were made as described in detail in Chapter II. Chlorophyll concentration of the samples was 1 µg/ml. Chlorophyll fluorescence decay traces were deconvoluted into three exponential components with the KaleidoGraph™ program. The fitting equation used was: $F_v/F_0 = A_1 \exp(t/\tau_1) + A_2 \exp(t/\tau_2) + A_3 \exp(t/\tau_3)$, where "A" represents the amplitude and "τ" the lifetime of the components. The fast component, A_1 , τ_1 which is in sub-ms range, reflects the characteristics of the component involved in direct

reoxidation of Q_A^- by Q_B (or Q_B^-). The intermediate component, A_2 , τ_2 which is in ms range is assumed to reflect the $[Q_A^-]$ equilibrium, partially controlled by the movement of plastoquinone to PSII without bound Q_B . The slow component, A_3 , τ_3 which is in seconds range, reflects the characteristics of the component involved in the back-reaction between Q_B^- and the S states of the oxygen evolving complex, mostly in the non- Q_B centers (see, Govindjee et al. 1996 and the references therein). As τ_3 is in the range of seconds, in actual regression analyses, it was assumed to be ∞ , thus, $A_3 \exp(t/\tau_3) = A_3$. The errors of the calculated values are normally within $\pm 20\%$.

To investigate differences in DCMU binding for the wild type and the two mutants, various concentrations of herbicide DCMU were added to the sample in complete darkness and samples were subjected to Chl fluorescence decay measurements as above.

7. Steady-state oxygen evolution

Steady-state oxygen evolution in intact *C. reinhardtii* cells was determined polarographically under saturating white light ($4,600 \mu E/m^2 \cdot s$) filtered through a 4% $CuSO_4$ solution in a round-bottom flask, using a Clark-type electrode (Yellow Springs Instrument Co., Yellow Springs, OH). A combination of two electron acceptors, 2,6-dichloro-*p*-benzoquinone (DCBQ) (0.1 mM) and potassium ferricyanide ($K_3Fe(CN)_6$) (1 mM) was used. DCBQ acts as the electron acceptor and the non-penetrating ferricyanide keeps DCBQ in the oxidized state. The measurement was done in the presence of $20 \mu M$ 2,5-dibromo-3-methyl-6-isopropyl-*p*-benzoquinone (DBMIB) in the reaction medium to block electron flow between the plastoquinone pool and PSI (see Trebst 1980). Thus, the effect of CO_2 due to CO_2 -fixing steps could be avoided. The temperature of the measurement was maintained at $25^\circ C$ with a water circulator. The Chl concentration used for oxygen evolution measurements was $10 \mu g/ml$. The reaction medium contains 100 mM sucrose, 10 mM NaCl, 5 mM $MgCl_2$, 20 mM HEPES (pH 6.5), and $2 \mu M$ nigericin.

8. Treatment of arginine specific reagents

To investigate the role of arginines in PSII electron transfer, two arginine-directed chemical modifying reagents phenylglyoxal (Takahashi 1968) and 2,3-butanedione (Riordan 1973) (both purchased from Sigma Chemical Co., St. Louis, MO) were used to study their effects on the steady state oxygen evolution of the *C. reinhardtii* cells. The mixotrophically grown wild type and D1-R257E, M mutant cells were incubated with either 50 mM phenylglyoxal or 5 mM 2,3-butanedione at the room temperature in the reaction buffer as described in the above section. However, the buffer pH was adjusted to 7.0 for optimal results. The reagents were incubated with the cells at room temperature for 2 min. in darkness before measurements. To test whether the reactions by the arginine reagents can be reversed by bicarbonate anions, the phenylglyoxal- or 2,3-butanedione-treated samples were centrifuged at 2000 g for 4 min to remove the inhibitors. The pellet was washed with the above buffer containing 20 mM bicarbonate (pH 7.0) once and resuspended in the same buffer. The samples were incubated with bicarbonate at room temperature for 5 min in darkness before measurements. The above experimental conditions were established through many pilot experiments.

C. Results

1. Site-directed mutagenesis of *psbA* and mutant confirmation

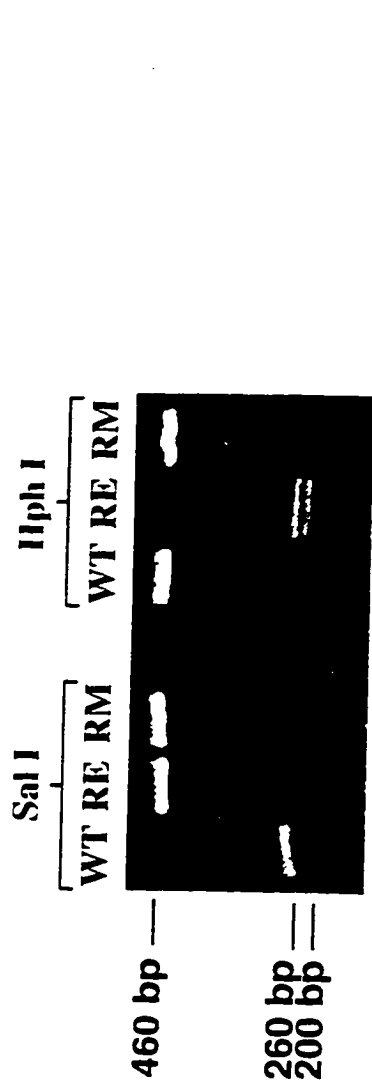
Using a newly developed protocol for site-directed mutagenesis of the D1 protein in *C. reinhardtii* (Minagawa and Crofts 1994) that involves the use of intron-less *psbA* gene, we have mutated D1-R257 into a glutamate and a methionine. These two amino acids with similar sizes in their sidechains but different electrostatic properties compared to arginine were designed to test the role of the positively charged guanido group in bicarbonate binding.

Prior to transformation, the mutagenized plasmid DNAs were sequenced to confirm the presence of both the introduced mutations (data not shown). After transformation, isolated algal transformants were further confirmed for the presence of the mutations. As shown in Fig. 3.2 (top panel), the PCR products (460 bp) of the chloroplast DNA of the transformants (putative mutants and intron-less wild type) were treated with Sal I restriction enzyme. The intrinsic Sal I restriction site at R257 position is confirmed in the wild type (intronless), resulting in 200 and 260 bp digestion fragments. In the putative D1-R257E (RE) and D1-R257M mutants, this site was removed, as expected, as shown by their inability to be cut by Sal I. Furthermore, DNA sequence analysis indicated that D1-R257E mutation should have introduced a new Hph I restriction site. This has also been confirmed in the putative D1-R257E mutant when its PCR product was treated with Hph I restriction enzyme, generating 200 and 260 bp fragments. The wild type and the D1-R257M mutant were not able to be cut by Hph I. The absence of contaminating bands at the 460 bp for the wild type and at 200 and 260 bp for the two putative mutants treated with Sal I and at 460 bp for D1-R257E treated with Hph I also verified the homoplasmy of the *psbA* transformants. No new restriction sites were generated for the D1-R257M mutant. The 460 bp PCR fragments of all the three samples were further sequenced and the presence of the two introduced mutations were confirmed (Fig. 3.2, bottom panel, shown are only the mutant sequences); no other mutations were found.

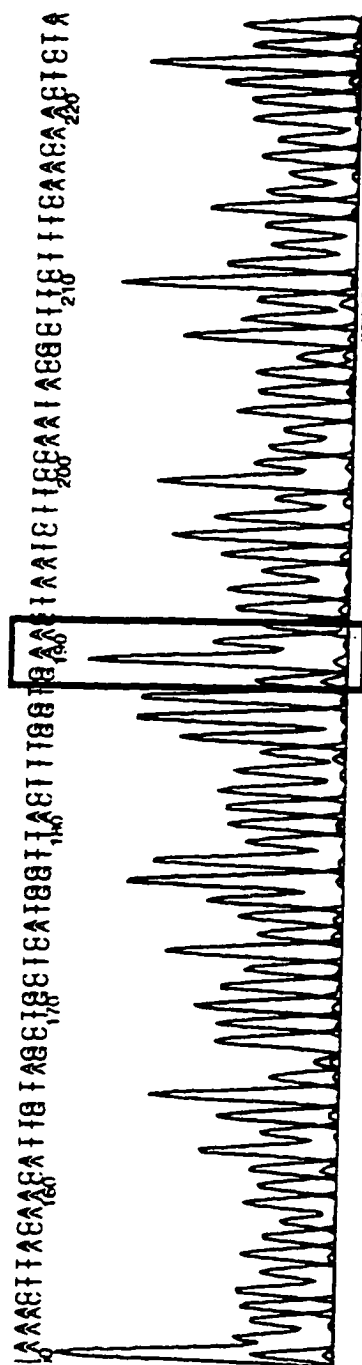
2. Growth characteristics

Photoautotrophic growth in the wild type and the isolated D1-R257E, M mutants were assayed by the optical density of the culture at 750 nm. Fig. 3.3 shows the growth curves of the wild type and the D1-R257E, M mutants in photoautotrophic conditions (in high salt). During the logarithmic growth phase, the doubling time for the wild type is ~12 hrs, and for the mutants 18 and 19 hrs for D1-R257E and D1-R257M, respectively. Thus, the mutations caused ~32-37% inhibition of the photosynthetic growth. However, under

Figure 3.2. Analyses confirming the presence of the introduced D1-R257E, M mutations. The top part shows that a fragment (460 bp) of the intronless *psbA* isolated from chloroplasts of wild type and putative mutants was PCR amplified and treated with Sal I restriction enzyme. Wild type DNA was cut by Sal I producing 200 and 260 bp fragments. However, D1-R257E (RE), M (RM) mutants have this site removed. Furthermore, the D1-R257E mutation introduces a new Hph I site generating 200 and 260 bp fragments. The 460 bp PCR fragments were further sequenced and the presence of the two introduced mutations were confirmed (highlighted by box) and no other mutations were found.



R257E



R257M

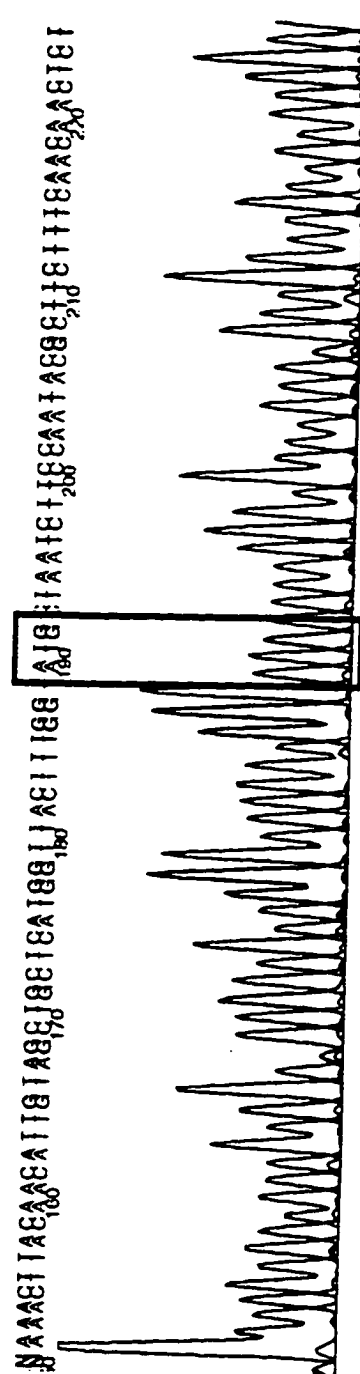
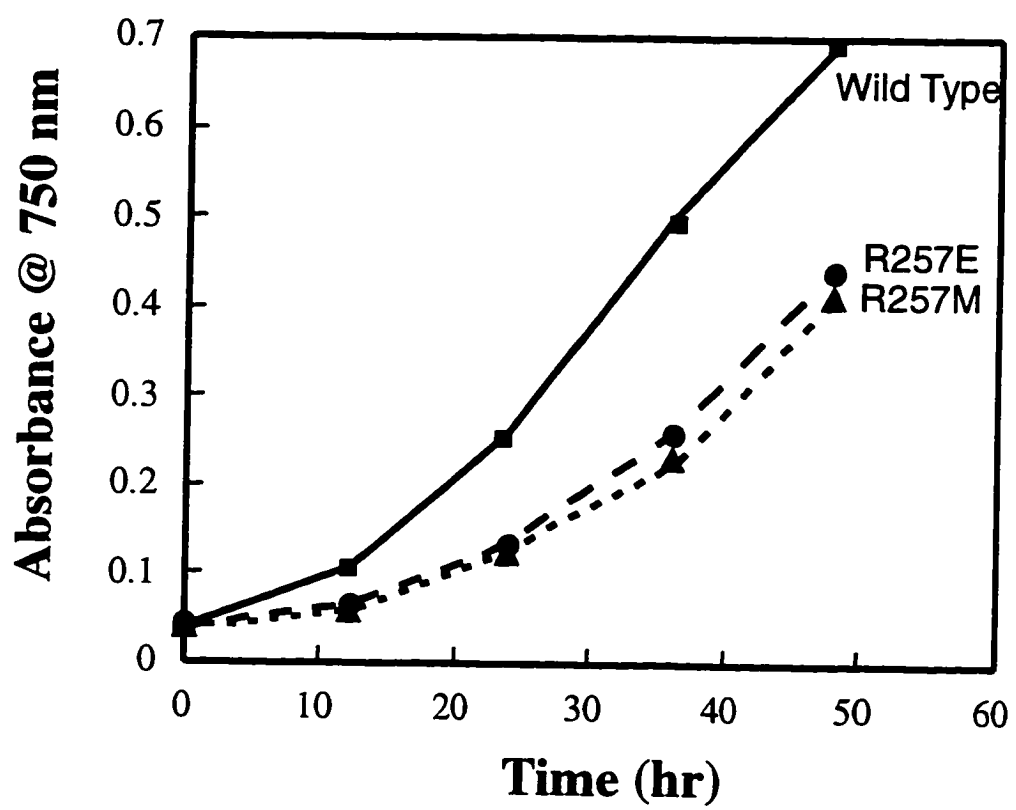


Figure 3.3. Photosynthetic growth determination of the wild type and D1-R257E, M mutants. The algal cells were cultured in a liquid high salt (HS, autotrophic) medium in light ($70 \mu\text{E}/\text{m}^2\text{s}$) and supplied with 5% CO_2 . The growth curve was determined by measuring the optical density of the cell culture at 750 nm. The doubling time for the wild type in the autotrophic condition is ~12 hrs, and for the mutants 18-19 hrs.



heterotrophic growth conditions (in TAP), the wild type and the two mutants have essentially the same rate of growth as the wild type with a doubling time of ~23 hrs.

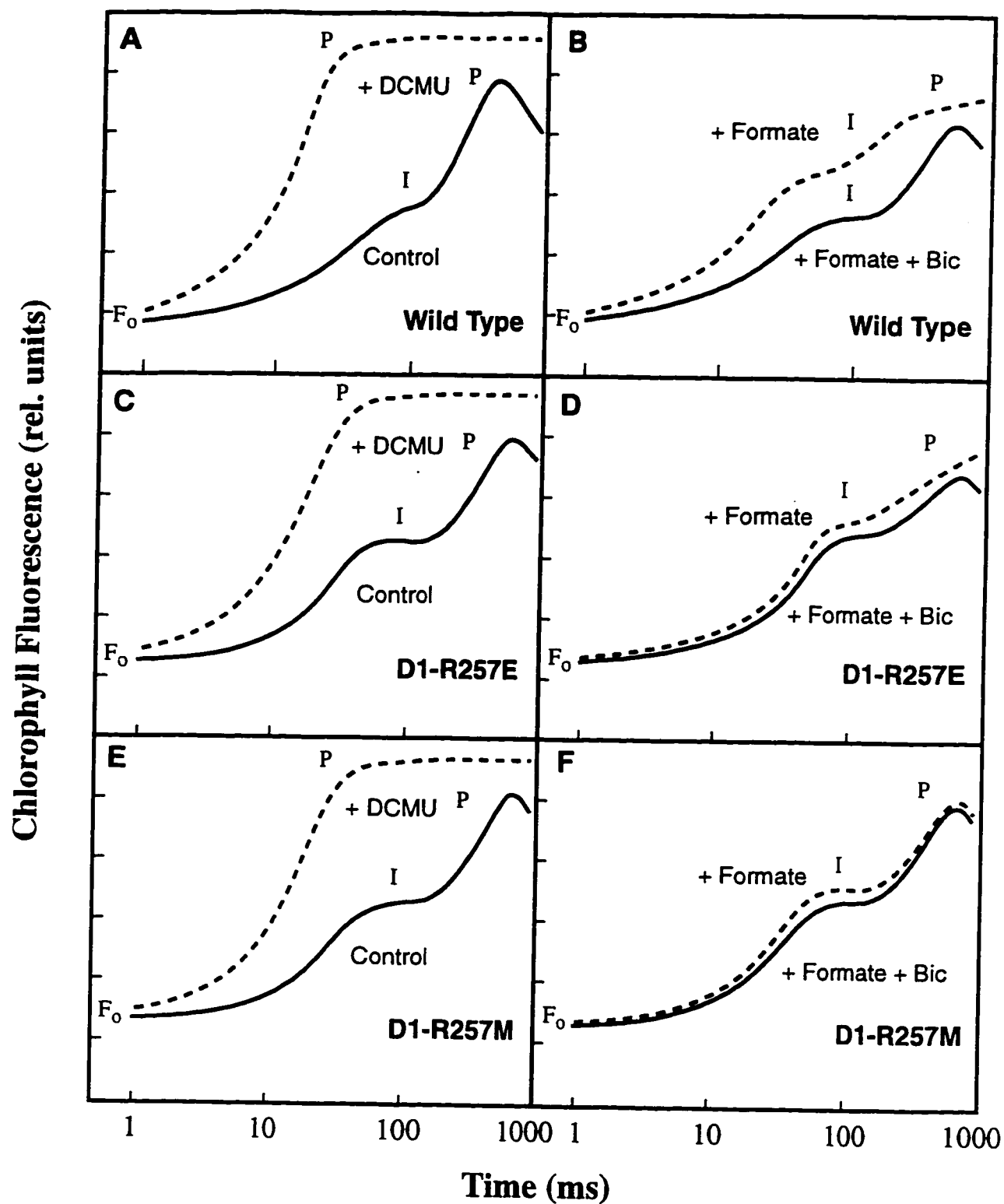
3. Chlorophyll *a* fluorescence induction

To obtain general information on the status of PSII photochemistry of the wild type and the D1-R257E, M mutants, chlorophyll fluorescence induction (up to 1 s) (see *e.g.*, Papageorgiou 1975; Briantais et al. 1986) was measured in the mixotrophically-grown wild type and mutant cells with a pulse-modulated fluorimeter. The induction kinetics of Chl *a* fluorescence of these samples were measured in the absence and the presence of herbicide DCMU, known to block electron flow by displacing Q_B , and in the presence of the bicarbonate analogue, formate, known to inhibit PSII electron transfer, and in the presence of both formate and bicarbonate (Fig. 3.4). The data of the induction kinetics were plotted on the logarithmic time scale, so that different rise components can be made visible. As reviewed in Govindjee (1995; also see Srivastava et al. 1995; Strasser et al. 1995), the first rise (photochemical phase) reflects the reduction of Q_A to Q_A^- but it also includes the influence of the S-states. The later rise to the P level is due to the filling up of the plastoquinone pool.

Figures 3.4A and 3.4B show the fluorescence induction kinetics of the wild type cells. The control curve shows the normal O to P rise. Under the experimental conditions used here, the rise to I is attained in about 50 ms, while the total time for reaching the final peak (Fp) is ~400 ms. The addition of DCMU (10 μ M), blocking the reoxidation of Q_A^- , caused the Chl fluorescence to rise from F_0 to F_m in only 30 ms, merging the various phases into one phase. The ratio of F_v/F_m which represents the maximum yield of PSII photochemistry in the wild type is 0.83 in agreement with previous results for the wild type *C. reinhardtii* (Srivastava et al. 1995).

The formate inhibition of the PSII electron transfer and subsequent recovery by the addition of bicarbonate have been studied extensively in the past (for reviews, see

Figure 3.4. Chlorophyll *a* fluorescence transients (as a function of time of illumination) of the mixotrophically-grown wild type and D1-R257E, M mutants in the absence and the presence of 10 μ M DCMU and in the presence of formate, and formate plus bicarbonate measured with a PAM-2000 fluorimeter. Each of the data points is an average of 10 raw data points measured at 300 μ s intervals. The data are plotted on the logarithmic scale. (A) The transient of the wild type cells in the absence and presence of DCMU. (B) The transients of wild type treated by formate and formate plus bicarbonate. (C) The transient of D1-R257E mutant in the absence and presence of DCMU. Note the elevated F_0 level. (D) The transients of D1-R257E mutant treated by formate and formate plus bicarbonate. (E) The transient of D1-R257M mutant in the absence and presence of DCMU. (F) The transients of D1-R257M mutant treated by formate and formate plus bicarbonate. In all measurements, the [Chl] of the samples was 5 μ g/ml, and the actinic illumination was 470 μ E/m²·s.



Blubaugh and Govindjee 1988a; Govindjee and van Rensen 1993). The results of this study show that, formate treatment (25 mM) of the wild type *C. reinhardtii* cells (Fig. 3.4B) results in a faster rise of the initial rise phases compared to the control indicative of a decrease in the electron transfer beyond Q_A . However, the I-P rise is significantly slowed down (the time reaching Fp is > 1 s) compared to the control suggesting the process of filling up the plastoquinone pool is inhibited. The addition of bicarbonate (10 mM) significantly restored the fluorescence kinetics close to the control level.

Chlorophyll *a* fluorescence induction measurements were also done with the D1-R257E, M mutants in the absence and presence of DCMU and in the presence of formate and formate plus bicarbonate (Figs. 3.4C-3.4F). The two mutants appear to have a higher rate of fluorescence rise in the O-I phase suggesting a moderate decrease in the electron transfer beyond Q_A^- caused by the mutations (Figs. 4C and 4E). The total time reaching the Fp is also slightly slower (~500 ms) compared to the wild type indicating a slight modification on the filling up the plastoquinone pool step. The addition of DCMU caused the two mutant samples to reach an Fm similar to that in the wild type. However, significant increase in Fo (~40%) was consistently observed in the mutant samples. This increase was confirmed by other crucial measurements (see later sections). The elevated Fo lowers the Fv/Fm level for the two mutants: 0.77 for D1-R257M and 0.75 for D1-R257E. Thus, the mutants have ~10% reduction in the calculated maximum yield of PSII photochemistry compared to the wild type.

The largest differences observed between the mutants and the wild type are the different sensitivity to the formate and formate plus bicarbonate treatments (Figs. 3.4D and 3.4F). The formate treatments of the two mutants only result in a very slight increase in the O-I phase compared to the control. Further, the addition of bicarbonate does not cause significant changes from the formate treatments. The results indicate a very low sensitivity of the mutant PSIIs to formate inhibition suggesting a modified binding capability of

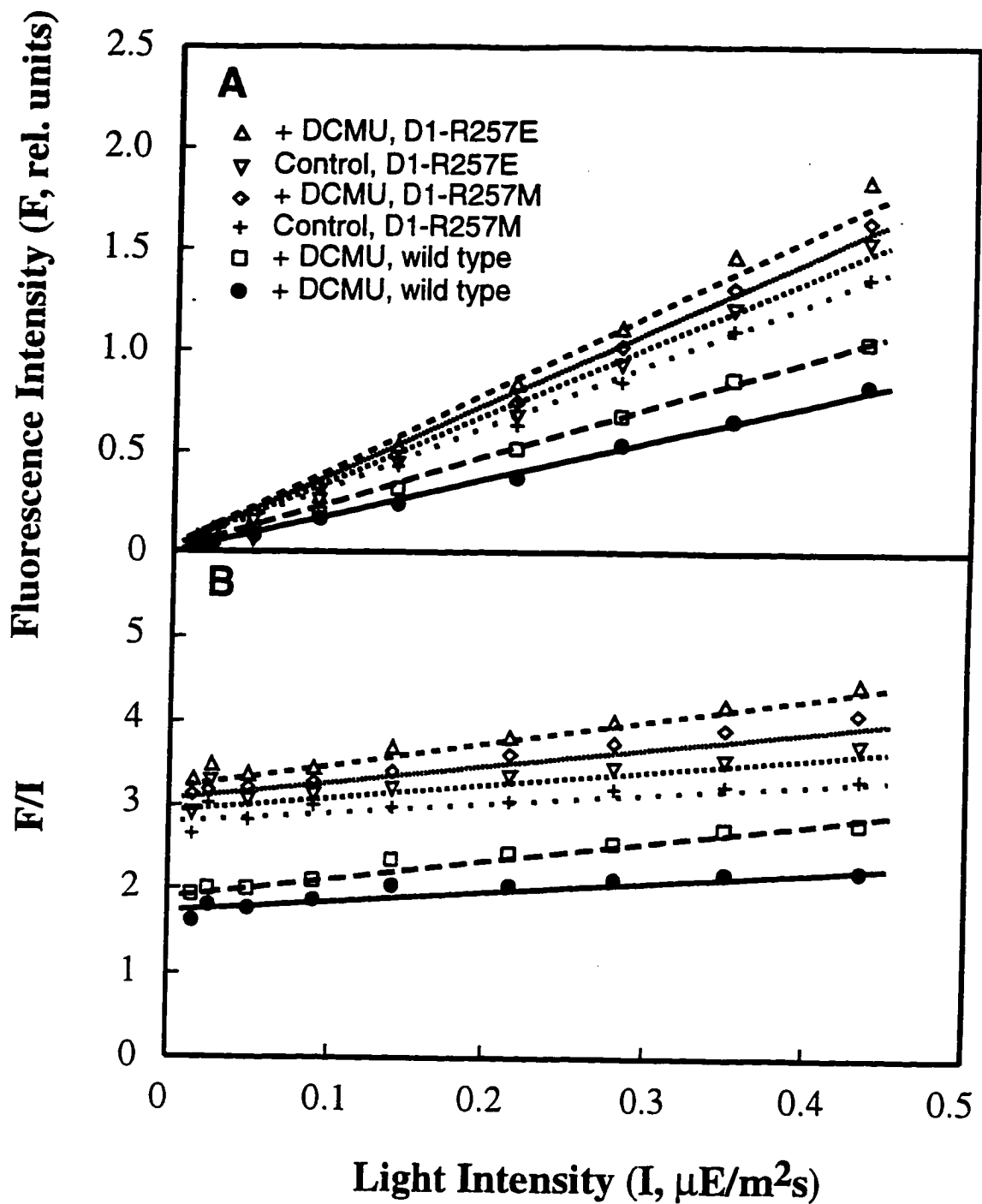
mutant PSIIIs for the formate/bicarbonate binding. The conclusion will be further tested by other experiments in later sections.

4. F_0

The above conclusion of lowered yield of photochemistry in the two mutants is dependent upon the measured F_0 being true F_0 . The two D1-R257 mutant samples have a consistently elevated F_0 ($> \sim 40\%$) compared to that of the wild type. As F_0 is the minimal level of chlorophyll fluorescence originating from antennae, in competition to the energy transfer to the PSII reaction center, an increase in F_0 may indicate a decreased excitation energy transfer to the active PSII reaction center, possibly due to a disconnection between antennae and the reaction center II, or due to the existence of inactive PSII (Lavergne and Briantais 1996) incompetent in trapping excitons arriving from antennae, which then can return to antennae and fluoresce. It may also be possible that there is an increase in the $[Q_A^-]$ in the dark or in the relative ratio of the antennae/PSII reaction (Vermaas et al. 1994). Although these last two hypotheses may not be the favored ones, the available data do not distinguish between the various possibilities. However, as shown in Fig. 3.4, the wild type cells display a small increase of F_0 when measured in the presence of DCMU which blocks the electron transfer beyond Q_A^- ; this may indicate that the measured F_0 level may not be all true F_0 . This slight increase in measured F_0 in the presence of DCMU is thought to be due to a small actinic effect of the measuring beam of the fluorimeter, or due to $[Q_A^-]$ in the dark. This small effect may become prominent when the process of Q_A reoxidation is decreased in the mutants. Thus, the measured F_0 required further investigation.

I conducted independent measurements of F_0 for the wild type and mutant cells. At very low light intensities of the measuring beam, fluorescence (F_0) intensity is shown to be a linear function of light intensities (I) (Fig. 3.5A). The quantum yield (F_0/I) remains constant as it should for true F_0 which should be independent of photochemistry (Fig. 3.5B) (see *e.g.*, Ref. Munday and Govindjee 1969). Further, at such low light intensities,

Figure 3.5. Measurements of minimal (baseline) fluorescence F_0 at low light intensities. (A) Baseline Chl *a* fluorescence (F_0) as a function of light intensities in the low intensity range, in the presence and the absence of 10 μ M DCMU. Measurements of the wild type *C. reinhardtii* and D1-R257E, M mutant cells were made as in Materials and Methods (section 2.3). (B) The quantum yield of F_0 , or the ratio of fluorescence intensity to the light intensity of the measuring beam, basically does not change with the light intensities indicating that the measured F_0 is the true F_0 . It is further confirmed by the absence of any significant effect of DCMU.



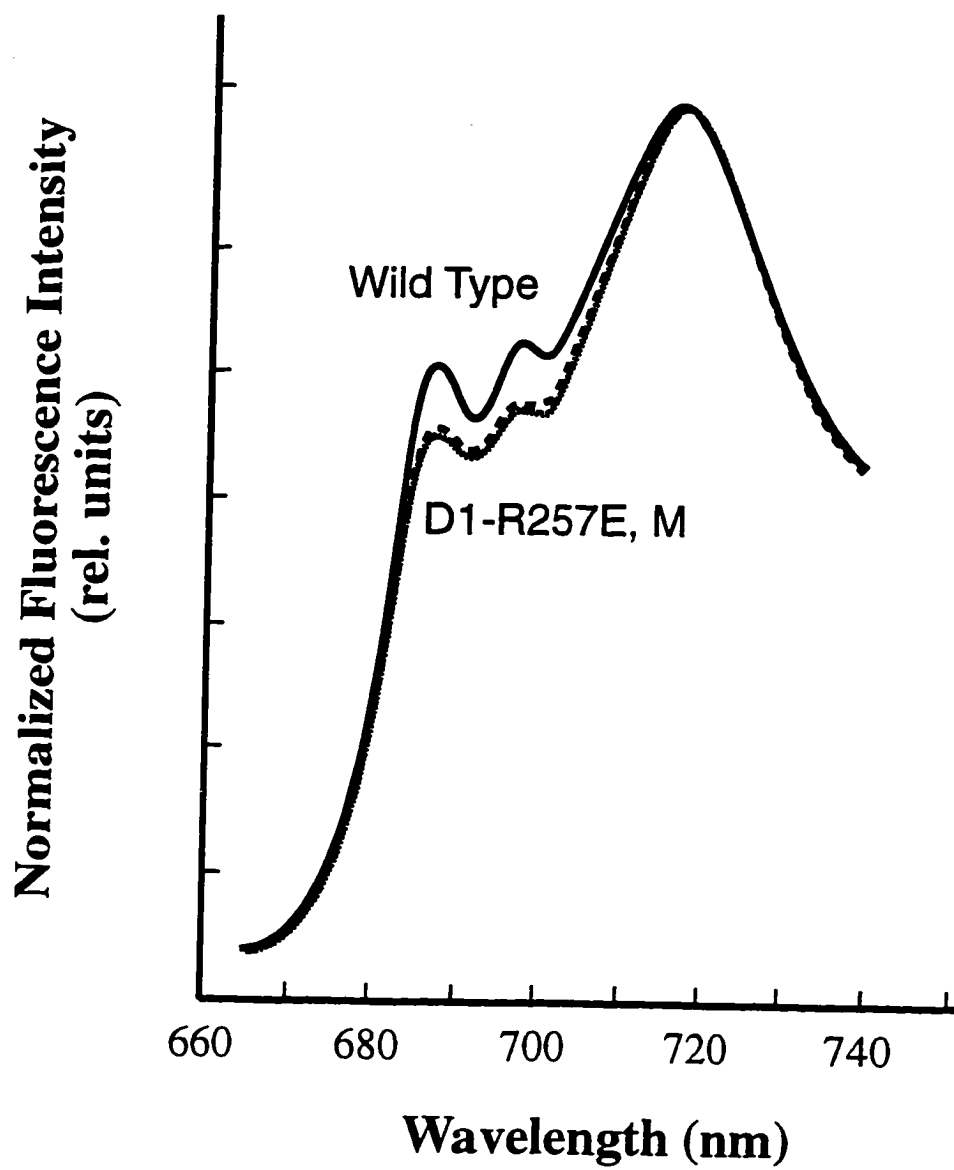
addition of DCMU did not cause significant increases in the measured F_0 levels, as it should since all $[Q_A]$ remains essentially unchanged. The F_0 of both mutants was consistently higher than that in the wild type (~50%). Thus, F_0 of the mutant is indeed higher than the wild type, and, F_v is therefore, indeed reduced in the mutant.

5. Low temperature fluorescence emission spectra

Based on the above measurements that indicate a lowered quantum yield of photochemistry and an elevated F_0 (indicating a lowered net excitation energy transfer from antennae to the PSII reaction center), it is reasonable to consider that the mutations on D1-R257 may have caused alterations on the structure and function of the PSII complex. As one of the means to investigate this effect, low temperature (77 K) fluorescence emission spectra of the wild type and D1-R257E, M mutants were measured (Fig. 3.6). At 435 nm excitation, PSII has two distinct emission bands at 685 nm (F685) and 695 nm (F695). F685 is thought to originate mostly from the CP43 polypeptide, and F695 from CP47 polypeptide (see Nakatani et al. 1984; Govindjee and Satoh 1986; Dekker et al. 1995). Haag et al. (1993) suggest that the intensity of these two bands, especially F695, correlates well with the level of the PSII core proteins in the mutants they examined and can be used as an indicator for the concentration of PSII. However, I realize that the intensities of F685 and F695 must also be influenced by the efficiency of excitation energy transfer from peripheral antenna chlorophylls to core antennae and from the core antennae to the PSII reaction center.

Assuming that no changes have occurred in PSI, analysis of the un-deconvoluted F685 and F695 bands (Fig. 3.6) shows that their intensities in both mutants were consistently reduced by ~10% compared to the those of the wild type. This result may indicate a reduction in these PSII antenna complexes *provided* the mutations had not caused changes in excitation energy transfer among these complexes and the PSII reaction center. Since there were assumed to be no changes in the CP43 and CP47 genes, this reduction

Figure 3.6. The 77 K chlorophyll *a* fluorescence emission spectra of the *C. reinhardtii* wild type and the D1-R257E, M mutant cells. Emission spectra of the samples (30 µg Chl/ml with 20% glycerol) were measured with a front-surface optics (excitation at 435 nm; corrected for the wavelength dependence of the sensitivity of the photodetector) and normalized to the 715-nm peak. Both F685 (from CP43) and F695 (from CP47) bands were lowered in the mutant with respect to F715 band (from PSI).

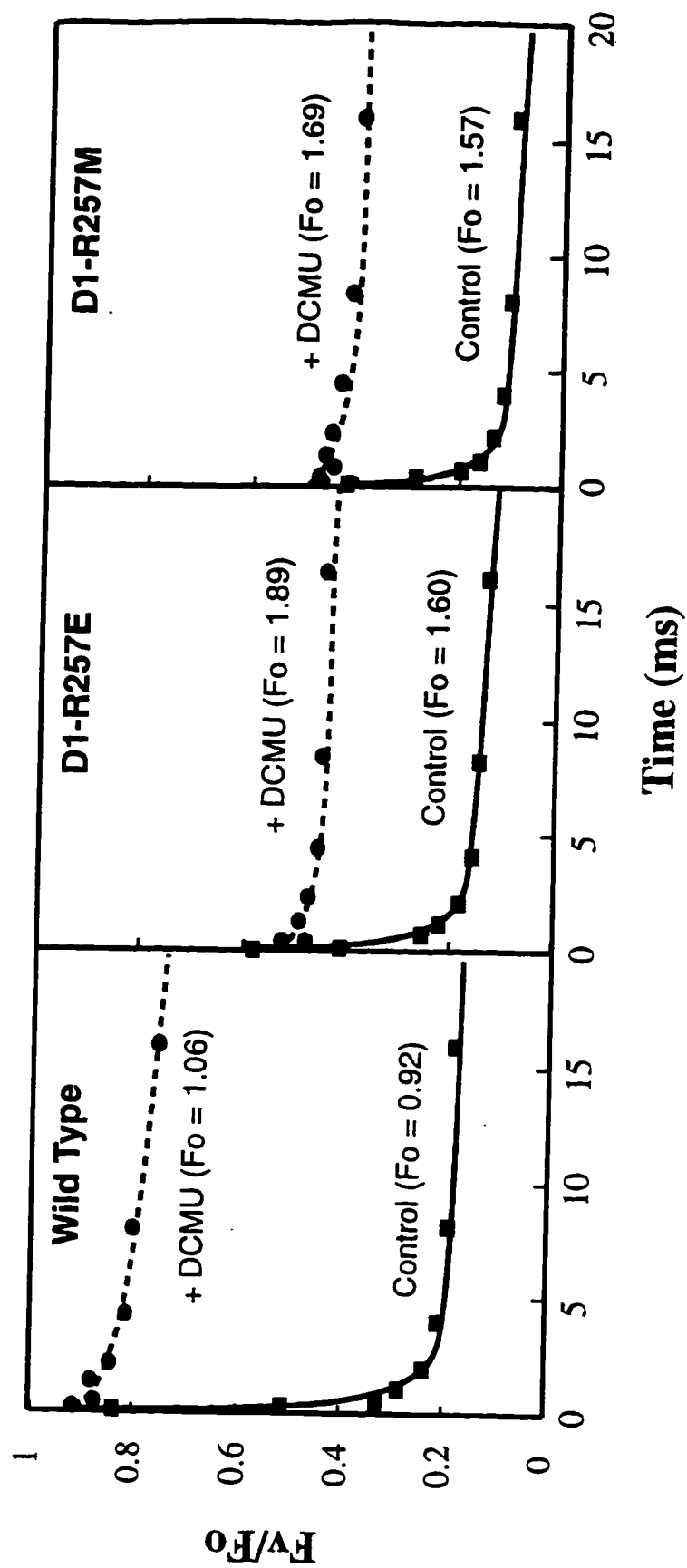


could be partly attributed to the changes in the stability of the D1/D2 complexes to which these inner antenna proteins are associated, and partly to the changes in the excitation energy transfer to and away from the PSII reaction center. Possible destabilization of PSII by the mutations on D1-R257 was further supported by the measurements of the mutant thylakoids which were found to have a complete blockage of electron transfer from Q_A^- to the plastoquinone pool, suggesting that the two mutants have a high sensitivity to biochemical preparations (data not shown).

6. Characterization of kinetics of $Q_A \rightarrow Q_B$ and DCMU binding

To further determine the mutational effects on the PSII electron transport from Q_A^- to the plastoquinone pool, Chl *a* fluorescence decay in the microsecond to millisecond time scale, after a series of single turnover flashes, was measured with the wild type and D1-R257E, M mutant cells in the absence or presence of DCMU (1 μ M). The kinetic measurements were done with 1 μ g Chl/ml samples. Only the second flash kinetic traces are shown (Fig. 3.7) which would have corresponded only to the electron flow from Q_A^- to Q_B^- , if all PSIIs started in dark with 100% Q_B . However, in unmodified intact cells, the ratio of Q_B to Q_B^- in darkness is close to 1 (see *e.g.* Xu et al. 1989). Q_A^- to Q_B and Q_A^- to Q_B^- reactions are not easily separable unless special efforts are made, such as the addition of excess *p*-benzoquinone. As shown in Fig. 3.7, the mutant cells have a significant reduction in the maximal ratio of F_v/F_o . The Chl *a* fluorescence yield change with time for the two mutant samples appears to be similar to that of the wild type. However, more accurate deconvolution studies indicate differences between the wild type and the two mutants. The lifetime of the fast component τ_1 is 90 μ s, whereas τ_1 of the D1-R257E and M mutants are 180 μ s and 160 μ s, respectively. This slowing down of fluorescence decay is more obvious when they are plotted on an expanded scale (up to 2 ms) (see later). There is ~50-55% decrease in the kinetics of electron flow from $Q_A \rightarrow Q_B$ in the mutants. This is confirmed by thermoluminescence experiments when almost equal $S_2Q_A^-$ (Q) and $S_2Q_B^-$

Figure 3.7. Flash-induced chlorophyll *a* fluorescence decay kinetics of the wild type and the D1-R257E. M mutant cells, treated with or without 1 μ M DCMU. Kinetic measurements were made with 1 μ g Chl/ml samples. Only the second-flash kinetic traces are shown. Note the elevated F_0 and the lowered levels of maximum F_v/F_0 level.



(B) bands were observed in D1-R257M cells after one flash (unpublished data of Govindjee, 1996). In agreement with the literature (see review by Vass and Govindjee 1996), the wild type had only B band under the same experimental condition.

The addition of 1 μ M DCMU almost fully inhibits the electron transfer in the wild type and in the mutant cells. As shown in Fig. 3.7, the measured F_0 levels of the mutants are ~70% higher than the wild type, in line with the results from the fluorescence induction studies (Fig. 3.4). To further quantitate the sensitivity of the wild type and the mutants to DCMU, the increase in variable Chl *a* fluorescence yield was determined as a function of DCMU concentration (Fig. 3.8). The fluorescence yield at 1 ms after the fifth saturating flash was plotted as a function of DCMU concentration. The ordinate of the graph is normalized by the measured fluorescence yield at the fully bound state. The DCMU concentration achieving the midpoint of the normalized F_v can be considered the dissociation constant (Cao et al. 1992). The calculated DCMU dissociation constant for the wild type is 54 nM, D1-R257E 47 nM, and D1-R257M 62 nM. However, given the errors in the raw data, the three constants are not statistically different from each other. The results suggest that the DCMU binding niche is not significantly altered by the mutations on D1-R257. This may be surprising as the residue is considered to be near the Q_B niche (see PSII three dimensional models in Chapter IV and IV) and, as presented in this paper, the mutations have somewhat inhibited photosynthetic growth, electron transfer and PSII photochemical yield. Thus, the cause of the phenotypic changes is beyond the modification of the DCMU binding pocket.

7. Effects of bicarbonate depletion on the kinetics of $Q_A \rightarrow Q_B$ electron transfer

Using Chl *a* fluorescence decay as a tool, the effect of bicarbonate depletion by formate in the wild type and the two mutants was further characterized. As shown in Fig. 3.9, the Chl *a* fluorescence decay kinetics at the second flash of the wild type is significantly inhibited by the addition of 25 mM formate. The addition of 10 mM

Figure 3.8. Determination of DCMU binding in the wild type and the D1-R257E, M mutants using normalized variable fluorescence yield (F_v/F_o) as a function of DCMU concentration. The Chl a fluorescence yield was measured at 1 ms after five actinic flashes spaced 1.5 s apart. No significant differences are found for the dissociation constant values of DCMU (47-62 nM) for these three samples.

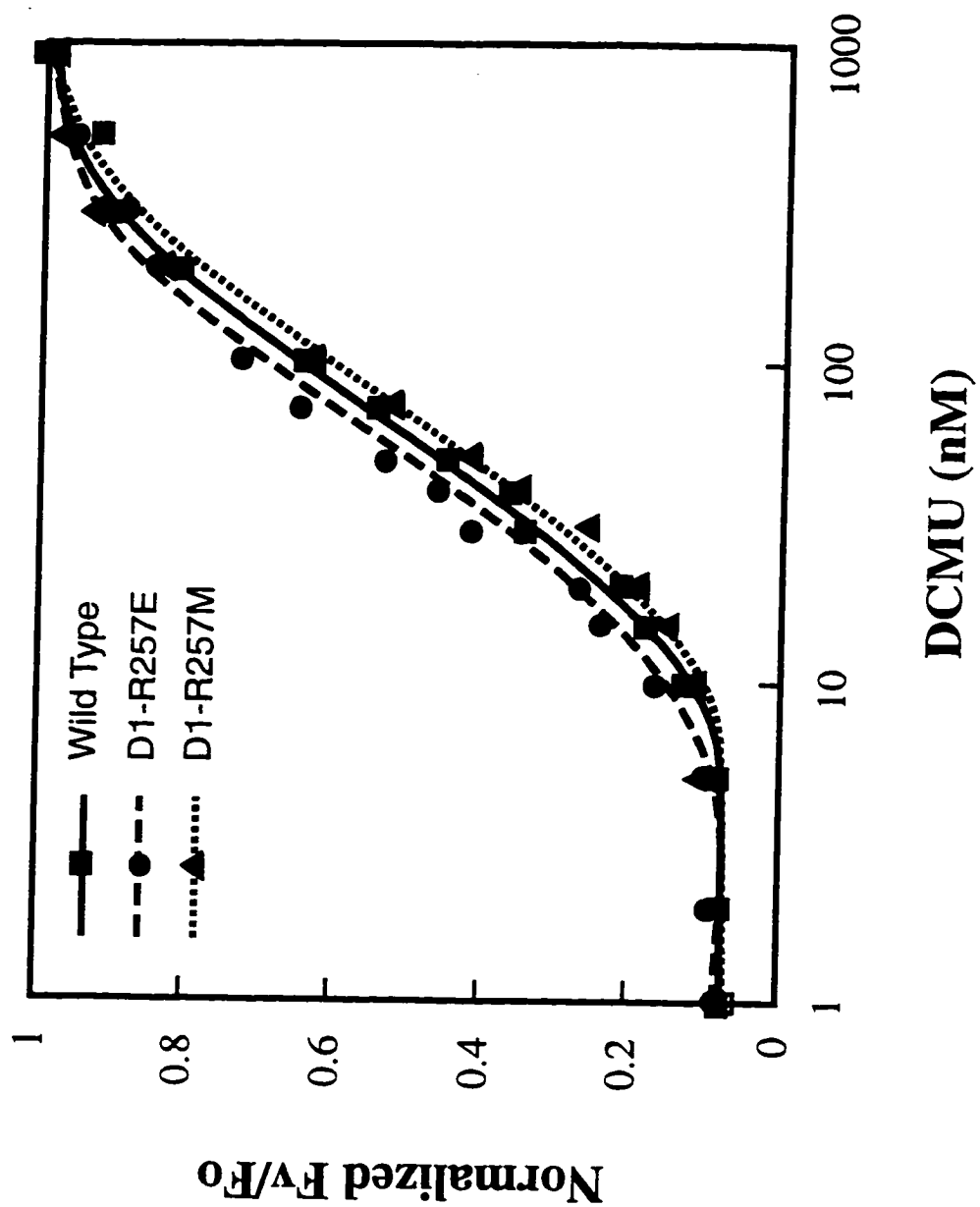
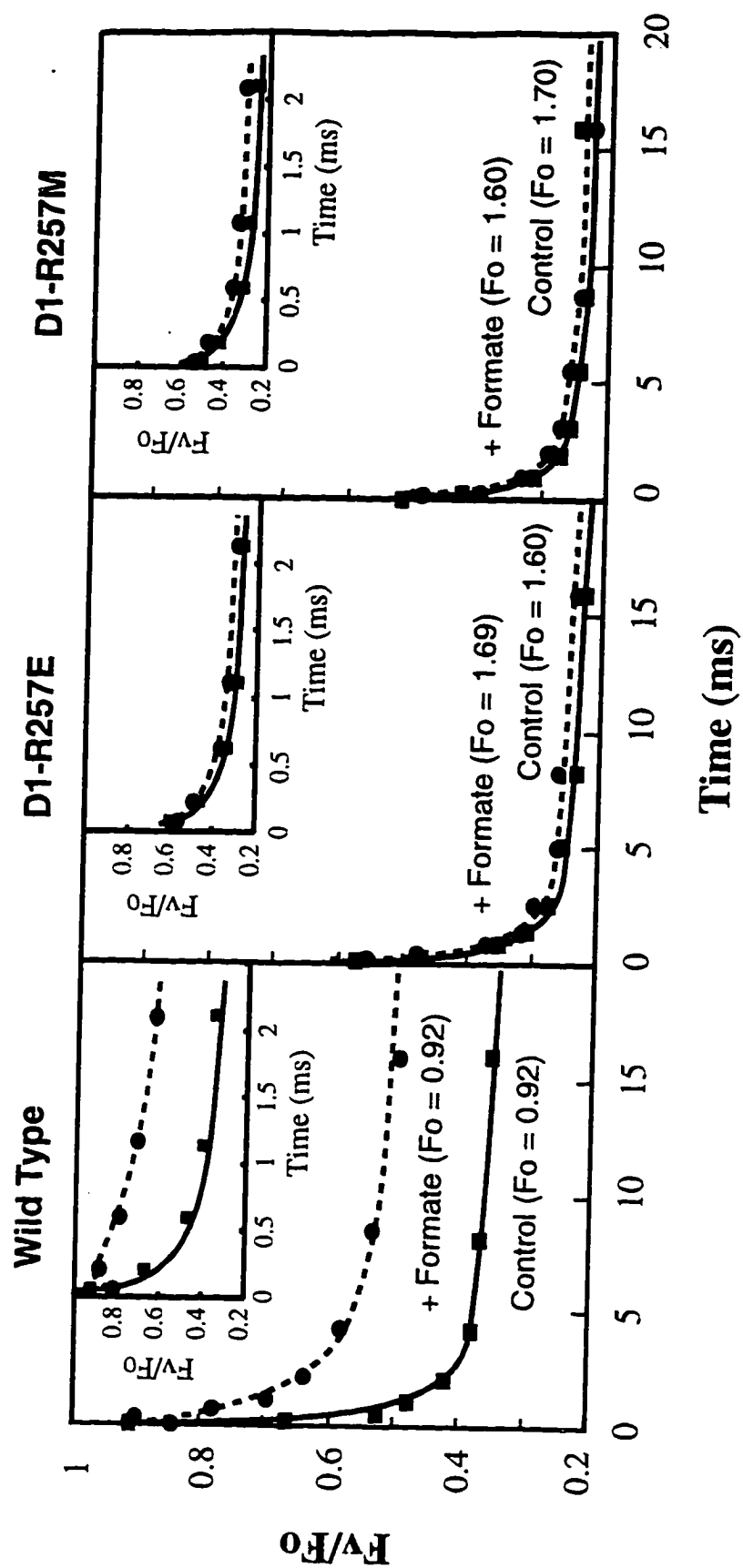


Figure 3.9. Chlorophyll *a* fluorescence decay kinetics of the wild type and D1-R257E, M mutants without formate (control) or treated with formate (25 mM). Only the second flash kinetic traces are shown. The insets with the fluorescence decay plotted on an expanded scale (up to 2 ms) show more clearly the slowing down of fluorescence decay in the mutants (control) compared to the wild type. Formate blocks electron flow from $Q_A^- \rightarrow Q_B^-$ in the wild type, but not in these two mutants.

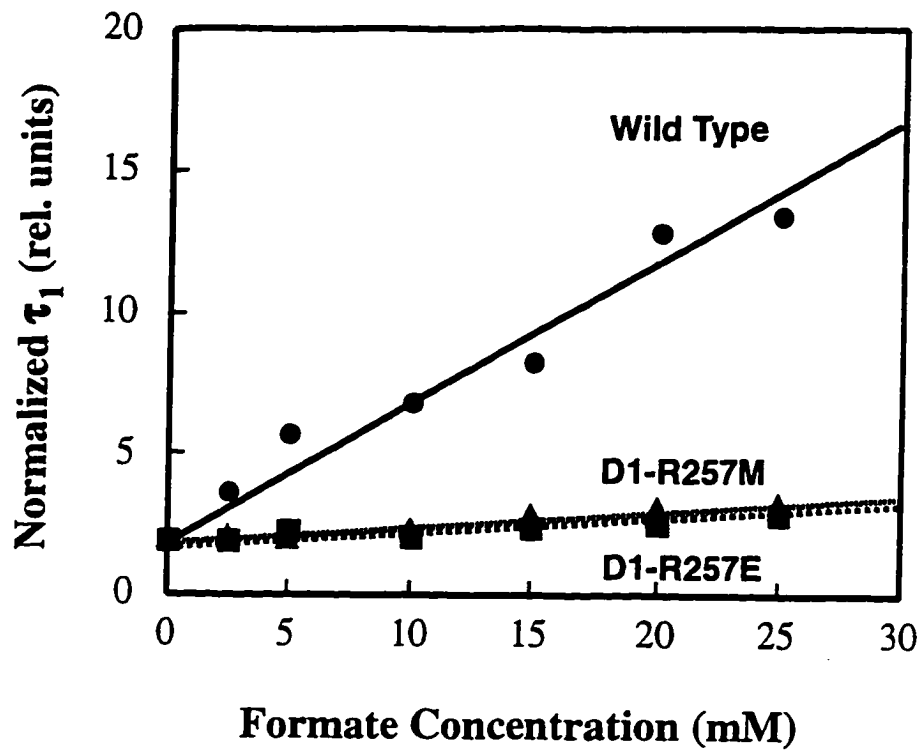
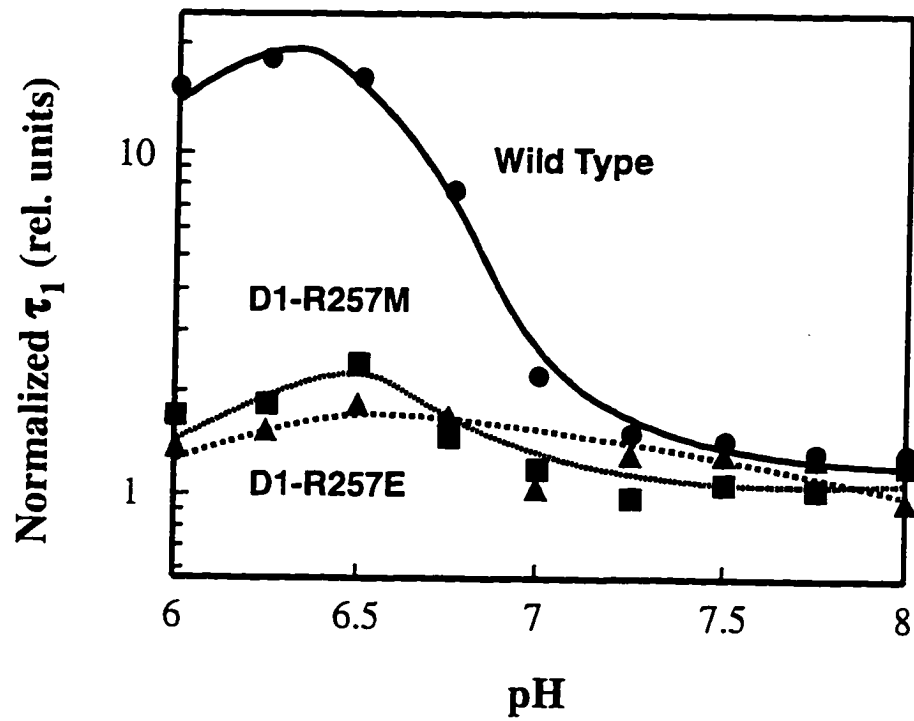


bicarbonate is able to fully restore the inhibition (data not shown). The lifetime for the fast component of the decay (τ_1) of the wild type is 90 μ s in the control and 1.3 ms in the presence of 25 mM formate, a 14 fold effect. This clearly shows a slowing down of the Q_A^- to Q_B^- electron flow. However, both the mutants show very little sensitivity to the inhibition by formate. The lifetime (τ_1) of D1-R257E is 180 μ s in the control compared to 340 μ s after being treated with formate. The τ_1 of D1-R257M is 160 μ s in the control and 420 μ s in formate treated sample. There are only 2-2.5 fold effects. The slowing down of fluorescence decay of the mutants in the control group compared to the wild type is shown more clearly in the expanded time scale (see insets of Fig. 3.9). Therefore in these two mutants, formate does not effectively block the $Q_A^- \rightarrow Q_B^-$ electron flow.

Further, the inhibition of the $Q_A \rightarrow Q_B$ kinetics by formate was titrated at various concentrations (Fig. 3.10). The relative lifetimes of the first component (τ_1) after two flashes are plotted as a function of formate concentration, when the τ_1 of the control is assumed to be 1. The data were fitted with simple linear regression (Fig. 3.10A). The regression equation for the wild type is $y = 2.54 + 0.45 x$; for the D1-R257E, $y = 1.80 + 0.044 x$; and D1-R257M, $y = 1.88 + 0.048 x$. If the plastoquinone reduction reaction measured in this assay is assumed to be a quasi-equilibrium enzymatic reaction inhibited by formate, Fig. 3.10A can be considered a Dixon plot with the lifetimes equivalent to the reciprocals of the rate of the reaction. The apparent dissociation constant (K_i) of formate can be calculated from the negative intercept of the regression lines on the X-axis (see Segel 1975). In this way, the calculated K_i for the wild type is 5.6 mM, for D1-R257E 40.9 mM, and for D1-R257M 39.5 mM. Judging from this parameter, there is an ~8 fold decrease in formate binding in these two mutants compared to the wild type.

To study the pH effect on the bicarbonate depletion, the formate inhibition reaction was titrated at various pHs (from 6 to 8) after the addition of 25 mM formate. The resulting decay curves after the second flash were deconvoluted as described in the previous section. The lifetimes of the first component (τ_1) of the control at specific pHs are set to arbitrarily

Figure 3.10. Effect of formate inhibition at various concentrations and pHs for the wild type and the mutants. (A) Chl *a* fluorescence decay analyses after two actinic flashes of the wild type and D1-R257E, M mutant cells treated with various concentrations of formate. The resulting decay curves were deconvoluted into three exponential components (see Materials and Methods). The lifetime of the first component (τ_1) of the decay curve after the second flash, corresponding only partially to the kinetics of Q_A^- to Q_B^- , is depicted as a function of formate concentration when the τ_1 of the control is assumed to be 1. The τ_1 of the wild type in the control is 90 μ s. The τ_1 of D1-R257E in the control is 180 μ s. The τ_1 of D1-R257M in the control is 160 μ s. (B) The Chl *a* fluorescence decay kinetic analyses for the wild type and D1-R257E, M mutants at various pHs with or without the addition of formate (25 mM). The resulting decay curves after the second flash were deconvoluted into three exponential components as above. The lifetimes (τ_1) of the fluorescence decays curves of the control are set to a value of 1. The normalized decay lifetimes after formate treatment are depicted as function of pH. The optimum pH for formate inhibition for the wild type is 6.25. The formate inhibitory effect in the wild type is only effective at pH below 7. The D1-R257E, M mutants did not show significant sensitivity to bicarbonate depletion at all the pHs investigated.

A**B**

read 1. No significant variations of the τ_1 values of the control group of each sample were observed for different pHs used here (data not shown). The normalized τ_1 s after the formate treatments are plotted as a function of pH (Fig. 3.10B). For the wild type, the optimum formate effect was reached at an acidic pH (6.25) where a ~15 fold of inhibition results. At above the neutral pH, formate inhibits the electron transfer reaction at a much lower efficiency in the wild type. However, the D1-R257E, M mutants did not show significant inhibition to bicarbonate depletion at all the pHs investigated (max. inhibition was ~2.5 fold).

8. Bicarbonate-reversible formate inhibition of the PSII electron transfer

Steady-state oxygen evolution of the *C. reinhardtii* cells (Hill reaction with DCBQ and ferricyanide) which directly measures the electron transfer by PSII was performed with the wild type and the mutants cell samples. As shown in Table 3.1, the electron transfer of the wild type was inhibited by ~85% after the treatment with 25 mM formate, and most of the inhibition was reversed by the addition of bicarbonate. The rate of electron transfer in the D1-R257E, M mutants are ~60% of the wild type level, which is consistent with the measurements on the photosynthetic growth in a previous section (Fig. 3.3) and fluorescence decay measurements (Figs. 3.7 and 3.9). The low sensitivity to formate inhibition in the D1-257E, M mutants is further confirmed. There is only 15-25% decrease after the formate treatment in both the mutant samples. The relative extent of inhibition in these two mutants appears to be slightly larger than what was observed in the above fluorescence decay measurements. This minor inconsistency was attributed to the fluorescence decay measurements not being a direct indicator of electron transfer or to natural variations among samples.

Table 3.1. Steady-state oxygen evolution of the mixotrophically grown wild type and D1-R257E, M mutant cells. Reaction mixture contained 100 mM sucrose, 10 mM NaCl, 5 mM MgCl₂, 20 mM HEPES (pH 6.5), 2 μ M nigericin, 0.1 mM DCBQ, 1 mM K₃Fe(CN)₆ and 20 μ M DBMIB. Measurements were done at 25°C. Chl *a* concentration was 10 μ g/ml. Twenty-five mM formate and 25 mM formate plus 10 mM bicarbonate treatments were done according to the Materials and Methods (section 2.4). Values (μ mole O₂/mg Chl·hr) are averages and standard errors of three separate measurements.

	Control	+ Formate	+ Formate, + Bicarbonate
Wild Type	189.7 \pm 6.5	27.7 \pm 1.5	160.9 \pm 8.5
D1-R257E	121.0 \pm 3.3	91.6 \pm 3.1	117.7 \pm 0
D1-R257M	117.8 \pm 6.6	101.4 \pm 3.3	114.5 \pm 3.3

9. Inhibition of PSII electron transfer by arginine specific reagents and recovery of inhibition by bicarbonate

Certain dicarbonyl reagents such as phenylglyoxal and 2,3-butanedione are able to specifically modify arginine residues (Takahashi 1968; Riordan 1973) and have been successfully used in many protein systems to probe arginine residues bound to anionic substrates (for review, see Lundblad 1991). The high specificity of these reagents is due to fact that arginine residues bound to anions tend to have lower pK_a than those arginine residues in other regions of the protein (Patty and Theze 1980). To study the effect of the arginine-specific reagents on the PSII electron transfer, I applied phenylglyoxal and 2,3-butanedione to the above Hill reactions and tested whether there is a reversal or competitive effect by bicarbonate anions.

As shown in Table 3.2, the addition of phenylglyoxal (50 mM) and 2,3-butanedione (5 mM) decreases the steady-state oxygen evolution in the wild type by ~45%, indicating that certain arginine residues in PSII are reactive to the two dicarbonyl reagents and that the interactions between the arginines and the reagents play an inhibitory role in oxygen evolution. Very interestingly, incubation of the phenylglyoxal- or 2,3-butanedione-pretreated samples with excess amount of bicarbonate (20 mM) reversed most of the inhibition (~90% of the control level). This indicates that bicarbonate is able to compete with the arginine-specific reagents and to restore the electron transfer, suggesting that the binding sites for bicarbonate overlap those for the arginine specific reagents. The results strongly suggest arginine residues in PSII are involved in bicarbonate binding. Thus, this provides evidence for the general involvement of arginines in PSII electron transfer which is to associate it with bicarbonate. However, the two mutations on D1-R257 almost abolish the sensitivity of PSII to the two arginine-specific inhibitors. This indicates the loss of binding sites for the dicarbonyl reagents in these two mutants. The addition of bicarbonate to these samples nearly did not cause significant changes in the electron transfer activity for

Table 3.2. Steady-state oxygen evolution measurements of mixotrophically grown wild type and D1-R257E, M mutant cells treated with arginine-specific reagents phenylglyoxal and 2,3-butanedione and subsequently with bicarbonate. The experimental conditions were similar as in Table 3.1, the buffer pH was 7.0. Phenylglyoxal (50 mM) and 2,3-butanedione (5 mM) were incubated with the cells at room temperature for 2 min in darkness before measurements. The bicarbonate reversal experiments were done by transferring the phenylglyoxal- or 2,3-butanedione-treated samples to the above buffer containing 20 mM bicarbonate and by incubating them for 5 min. in darkness. Values ($\mu\text{mole O}_2/\text{mg Chl}\cdot\text{hr}$) are averages and standard errors of three separate measurements.

	Control	+ phenyl- glyoxal	+ bicarbonate after phenyl- glyoxal pre- treatment	+ 2,3- butanedione	+ bicarbonate after 2,3- butanedione pretreatment
Wild Type	199.3 \pm 12.2	106.2 \pm 8.1	173.3 \pm 16.7	112.7 \pm 16.2	175.5 \pm 5.3
D1-R257E	113.8 \pm 4.6	106.0 \pm 8.1	117.3 \pm 6.5	96.3 \pm 8.1	98.3 \pm 10.2
D1-R257M	104.0 \pm 10.6	119.2 \pm 16.2	109.4 \pm 8.5	93.3 \pm 8.5	101.0 \pm 6.6

the two site-directed mutants, strongly implicating that the essentiality of D1-R257 in binding to bicarbonate anions.

D. Discussion

Two site-directed mutants on D1-R257 (D1-R257E, M) were first constructed in this study and the role of the arginine residue in bicarbonate/formate binding in PSII was investigated. The results indicate that the mutations on this residue: slow down the photosynthetic growth (Fig. 3.3) and the PSII electron transfer (Figs. 3.7 and 3.9; Table 3.1); lower the maximal yield of photochemistry (Fig. 3.4) and raise the F_0 level (Fig. 3.5); possibly destabilize PSII (Fig. 3.6); and most importantly, cause a near absence of the bicarbonate/formate effect on the PSII electron transfer (Figs. 3.4, 3.9 and 3.10; Table 3.1). The use of arginine-specific reagents helped further establish the role of the arginine residue in bicarbonate binding (Table 3.2).

The slower rate of photosynthetic growth and electron transfer of the D1-R257E, M mutants of *C. reinhardtii* agree well with the characterization of a similar mutant (D1-R257V) constructed in cyanobacteria (Kless et al. 1994). This phenotype was attributed to the possible role of the arginine to balance the negative charge formed by the dipole moment of the D1-*de* α -helix. However, the characterization of the cyanobacterial D1-R257V mutant showed a 38 fold increase in diuron (DCMU) tolerance judged by DCPIP reduction. The D1-R257M and D1-R257E mutants of *C. reinhardtii*, however, showed no apparent changes in DCMU sensitivity to that in the wild type as judged by Chl *a* fluorescence measurements. Though the mutant and species used by Kless et al (1994) are different from what was used in this study, the question of whether mutations on D1-R257 can induce significant herbicide resistance is certainly worth further investigation.

The lowered yield of photochemistry and significantly elevated F_0 level for the two mutants were constantly observed (Figs. 3.4, 3.5, 3.7 and 3.9). The low temperature Chl fluorescence spectra (Fig. 3.6) also indicate a slight but consistent decrease in the F685 and F695 emission bands after the spectra were normalized at 715 nm (F715). The reduction could be interpreted either by changes in excitation energy transfer or by decreased PSII core stability in the mutants. The severe damage observed in PSII in the mutant thylakoid preparations may partially support the possible destabilization of the PSII complex. In the cyanobacterial D1-R257V mutant (cited in Kless et al. 1994), a marked change in electrophoretic mobility of the D1 protein was observed suggesting significant conformational changes caused by the mutation. Computer modeling of the PSII reaction center (see Chapters IV and V) indicated that D1-R257 is a contact residue located in between D1 and D2. The mutations thus are expected to disrupt at least part of the putative protein-protein interactions destabilizing the conformation of reaction center core complex. Site-directed mutations of other proposed contact residues (see Chapters IV and V) have induced severe structural changes in PSII. These residues include D1-R269, D2-H214, D2-G215, and D2-H268 (see Chapter II, Vermaas et al. 1987; 1990).

The most striking phenotypic effect observed between these two mutants (D1-R257M and E) and the wild type are their significantly lowered sensitivity to the bicarbonate-reversible formate inhibition (Figs. 3.4, 3.9 and 3.10; Table 3.1). The results strongly implicate the relevance of D1-R257 in formate/bicarbonate binding *in vivo*. Inhibition of PSII electron transfer of pea chloroplasts by arginine specific reagent phenylglyoxal was first reported by Vermaas et al. (1982). However, no reversal of inhibition was shown by co-incubation of phenylglyoxal and bicarbonate with the chloroplasts. I have also obtained similar results by incubating bicarbonate and the arginine inhibitor (phenylglyoxal) with the wild type cell samples (data not shown). I attribute the difficulty of reversing the inhibition to the covalent nature of the interactions between arginines and phenylglyoxal. This problem can be resolved if the excess arginine inhibitors

are removed before the bicarbonate treatment. Thus, for the first time, I have shown the bicarbonate-reversible inhibition of PSII electron transfer by the arginine specific chemical modifying reagents. This provides evidence for the general involvement of arginine residues in bicarbonate binding in PSII. The use of two different arginine reagents (phenylglyoxal and 2,3-butanedione) strengthens the implication of arginines being involved in inhibition of the PSII electron transfer, because under certain circumstances, phenylglyoxal may have low reactivity to the amino group of lysine residues (Riordan 1979). 2,3-Butanedione is, however, more selective for arginine residues. The use of both reagents in the inhibitory study excludes the possibility of lysines being involved in interacting with the reagents. The bicarbonate-reversible inhibition by arginine-specific reagents had also been studied in the anion transporters located on the plasma membrane of marine macroalgae (Drechsler et al. 1994). However, in these systems, much lower concentrations of phenylglyoxal and 2,3-butanedione and higher pHs were needed to exert the inhibition.

The combination of the use of site-directed mutants and arginine-directed chemical reagents allowed me to establish the essentiality and specificity of D1-R257 in bicarbonate binding in PSII. The results may also be taken to verify the hypothesis that the positively charged sidechain of the arginine residue is important for providing forces for liganding bicarbonate anions. I also realize that there could be more than one arginine residues in the PSII reaction center that may be involved in anion binding, thus reactive to the arginine specific reagents. Slight inhibition of the PSII electron transfer by 2,3-butanedione in the two mutants in this study (Table 3.2) may support such a possibility. Thus, non-essential or low affinity bicarbonate binding arginine residues may exist.

Site-directed mutagenesis on the D2 protein in cyanobacteria (cited in Diner et al. 1991) have shown that D2-R265 near the non-heme iron may play a role in associating with bicarbonate. However, the unpublished study seems to favor D2-K264 as a better candidate for bicarbonate binding in the non-heme iron site. The involvement of several

other positively charged residues in bicarbonate binding near the non-heme iron have been investigated in cyanobacteria or green algae (Cao et al. 1991; Govindjee 1993; Chapter II). D2-R233 and D2-R251 have been shown to increase the PSII susceptibility to formate inhibition of the PSII electron transfer by 10 fold relative to the wild type and are suggested to function in stabilizing bicarbonate binding *in vivo* (Cao et al. 1991). However, a mutation on D2-R139 (D2-R139H) did not show any effect on bicarbonate-reversible formate inhibition (Govindjee 1993). Thus, there is a clear specificity. Recently, a non-conservative mutation was made on D1-R269 (D1-R269G) (see Chapter II). Despite the wide range significant structural and functional perturbations in the mutant, its reaction from Q_A^- to the plastoquinone pool was ~4 fold less sensitive to formate inhibition compared to the wild type. However, taken together with other available experimental evidence, the study indicates that the residue is less likely to be a bicarbonate ligand *in vivo*.

Using the recently constructed three-dimensional PSII reaction center model (Chapter IV) and ideas in Blubaugh and Govindjee (1988), a hypothesis was proposed for the function of D1-R257 in bicarbonate-mediated Q_B^{2-} protonation (Chapter IV). Although the current observations do not shed any new light on that hypothesis, yet it shows clearly the importance of D1-R257 for the bicarbonate effect. The characterization of the two D1-R257 mutants showed profound differences in formate and bicarbonate binding but apparently little difference in DCMU binding compared to the wild type, both through Chl *a* fluorescence measurements. This suggests that the mutational effect may be rather localized. This local effect may lead somehow to the observed slower rate of photosynthetic growth and the PSII electron transfer. However, the fact that the mutant cells can still manage to grow photoautotrophically at a considerable rate suggests that the algal cells may have alternative mechanisms of protonating Q_B which is important for survival. In the bacterial reaction center where there is no formate/bicarbonate effect (Shopes et al. 1989) and no conserved counterpart for D1-R257, the Q_B protonation relies on the presence of

water molecule in the Q_B niche (Ermler et al. 1994). I speculate that the mutant PSII's from this work may function in similar manner in which water molecules may replace the role of bicarbonate in Q_B protonation when the binding environment for bicarbonate becomes unfavorable. If this speculation is valid, the pattern of Q_B protonation in these two mutant PSII reaction centers would resemble that in the bacterial reaction center. It seems that only the availability of a high resolution X-ray crystal structure of the PSII reaction center, both in the wild type and mutant forms, would provide the answers.

Data presented in this chapter are based on the work to be published by the author and his collaborators (Xiong et al. 1996).

E. References

- Aime, S., Fasano, M., Paoletti, S., Cutruzzolà, F., Desideri, A., Bolognesi, M., Rizzi, M. and Ascenzi, P. (1996) Structural determinants of fluoride and formate binding to hemoglobin and myoglobin: Crystallographic and ^1H -NMR relaxometric study. *Biophys. J.* 70: 482-488.
- Anderson, B.F., Baker, H.M., Norris, G.E., Rice, D.W. and Baker, E.N. (1989) Structure of human transferrin: Crystallographic structure analysis and refinement at 2.8 Å resolution. *J. Mol. Biol.* 209: 711-734.
- Blubaugh, D. and Govindjee. (1986) Bicarbonate, not CO_2 , is the species required for the stimulation of Photosystem II electron transport. *Biochim. Biophys. Acta* 848: 147-151.
- Blubaugh, D.J. and Govindjee. (1988a) The molecular mechanism of the bicarbonate effect at the plastoquinone reductase site of photosynthesis. *Photosynth. Res.* 19: 85-128.

- Blubaugh, D.J. and Govindjee. (1998b) Kinetics of the bicarbonate effect and the number of bicarbonate-binding sites in thylakoid membranes. *Biochim. Biophys. Acta* 936: 208-214.
- Briantais, J.-M., Vernotte, C., Krause, G.H. and Weis, E. (1986) Chlorophyll *a* fluorescence of higher plants: Chloroplasts and leaves. In: Govindjee, Ames, J. and Fork, D.C. (eds.) *Light Emission by Plants and Bacteria* pp. 539-583. Academic Press, Orlando.
- Cao, J., Vermaas, W.F.J. and Govindjee. (1991) Arginine residues in the D2 polypeptide may stabilize bicarbonate binding photosystem II of *Synechocystis* sp. PCC 6803. *Biochim. Biophys. Acta* 1059: 171-180.
- Cao, J., Ohad, N., Hirschberg, J., Xiong, J. and Govindjee. (1992) Binding affinity of bicarbonate and formate in herbicide-resistance D1 mutants of *Synechococcus* sp. PCC 7942. *Photosyn. Res.* 34: 397-408.
- Dekker, J.P., Hassoldt, A., Petterson, A., van Roon, H., Groot, M.L. and van Grondelle, R. (1995) On the nature of the F695 and F685 emission of photosystem II. In: Mathis, P. (ed.) *Photosynthesis: from Light to Biosphere*, Vol. I, pp. 53-56. Kluwer, Dordrecht.
- Diner, B.A., Petrouleas, V. and Wendoloski, J.J. (1991) The iron-quinone electron-acceptor complex of photosystem II. *Physiol. Plant.* 81: 423-436.
- Drechsler, Z., Sharkia, R. Cabantchik, Z.I. and Beer, S. (1994) The relationship of arginine groups to photosynthetic HCO_3^- uptake in *Ulva* sp. mediated by a putative anion exchanger. *Planta* 194: 250-255.
- Eaton-Rye, J.J. and Govindjee. (1988a) Electron transfer through the quinone acceptor complex of photosystem II in bicarbonate-depleted spinach thylakoid membranes as a function of actinic flash number and frequency. *Biochim. Biophys. Acta* 935: 237-247.

- Eaton-Rye, J.J. and Govindjee. (1988b) Electron transfer through the quinone acceptor complex of photosystem II after one or two actinic flashes in bicarbonate-depleted spinach thylakoid membranes. *Biochim. Biophys. Acta* 935: 248-257.
- El-Shintinawy, F., Xu, C. and Govindjee. (1990) A dual bicarbonate-reversible formate effect in *Chlamydomonas* cells. *J. Plant. Physiol.* 136: 421-428.
- Ermler, U., Fritzsche, G., Buchanan, S.K. and Michel, H. (1994) Structure of the photosynthetic reaction centre from *Rhodobacter sphaeroides* at 2.65 Å resolution: Cofactors and protein-cofactor interactions. *Structure* 2: 925-936.
- Govindjee. (1993) Bicarbonate-reversible inhibition of plastoquinone reductase in photosystem II. *Z. Naturforsch.* 48c: 251-258.
- Govindjee. (1995) Sixty-three years since Kautsky: Chlorophyll *a* fluorescence. *Aust. J. Plant Physiol.* 22: 131-160.
- Govindjee and Satoh, K. (1986) Fluorescence properties of chlorophyll *b*- and chlorophyll *c*- containing algae. In: Govindjee, Ames, J., and Fork, D.C. (eds.) *Light Emission by Plants and Bacteria*, pp. 497-537. Academic Press, Orlando.
- Govindjee and van Rensen, J.J.S. (1993) Photosystem II reaction center and bicarbonate. In: Deisenhofer, J. and Norris, J. (eds.), *The Photosynthetic Reaction Center*, Vol. I, pp. 357-389, Academic Press, Inc., San Diego.
- Govindjee, Vernotte, C., Peteri, B., Astier, B. and Etienne, A.-L. (1990) Differential sensitivity of bicarbonate-reversible formate effects on herbicide resistant mutants of *Synechocystis* 6714. *FEBS Lett.* 267: 273-276.
- Govindjee, Eggenberg, P., Pfister, K. and Strasser, R.J. (1992) Chlorophyll *a* fluorescence decay in herbicide-resistant D1 mutants of *Chlamydomonas reinhardtii* and the formate effect. *Biochim. Biophys. Acta* 1101: 353-358.
- Govindjee, Xu, C., Schansker, G., and van Rensen, J.J.S. (1996) Chloroacetates as inhibitors of photosystem II: Effects on electron acceptor side. *J. Photochem. Photobiol.* (in press)

- Haag, E., Eaton-Rye, J.J., Renger, G., and Vermaas, W.F.J. (1993) Functionally important domains of the large hydrophilic loop of CP47 as probed by oligonucleotide directed mutagenesis in *Synechocystis* sp. PCC 6803. *Biochemistry* 32: 4444-4454.
- Harris, E.H. (1989) In: *The Chlamydomonas Sourcebook, A Comprehensive Guide to Biology and Laboratory Use*. pp. 25-31. Academic Press, San Diego.
- Hienerwadel, R. and Berthomieu, C. (1995) Bicarbonate binding to the non-heme iron of photosystem II investigated by Fourier transform infrared difference spectroscopy and ^{13}C -labeled bicarbonate. *Biochemistry* 34: 16288-16297.
- Kless, H., Oren-Shamir, M., Malkin, S., McIntosh, L. and Edelman, M. (1994) The *D-E* region of the D1 protein is involved in multiple quinone and herbicide interactions in photosystem II. *Biochemistry* 33: 10501-10507.
- Klimov, V.V., Allakhverdiev, S.I., Feyziev, Y.M. and Baranov, S.V. (1995) Bicarbonate requirement for the donor side of photosystem II. *FEBS Lett.* 363: 251-255.
- Kramer, D.M., Robinson, H.R. and Crofts, A.R. (1990) A portable multi-flash fluorimeter for measurements of donor and acceptor reactions of photosystem 2 in leaves of intact plants under field conditions. *Photosynth. Res.* 26: 181-193.
- Lavergne, J. and Briantais, J.-M. (1996) In: Ort, D.R. and Yocum, C. (eds.) *Oxygenic Photosynthesis: The Light Reactions*. Kluwer Academic Publishers, Dordrecht. (in press)
- Lindley, P.F., Evans, M.B., Evans, R.W., Garratt, R.C., Hasnain, S.S., Kuser, H.J., Kuser, P., Neu, M., Patel, K., Sarra, R., Strange, R., and Walton, A. (1993) The mechanism of iron uptake by transferrins: The structure of an 18 kDa NII-domain fragment from duck ovotransferrin at 2.3 Å resolution. *Acta Cryst. D* 49: 292-304.
- Lundblad, R.L. (1991) In: *Chemical Reagents for Protein Modification*, 2nd Edn. CRC Press, Boca Raton, FL.

- Mäenpää, P., Miranda, T., Tyystjärvi, E., Tyystjärvi, T., Govindjee, Ducruet, J.-M., Etienne, A.-L. and Kirilovsky, D. (1995) A mutation in the D-de loop of D₁ modifies the stability of the S₂Q_A⁻ and S₂Q_B⁻ states in photosystem II. *Plant Physiol.* 107: 187-197.
- Michel, H. and Deisenhofer, J. (1988) Relevance of the photosynthetic reaction center from purple bacteria to the structure of photosystem II. *Biochemistry* 27: 1-7.
- Minagawa, J. and Crofts, A.R. (1994) Photosyn. Res. A robust protocol for site-directed mutagenesis of the D1 protein in *Chlamydomonas reinhardtii*: A PCR-spliced *psbA* gene in a plasmid conferring spectinomycin resistance was introduced into a *psbA* deletion strain. 42: 121-131.
- Munday, J.C.M. Jr. and Govindjee. (1969) Light-induced changes in the fluorescence yield of chlorophyll *a* in vivo. IV. The effect of preillumination on the fluorescence transient of *Chlorella pyrenoidosa*. *Biophys. J.* 9: 22-35.
- Nakatani, H.Y., Ke, B., Dolan, E., and Arntzen, C.J. (1984) Identity of the photosystem II reaction center polypeptide. *Biochim. Biophys. Acta* 765: 347-352.
- Papageorgiou, G. (1975) Chlorophyll fluorescence: an intrinsic probe of photosynthesis. In: Govindjee, (ed.) *Bioenergetics of Photosynthesis* pp. 319-371. Academic Press, New York.
- Patty, L. and Theze, J. (1980) Origin of the selectivity of α -dicarbonyl reagents for arginyl residues of anion-binding sites. *Eur. J. Biochem.* 105: 387-393.
- Petrouleas, V. and Diner, B. (1990) Formation of NO of nitrosyl adducts of redox components of the photosystem II reaction center. I. NO binds to the acceptor-side non-heme iron. *Biochim. Biophys. Acta* 1015: 131-140.
- Porra, R.J., Thompson, W.A. and Kriedemann, P.E. (1989) Determination of accurate extinction coefficients and simultaneous equations for assaying chlorophylls *a* and *b* extracted with four different solvents: verification of the concentration of

- chlorophyll standards by atomic absorption spectroscopy. *Biochim. Biophys. Acta* 975: 384-394.
- Riordan, J.F. (1973) Functional arginyl residues in carboxypeptidase A. Modification with butanedione. *Biochemistry* 20, 3915-3923.
- Riordan, J.F. (1979) Arginyl residues and anion binding sites in proteins. *Mol. Cell. Biochem.* 26: 71-92.
- Segel, I.H. (1975) In: *Enzyme Kinetics*. John Wiley & Sons, New York.
- Shopes, R.J., Blubaugh, D., Wraight, C. and Govindjee. (1989) Absence of a bicarbonate-depletion effect in electron transfer between quinones and reaction centers of *Rhodobacter sphaeroides*. *Biochim. Biophys. Acta* 974: 114-118.
- Srivastava, A., Strasser, R.J. and Govindjee. (1995) Polyphasic rise of chlorophyll *a* fluorescence in herbicide-resistant D1 mutants of *Chlamydomonas reinhardtii*. *Photosyn. Res.* 43: 131-141.
- Strasser, R.J., Srivastava, A. and Govindjee. (1995) Polyphasic chlorophyll *a* fluorescence transient in plants and cyanobacteria. *Photochem. Photobiol.* 61: 32-42.
- Takahashi, K. (1968) The reaction of phenylglyoxal with arginine residues in proteins. *J. Biol. Chem.* 243: 6171-6179.
- Trebst, A. (1980) Inhibitors in electron flow: Tools for the functional and structural localization of carriers and energy conservation sites. *Methods in Enzymol.* 69: 675-715.
- van Rensen, J.J.S., Tonk, W.J.M. and de Bruijn, S.M. (1988) Involvement of bicarbonate in the protonation of the secondary quinone electron acceptor of photosystem II via the non-heme iron of the quinone-iron acceptor complex. *FEBS Lett.* 226: 347-351.
- Vass, I. and Govindjee. (1996) Thermoluminescence of photosynthetic apparatus. *Photosyn. Res.* (in press)

- Vermaas, W.F.J. and Rutherford, A.W. (1984) EPR measurements on the effects of bicarbonate and triazine resistance on the acceptor side of photosystem II. *FEBS Lett.* 175: 243-248.
- Vermaas, W.F.J., van Rensen, J.J.S. and Govindjee. (1982) The interaction between bicarbonate and the herbicide ioxynil in the thylakoid membrane and the effects of amino acid modification on bicarbonate action. *Biochim. Biophys. Acta* 681: 242-247.
- Vermaas, W.F.J., Williams, J.G.K., Arntzen, C.J. (1987) Site-directed mutations of two histidine residues in the D2 protein inactivate and destabilize photosystem II in the cyanobacterium *Synechocystis* 6803. *Z. Naturforsch.* 42c: 762-768.
- Vermaas, W.F.J., Charité, J. and Shen, G. (1990) Glu-69 of the D2 protein in photosystem II is a potential ligand to Mn involved in photosynthetic oxygen evolution. *Z. Naturforsch.* 45c: 359-365.
- Vermaas, W., Vass, I., Eggers, B. and Styring, S. (1994) Mutation of a putative ligand to the non-heme iron in photosystem II: Implications for Q_A reactivity, electron transfer, and herbicide binding. *Biochim. Biophys. Acta* 1184: 263-272.
- Vernotte, C., Briantais, J.-M., Astier, C. and Govindjee. (1995) Differential effects of formate in single and double mutants of D1 in *Synechocystis* sp. PCC 6714. *Biochim. Biophys. Acta* 1229: 296-301.
- Xiong, J., Minagawa, J., Antony, C. and Govindjee. (1996) Construction and characterization of bicarbonate/formate binding site mutants on arginine-257 in the photosystem II D1 protein of *Chlamydomonas reinhardtii*. to be submitted to *Biochim. Biophys. Acta*
- Xu, C., Rogers, S.M.D., Goldstein, C., Widholm, J.M. and Govindjee (1989) Fluorescence characteristics of photoautotrophic soybean cells. *Photosynth. Res.* 21: 93-106.

- Xu, C., Taoka, S., Crofts, A.R. and Govindjee. (1991) Kinetic characteristics of formate/formic acid binding at the plastoquinone reductase site in spinach thylakoids. *Biochim. Biophys. Acta* 1098: 32-40.
- Yano, M., Terada, K., Umiji, K. and Izui, K. (1995) Catalytic role of an arginine residue in the highly conserved and unique sequence of phosphoenolpyruvate carboxylase. *J. Biochem.* 117: 1196-1200.

CHAPTER IV. MODELING OF THE D1/D2 PROTEINS AND COFACTORS OF THE PHOTOSYSTEM II REACTION CENTER: IMPLICATIONS FOR HERBICIDE AND BICARBONATE BINDING

A. Introduction

The primary photosynthetic reactions of plants, algae, and cyanobacteria occur in photosystem II (PSII) and photosystem I (PSI) protein complexes located in thylakoid membranes. The study of the photochemical mechanism of PSII has been a focus of photosynthesis research as this protein complex is the only one in nature, which is able to evolve oxygen by splitting water (Renger 1993). The PSII reaction center lies at the core of the PSII protein complex and carries out the chemical reactions including the primary charge separation at the reaction center chlorophylls (P680) and a subsequent electron transfer from water to plastoquinone via a number of redox active intermediates, while releasing oxygen as a byproduct (for reviews, see Vermaas et al. 1993; Diner and Babcock 1996). The photochemically active PSII reaction center contains six polypeptides, D1, D2, a heterodimer of cytochrome b559, *psbI* and *psbW* gene products (see *e.g.* Satoh 1993; and Lorkovic et al. 1995). The central core of the PSII reaction center is composed of D1 and D2 proteins where all the redox active components are embedded. These components include a tetra-manganese cluster, two redox active tyrosine residues, four to six chlorophyll *a* molecules, two pheophytins, and plastoquinones Q_A and Q_B. A non-heme iron, located between Q_A and Q_B, does not participate directly in the electron transfer but is vital for the transfer process. A β -carotene is also found in the PSII reaction center and is believed to be involved in the photoprotective process.

An X-ray structure of the PSII reaction center is not available to this date. However, low resolution electron microscopy structures are available (Holzenburg et al. 1993; Santini et al. 1994; Boekema et al. 1995). Significant sequence and functional

homology is known to exist between the PSII reaction center proteins D1 and D2 and the L and M subunits of the photosynthetic reaction centers of purple bacteria, *Rhodobacter (Rb.) sphaeroides* and *Rhodospseudomonas (Rps.) viridis* (see review by Diner and Babcock 1996) for which high resolution crystal structures are available (see review by Lancaster et al. 1995). It is, thus, of considerable interest to construct a reasonable working model for the PSII reaction center, based on the homology with bacterial reaction centers. The availability of the PSII three dimensional model will enable accurate structural interpretation of experimental data, be useful for proposing functional hypotheses for the electron transfer mechanism and for suggesting designs of site-directed mutants for elucidating the structure-function relationship in PSII.

Several attempts have already been made to construct a three dimensional model for the PSII reaction center. Trebst (1986) first aligned the D1 and D2 sequences of the higher plant PSII reaction center with the L and M sequences of the bacterial reaction center and used the homology information to predict the folding of D1 and D2. Based on the model, he also proposed important residues involved in Q_B and the non-heme iron binding. Bowyer et al. (1990) constructed a model (using the sequence from *Synechococcus* 7942) for the Q_B and herbicide binding niche in the D1 protein, by digitizing the stereoimage of part of the *Rps. viridis* structure. Other Q_B and herbicide binding niche models have also been constructed by various groups (Tietjen et al. 1991; Ohad et al. 1992; Draber et al. 1993; Egner et al. 1993; Sobolev and Edelman 1995). Svensson et al. (1990) built a PSII donor side model with the redox active tyrosine residues by using part of the consensus D1/D2 sequences. The model was constructed by replacing a small number of side chains in the related region of the L subunit of *Rps. viridis* structure. A more complete spinach PSII model from this group is now available with refined structures for P680, the pheophytins, and the redox active tyrosyl residues (Svensson et al. 1995a, b; Svensson 1995). Another comprehensive modeling study for pea PSII was presented by Ruffle et al. (1992), who compared sequences of 23 D1, 9 D2 and 8 bacterial L and 8 bacterial M

proteins and showed a strong sequence similarity amongst them, especially in the transmembrane regions. An environment-dependent substitution table was applied in the sequence alignment, and the structurally conserved regions of D1, D2 and the bacterial L and M subunits were identified. Using SYBYL molecular modeling package, a partial (73% complete) PSII reaction center model was generated from pea D1 and D2 sequences. With this pea PSII model, Mackay and O'Malley (1993a, b, c, d) have conducted a series of herbicide binding analyses. Their calculations on the intermolecular interactions of several herbicides (*e.g.* 3-(3,4-dichlorophenyl)-1,1-dimethylurea or DCMU) with PSII indicate that van der Waals forces play a major role in stabilizing the herbicides in the Q_B niche.

Bicarbonate has been suggested to be a positive regulator for the function of the PSII reaction center (see reviews by Blubaugh and Govindjee 1988a; Govindjee and van Rensen 1993; Govindjee 1993). The depletion of bicarbonate by its analogue formate results in a significant inhibition of the electron transfer on the acceptor side, *i.e.* from Q_A⁻ to the plastoquinone pool (see references in Blubaugh and Govindjee 1988a; Govindjee and van Rensen 1993). Studies have also suggested that bicarbonate may affect the donor side function of PSII (El-Shintinawy and Govindjee 1990; Jursinic and Dennenberg 1990; Stemler and Jursinic 1993; Klimov et al. 1995; Wincencjusz et al. 1996).

Regarding the role of bicarbonate in PSII function, Michel and Deisenhofer (1988) suggested that bicarbonate may serve as a functional homologue to the glutamate residue in the bacterial reaction center (M232 in *Rps. viridis* numbering) which provides ligands to the non-heme iron. This was based on the finding that there is no homologous glutamate residue in the D1 and D2 sequences, and there is no bicarbonate stimulatory effect in the bacterial system (Shopes et al. 1989). Although the involvement of M232 in the bacterial reaction center as a substitute for bicarbonate could not be confirmed by site-directed mutagenesis experiments (Wang et al. 1992), EPR experiments in PSII confirmed the binding of bicarbonate to the non-heme iron (Petrouleas and Diner 1990; Diner and

Petrouleas 1990). Further, a hypothesis for the involvement of bicarbonate in the Q_B protonation is supported by other experimental evidence (see Blubaugh and Govindjee 1988a; Govindjee and van Rensen 1993). Blubaugh and Govindjee (1988a) presented a hypothesis for the possible involvement of D1-R257 or D1-R269 (with D1-R257 as the more favored residue) in facilitating the bicarbonate-mediated Q_B protonation. Diner et al. (1991a) suggested two patterns of the bicarbonate-iron binding, in which bicarbonate either binds to the iron as a mono or bidentate ligand. Different ways of bicarbonate liganding to the non-heme iron were also discussed by Govindjee and van Rensen (1993), in which the bicarbonate is stabilized by hydrogen bonding interactions with lysine 265 (pea numbering) in D2. Involvement of other amino acids in this stabilization process has been discussed by Govindjee (1993).

In this chapter, I present a complete D1/D2 model of the PSII reaction center of a cyanobacterium *Synechocystis* sp. PCC (Pasteur culture collection) 6803. I chose to model D1 and D2 of this species because it is one of the most widely used systems for site-directed mutagenesis in photosynthesis (Vermaas 1993). In this modeling, I take into account the alignment of the structurally conserved regions (SCRs) in Ruffle et al. (1992) and use this information in my SCR alignment of the cyanobacterial D1 and D2 with the L and M subunits. In addition, I modeled the loop regions with a novel sequence-specific approach by searching for the best-matched protein segments in the Protein Data Bank with the "basic local alignment search tool" (BLAST) (Altschul et al. 1990), and fitting the matching fragment conformations onto the corresponding D1 and D2 regions. With the inclusion of all the cofactors important for the PSII functions, a complete model of the central core of the PSII reaction center was constructed and refined through energy minimization. Various issues important in the study of the PSII reaction center including protein binding environment for the cofactors and residues involved in inter-protein interactions were analyzed. Three alternative conformations of P680 chlorophylls different from that of the bacterial counterparts were also proposed based on various experimental

suggestions. For the first time, a β -carotene was included in the PSII reaction center model. Redox active residues important for the $P680^+$ reduction, i.e. D1-Y161 and D2-Y160, have also been studied and their modeled distances to the several cofactors have been shown to match well with the experimental suggestions. This model was further applied to the modeling of herbicide DCMU in the Q_B binding niche. I focus in the modeling on the bicarbonate binding and its function in photosystem II. A bicarbonate anion was modeled in the non-heme iron site providing a bidentate ligand to the iron. By modifying the previous hypothesis of Blubaugh and Govindjee (1988a), I modeled a second bicarbonate and a water molecule in the Q_B site and propose a hypothesis to explain the mechanism of Q_B protonation mediated by a bicarbonate and a water molecule, in which the bicarbonate, stabilized by D1-R257, donates a proton to Q_B^{2-} through an intermediate of D1-H252; the water molecule is proposed to donate another proton to the doubly reduced Q_B . Based on the structure of the "water transport channel" in the bacterial reaction center, I propose a similar, but not identical, channel for transporting water and bicarbonate in PSII. The model indicates a more positively charged binding domain near Q_B and the non-heme iron, in contrast to the situation in the bacterial reaction center which lacks the bicarbonate effect.

B. Materials and Methods

Homology modeling of the PSII reaction center of *Synechocystis* sp. PCC 6803 was performed using QUANTA/CHARMm (version 4.0) molecular modeling package. Based upon the assumption that D1 is an equivalent of L and D2 is an equivalent of M, I used the coordinates of the L and M subunits from *Rb. sphaeroides* and *Rps. viridis* as the templates for D1 and D2, respectively. The coordinates of the bacterial reaction centers (1PRC and 2RCR) were obtained from the Brookhaven Protein Data Bank (Bernstein et al.

1977; Abola et al. 1987). The amino acid sequence information of D1 (from *psbA*-2) and D2 (from *psbD*-2) was obtained from Ravnikar et al. (1989) and Williams and Chisholm (1987), respectively. The post-translational truncation on the C-terminus (16 amino acid residues) of *Synechocystis* 6803 was also taken into account (see Diner et al. 1991b).

The modeling started from the primary structure alignment of D1 and D2 with the bacterial L and M subunits, respectively. The structurally conserved regions (SCRs) of D1 and D2 proteins with the L or M subunits were based on the pea model by Ruffle et al. (1992). In this model, I chose to use the L subunit for aligning D1 and the M subunit for D2, respectively, rather than using all the four bacterial subunits together for aligning both D1 and D2. The alignment for the sequences outside the SCRs which are either partially conserved or structurally varied was done on the Protein Design subprogram of QUANTA. The QUANTA alignment process is based on the multiple sequence alignment algorithm of Feng and Doolittle (1987). The alignment was done with the statistical weight for the sequence homology parameter set at 0.6. Raw alignment results were manually refined using the interactive alignment tools in the Protein Design module. After alignment, the template proteins were matched and superimposed, the coordinates of the aligned sequences were averaged and copied to the modeled sequences. The newly defined coordinates in D1 and D2 were refined with the Structural Regularization tool which is a limited energy minimization function, with 50 steps using the Steepest Descents method followed by 200 steps of Adopted Basis Newton Raphson method (ABNR). The regularization was carried out with less than 20 residues at a time.

Certain stretches of D1 and D2 sequences in between the aligned regions clearly do not exhibit homology with the L and M sequences. The connecting loop sequences (including the C-terminal region of D1) were treated in two different ways. For the loop sequences of less than or equal to four residues, the conformation of the loops was built using the "Build Coordinates" function in the Protein Design subprogram. The newly built peptide conformation was regularized as above. The longer loops with more than five

residues were modeled with a sequence-specific approach. A "basic local alignment search tool" (BLAST, Altschul et al. 1990) was applied in searching for the best matched protein fragments among the protein sequences that already have crystal coordinates available from the Brookhaven Protein Data Bank. Once the most homologous fragment from a protein is selected, the conformation of the fragment flanked by two extra anchor residues on either end was excerpted from the original protein. As the anchor residues of the template peptide on either side were superposed onto the two residues immediately next to the gap, the conformation of the template peptide was copied to the modeled sequences. The newly built loop conformation was then regularized as above.

The PSII chromophores which include chlorophylls, pheophytins and plastoquinones were modified from their counterparts in the *Rb. sphaeroides* reaction center using the interactive graphic tools in the Molecular Editor function of QUANTA. The PSII chromophore structures were based on those reviewed by Cramer and Knaff (1990). The corrected PSII chromophores were then added to the assembly of D1 and D2. To accommodate the existing experimental data on the measurements of P680 chlorophyll, four alternative models of P680 conformations are proposed. One is based on the bacterial special pair while the other three involve significant rotations of the two chlorophyll monomers. As the latter three P680 conformations (see Results and Discussion) introduced enormous, unrelievable strains in the protein part of the reaction center model which had been generated by homology, they were modeled separately along with the liganding histidines and the redox active tyrosines. Another PSII chromophore, β -carotene, was also introduced into the model by modifying the dihydro-neurosporene in *Rps. viridis* structure and added into the model by using the Molecular Similarity Tools in QUANTA. The non-heme iron coordinate was directly transferred from the *Rb. sphaeroides* structure. The raw PSII reaction center complex structure was energy-minimized using the CHARMM procedure (Brooks et al. 1983). The energy minimization was performed with 100 iterations of Steepest Descents followed by ABNR energy minimization until fully

converged (rms force < 0.01 kcal/mol·Å²), during which the coordinates of all the cofactors were constrained in place and only the D1 and D2 polypeptides could be moved. The hydrogen bonding pattern of the constructed PSII model was calculated on the Protein Design module and the secondary structure of D1 and D2 proteins were derived. The model was evaluated using the Protein Health subprogram in QUANTA and the PDF method (Subramaniam et al. 1996).

The herbicide DCMU was also modeled in the PSII reaction center replacing Q_B in its binding niche. Its structure in *trans*-amide form was obtained by editing the phenyl ring of Q_B on the Molecular Editor subprogram and was added to a Q_B-lacking PSII model. The DCMU structure was manually moved to match the DCMU binding pattern determined in the crystal structure in a mutant *Rps. viridis* reaction center (T4) (Sinning et al. 1990; Sinning 1992). All residues surrounding DCMU were fully energy minimized with ABNR. The DCMU binding environment was further refined by molecular dynamics simulations, during which the herbicide binding environment was heated from 0 K to 300 K in 0.3 ps with an integration time of 1 fs. The structure was then equilibrated at 300 K for 25 ps with 1 fs integration time, followed by a final simulation at 300 K for 5 ps with 1 fs integration time. The structure was again fully energy minimized with ABNR. During the above energy minimization and molecular refinement processes, all the alpha-carbons of the amino acid residues were constrained so that only the residue side chains in the herbicide binding environment were allowed to move.

A bicarbonate anion (HCO₃⁻) was modeled to the non-heme iron site to satisfy the iron valence requirement based on suggestions from previous experimental data (Petrouleas and Diner 1990; Diner and Petrouleas 1990). The docking of HCO₃⁻ was performed by manually placing the anion close to the Fe center and its position is compared and matched to carboxylic group of the M-E232 residue of the *Rb. sphaeroides*. A second bicarbonate as well as a water molecule were modeled into the Q_B niche in an attempt to study the possible

involvement of bicarbonate and water in Q_B protonation. They were docked in the vicinity of D1-H252 and D1-R257 and energy minimized as above.

The entire modeling work was performed on UNIX Silicon Graphics Power Series Workstation 4D/440VGXT.

C. Results and Discussion

1. Sequence alignment and sequence-specific loop modeling

Ruffle et al. (1992), using an environment-dependent substitution table, aligned the bacterial L and M subunits with the D1 and D2 sequences and derived the SCRs for pea D1 and D2. This alignment information for the SCRs, with further refinements, was applied in the current D1/D2 alignment of *Synechocystis* sp. PCC 6803 with the bacterial templates.

In contrast to Ruffle et al. (1992), who used all the four bacterial subunits as templates, I used two L subunits as homology templates for modeling D1 and two M subunits as templates for D2, based on the long standing assumption that D1 is the equivalent of L and D2 is the equivalent of M (Trebst 1986; Michel and Deisenhofer 1988). This option is thought to yield a more reliable sequence alignment, since examination of the secondary structure of L and M in loop regions shows significant variations between the L and M subunits. If the averaged coordinates of all the four template proteins were applied in modeling on subunit, many regions, especially those in the between the SCRs, would expect to have significant errors and structural constraints.

The alignment of the D1 protein with the L subunits of both *Rps. viridis* and *Rb. sphaeroides* is shown in Fig. 4.1. After alignment, 20% sequence identity (69 identical residues) and 60% sequence similarity of D1 with the L subunit (205 similar residues) were found. The alignment of D2 with the M subunit sequences is shown in Fig. 4.2. After alignment, the sequence identity of D2 with the M subunit is 24% (85 identical residues)

Figure 4.1. Sequence alignment of the D1 protein of *Synechocystis* sp. PCC 6803 with the L subunit of photosynthetic bacterial reaction center of *Rhodobacter sphaeroides* (SL) and *Rhodopseudomonas viridis* (VL). The D1 sequence is in lower case and the bacterial L sequences are in upper case.

SL *1 *ALLSFERKYR*11 *VPGGTLVGGN*21 *LFDFWVGP--*29 *--FYVGFPGV
 VL *1 *ALLSFERKYR*11 *VRGGTLIGGD*21 *LFDFWVGP--*29 *--YFVGFFGV
 D1 *1 *----mtttlq*7 *qresaslweq*17 *fcq-wvtstn*26 *nriyvgwfgt

SL *37 *ATFFFAALGI*47 *ILIAWSAVLQ*57 *GT-----WN*61 *P-----
 VL *37 *SAIFFIFLGV*47 *SLIGYAASQG*57 *PT-----WD*61 *P-----
 D1 *36 *lmiptlltat*46 *tcfiiafiaa*56 *ppvddidgire*66 *pvagsllygn

SL *62 *QLISVY--PP*70 *----ALE-YG*75 *L-GGAPL---*81 *A-KGGLWQII
 VL *62 *FAISIN--PP*70 *----DLK-YG*75 *L-GAAPL---*81 *L-EGGFQWAI
 D1 *76 *niisgavvps*86 *snaighlfyp*96 *iweaasldew*106*lynggpyqlv

SL *90 *TICATGAFVS*100*WALREVEICR*110*KLGI-GYHIP*119*FAFAFAILAY
 VL *90 *TVCALGAFIS*100*WMLREVEISR*110*KLGI-GWEVP*119*LAFCVPIFMF
 D1 *116*vfhfligifc*126*ymgrqwelsy*136*rlgmrpw-ic*145*vaysapvsaa

SL *129*LTLVLFRPVM*139*MGAWGYAFFY*149*GIWTHLDWVS*159*NTGYTYGNFH
 VL *129*CVLQVFRPLL*139*LGSWGHAFY*149*GILSHLDWVN*159*NFGYQYLNWH
 D1 *155*tavfliypig*165*qgsfsdgmpl*175*gisgtfnfmi*185*vfqaeh-nil

SL *169*YNPAHMIAIS*179*FFFTNALALA*189*LEGALVLSAA*199*N-----PE
 VL *169*YNPGHMSSVS*179*FLFVNAMALG*189*LEHGLILSVA*199*N-----PG
 D1 *194*mhpfhmlgva*204*gvfggsifsa*214*mhgslytss1*224*vrettevesq

SL *202*K-GKE-----*206*----MRTPDE*212*EDTFF-RD-L*220*VGY-S-IGTL
 VL *202*D-GDK-----*206*----VKTAEH*212*ENQYF-RD-V*220*VGY-S-IGAL
 D1 *234*nygykfgqee*244*etyni---va*251*ahgyfgr-li*260*fqyasfnnsr

SL *228*GIHRLGLLLS*238*LSAVFFSALC*248*MIIT-----G*253*-TI-----
 VL *228*SIHRLGLFLA*238*SNIFLTGAFG*248*TIAS-----G*253*-PF-----
 D1 *270*slhfflgawp*280*vigiwftamg*290*vstmafning*300*fnfnqsilds

SL *255*WFDQWVDWWQ*265*WWVKL--PW-*272*-----W*273*A-NIPGG
 VL *255*WTRGWPEWWG*265*WWLDI--PF-*272*-----W*273*S
 D1 *310*qgrvigtwad*320*vlnranigfe*330*vmhernahnf*340*p1d1a

Figure 4.2 Sequence alignment of D2 protein of *Synechocystis* sp. PCC 6803 with the M subunit of the photosynthetic bacterial reaction center of *Rhodobacter sphaeroides* (SM) and *Rhodopseudomonas viridis* (VM). The D2 sequence is in lower case and the bacterial M sequences are in upper case.

SM *1 *AEYQNIFSQV*11 *QVRGPADLGM*21 *TEDVNLANRS*31 *GVGPFSTLLG
 VM *1 *ADYQTIYTQI*11 *QARGPHITVS*21 *GEWGDNDRV-*30 *GKPFYSYWL
 D2 *1 * * m*2 *tiavgrapv-*11 *egrwfdvldd

SM *41 *WFGNAQLGPI*51 *YLGS LGVLSL*61 *FSGLMWFFTI*71 *GIWFWYQAGW
 VM *40 *KIGDAQIGPI*50 *YLGASGIAAF*60 *AFGSTAILII*70 *LFNMAAEVHF
 D2 *21 *wl-kdrf-v*29 *figwsglllf*39 *pcafmalggw*49 *ltgttfvtsw

SM *81 *--NPAV--FL*87 *RDLFFFSLE-*96 *-PPAPEYG--*103*LSF---AAP-
 VM *80 *--DPLQ--FF*86 *RQFFWLGLY-*95 *-PPKAQYG--*102*MGI---P-P-
 D2 *59 *ythglassyl*69 *eganfltvav*79 *sspadafghs*89 *llflwgspeaq

SM *109*-----LKEG*113*GLWLIASFFM*123*FVAVSWWGR*133*TYLRAQALGM
 VM *107*-----LHDG*111*GWWMAGLFM*121*TLSLGSSWIR*131*VYSRARALGL
 D2 *99 *gnltrwfqig*109*glwvfvalhg*119*afgligfmlr*129*qfeisrlvgi

SM *143*GKHTAWAFLS*153*AIWLWMVLGF*163*IRPILMGWSWS*173*EAVPYGIFSH
 VM *141*GTHIAWNFAA*151*AIFFVLCIGC*161*IHPTLVGSWS*171*EGVPFGIWPH
 D2 *139*rpynaiafsg*149*piavfvsvfl*159*myplgqsswf*169*fapsfgvagi

SM *183*LDWTNNFSLV*193*HGNLFYNPFH*203*GLSIAFLYGS*213*ALLFAMHGAT
 VM *181*IDWLTAFSIR*191*YGNFYCPWH*211*GFSIGFAYGC*221*GLLFAAHGAT
 D2 *179*frfilflqgf*189*h-nwtlnpfh*198*mmgvagilgg*208*allcaihgat

SM *223*ILAVSR-----*229*-----FGGERE*235*LEQIADRGT-*244*AAERAALFWR
 VM *231*ILAVAR-----*227*-----FGGDRE*233*IEQITDRGT-*242*AVERAALFWR
 D2 *218*ventlfedge*228*dsntf---ra*235*feptqaeety*245*smvtanrfws

SM *254*--WTMGFNAT*262*MEGIHRWAIW*272*MAVLVTLTGG*282*IGIL-LS---
 VM *252*--WTIGFNAT*260*IESVHRWGWF*270*FSLMVMVSAS*280*VGIL-LT---
 D2 *255*qifgiaf-sn*264*krwlhffmlf*274*vpvtglwmss*284*vgivglaln1

SM *288*-G-TVV-----*292*-----D-NWYV*297*WGQNEGMA--*306*P
 VM *286*-G-TFV-----*290*-----D-NWYL*295*WCVKEGAA--*303*P-----D
 D2 *294*raydfvsqel*304*raaedpefet*314*fytknillne*324*gmrawmapqd

SM
 VM *305*YP--AYL-PA*312*TPDPASLPGA*322*PK
 D2 *334*qphenfifpe*344*evlprgnal

and the sequence similarity is 58% (204 similar residues). Since template structures were well characterized and the sequence alignment is based on the homology of the three-dimensional structures, the homology were counted with either of the template sequences. This is a standard protocol followed in family sequence alignments based on structural criteria. However, if the homology is counted with both of the template sequences, both the identity and similarity values will be lower than noted above.

The loop regions which represent insertion sequences were modeled using a bits-and-pieces sequence homology modeling strategy. The loop regions are presumably all solvent exposed, it is thus justifiable to use structural fragments from other proteins even soluble proteins because loop regions are well characterized by sequences (Han and Baker 1996). This was done by searching for highly homologous sequences in proteins whose high resolution structures are available. The search was done using a "basic local alignment search tool" (BLAST, Altschul et al. 1990). Table 4.1 gives sequences from highly resolved structures which are homologous to the D1 and D2 loop sequences. In all the hits, the smallest Poisson probability is above 0.95, hence the sequence similarity is significant enough to allow me copy the fragment structures for homology modeling.

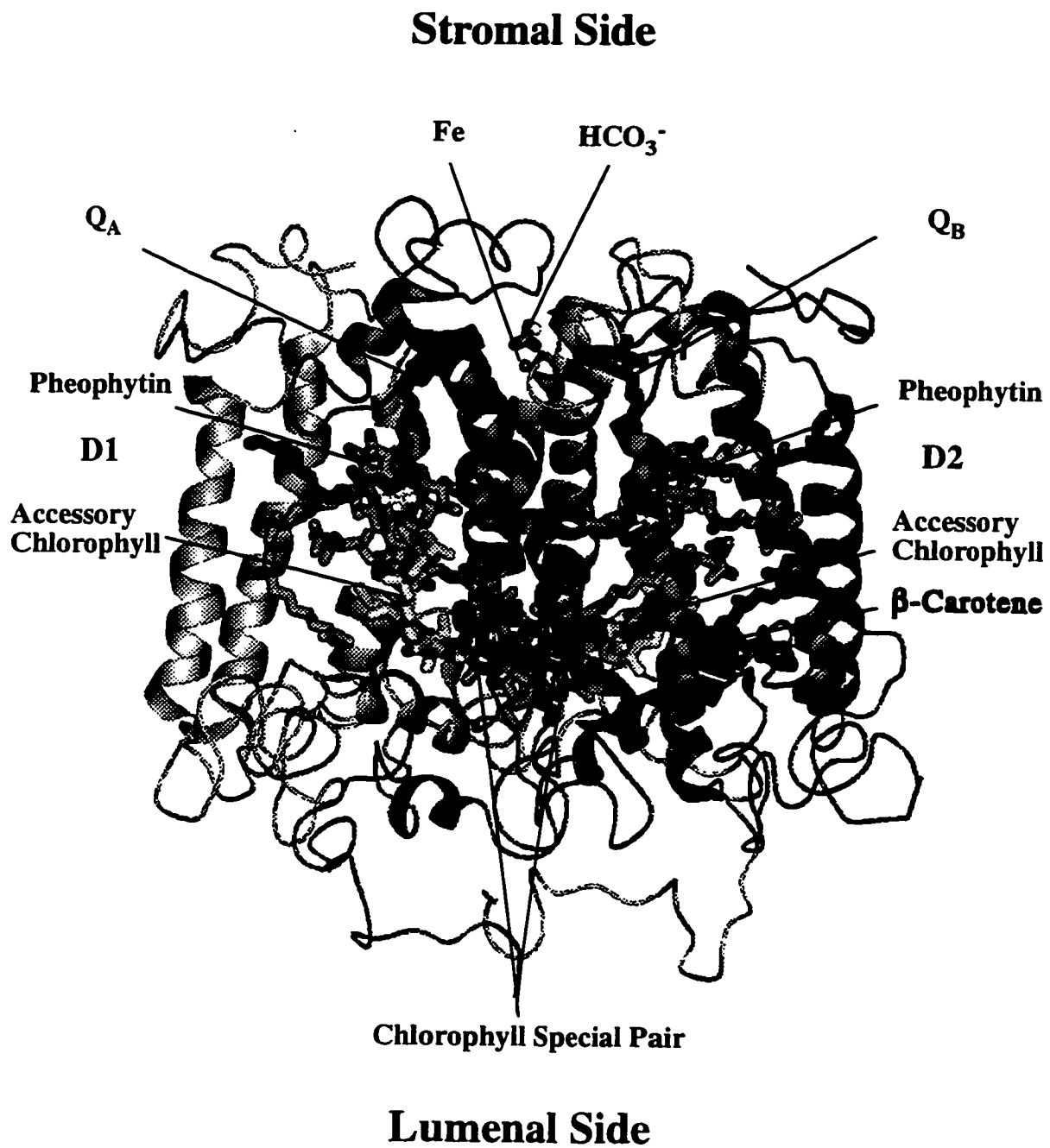
2. General topology and evaluation of the model

The constructed PSII reaction center model, presented here, was refined using energy minimization methods in CHARMM (Brooks et al. 1983). At the end of the minimization, the energy of the model was -33,350 kcal/mol, compared to 2.39×10^{10} kcal/mol at the beginning of the minimization process (all measured with cofactors constrained). The general topology of the final PSII reaction center model resembles that of the bacterial reaction center (Fig. 4.3). The main chain atoms of the constructed homology model deviates from their equivalent atoms in the *Rb. sphaeroides* reaction center by 0.818 Å root mean square. Like its bacterial counterpart, the model has a two fold symmetry with an axis running from the center of the two chlorophylls of P680 to the non-heme iron. Both

Table 4.1. Search results by the BLAST program through the Brookhaven Protein Data Bank for the unconserved loop sequences of *Synechocystis* sp. PCC 6803 D1 and D2 proteins.

SEARCH QUERY		SEARCH RESULTS	
Protein and Residue Range	Sequence	Protein, PDB File Code and Residue Range	Sequence
D1 (58-63)	VDIDGI	Aspartate aminotransferase, 3AAT (71-76)	LGIDGI
D1 (67-75)	VAGSLLYGN	Photosynthetic reaction center of <i>Rb. spaeroides</i> , H-subunit, 4RCR.H (237-245)	VAGGLMYAA
D1 (225-231)	RETTEVE	Poliovirus, subunit 3, 2PLV.3 (226-232)	RDTHIE
D1 (239-248)	FGQEEETYNI	Tryptophan synthase, Subunit B, 1WSY.B. (291-300)	DGQIEESYSI
D1 (294-298)	AFNLN	Tomato bushy stunt virus, Subunit A, 2TBV.A. (311-315)	TFNLS
D1 (303-309)	NQSILDS	Phosphoglucomutase, Subunit A, 2PMG.A. (39-45)	IQSIIST
D2 (98-104)	QGNLTRW	Cardio picornavirus coat protein, Subunit 1 2MEV.1 (139-145)	HGLLVRW
D2 (224-232)	EDGEDSNTF	Porin, 2POR (54-62)	ETGEDGTVF
D2 (300-307)	SQELRAAE	Apolipoprotein-E2, 1LE2 (57-64)	TQELRALM
D2 (325-332)	MRAWMAPQ	Methyltransferase, 3TMS (98-105)	WRAWPTPD

Figure 4.3 The ribbon drawing diagram of the modeled three dimensional structure of the PSII reaction center including cofactors. The ribbon form indicates the α -helix structure. D1 and D2 have five transmembrane helices each and several amphipathic helices in the luminal and stromal (cytoplasmic in cyanobacteria) sides. The D1 protein is shown in light gray and D2 is shown in dark gray. The cofactors are represented in licorice bond forms. Two bicarbonate anions were modeled in this structure, one in the non-heme iron site and the other in the Q_B binding niche (not shown as it is behind the D1 stromal (cytoplasmic) non-membrane helix).

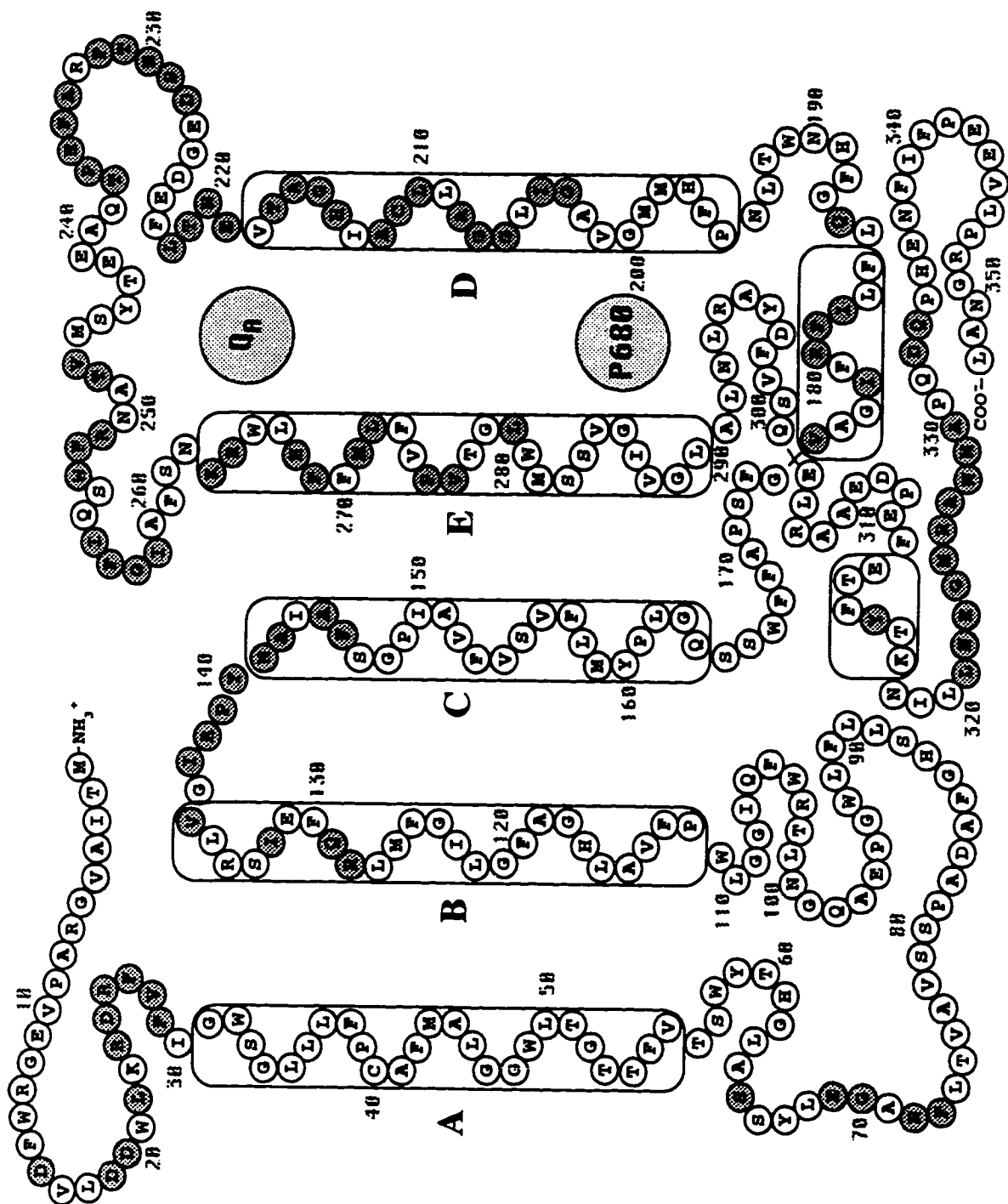


D1 and D2 proteins have five transmembrane α -helices in which cofactors responsible for the primary photochemistry are anchored. The transmembrane helices of D1 and D2 are denoted as A, B, C, D, E. The topology of five transmembrane helices for D1 and D2 is consistent with the evidence of the immunological assays (Sayre et al. 1986). There are also several short non-membrane helices between the transmembrane helices on either the lumenal side or the stromal (cytoplasmic in cyanobacteria) side. These non-membrane helices were based on the bacterial templates because the sequences are well conserved. No new secondary structures were introduced by the BLAST-searched protein fragments. In this model, there is very little β -sheet content which is in agreement with the Fourier transform infra-red spectroscopy data (He et al. 1991). The detailed secondary structure profiles analyzed from the modeled D1 and D2 are shown in Figs. 4.4 and 4.5, respectively. The definition for the boundaries of the transmembrane α -helices are slightly different from what was previously reported (Ruffle et al. 1992; Vermaas et al. 1993; Nixon and Diner 1994; Svensson 1995). The differences can be attributed to the different alignment and refinement procedures used in the modeling. The general profile of the residue polarity was also examined: most of the charged or polar residues in the model are on the outside of the putative transmembrane spans and in the putative lumenal and stromal (cytoplasmic) sides, while the non-polar and hydrophobic residues are in the putative membranous region, making the structure more stable.

The D1 and D2 interface is mostly composed of residues either in the transmembrane helices D and E or in the non-transmembrane regions. The contact residues between D1 and D2 are highlighted in Figs. 4.4 and 4.5. The interactions between these contact residues are considered to play a key role in the assembly of the PSII reaction center and in maintaining a proper conformation of this protein complex. Mutations of some of these residues may result in complicated local and/or global effects, such as destabilization of the reaction center (Vermaas et al. 1987; 1990; 1994; Xiong et al. 1995; Hutchison et al. 1996), transduction of donor side mutational effect to the acceptor side (Roffey et al. 1994)

Figure 4.4. The secondary structure profile of the modeled D1 protein. The predicted α -helical residues are boxed. The residues that are predicted to interact with D2 protein are highlighted. The stromal (cytoplasmic) side is on top, the luminal side on the bottom.

Figure 4.5. The secondary structure profile of the modeled D2 protein. The predicted α -helical residues are boxed. The residues that are predicted to interact with D1 protein are highlighted. The stromal (cytoplasmic) side is on top, the luminal side on the bottom.



or vice versa (Hutchison et al. 1996), transduction of D2 mutational effects to D1 (Kless et al. 1993; Vermaas et al. 1994) or vice versa.

The final PSII reaction center model was evaluated with the Protein Health subprogram in QUANTA. The D1 and D2 main chain torsion angles were analyzed using the phi-psi plot (Ramachandran et al. 1963) which shows that 83.8% of the backbone conformations are within the most favoured regions as compared to 88.0% in the structure of *Rb. sphaeroides* L and M subunits. The quality of the model was also assessed using the newly developed Probability Density Functions (PDF) method (Subramaniam et al. 1996) which profiles the modeled structures against a standardized database of atom-pair probability density functions, which includes information on the distribution of distances between each pair of atoms in any pair of residues. The total number of atom types corresponding to the heavy atoms in the twenty amino acids is 167. The pairwise atomic distance PDFs are generated intra residues, residues related by positions, $n-n+1$, $n-n+2$, and $n-n+3$ and tertiary PDFs are computed separately for N to C and C to N terminal directions. The PDFs are assumed independent to each other. The total number of PDFs thus amount to 112,226 types and the number of atomic distance pairs in the 380 proteins considered are 80,670,588. Summary profiles at the atomic and residue level were generated for the modeled structure. In profiling, negative probabilities are unfavorable and probabilities above zero correspond to favorable contacts in resolution protein structures. The calculated results show that there are 0.0019% of highly improbable ($\log(P) < -9$) interatomic distances found in the model (440 out of 22,535,541 interatomic distances measured), as compared to 0.0016% of such improbable distances (250 out of 15,193,828 interatomic distances measured) found in one of the templates used, the L and M subunits of *Rb. sphaeroides* reaction center. Thus, the comparison of PSII with bacterial reaction center is highly favorable.

Due to the varied sequence homology, different regions of the PSII reaction center model may have different levels of correctness. The transmembrane regions and the

quinone binding sites are highly conserved and have been modeled with a high degree of confidence. The stromal (cytoplasmic) and lumenal parts of the sequences, having many occurrences of insertions and deletions, can only be predicted with a relatively low degree of confidence. The conformation of the modeled C-terminal regions of both polypeptides, which are non-homologous to the bacterial template and are, perhaps, in contact with other PSII subunits, are more speculative than other regions of the model.

3. General description of important cofactors

In this model, the cofactors essential for the PSII electron transfer include four chlorophylls, two pheophytins, one β -carotene, two plastoquinones, one non-heme iron and two bicarbonate ions. Except for bicarbonate, other cofactors were modeled in the same location and the same geometric orientation as their counterparts in the bacterial reaction centers. Experimental evidence on the cofactor composition, P680 charge separation and the electron transfer of PSII reaction center preparations supports the notion that the PSII chromophores are oriented similarly to those in the bacterial reaction center (Barber et al. 1987; van Dorssen et al. 1987; Shuvalov et al. 1989; Diner et al. 1991b). Quantitation of the PSII reaction center chromophores indicate that there are four to six chlorophylls, two pheophytins and two plastoquinones (Nanba and Satoh 1987; Gounaris et al. 1990; Kobayashi et al. 1990; van Leeuwen et al. 1991; Chang et al. 1994). Based on hole burning experiments, Chang et al. (1994) consider four chlorophylls to be the functionally limiting number in the PSII reaction center, making the pigment composition of PSII more homologous to that in the purple bacterial reaction centers.

4. Chlorophyll P680

There have been controversies concerning the number and orientation of the bound primary donor P680 chlorophylls in the PSII reaction center. On the basis of optical absorption difference measurements, van der Vos et al. (1992) proposed that P680 is a

monomer chlorophyll. However, an electron nuclear double resonance (ENDOR) study by Nugent et al. (1994) showed that the P680⁺ radical involves two weakly interacting chlorophylls. EPR studies showed that the ground state P680 is a dimer (Nugent et al. 1994). The measurement by Kwa et al. (1994) also ruled out the simple monomer model and suggested that P680 is most likely a dimer but did not rule out the possibility of more than two excitonically-coupled chlorophylls. Schelvis et al. (1994) suggested that P680 is a dimer asymmetrically oriented in the PSII reaction center. Thus, the majority of the studies appear to indicate that P680 is a dimer, at least in the singlet excited state. However, there are other suggestions as well. Vermaas (1993) suggested that P680 may consist of three chlorophylls (two homologous to the bacterial special pair and one to an accessory bacteriochlorophyll) which are in sufficient proximity that the positive charge and the triplet state are delocalized over the three molecules. Recently, Durrant et al. (1995) proposed that P680 should not be considered a strongly coupled dimer but rather a weakly coupled multimer including the pheophytin electron acceptor. The final resolution of these possibilities will be available only from a high resolution crystal structure of the PSII reaction center.

The orientation measurements of a light-induced spin-polarized chlorophyll triplet by van Mieghem et al. (1991) led to the conclusion that in the PSII reaction centers the ring of the triplet chlorophyll is at a 30° angle relative to the membrane plane, in contrast to the primary donor in the purple bacterial reaction center where they are essentially perpendicular to the membrane plane. It was suggested that this chlorophyll which is P680 may resemble in geometry one of the accessory bacteriochlorophylls. Similar results were obtained by Bosch et al. (1995) who proposed a structural model of P680 based on the magnetophotoselection measurement of the triplet state P680, in which P680 is an excitonically-coupled dimer of chlorophyll *a*. Their model shows that two chlorophyll components of P680 are separated by 11 Å (center to center) and make an angle of 60°. The model of Svensson et al. (1995b), based on optical spectroscopic data, indicates that the

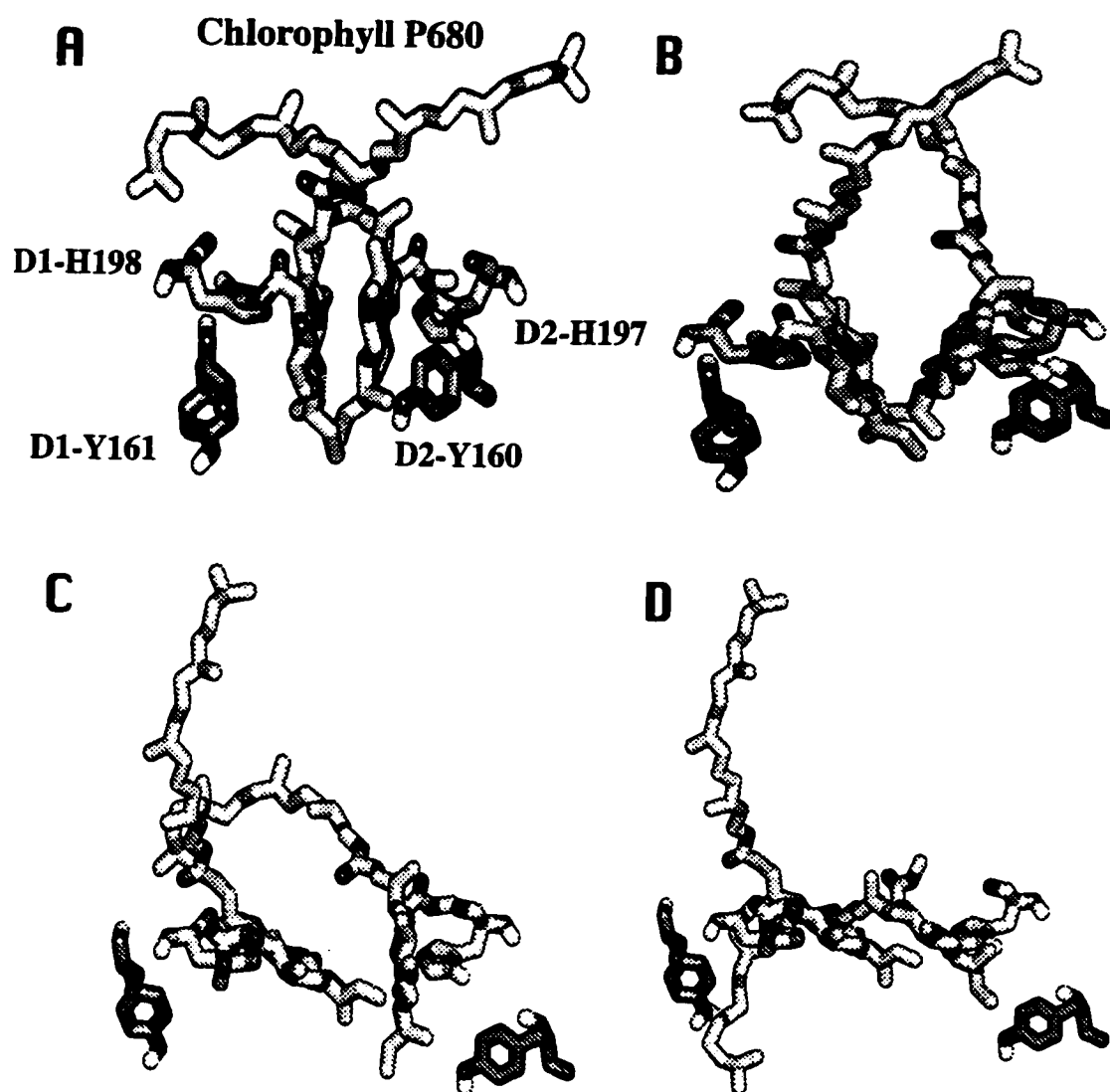
dimeric P680 chlorophylls, which are symmetrically oriented and parallel to each other, are separated by 10 Å and the angle between the excitonic transition moments (Q_y) is 150°.

In view of the existing experimental suggestions, several possible alternative conformations for the chlorophyll P680 are proposed here (Fig. 4.6). In the first model (Fig. 4.6A), the arrangement of the special pair chlorophyll is assumed to be similar to the bacterial counterpart. In this model, the two monomers of the P680 chlorophyll dimer are parallel to each other and perpendicular to the membrane plane. The magnesium ions in the center of the chlorophyll special pair are separated by 8.4 Å. The center to center distance of the primary donor is larger than that in the *Rps. viridis* reaction center, which may allow a more even distribution of exciton interactions between all pigments in PSII. The P680 model of Svensson et al. (1995b) and Svensson (1995), in which the special pair chlorophyll is also perpendicular to the membrane plane, has an even larger separation between the two monomers (10.1 Å).

In the P680 chlorophylls, the magnesium ions at the center of the P680 monomers are liganded by the specific histidine residues, D1-H198 and D2-H197, which, according to sequence comparison, match well with L-H173 and M-H210 (*Rps. viridis* numbering) of the bacterial special pair ligands. The ϵ 2-nitrogen atoms of D1-H198 and D2-H197 are modeled 2.4 Å and 2.3 Å away from the coordinating magnesium, respectively. These two histidine residues are conserved in all known D1 and D2 sequences throughout the plants, algae, and cyanobacteria. Mutations made at these two histidine residues either lead to the loss of the PSII reaction center (see Vermaas et al. 1988; Nixon et al. 1992) or show a shift of 20-30 mV in midpoint potentials for P680⁺/P680, thus supporting the role of these histidines in coordinating P680 (unpublished data, cited in Vermaas 1993).

Most of the residues lining the binding pocket for the P680 chlorophyll pair are hydrophobic and non-polar. The P680 chlorophyll on the D2 side appears to be stacked by an aromatic residue, D2-W191. The closest modeled distance between the residue and the chlorophyll is 3.4 Å. Similar interaction was also suggested by Svensson (1995). No such

Figure 4.6. Various possible models for the structures of P680 chlorophylls. The two histidines (D1-H198 and D2-H197) that ligand the magnesium in the center of the chlorophylls and the two redox active residues D1-Y161 (Z) and D2-Y160 (D) as electron donors to P680 are also shown. (A) The possible conformation of P680 based on homology. The P680 chlorophyll dimer which is assumed to be a homologous to the bacteriochlorophyll special pair have two monomers parallel to each other and perpendicular to the membrane plane, which are separated by 8.4 Å. (B) The possible conformation of P680 dimer based on the suggestion of Bosch et al. (1995). The two chlorophylls of the special pair are modeled to be distanced by 10 Å and to make an angle of $\sim 60^\circ$ ($\sim 30^\circ$ with the vertical membrane axis). (C) The possible conformation of P680 dimer based on the suggestion of Noguchi et al. (1993). The two chlorophylls of the special pair are arranged asymmetrically, with one of the chlorophylls perpendicular with the membrane plane and the other tilted by 30° relative to the membrane plane. They are separated by 8.4 Å. (D) The possible conformation of P680 dimer based on the suggestion of Schelvis et al. (1994). The two chlorophylls are parallel to each other and make a 30° angle to the membrane plane and are separated by 8.4 Å.



ring stacking is observed for the P680 on the D1 side. Svensson (1995) suggested that the above tryptophan residue may also form a hydrogen bond to the ester group on the ring IV of D2 P680 chlorophyll. This hydrogen bonding was not observed in this model as the modeled distance is 8.6 Å. Svensson (1995) also suggested that residues D1-T286 and D2-S283 hydrogen bond to the ester groups on the ring IV of P680 on both the D1 and D2 sides. However, this was not supported in this model either. D1-M183 is positioned on the opposite side of the liganding D1-H198 and was suggested to have an electrostatic interaction with the magnesium ion and one of the nitrogens of D1 P680 by Svensson (1995). I consider such interaction unlikely as the modeled distances between the sulfur atom and the above two atoms are 5.5 and 5.8 Å, respectively, in this model. I consider the possibility that the residue may form a van der Waals interaction instead with the chlorophyll since the methyl group is modeled to be 3.1 Å away from the chlorophyll.

Alternative structural models for the P680 special pair are proposed or re-proposed here to account for the existing experimental data in literature. One such possible conformation of the chlorophyll P680 based on the suggestion of Bosch et al. (1995) results in a symmetrical structure for the two chlorophyll components. In this model (Fig. 4.6B), the two chlorophylls were separated by 10 Å, which make an angle of ~60° with each other. Each chlorophyll in the model has a ~60° angle relative to the membrane plane. This model matches the experimentally measured distance of 10.5 Å and an angle of 60° (Bosch et al. 1995).

According to a Fourier transform infra-red spectroscopic study which indicates the existence of an asymmetric dimer of chlorophyll *a* in the triplet state (Noguchi et al. 1993), an asymmetric P680 model was proposed (see review by Diner and Babcock 1996). This conformation of P680 dimer suggests that one of the chlorophyll monomers is perpendicular to the membrane plane and the other tilted by 30° relative to the membrane plane. I have thus provided such a model with the two asymmetric chlorophylls (Fig. 4.6C). The distance between the centers of the two chlorophylls in the model is 8.4 Å.

Another possible conformation of P680 dimer which seems to account for more experimental data was proposed by Schelvis et al. (1994) (see Diner and Babcock 1996). This suggestion implicates that the two chlorophyll monomers are still parallel to each other but both are tilted by a 30° angle relative to the membrane plane. Thus another alternative model for P680 is presented here (Fig. 6D). The modeled distance between the two chlorophylls is 8.4 Å which is greater than that between the two monomers of the bacterial special pairs, as suggested by Diner and Babcock (1996).

The latter three alternative conformations (Figs. 6B-D) introduced enormous structural constraints to the protein part of the model which was constructed based on homology. Thus, these chlorophylls were modeled separately from the main protein model. These models are only considered speculative suggestions for motivating further experimental verification. Currently, the P680 model that was based on analogy with the bacterial primary donor is the favored one (Fig. 6A), since it is the most energetically favorable conformation in the current PSII reaction center model. In particular, the similar model of Svensson et al. (1995b) indicates that when the two P680 monomers which are perpendicular to the membrane plane are more than 10 Å away from each other, the conformation can be made to fit all existing experimental data.

5. Accessory chlorophylls

The modeling of the two accessory chlorophylls that are not directly involved in primary charge separation was strictly based on their bacterial counterparts. The protein binding environment of the accessory chlorophylls appears to be somewhat different from the ones in the bacterial reaction center if the chlorophylls occupy the same spatial position in PSII. The histidine residues which are coordinated with the magnesium ions in the bacteriochlorophylls (L-H153 and M-H180) are not conserved in D1 and D2. In this model, the residues close to the center of the two accessory chlorophylls are D1-T179 and D2-I178, which are modeled 3.9 Å and 4.2 Å to the magnesium, respectively. However

these two residues do not appear to be able to provide ligands to the respective magnesium ions as previously noticed in the pea model of Ruffle et al. (1992). Svensson (1995) proposed a possibility of water molecules acting as ligands for the chlorophylls. Aromatic residues D1-F180 and D2-F179 are found to be close (3.7 Å) to one of the pyrrole rings of the chlorophylls on either side, and it is expected that they may provide important ring-stacking interactions to the chlorophylls. Residue D2-L205 is in between the accessory chlorophyll and the active pheophytin on the Q_A side and is thought to serve as a conduit for electron transport, as noted in Ruffle et al. (1992).

Experimental models of accessory chlorophylls also exist. Based on the results from polarized fluorescence spectroscopy that the average orientations of the PSII chlorophylls are markedly different from those of the bacterial accessory chlorophylls, van Gorkom and Schelvis (1993) argued that a close association of the accessory chlorophylls with the P680 dimer is unlikely, and suggested that they should be separated by ~23 Å to allow an effective antenna function while minimizing the photo-oxidation process. Schelvis et al. (1994) further postulated that D1-H118 and D2-H117 may be the likely candidates for liganding the accessory chlorophylls. These two histidine residues in the PSII reaction center model are separated from the nearest accessory chlorophylls by more than 10 Å and thus a non-covalent interaction is considered unlikely without introducing new chlorophylls onto these two ligands.

6. *Pheophytins*

Modeling of the two pheophytins is also based on a strict homology with the bacteriopheophytins which are positioned in the center of the hydrophobic membrane spanning region. The most prominent binding interactions to the "redox active" pheophytin on the Q_A side are the hydrogen bonds to the keto group of the pheophytin provided by D1-R27 and D1-Q130 (modeled bond distances 2.3 Å and 2.5 Å, respectively). In many other species, D1-130 residue is a glutamate instead. Ruffle et al. (1992) and Svensson

(1995) have modeled similar hydrogen bonding interactions between the pheophytin and D1-E130 (but not the arginine) in pea and spinach. In *Synechocystis* sp. PCC 6803, D1-Q130E mutation caused the pheophytin difference absorption spectrum to shift to the red by 3 nm (Giorgi et al. 1996) making it resemble the spectrum of the higher plants. It is suggested that in the higher plant system the glutamate may provide a stronger hydrogen bond to the pheophytin. In a related cyanobacterial species, *Synechococcus* sp. PCC 7942, there are two distinct forms of D1 protein, one (form I, encoded by *psbA*-1) having a lower photochemical yield and higher susceptibility to photoinhibitory damage than the other (form II, encoded by *psbA*-2 and -3) (Clarke et al. 1993; Kulkarni and Golden 1994; 1995). The more efficient form II turns out to have a glutamate at 130 position, while the less efficient form I has a glutamine (see Svensson et al. 1991). Since this keto oxygen is part of the conjugated double bond system in the porphyrin, it is expected that a modified interaction at this position will have a considerable effect on the redox potential of the pheophytin (Svensson 1995). Analogous situations were observed in purple bacteria when mutations affected the hydrogen bonding pattern with the bacteriochlorophylls, the redox potentials of the bacteriochlorophylls were changed (see, *e.g.*, Wachtveitl et al. 1993).

In addition to the hydrogen bonding provided by D1-Q130, aromatic residue D1-Y147 is found to be close to one of the pyrrole rings and are thought to play a role in stabilizing the pheophytins. The side chain of D1-Y147 may also provide hydrogen bonding to the ester oxygen of the phytol branch (modeled distance 3.3 Å) consistent with the modeling result of Svensson (1995). The carbonyl group of the phytol branch of the same pheophytin probably forms a weak hydrogen bond with the hydroxyl group of D1-Y126, as the modeled distance between them is 3.4 Å. However, Svensson (1995) suggests that this tyrosine residue hydrogen bonds to the ester group on the ring IV of the pheophytin instead. An aromatic residue D2-W253 is found to be located between the Q_A head group and the "active" pheophytin and is separated from the porphyrin by 3.1 Å and from the Q_A by 3.7 Å. This residue has been suggested to be a "superexchange" mediator

for the electron transport between pheophytin and plastoquinone (Plato et al. 1989). Another residue in between the same pheophytin and Q_A is D2-I213 which is positioned 4.5 Å from the porphyrin of pheophytin and 4.7 Å from the head group of Q_A and may play a similar role as D2-W253.

In the current model, the keto group on the ring V of the "inactive" pheophytin on the Q_B side is hydrogen-bonded to D2-Q129 and D2-N142 (modeled bond distances from donor hydrogens to the hydrogen acceptors are 1.9 Å and 2.3 Å, respectively). The previous models (Ruffle et al. 1992; Svensson 1995) had only the glutamine residue providing such hydrogen bonding interactions with the pheophytin. D2-F146 is modeled close to the ring IV of the pheophytin (3.1 Å) and its aromatic ring is also parallel to the pyrrole ring allowing a ring stacking interaction between them. The key hydrophobic residues located in between the "inactive" pheophytin and Q_B are D1-F255 and D1-M214 which are modeled to be 3.6 Å and 4.9 Å, respectively, away from the pheophytin, and 4.7 Å and 4.0 Å, respectively, from Q_B . The geometric orientation of D1-F255 is different compared to that of D2-W253. It is speculated that the distances and orientation of the two aromatic residues relative to the pheophytins may partially contribute to the unidirectional electron flow after the primary charge separation is over.

Supporting evidence for the above pheophytin modeling based on homology includes measurements on PSII chromophore stoichiometry (*e.g.* Chang et al. 1994) and the influence of site-directed mutagenesis on the pheophytin binding site on PSII electron transfer (see Diner and Babcock 1996). However the linear dichroism (LD) data that indicate oppositely signed LD features for pheophytins appear to argue against the strict analogy used above (Breton 1990; van der Vos et al. 1992; van Gorkom and Schelvis 1993).

7. β -Carotene

In the PSII reaction center model presented in this chapter, I have one β -carotene molecule modeled on the D2 side, from modifying the structure of dihydro-neurosporene from *Rps. viridis* (1PRC). This is the first effort in modeling of this chromophore in PSII. The carotenoid is located in the middle of the transmembrane region. The protein binding environment for the carotenoid is exclusively hydrophobic, which includes D2-L45, D2-W48, D2-L49, D2-A71, D2-L74, D2-F91, D2-W111, D2-D112, D2-F113, D2-A115, D2-A119, D2-L116, D2-F153, D2-V154, D2-F157, D2-L158, D2-S172, D2-F173, D2-G174, D2-V175. The conformation of β -carotene is kinked with a conjugated π -system parallel to the membrane. The molecule was modeled to be within van der Waals contact with the accessory chlorophyll on the D2 side.

The carotenoid in the bacterial system is suggested to protect the reaction center against photo-oxidation by quenching the triplet state of the bacteriochlorophyll special pair (see review, Lancaster et al. 1995). Similarly, the function of β -carotene in the PSII reaction center is thought to be related to the protection of PSII reaction center from damage by excess light through dissipation of excess excitation energy, as heat, on the special pair chlorophyll (Telfer et al. 1994). The close proximity of β -carotene to the accessory chlorophyll supports a high probability that it may function in quenching the triplet state of primary donor P680 via the accessory chlorophyll, analogous to the role of carotenoid in the bacterial reaction center.

8. Donors to P680⁺

Oxygen evolution takes place in PSII only when the PSII reaction center is in association with several other PSII proteins (for reviews, see Ghanotakis and Yocum 1990; Vermaas and Ikeuchi 1991; Vermaas et al. 1993). The D1 and D2 residues at the luminal side have high affinity for a manganese cluster (Coleman and Govindjee 1987; Debus 1992) which serves as a charge accumulator device during water oxidation (for reviews,

see Hansson and Wydrzynski 1990; Diner et al. 1991b, Debus 1992; Renger 1993; Babcock 1995). Site-directed mutagenesis studies on D1 and D2 have led to the identification of two redox active residues, D1-Y161 and D2-Y160, which are electron donors to chlorophyll P680⁺. D1-Y161, or the donor Z (also called Y_Z), is a rapid electron donor to the P680⁺ (Debus et al., 1988a; Metz et al., 1989); and the D2-Y160, or the donor D (also called Y_D), is a slow donor (Debus et al. 1988b; Vermaas et al. 1988).

The two tyrosine residues in the model were arranged symmetrically around the special pair chlorophylls and in relation to the non-heme iron. Both of the residues are positioned such that their hydroxyl groups are pointing toward the lumen. The spatial relationships of the residues with D1-H198 and D2-H197 that serve as ligands for the chlorophyll special pair are shown in Fig. 6. The modeled distance from the D1-Y161 phenolic oxygen to the center of the nearest chlorophyll P680 monomer is 12.8 Å. This matches well with the experimentally determined distance of 10-15 Å (Hoganson and Babcock 1989). The measured distance between D1-Y161 and D2-Y160 are 30.6 Å which matches closely with the experimentally measured 29-30 Å distance (Astashkin et al. 1994; Kodera et al. 1995). The modeled distances of the tyrosines Z and D to the non heme iron is 36.5 Å and 34.2 Å, respectively, which fall in the range of the EPR spectroscopic measurements of 37 ± 5 Å by Hirsch and Brudvig (1993) and Koulougliotis et al. (1995). The EPR-estimated distance from donor D to the non-heme iron by Kodera et al. (1992) is 26-33 Å. The above experimental studies provide strong support to the validity of this PSII three-dimensional model.

The amino acid environment surrounding the two tyrosine residues may affect the functions of Z and D. In this model, the residues that are located between D1-Y161 and the nearest P680 chlorophyll are D1-A156, D1-F186, D1-A287, D1-M288, D1-G289, D1-V290, D1-S291, D1-T292, and D1-M293. Most of these residues may be crucial in mediating the electron transfer from the donor Z to P680⁺. The modeled Z and D residues do not seem to hydrogen bond with the histidine residues that coordinate P680 as

previously noted (Svensson et al. 1990). Other residues surrounding D1-Y161 within 5 Å are D1-T155, D1-V157, D1-F158, D1-L159, D1-I160, D1-P162, D1-I163, D1-G164, D1-Q165, D1-G166, D1-N298, D1-G299, D1-N301, D1-N303, and D1-Q304. The binding environment is somewhat hydrophilic for the donor Z. Some of the residues such as D1-S167 were suggested to provide ligands to the manganese cluster (Ruffle et al. 1992). Site-directed mutagenesis of D1-H190 in *Chlamydomonas reinhardtii* indicates that this residue may be involved in assembly of manganese cluster (Roffey et al. 1994). D1-H190 was suggested to be in close vicinity to donor Z (4 Å) by Svensson (1995) and an electrostatic interaction between the two residues was proposed. However, this is not in agreement with the current model, as the respective distance from the tyrosine to the histidine is 9.0 Å. Mutation of this residue to a phenylalanine resulted in a spectrum very similar to the wild type suggesting that the histidine may not be in such a close contact with the donor Z (Roffey et al., 1994; Kramer et al., 1994). Mutations on D1-H195 were shown to have lowered oxygen evolution and a shifted equilibrium constant between $\text{Tyr}_Z\text{P680}^+$ and $\text{Tyr}_Z^{\text{ox}}\text{P680}$ most likely due to a change in the midpoint potential for $\text{Tyr}_Z/\text{Tyr}_Z^{\text{ox}}$ couple (Roffey et al. 1994; Kramer et al. 1994). This residue was modeled to be off the contact distance from either Z or P680. However, it is positioned 3.1 Å from D1-M293 which is also 3.1 Å from Z. Thus impacts of indirect structural changes in the binding environment for the donor Z may be attributed to its slowed electron transfer to P680.

Manganese cluster which is crucial in water oxidation and reduction of the donor Z was not included in this model. An aspartate residue, D1-D170, was experimentally implicated in binding to the Mn cluster at the PSII donor side (Nixon and Diner 1992; Chu et al. 1995). The distance between the manganese cluster and the donor Z measured by the electron spin echo electron-nuclear double resonance experiments was shown to be 4.5 Å (Gilchrist et al. 1995). It is conceivable that one of the manganese ligands, D1-D170, should be located in close proximity to the donor Z as presented in Svensson (1995). In

this PSII reaction center model, this aspartate residue was modeled at slightly more than the van der Waals contact distance (6.4 Å) which is somewhat in agreement with the previous experimental and theoretical studies. However, another acidic residue, D1-E189, which was also suggested to be close to D1-Y161 (Svensson 1995), is not observed in the current model as the inter-residue distance is 12.2 Å.

The model of Svensson (1995) suggests that D2-H190 (higher plant numbering) is hydrogen bonded to the donor D, as the distance between the ϵ 2-nitrogen of D2-H190 and the phenolic oxygen of D2-Y160 is 2.8 Å. This is not in agreement with this model, as the corresponding distance in the model is 7.9 Å. D2-Q164 was proposed to hydrogen bond to the donor D in Svensson (1995); also this is inconsistent with the model presented here as the corresponding distance is 6.2 Å. Instead, the phenolic oxygen of the donor D appears to hydrogen bond to the main chain oxygen of D2-F169 (the modeled distance is 2.8 Å).

Diner et al. (1991b) suggested that some of the D1 C-terminal residues (D1-H332, D1-D342, D1-A344) are involved in the assembly of the oxygen evolving complex and in manganese binding. However, these residues are found at a long distance (more than 27 Å) from the donor Z in this model. It is not clear how their role can be exerted at such a distance. It may be possible that the C-terminus is folded under the transmembrane helices as suggested by Nugent et al. (1994). However, without further experimental evidence to direct the modeling, this question has to be left open. As oxygen evolution is unique in PSII and the primary structures of D1 and D2 tend to have low homology with the bacterial reaction center in the C-terminal region, accurate modeling of the oxygen evolving complex may be difficult at this stage.

9. Plastoquinone Q_A and its binding niche

The primary plastoquinone Q_A , a bound one electron carrier, was modeled in the region between helices D and E of D2, though the rest of the transmembrane regions on the "active" side are dominated by the D1 protein. The D2 residues that provide specific

interactions to Q_A include D2-T217, D2-N230, D2-S262 and D2-N263; they may contribute to the Q_A binding by providing hydrogen bonds to the carbonyl oxygen of Q_A . One of the Q_A carbonyl oxygen atoms can form a bifurcal hydrogen bond to the side chain hydroxyl group of D2-T217 and the amide group of D2-N230. The modeled bond distances are 2.8 and 2.3 Å (from the donor hydrogens to the acceptor oxygen), respectively. Another Q_A carbonyl oxygen may also hydrogen bond to more than one residue donor atoms. The main chain amide hydrogens of D2-S262 and D2-N263 are both possible donors for the hydrogen bonds since the modeled distances from the Q_A oxygen atom to the hydrogen donors of D2-S262 and D2-N263 are 2.4 and 2.8 Å, respectively. Among the residues that form a tight binding niche, those that are considered to be involved in interacting with the head group of Q_A are mostly polar or positively charged. They are D2-H214, D2-T217, D2-T221, D2-N230, D2-A249, D2-N250, D2-W253, D2-S254, D2-S262, D2-N263, D2-K264, D2-L267. Those residues that are considered to be more likely to interact with the isoprenoid chain of Q_A are mostly hydrophobic. They are D2-L209, D2-L210, D2-I213, D2-Q255, D2-I259, D2-A260, D2-F261, and D2-W266. As mentioned previously, D2-W253 is a critical residue that may function in mediating the electron transfer between pheophytin and Q_A . In addition, the ring system of D2-W252 is parallel to Q_A and thus may allow the residue to stack with Q_A and stabilize Q_A binding.

An electron spin echo envelope modulation experiment suggested hydrogen bonding between Q_A^- and a histidine residue (Astashkin et al. 1995). If this bonding pattern indeed exists, I consider D2-H214 to be a likely candidate to provide such a bonding because its $\delta 1$ -hydrogen is modeled to be 3.5 Å away from one of the Q_A carbonyl oxygens. However, the isotopic labeling experiment of Tang et al. (1995) did not confirm the coupling of a histidine nitrogen with Q_A^- .

10. Plastoquinone Q_B and its binding niche

The secondary plastoquinone Q_B is a two electron carrier and can be doubly reduced by Q_A^- . The Q_B binding niche has long been the subject of intensive research as this binding site is also the site for herbicide binding (see reviews, Oettmeier 1992; Vermaas 1993).

The Q_B binding niche is formed predominantly by D1 residues which fall between the helices D and E of the D1 protein. Interestingly, there are also a number of D2 residues that are identified to be in the Q_B niche. The residues that are modeled to provide hydrogen bonding to the carbonyl oxygen atoms of Q_B are D1-H215, D1-H252 and D1-S264. The modeled hydrogen bond distances between one of the Q_B oxygens and the hydrogen donors of D1-H252 and D1-S264 are 3.1 Å and 2.8 Å, respectively. The other Q_B oxygen is hydrogen bonded to D1-H215 at a bond distance of 2.3 Å. D1 residues identified to be more likely related to the binding of the head group of Q_B are D1-H215, D1-V219, D1-Y246, D1-A251, D1-H252, D1-F255, D1-S264, D1-N266, and D1-L271. A D2 residue D2-F232 is found in close association with the Q_B head group. The residues that are identified to be responsible for interacting with the isoprene tail also involve both D1 and D2 proteins. They are D1-F211, D1-M214, D1-I259, D1-F260, D1-Y262, D1-A263, D1-F265, D2-I30, D2-L37, D2-F38, D2-F125, D2-R128.

Mutational studies on D1-S264 and D1-H252 have implicated their close association with Q_B . Taoka and Crofts (1990) show that D1-S264G mutation raises the dissociation constant (K_Q) of Q_B by a factor of ten, though it has little effect on the forward rate constant that is related to the Q_B protonation. The bacterial homologue of D1-S264, L-S233 (*Rps. viridis* numbering) has been suggested to play a role in stabilizing the Q_B protonation intermediate, Q_BH^+ (Lancaster and Michel 1996). It is not yet known whether D1-S264 may assume a similar role in PSII. Mutations of D1-H252 to leucine or glycine have been shown to lower the apparent equilibrium constant (K'_{AB}) by a factor of ten for the reaction $Q_A^- + PQ + Q_A^-Q_B = Q_AQ_B^-$ (Diner et al. 1991a; b; Nixon et al. 1992). More

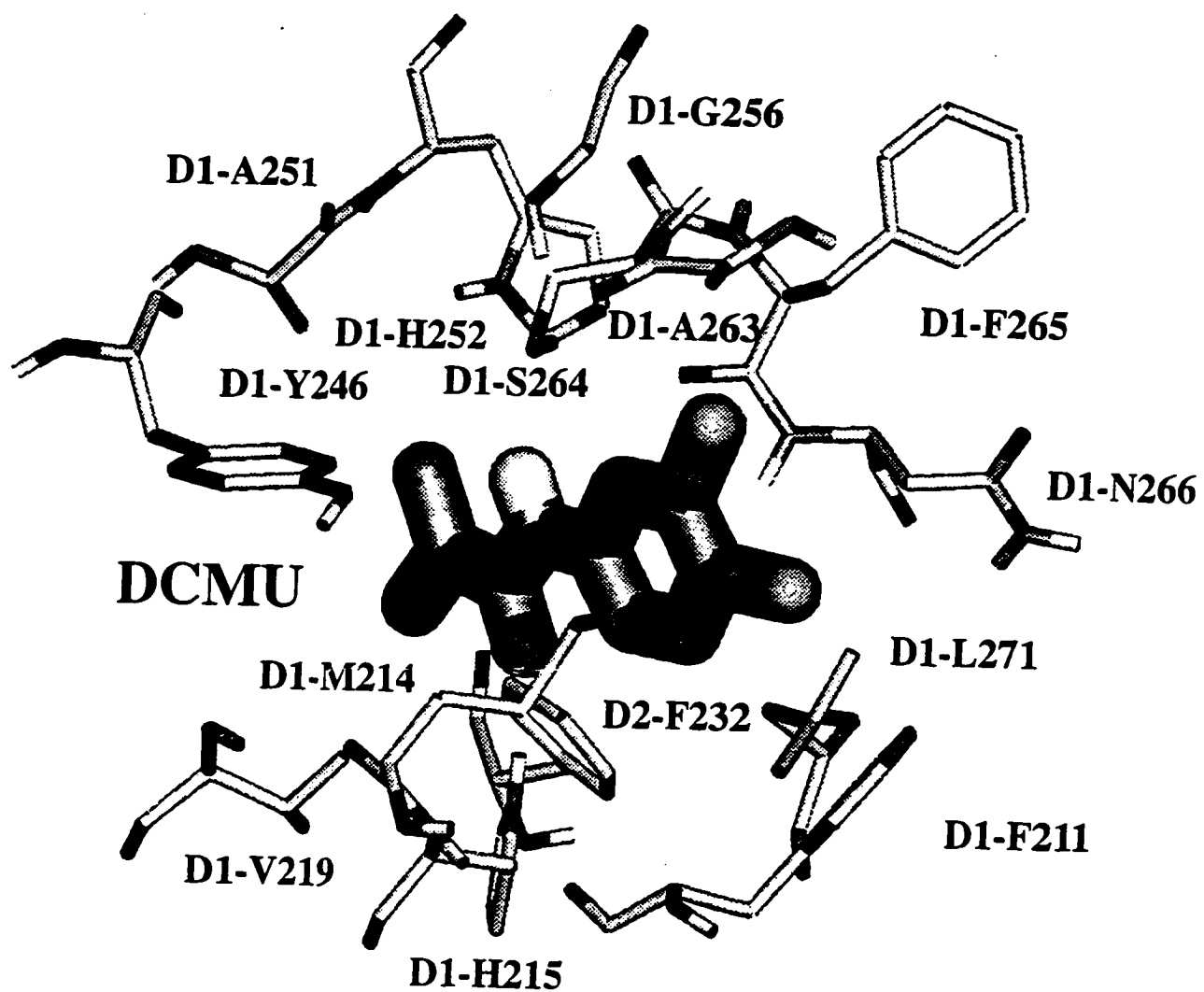
detailed discussion on the role of D1-H252 in the Q_B protonation will be presented in a later section. D1-F255 may also be a critical residue in Q_B binding as its bacterial counterpart, L-F216, in the refined model of Lancaster et al. (1995) where the phenyl ring of L-F216 appears to stack with the Q_B head group. Though the phenyl ring of D1-F255 in my model is not parallel to the aromatic ring of Q_B corresponding to the structure in the bacterial templates (1PRC and 2RCR), it is still modeled within van der Waals contact distance to Q_B (4.2 Å), which may support its role in providing strong hydrophobic interactions with the plastoquinone.

11. Herbicide DCMU binding

PSII herbicides are known to displace Q_B from its binding niche and to inhibit the electron transfer from Q_A to Q_B (Velthuys 1981; Wraight 1981). In this study, DCMU which is one of the most commonly used phenylurea type of herbicides was modeled in the Q_B site.

Modeling of DCMU to the Q_B niche (Fig. 4.7) was based on the available crystal structure information of DCMU binding in a bacterial reaction center. DCMU that binds to PSII does not normally bind to the bacterial reaction center. However, analyses of *Rps. viridis* mutants showed that a mutation (L-Y222F) resulted in the reaction center being "PSII-like" by becoming receptive to urea type herbicides (*e.g.* DCMU) (Sinning et al. 1989). The X-ray structure of this mutant (T4) reaction center with bound DCMU is available (Sinning et al. 1990; Sinning 1992). The structure shows that the mutation eliminates the hydrogen bonding between the L-Y222 and M-D43, causing a slight movement of a stretch of M residues that shield the Q_B site thus widening the Q_B binding pocket. DCMU phenyl ring was turned by 180° as compared with Q_B . During modeling, I assumed that DCMU adopted a conformation similar to that in the bacterial reaction center. This assumption was supported by the evidence that DCMU binding to T4 resulted in similar semiquinone-EPR signals to that in PSII (Sinning et al. 1989). Following the

Figure 4.7. Herbicide DCMU modeled in the Q_B binding niche according to its binding pattern determined in the crystal structure of a mutant *Rps. viridis* reaction center. The protein binding environment for DCMU is shown. The side chain of D1-H215 is predicted to provide hydrogen bonding to the carboxyl oxygen of DCMU. D1-S264 may provide a hydrogen bond with the amide group of DCMU.



insertion of DCMU, protein binding environment surrounding the herbicide was refined through energy minimization and molecular dynamics simulations. The final CHARMM energy of the DCMU binding niche is -1,200.5 kcal/mol compared to 95969.7 kcal/mol before minimization.

The protein binding environment for DCMU is found to be overlapping with that for Q_B, though not identical. The residues that appear to coordinate the herbicide binding are D1-F211, D1-M214, D1-H215, D1-V219, D1-F232, D1-Y246, D1-A251, D1-H252, D1-G256, D1-A263, D1-S264, D1-F265, D1-N266, and D1-L271 as shown in Fig. 7. D1-H215 δ 1-hydrogen is likely to provide a hydrogen bond to the carbonyl group of DCMU with the modeled bond distance at 2.3 Å. D1-H215 is homologous to L-H190 in bacterial reaction center, which was also found to hydrogen bond to DCMU in the T4 mutant reaction center (Sinning 1992). D1-S264 may provide another hydrogen bond through its hydroxyl oxygen to the amide hydrogen of DCMU. The modeled bond distance is 2.7 Å. It is possible that the herbicide may also hydrogen bond with the amino acid residues via water molecules as is the case in triazine binding to the bacterial reaction centers (Lancaster et al. 1995).

Numerous studies have been conducted on site-specific mutations in the Q_B niche that induce modified binding specificities for DCMU (for review, see Oettmeier 1992). Well known single mutations that have caused DCMU resistance such as D1-F211S, D1-V219I, D1-G256D, D1-A251V, and D1-S264A can all be explained by the newly constructed model as these residues are found within the van der Waals contact sphere with DCMU (Fig. 4.7). The herbicide resistance mutations may thus be due to the modified van der Waals or electrostatic interactions of DCMU with its protein binding environment.

12. Non-heme iron and the liganding histidines and bicarbonate

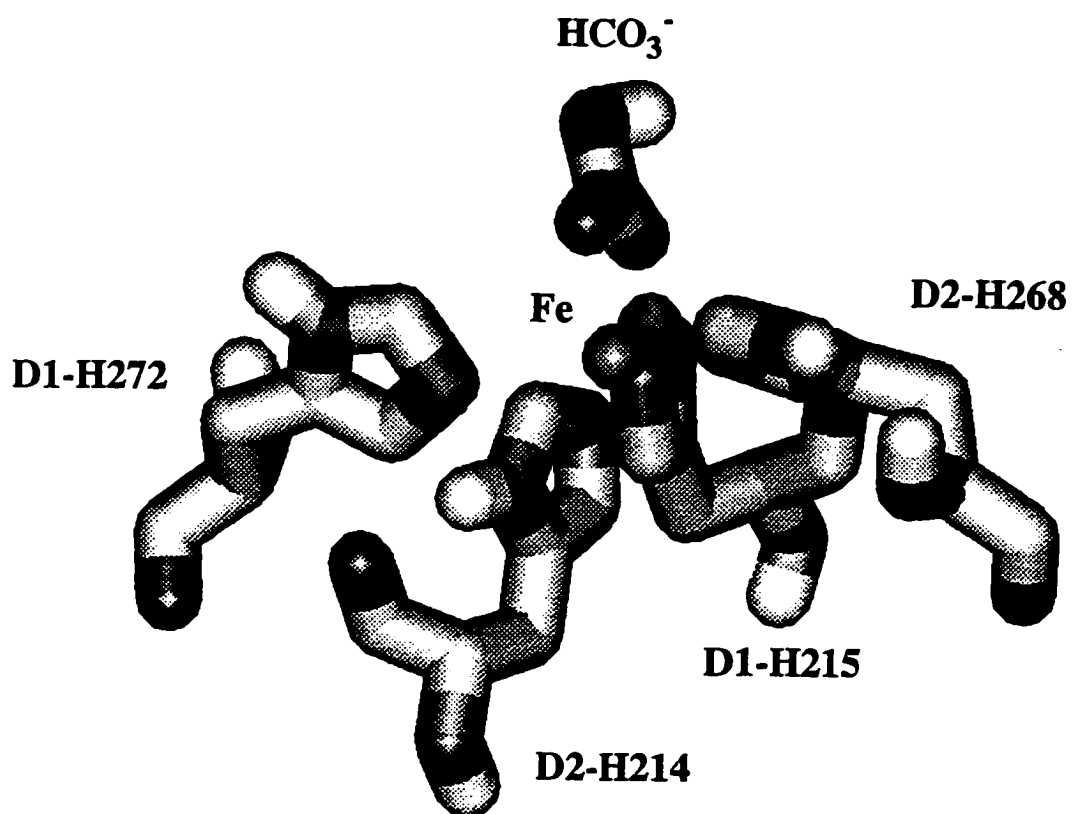
In the bacterial reaction center, the non-heme iron is coordinated by six ligands, one from each of the four histidines (L-H190, L-H230, M-H227, M-H264) and two from a

glutamate (M-E232, *Rps. viridis* numbering) (cf. Michel and Deisenhofer 1988). The four histidines are conserved in all known D1/D2 sequences. The involvement of histidine ligation in PSII is supported by the extended X-ray absorption fine structure spectroscopic studies (Bunker et al. 1982). However, the M-E232 residue is not conserved in the D1/D2 polypeptides. Michel and Deisenhofer (1988) and van Rensen et al. (1988) proposed that bicarbonate could serve as a functional homologue of M-E232 in PSII. The possible role of bicarbonate liganding with the non-heme iron was further supported by EPR and Mössbauer measurements (Petrouleas and Diner 1990; Diner and Petrouleas 1990).

In this PSII reaction center model, the four histidine residues, D1-H215, D1-H272, D2-H214, and D2-H268, as in the bacterial template, ligand with the non-heme iron (Fig. 4.8). Their ϵ 2-nitrogens are liganded to the non-heme iron and the modeled bond distances are from 1.9 to 2.0 Å. Mutation on D2-H268 changing it to glutamine (Vermaas et al. 1994) caused the mutant to lose the autotrophic growth and result in a total inhibition of electron transport from Q_A^- to the plastoquinone pool. Both Q_A and Q_B niches were shown to be significantly perturbed in the mutant, which could be explained by the loss of the non-heme iron. Since this mutation also caused destabilization of the PSII assembly, part of the phenotypic effect can also be attributed to the residue being at the interface of D1 and D2 (see above). Mutations on D2-H214 and nearby residue D2-G215 also resulted in destabilization of the PSII reaction center and disturbed local structure around Q_A and the non-heme iron (Vermaas et al. 1987; 1990). The above experimental evidence supports the ligation of the non-heme iron to the histidine residues.

In the refined PSII reaction center model, no D1 nor D2 glutamate residue appears to substitute the bacterial M-E232. Therefore, to satisfy the iron liganding requirement, a bicarbonate ion was docked to the iron center and allowed to assume the same position as the carboxyl group of M-E232 in the bacterial reaction center based on the available experimental and theoretical suggestions. The modeled distances between the carboxylic oxygens of the bicarbonate and the non-heme iron are modeled to be 2.7 and 3.2 Å,

Figure 4.8. The non-heme iron of the modeled PSII reaction center shown to be coordinated by four histidines, D1-H215, D1-H272, D2-H214, D2-H268, and a bicarbonate (HCO_3^-). The bicarbonate anion was modeled to provide a bidentate ligand to the iron.



respectively. Thus, the bicarbonate appears to provide the fifth and the sixth ligand to the non-heme iron. In contrast, in the pea PSII model (Ruffle et al. 1992), D1-E231 was modeled to assume the structural homologue of M-E232 from the bacterial reaction center and appears to provide two ligands to the iron. In the absence of a final crystal structure, this possibility can be tested using site-directed mutagenesis.

The direct involvement of bicarbonate in binding to the iron is supported by several lines of evidence. Vermaas and Rutherford (1984) found that formate treatment to thylakoid membranes increases the Q_A^- -Fe²⁺ EPR signal ($g = 1.82$) by ten fold. Mössbauer spectrum of Fe signal, indicative of the inner coordination sphere of iron, was found to be significantly affected by the addition of formate and the signal was restored upon the readdition of bicarbonate (Diner and Petrouleas 1987; Semin et al. 1990). NO has been shown to be able to ligand to the non-heme iron of PSII and to exhibit a characteristic Fe²⁺-NO-EPR signal ($g = 4$). Addition of bicarbonate is able to suppress the Fe²⁺-NO-EPR signal (Petrouleas and Diner, 1990). A recent Fourier transform infrared difference spectroscopy study using ¹³C-labeled bicarbonate has further indicated that bicarbonate is a bidentate ligand of the non-heme iron in PSII (Hienerwadel and Berthomieu 1995). All these experiments strongly suggest that bicarbonate is able to compete with formate or NO for ligation with the non-heme iron.

In this model, two residues from D1 and D2, D1-V219 and D2-F232, may also form a part of the close binding niche (5 Å sphere) for the non-heme iron. This binding pocket is similar to that in the bacterial reaction center where L-I194 and M-I223 occupy similar spatial positions and participate in forming the binding pocket for the iron. The partial PSII model of Svensson (1995) indicates that D1-S268 and D2-K265 (higher plant numbering) form hydrogen bonds with the ϵ 2-hydrogens of D1-H272 and D2-H268, respectively. However, this is not supported in the model as the corresponding distances are 4.9 Å and 3.8 Å, respectively.

In this PSII model containing the bicarbonate, the residues that seem to form a binding pocket for the bicarbonate are positively charged and hydrophobic, which include D1-L233, D1-V219, D2-N230, D2-T231, D2-F232, D2-R233, D2-A234, D2-P237, and D2-K264, in addition to the four iron-liganding histidines mentioned above. Among these residues, D2-R233 was shown to be involved in binding and/or stabilizing bicarbonate and formate *in vivo* (Cao et al. 1991). The hydroxyl oxygen of the bicarbonate is separated from the main chain amide hydrogen of D2-R233 by 4.8 Å. However, D2-K264 appears to be the most likely candidate to directly interact with the bicarbonate anion; the modeled distance from one of the ζ hydrogens of the lysine to the closest carbonyl oxygen of bicarbonate is 3.9 Å. The involvement of D2-K264 for binding with the bicarbonate has been confirmed by Diner et al. (1991a).

An *in vivo* role of bicarbonate binding to the non-heme iron has been postulated (Govindjee and van Rensen, 1993). The bound bicarbonate, in addition to effects on the donor side of PSII (El-Shintinawy and Govindjee, 1990; Klimov et al., 1995), may serve to stabilize the Q_A -Fe- Q_B structure; and upon the removal of bicarbonate, the distance between Q_A and Q_B may be altered, slowing the electron transfer rate, although a larger effect is in the protonation of reduced Q_B .

I speculate here that there may be a channel within the PSII complex that leads to the iron center from the outside environment. The channel may be just small enough to allow small molecules or ions such as water or bicarbonate to pass through. If such a channel exists, certain positively charged residues in both D1 and D2 may serve to increase the affinity of bicarbonate. Within 20 Å distance to the bicarbonate modeled in this PSII reaction center, several positively charged residues are identified. They are D1-R27, D1-R225, D1-R140, D1-R225, D1-K238, D1-H252, D1-R257, D1-R269, D2-K23, D2-R24, D2-R26, D2-R239, D2-R233, D2-R251, D2-K264 and D2-R265. As discussed below, some of these residues such as D1-R269, D2-R233, D2-R251, D2-K264 and D2-R265 have been shown to have dramatic influence on the binding, stabilization and functioning of

bicarbonate in PSII (Xiong et al. 1995; Cao et al. 1991; Diner et al. 1991a). It is likely that the physiological role of these residues may extend beyond the binding to bicarbonate. It may also be involved in PSII assembly.

D2-K264 is modeled 3.9 Å away from bicarbonate suggesting its crucial role in bicarbonate binding to the iron center. Site-directed mutations at D2-K264 showed that the mutants have a reduced rate of electron flow from Q_A^- to Q_B and are very resistant to formate and NO treatment (unpublished data, cited in Diner et al. 1991a). In addition, the D2-K264X mutants require much higher levels of bicarbonate to increase the electron flow from Q_A^- to Q_B , suggesting that the residue is involved in the binding of bicarbonate. The mutants of another nearby positive residue (D2-R265) showed a similar behavior though to a lesser extent (Diner et al. 1991a). Two other positively charged residues on the D2 protein (D2-R233 and D2-R251, but not D2-R139) of cyanobacteria near the non-heme iron have been investigated for involvement in bicarbonate effect. Both have been shown to strongly affect the formate susceptibility of PSII and were suggested to stabilize the bicarbonate binding *in vivo* (Cao et al. 1991; Govindjee 1993). Govindjee et al. (1991) showed that a herbicide-resistant mutant in *Chlamydomonas reinhardtii* D1-L275F fails to show the bicarbonate-reversible formate effect. This residue is located near the middle of transmembrane helix E and is not close to the iron-liganding bicarbonate (8.1 Å). However, it is separated from one non-heme iron ligand D2-H214 by 4.0 Å. It is speculated that this mutation significantly perturbs the binding environment of the non-heme iron and thus the binding of bicarbonate. To investigate the involvement of D1 arginine residues in the bicarbonate binding, a D1 arginine nearest to the bicarbonate in the iron site, D1-R269 which is 8.5 Å away from the putative bicarbonate (α -carbon of D1-R269 to the hydroxyl oxygen of bicarbonate), was mutated to a glycine (see Chapter II). The mutant appears to be ~4 fold less sensitive to formate inhibition than the wild type. The EPR analysis of the mutant suggests that the putative iron-formate (a bicarbonate analog) liganding still exists but is greatly perturbed suggesting that D1-R269 may not be directly

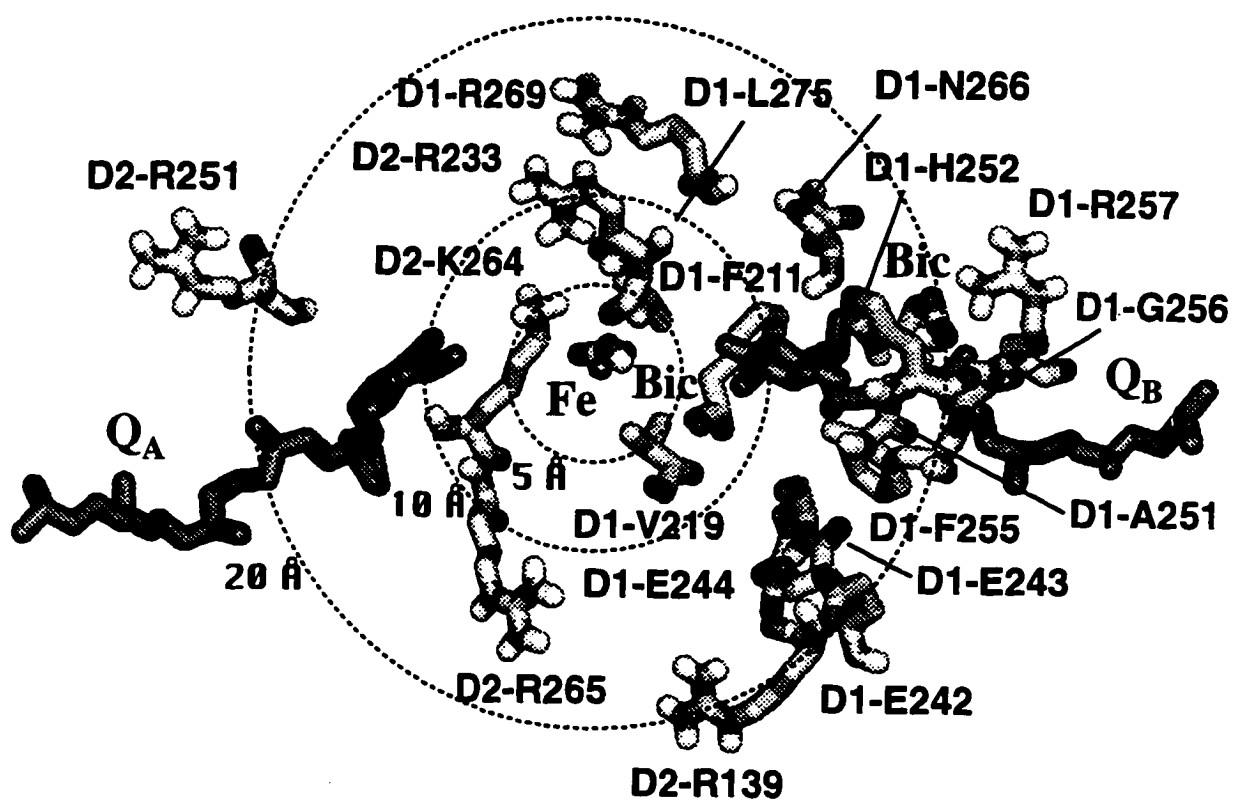
involved in binding the bicarbonate at the iron but may affect the conformation of the bicarbonate-iron center. It is thought that the general characteristics of the electrostatic field near the non-heme iron sometimes plays an important role in allowing the bicarbonate anion to diffuse to the site.

13. Bicarbonate in the Q_B niche

In addition to liganding to the iron, many experiments have suggested that bicarbonate may also function in promoting the protonation of Q_B^- or Q_B^{2-} (Eaton-Rye and Govindjee 1988a; b; van Rensen et al. 1988; Xu et al. 1991). Kinetic studies by Blubaugh and Govindjee (1988b) suggested the possibility of two high affinity bicarbonate binding sites in the PSII reaction center. This second binding site is likely to exist in the Q_B niche and is considered to be related to the protonation of plastoquinone. Characterization of a number of Q_B mutants which are also herbicide resistant have implicated the Q_B binding niche to be involved for the bicarbonate functioning in PSII (Govindjee et al. 1990; Govindjee et al. 1992; Cao et al. 1992; Strasser et al. 1992; Mäenpää et al. 1995; Srivastava et al. 1995; Vernotte et al. 1995). The tested residues involved are: D1-F211, D1-V219, D1-E242, D1-E243, D1-E244, D1-A251, D1-F255, D1-G256, D1-S264, D1-N266, D1-L275. These residues and others near the non-heme iron mentioned above that affect the bicarbonate stabilization, binding and functioning in the PSII reaction center are shown in Fig. 4.9.

In the bacterial reaction centers, aspartate 213 and glutamate 212 on the L subunit are in close proximity to the ubiquinone and were shown to be important for Q_B protonation (see a review by Okamura and Feher 1995). However, on the Q_B binding domain in D1, there are no carboxylate residues near the quinone head group. It is considered likely that there may be a bicarbonate anion in this site functioning as a homologue of an aspartate or a glutamate in the bacterial reaction center, shuttling protons

Figure 4.9. Amino acid residues that are experimentally implicated in the bicarbonate stabilization, binding and functioning in the acceptor side of the PSII reaction center. The concentric rings indicate the distances away from the non-heme iron.



between Q_B and external aqueous environment (also see Blubaugh and Govindjee 1988a; Govindjee and van Rensen 1993).

Since bicarbonate is anionic, it is very likely that its binding at the Q_B niche would be electrostatic in nature and therefore positively charged amino acid residues in D1 are likely to participate in bicarbonate binding. In the 6 Å vicinity from Q_B , two histidines (D1-H215 and D1-H252) and only one arginine (D1-R257) are found. Since D1-H215 is modeled in the middle of the transmembrane helix D, providing ligands to the non-heme iron, it seems unlikely that it also serves the role of bicarbonate binding as this would be expected to perturb the liganding with the iron while bicarbonate undergoes the cycle of being deprotonated and protonated. Though I cannot rule out this possibility, I consider it more reasonable to assume that a bicarbonate may be located closer to D1-H252 and/or D1-R257. This suggestion is consistent with that of Blubaugh and Govindjee (1988a) in which D1-R257 binds a bicarbonate at the Q_B site, transferring protons between D1-R257 and D1-H252.

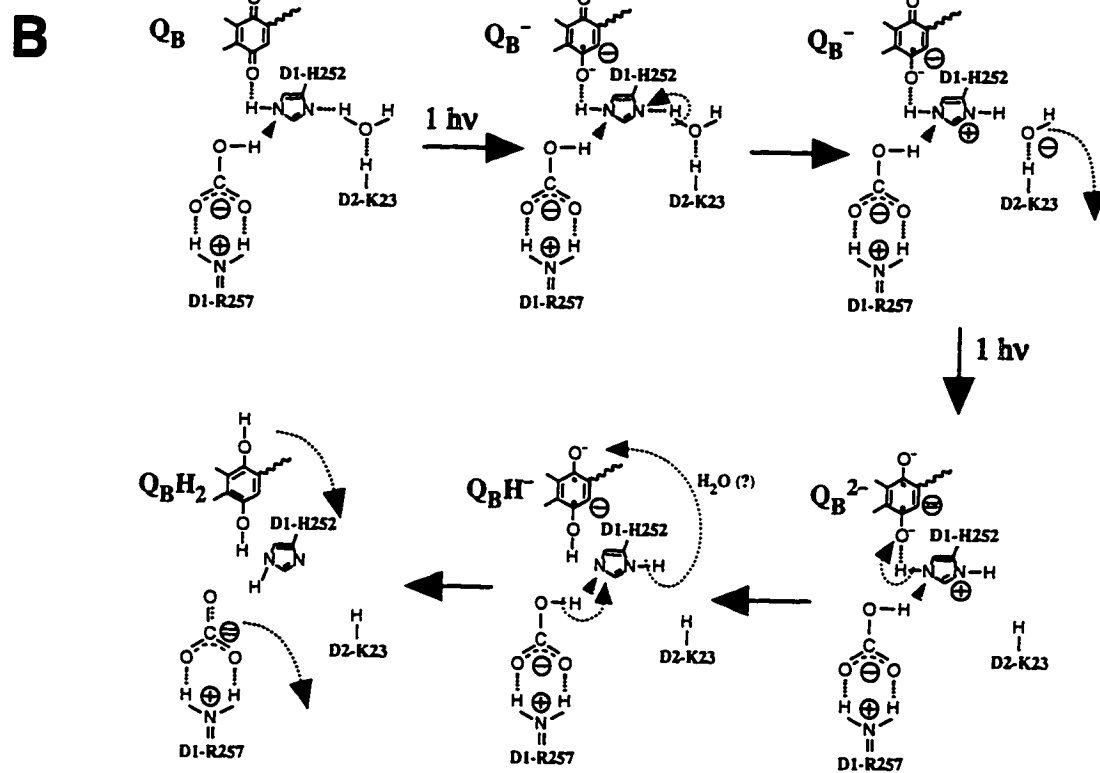
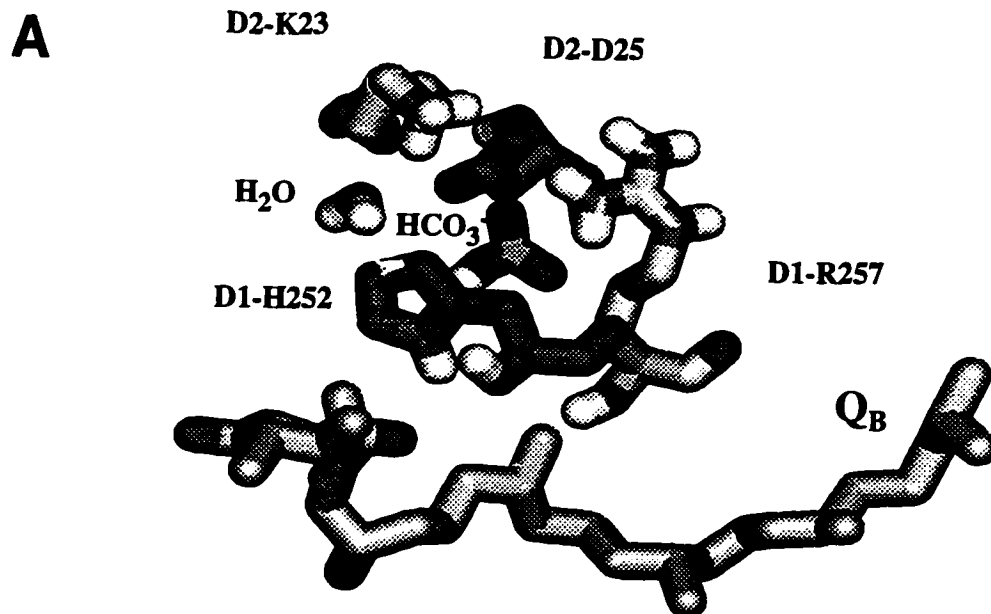
In the Q_B niche of the model, the carbonyl oxygens of Q_B appear to provide a bifurcated hydrogen bond with both D1-H252 and D1-S264. This is different from the model of Blubaugh and Govindjee (1988a) in which D1-H252 does not hydrogen bond with Q_B in its fully oxidized form. In that model, a bicarbonate was modeled in between D1-H252 and D1-R257 in an attempt to explain the Q_B protonation. The bicarbonate anion is stabilized by D1-R257 and provides a proton, through D1-H252 intermediate, to Q_B in both the singly and doubly reduced forms after each charge separation.

As studies of the protonation of Q_B in the bacterial reaction centers (Wraight 1979; Maróti and Wraight 1988; McPherson et al. 1988) suggest that when Q_B is in the semiquinone form (Q_B^-), it is not protonated but only partially neutralized by the protein environment of the reaction center and that Q_B is only protonated after it is doubly reduced, I modified the model of Blubaugh and Govindjee (1988a) and allowed the protonation to occur only after Q_B becomes Q_B^{2-} . In this current model, the bicarbonate is anchored in

such a way that its hydroxyl group is hydrogen bonded to the $\delta 1$ -nitrogen of D1-H252, while its carboxyl group is hydrogen bonded to the positively charged δ -guanido group of D1-R257 (Fig. 4.10A). In order to explain that Q_B is in fact stabilized by a positive charge in the binding environment, a water molecule which serves as a potential proton donor to D1-H252 is introduced in this model. This water molecule is docked near the $\epsilon 2$ -nitrogen of the histidine while it is stabilized by a nearby D2-K23 through a hydrogen bond. This lysine on D2 does not appear to be able to bind a bicarbonate through electrostatic forces as its positive charge appears to be neutralized by a nearby aspartate, D2-D25.

Based on some earlier ideas of Blubaugh and Govindjee (1988a) and the refined three dimensional PSII reaction center model, I propose a working hypothesis concerning the Q_B protonation (Fig. 4.10B). My hypothesis suggests that once Q_B receives one electron from Q_A^- , D1-H252 is protonated and becomes positively charged. The protonation of the histidine can be made possible by withdrawing a proton from the nearby hydrogen-bonded water molecule. The protonated D1-H252 presumably serves to stabilize the negative charge on Q_B^- . The resulting hydroxyl anion is thought to either diffuse away from the site or is protonated by other nearby water molecules if there are any. When Q_B is doubly reduced, direct protonation on Q_B^{2-} occurs in an acid/base mechanism, in which the $\delta 1$ -hydrogen of D1-H252 is donated to the nearby oxygen atom of Q_B and the $\epsilon 2$ -hydrogen of D1-H252 is donated to the other oxygen atom of Q_B . This may be made possible through a proton shuttle mediated by other water molecules in the Q_B niche or simply by the vibrational motions in the plastoquinone that allows its second oxygen atom to move close enough to the $\epsilon 2$ -hydrogen of D1-H252. The resulting plastoquinol (Q_BH_2) will leave the binding niche which will then be re-occupied by another plastoquinone. The deprotonated histidine will be recovered by picking up a proton from the nearby bicarbonate, producing a carbonate anion (CO_3^{2-}) which will then leave the site to let another bicarbonate to diffuse in. It is also likely that the carbonate anion is reprotonated from the nearby environment to recover a bicarbonate. Substitution of bicarbonate

Figure 4.10. Modeling of the second bicarbonate anion in the PSII reaction center and proposed mechanism for the bicarbonate mediated Q_B protonation. (A) A second bicarbonate modeled in the Q_B binding niche as an attempt to explain its involvement in Q_B protonation. A bicarbonate anion (HCO_3^-) modeled in between the side chains of D1-H252 and D1-R257 appears to be coordinated by the hydrogen bonding with the $\delta 1$ -nitrogen of D1-H252 and by the hydrogen bonding/electrostatic interactions with the δ -guanido group of D1-R257. In between the imidazole group of D1-H252 and the amino group of D2-K23, a water molecule was modeled, appearing to be hydrogen bonded by both residues. (B) A working hypothesis for the bicarbonate involvement in the protonation of Q_B . When Q_B is in the oxidized form, its carbonyl oxygen is hydrogen-bonded with D1-H252 and D1-H215 (not shown). The bicarbonate and water are presumably to be anchored on D1-R257 and D2-K23, respectively, through hydrogen bonding and/or electrostatic interactions. When Q_B receives one electron from Q_A^- , D1-H252 is thought to be protonated in response to the inductive forces from the negative charge on Q_B^- . The histidine protonation can be made possible by withdrawing a proton from the nearby hydrogen-bonded water molecule. The protonated D1-H252 presumably serves to stabilize the negative charge on Q_B^- . The resulting hydroxyl anion is thought to diffuse away from the site. When Q_B is doubly reduced, direct protonation on Q_B^{2-} occurs when the $\delta 1$ -hydrogen of D1-H252 is donated to the nearby oxygen atom of Q_B and the $\epsilon 2$ -hydrogen of D1-H252 is donated to the other oxygen atom of Q_B , which may be made possible through other water molecules or by the vibrational actions of the plastoquinone that allows its second oxygen atom to move close enough to the $\epsilon 2$ -hydrogen of D1-H252. The resulting plastoquinol (Q_BH_2) will then leave the binding niche and be replaced by another plastoquinone. The deprotonated histidine will be recovered by picking up a proton from the nearby bicarbonate, and producing a carbonate ion (CO_3^{2-}) which will then leave the site and be replaced by another bicarbonate.



(HCO_3^-) with formate (HCO_2^-) will abolish the donation of the proton to D1-H252 resulting in an inhibition of the process of Q_B^{2-} protonation (Fig. 4.10B).

The hypothesis that an arginine is involved in bicarbonate binding was partially supported from the analogy found in the x-ray crystal structure of human lactoferrin which has a (bi)carbonate binding to an iron at the active site (Anderson et al. 1989). In this protein, the (bi)carbonate is stabilized by hydrogen bonding interactions with an arginine and several other adjacent amino acid residues. A similar example is found in the x-ray crystal structure of hemoglobin and myoglobin with a formate (a bicarbonate analog) bound to the heme iron and an arginine residue interacting with the formate (Aime et al. 1996). The involvement of histidines in the protonation after Q_B^- formation is supported by the observation that the pK_a of a PSII protein group shifts from 6.4 to 7.9 upon the formation of Q_B^- (Crofts et al. 1984). Crofts et al. (1987) had earlier suggested the role of D1-H252 as a proton donor to Q_B^{2-} . Site-directed mutagenesis on D1-H252 has demonstrated a dramatic influence on the PSII electron flow (see Diner et al. 1991a; b; Nixon et al. 1992). Mutational studies on the other two residues, D1-R257 and D2-K23, certainly will help further test the hypothesis. As shown in Chapter III, site-directed mutants D1-R257E and D1-R257M in *C. reinhardtii* were constructed and characterized, which show an inhibited rate of growth and PSII electron transfer. There is a near absence of bicarbonate-reversible formate inhibition on the electron transport from Q_A^- to the plastoquinone pool, especially on the step of protonation of Q_B^{2-} . This evidence strongly supports the validity of the above hypothesis.

14. Bicarbonate/water transport in PSII

The presence of multiple water molecules in the Q_B binding region was experimentally shown in the newly refined bacterial reaction center structures (Ermler et al. 1994; Deisenhofer et al. 1995; Lancaster and Michel 1996). In the structure of *Rb. sphaeroides*, an uninterrupted chain of fixed water molecules is found leading from the

cytoplasmic surface to the Q_B molecule (Ermler et al. 1994). The water molecules in the chain are connected by hydrogen bonds to each other and to the nearby protonable residues. Their role is presumably to facilitate the protonation of doubly reduced Q_B . Some of the protonable residues that form the water channel have been confirmed to be relevant to the proton transfer process (see Lancaster et al. 1995). Interruption of the water chain near the Q_B site by site-directed mutagenesis (L-P209Y) caused a reduction of the protonation of Q_B (Bacjou and Michel 1995).

The above experimental evidence revealed the proton transfer pathway to Q_B which is deeply buried in the protein complex. The water-lining residues are found to be primarily charged; they are negatively charged near the Q_B niche (Ermler et al. 1994, redrawn in Fig. 4.11A). It is thus conceivable that bicarbonate anions will be easily excluded from the bacterial Q_B binding site due to the electrostatic repulsions. This cluster of negatively charged residues may thus help explain the fact that there is no bicarbonate effect in the bacterial reaction center.

Since the Q_B molecule in PSII is also believed to be buried inside the protein complex and its protonation must ultimately result in protons being transferred from the outer environment, it is reasonable to consider the existence of a similar transport channel, which carries protonating agents from the stroma/cytoplasm to the Q_B site. As mentioned above, the protonating agents for Q_B in PSII could be *both* water and bicarbonate.

To construct a tentative model for a similar transport channel for water and bicarbonate in PSII, I have made the following assumptions, (1) the direction of the transport channel in the PSII reaction center is similar to that in the bacterial reaction center by assuming that a good homology exists in this respect; this allows me to focus on a more specific region for constructing the model of water/bicarbonate transport; (2) the charged residues form the putative "transport channel", as in the bacterial reaction center; (3) the local electrostatic characteristic of the binding region weighs more than the precise

geometric match with the bacterial water-binding residues; (4) the channel to be constructed has another end at the non-heme iron site.

In my effort to determine the location of this large bicarbonate/water binding niche or "channel" in PSII, I simply superimposed the bacterial structure (2RCR) and the constructed PSII reaction center model and identify specific D1/D2 charged residues that are positioned as in the L and M residues that form the bacterial water channel.

The following charged residues in D1 and D2 are included in the tentative transport channel: D1-H215, D1-K238, D1-E242, D1-E243, D1-E244, D1-H252, D1-R257, D1-R269, D2-K23, D2-D25, D2-E224, D2-R233, D1-E236, D2-E241, D2-E242, D2-K264, and D2-R265 (Fig. 11B). A striking feature of these charged residues is that near Q_B and the non-heme iron they are predominantly positively charged. This more basic Q_B /Fe binding domain is in contrast to the situation in the bacterial reaction center. This feature appears to further support the possibility of a negatively charged species *i.e.* bicarbonate to bind and function in these sites.

The available experimental evidence that indicates the strong relevance of the above residues for binding bicarbonate/formate includes results on the aforementioned D1-R257E and D1-R257M mutants (Chapter III), the D1-R269G mutant (Chapter II); the D2-R233Q mutant (Cao et al. 1991) and the D2-K264 and D2-R265 mutants (see Diner et al. 1991a). These mutants except D2-R233Q all have shown various levels of resistance to formate inhibition in support of the current model. D2-R233Q was shown to be 10 fold more susceptible to formate inhibition than the wild type. This can also be interpreted using the above model that the mutations resulted in a more widely "opened" transport channel making the target site more accessible to formate. Interestingly, a deletion mutant for the above three D1 glutamate residues (D1-E242, D1-E243, and D1-E244) was also shown to be seven fold less sensitive to formate inhibition than the wild type (Mäenpää et al. 1995). As these are negatively charged residues, they may be more likely to serve a role for binding water molecules and providing the correct electrostatic environment in the above

geometric match with the bacterial water-binding residues; (4) the channel to be constructed has another end at the non-heme iron site.

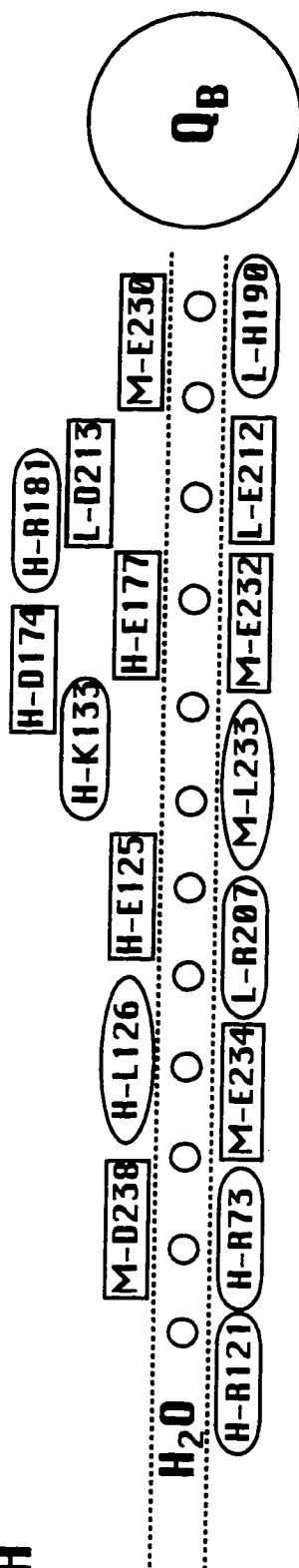
In my effort to determine the location of this large bicarbonate/water binding niche or "channel" in PSII, I simply superimposed the bacterial structure (2RCR) and the constructed PSII reaction center model and identify specific D1/D2 charged residues that are positioned as in the L and M residues that form the bacterial water channel.

The following charged residues in D1 and D2 are included in the tentative transport channel: D1-H215, D1-K238, D1-E242, D1-E243, D1-E244, D1-H252, D1-R257, D1-R269, D2-K23, D2-D25, D2-E224, D2-R233, D1-E236, D2-E241, D2-E242, D2-K264, and D2-R265 (Fig. 11B). A striking feature of these charged residues is that near Q_B and the non-heme iron they are predominantly positively charged. This more basic Q_B /Fe binding domain is in contrast to the situation in the bacterial reaction center. This feature appears to further support the possibility of a negatively charged species *i.e.* bicarbonate to bind and function in these sites.

The available experimental evidence that indicates the strong relevance of the above residues for binding bicarbonate/formate includes results on the aforementioned D1-R257E and D1-R257M mutants (Chapter III), the D1-R269G mutant (Chapter II); the D2-R233Q mutant (Cao et al. 1991) and the D2-K264 and D2-R265 mutants (see Diner et al. 1991a). These mutants except D2-R233Q all have shown various levels of resistance to formate inhibition in support of the current model. D2-R233Q was shown to be 10 fold more susceptible to formate inhibition than the wild type. This can also be interpreted using the above model that the mutations resulted in a more widely "opened" transport channel making the target site more accessible to formate. Interestingly, a deletion mutant for the above three D1 glutamate residues (D1-E242, D1-E243, and D1-E244) was also shown to be seven fold less sensitive to formate inhibition than the wild type (Mäenpää et al. 1995). As these are negatively charged residues, they may be more likely to serve a role for binding water molecules and providing the correct electrostatic environment in the above

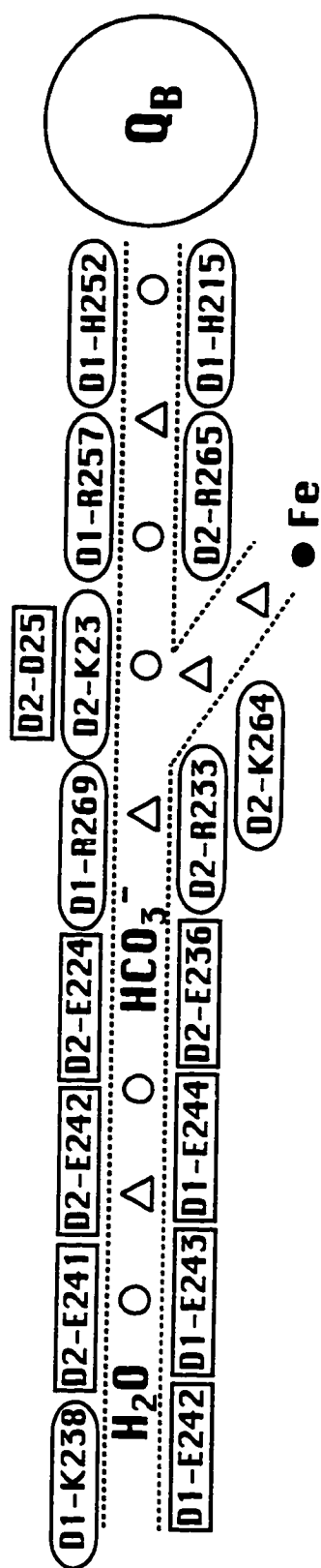
Figure 4.11 Schematic diagram of the water transport channel in the bacterial reaction center (Ermeler et al. 1994) and hypothesis for a similar transport channel for water and bicarbonate in the PSII reaction center. (A) A schematic drawing of the water chain and the surrounding amino acids in the *Rb. sphaeroides* reaction center. The water molecules presumably aid in the Q_B protonation. The polarity of the surrounding residues are boxed or circled differently. The negatively charged residues are boxed with rectangles, the positively charged ones rectangles with rounded corners, and the non-polar ones ovals (modified from Ermeler et al. 1994, but with the same numbering). Several water molecules branching out from the major chain and their associating amino acid residues were omitted. Water molecules are shown as small circles. (B) A hypothetical water and bicarbonate transport channel in PSII reaction center constructed based on the assumptions made in the text. Charged residues in the PSII model considered to be important for associating with the bicarbonate and water molecules are shown. The predominately positively charged protein environment near the Q_B and the non-heme iron suggests a more favorable binding environment for bicarbonate. Water molecules are shown as small circles and bicarbonate as triangles. The residues are circled or boxed as in (A).

A



● Fe

B



● Fe

channel. However, the removal of the three residues results in an interruption of the transport channel and thus affects the bicarbonate/formate binding and diffusion as well.

Further mutagenesis of the arginine or lysine residues forming the "channel" by changing them to all negatively charged or neutral ones may be a good experiment to test the above hypothesis. On the other hand, mutations that change the negatively charged residues into positive ones in the "water channel" of the bacterial reaction center may serve to test the hypothesis of the above bicarbonate transport and function, provided the mutations do not introduce drastic conformational changes which seriously affect the assembly of the protein complex.

It is noted that in the bacterial water channel, pairs of charged residues, such as L-D213/H-R181 and H-K133/H-D174, exist (Fig. 4.11A). This close interaction is believed to cancel the negative or positive charges on the residues and to alleviate the electrostatic repulsions (Ermler et al. 1994). Similar interactions between opposite charged residues may also exist in PSII as predicted in the D2-K23/D2-D25 pair (Fig. 4.11B). In this case, the residue may bind water molecules instead.

As the bacterial water transport channel consists of a number of residues from the H subunit, I consider that a similar situation may exist in PSII in which certain residues from other nearby PSII core polypeptides may participate in the binding of the water and bicarbonate. As this is beyond the scope of homology modeling, I have to leave this question open.

Data presented in this chapter are based on the published work of the author (Xiong et al. 1996).

D. References

- Abola, E.E., Bernstein, F.C., Bryant, S.H., Koetzle, T.F. and Weng, J. (1987) Protein Data Bank. In: Allen, F.H., Bergerhoff, G., Sievers, R. (eds.) Crystallographic Databases. pp. 107-132. International Union of Crystallography, Bonn.
- Aime, S., Fasano, M., Paoletti, S., Cutruzzolà, F., Desideri, A., Bolognesi, M., Rizzi, M. and Ascenzi, P. (1996) Structural determinants of fluoride and formate binding to hemoglobin and myoglobin: Crystallographic and ^1H -NMR relaxometric study. *Biophys. J.* 70: 482-488.
- Altschul, S.F., Gish, W., Miller, W., Myers, E.W. and Lipman, D.J. (1990) Basic local alignment search tool. *J. Mol. Biol.* 215: 403-410.
- Anderson, B.F., Baker, H.M., Norris, G.E., Rice, D.W. and Baker, E.N. (1989) Structure of human transferrin: Crystallographic structure analysis and refinement at 2.8 Å resolution. *J. Mol. Biol.* 209: 711-734.
- Astashkin, A.V., Koder, Y., Kawamori, A. (1994) Distance between tyrosines Z⁺ and D⁺ in plant photosystem II as determined by pulsed EPR. *Biochim. Biophys. Acta* 1187: 89-93.
- Astashkin, A.V., Kawamori, A., Koder, Y., Kuroiwa, S. and Akabori, K. (1995) An electron spin echo envelope modulation study of the primary acceptor quinone in Zn-substituted plant photosystem II. *J. Chem. Phys.* 102: 5583-5597.
- Babcock, G.T. (1995) The oxygen-evolving complex in photosystem II as a metalloradical enzyme. In: Mathis, P. (ed.) *Photosynthesis: From Light to Biosphere*. Vol. II. pp 209-215. Kluwer Academic Publishers, Dordrecht.
- Bacjou, L. and Michel, H. (1995) Role of the water chain in the reaction center from *Rb. sphaeroides*. In: Mathis, P. (ed.) *Photosynthesis: From light to biosphere*. Vol. I. pp. 683-686. Kluwer Academic Publishers, Dordrecht.

- Barber, J., Chapman, D.J. and Telfer, A. (1987) Characterization of a PSII reaction centre isolated from the chloroplasts of *Pisum sativum*. FEBS Lett. 220: 67-73.
- Bernstein, F.C., Koetzle, T.F., Williams, G.J.B., Meyers, E.F. Jr., Brice, M.D., Rodgers, J.R., Kennard, O., Shimanouchi, T., Tasumi, M. (1977) The protein data bank: A computer-based archival file for macromolecular structures. J. Mol. Biol. 112: 535-542.
- Blubaugh, D.J. and Govindjee. (1988a) The molecular mechanism of the bicarbonate effect at the plastoquinone reductase site of photosynthesis. Photosyn. Res. 19: 85-128.
- Blubaugh, D.J. and Govindjee. (1998b) Kinetics of the bicarbonate effect and the number of bicarbonate-binding sites in thylakoid membranes. Biochim Biophys Acta 936: 208-214.
- Boekema, E.J., Hankamer, B., Bald, D., Kruip, J., Nield, J., Boonstra, A.F., Barber, J. and Rogner, M. (1995) Supramolecular structure of the photosystem II complex from green plants and cyanobacteria. Proc. Natl. Acad. Sci. USA 92: 175-179.
- Bosch, M.K., Proskuryakov, I.I., Gast, P., Hoff, A.J. (1995) Relative orientation of the optical transition dipole and triplet axes of the photosystem II primary donor. A magnetophotoselection study. J. Phys. Chem. 99: 15310-15316.
- Bowyer, J., Hilton, J.M., Whitelegge, J., Jewess, P., Camilleri, P., Crofts, A., Robinson, H. (1990) Molecular modelling studies on the binding of phenylurea inhibitors to the D1 protein of photosystem II. Z. Naturforsch. 45c: 379-387.
- Breton, J. (1990) Orientation of the pheophytin primary electron acceptor and of the cytochrome b-559 in the D1-D2 photosystem II reaction center. In: Jortner, J. and Pullman, B. (eds.) Perspectives in photosynthesis. pp 23-28. Kluwer Academic Publishers, Dordrecht.
- Brooks, B.R., Bruccoleri, R.E., Olafson, B.D., States, D.J., Swaminathan, S., Karplus, M. (1983) CHARMM: A program for macromolecular energy, minimization, and dynamics calculations. J. Computational. Chem. 4: 187-217.

- Bunker, G., Stern, E.A., Blankenship, R.E. and Parson, W.W. (1982) An X-ray absorption study of the iron site in bacterial photosynthetic reaction centers. *Biophys. J.* 37: 539-551.
- Cao, J., Vermaas, W.F.J. and Govindjee. (1991) Arginine residues in the D2 polypeptide may stabilize bicarbonate binding photosystem II of *Synechocystis* sp. PCC 6803. *Biochim. Biophys. Acta* 1059: 171-180.
- Cao, J., Ohad, N., Hirschberg, J., Xiong, J. and Govindjee. (1992) Binding affinity of bicarbonate and formate in herbicide-resistance D1 mutants of *Synechococcus* sp. PCC 7942. *Photosyn. Res.* 34: 397-408.
- Chang, H.C., Jankowiak, R., Reddy, N.R.S., Yocum, C.F., Picorel, R., Seibert, M. and Small, G.J. (1994) On the question of the chlorophyll *a* content of the photosystem II reaction center. *J. Phys. Chem.* 98: 7725-7735.
- Chu, H.-A., Nguyen, A.P. and Debus, R.J. (1995) Amino acid residues that influence the binding of manganese or calcium to photosystem II .1. The lumenal interhelical domains of the D1 polypeptide. *Biochemistry* 34: 5839-5858.
- Clarke, A.K., Soitamo, A., Gustafsson, P., Öquist, G. (1993) Rapid interchange between two distinct forms of cyanobacterial photosystem II reaction-center protein D1 in response to photoinhibition. *Proc. Natl. Acad. Sci. USA* 90: 9973-9977.
- Coleman, W.J. and Govindjee. (1987) A model for the mechanism of chloride activation of oxygen evolution in photosystem II. *Photosyn. Res.* 13: 199-223.
- Cramer, W.A. and Knaff, D.B. (1990) *Energy Transduction in Biological Membranes*, A Textbook of Bioenergetics. pp. 194-195; 253. Springer-Verlag, New York.
- Crofts, A.R., Robinson, H.H., Snozzi, M. (1984) Reactions of quinones at catalytic sites; a diffusional role in H-transfer. In: Sybesma, C. (ed.) *Advances in photosynthesis research*. pp. 461-468. Martinus Nijhoff/Dr W. Junk Publishers, Hague.

- Crofts, A.R., Robinson, H.H., Andrews, K. and van Doren, S., Berry, E.D. (1987) Catalytic site for reduction and oxidation of quinones. In: Papa, S., Chance, B. and Ernster, L. (eds.) *Cytochrome systems*. pp. 617-624. Plenum Press, New York.
- Debus, R. (1992) The manganese and calcium ions of photosynthetic oxygen evolution. *Biochim. Biophys. Acta* 1102: 269-352.
- Debus, R., Barry, B.A., Sithole, I., Babcock, G.T. and McIntosh, L. (1988a) Directed mutagenesis indicates that the donor to P680⁺ in photosystem II is tyrosine-161 of the D1 polypeptide. *Biochemistry* 27: 9071-9074.
- Debus, R., Barry, B.A., Babcock, G.T. and McIntosh L. (1988b) Site-directed mutagenesis identifies a tyrosine radical in the photosynthetic oxygen-evolving system. *Proc. Natl. Acad. Sci. USA* 85: 427-430.
- Deisenhofer, J., Epp, O., Sinning, I. and Michel, H. (1995) Crystallographic refinement at 2.3-angstrom resolution and refined model of the photosynthetic reaction centre from *Rhodospseudomonas viridis*. *J. Mol. Biol.* 246: 429-457.
- Diner, B.A. and Petrouleas, V. (1987) Q₄₀₀, the non-heme iron of the photosystem II iron-quinone complex. A spectroscopic probe of quinone and inhibitor binding to the reaction center. *Biochim. Biophys. Acta* 895: 107-125.
- Diner, B.A. and Petrouleas, V. (1990) Formation by NO of nitrosyl adducts of redox components of the photosystem II reaction center. II. Evidence that HCO₃⁻/CO₂ binds to the acceptor-side non-heme iron. *Biochim. Biophys. Acta* 1015: 141-149.
- Diner, B.A. and Babcock, G.T. (1996) Structure, dynamics, and energy conversion efficiency in photosystem II. In: Ort, D.R. and Yocum, C.F. (eds.) *Oxygenic Photosynthesis: The Light Reactions*. Kluwer Academic Publishers, Dordrecht. (in press)
- Diner, B.A., Petrouleas, V. and Wendoloski, J.J. (1991a) The iron-quinone electron-acceptor complex of photosystem II. *Physiol. Plant.* 81: 423-436.

- Diner, B.A., Nixon, P.J. and Farchaus, J.W. (1991b) Site-directed mutagenesis of photosynthetic reaction centers. *Curr. Op. Struct. Biol.* 1: 546-554.
- Draber, W., Hilp, U., Likusa, H., Schindler, M. and Trebst, A. (1993) Inhibition of photosynthesis by 4-nitro-6-alkylphenols: Structure-activity studies in wild type and five mutants of *Chlamydomonas reinhardtii*. *Z. Naturforsch.* 48c: 213-223.
- Durrant, J.R., Klug, D.R., Kwa, S.L.S., Vangrondelle, R., Porter, G. and Dekker, J.P. (1995) A multimer model for P680, the primary electron donor of photosystem II. *Proc Natl Acad Sci* 92: 4798-4802.
- Eaton-Rye, J.J. and Govindjee. (1988a) Electron transfer through the quinone acceptor complex of photosystem II in bicarbonate-depleted spinach thylakoid membranes as a function of actinic flash number and frequency. *Biochim. Biophys. Acta* 935: 237-247.
- Eaton-Rye, J.J. and Govindjee. (1988b) Electron transfer through the quinone acceptor complex II after one or two actinic flashes in bicarbonate-depleted spinach thylakoid membranes. *Biochim. Biophys. Acta* 935: 248-257.
- Egner, U., Hoyer, G.-A. and Saenger, W. (1993) Modeling and energy minimization studies on the herbicide binding protein (D1) in photosystem II of plants. *Biochim. Biophys. Acta* 1142: 106-114.
- El-Shintinawy, F. and Govindjee. (1990) Bicarbonate effects in leaf discs from spinach. *Photosyn. Res.* 24: 189-200.
- Ermler, U., Fritsch, G., Buchanan, S.K. and Michel, H. (1994) Structure of the photosynthetic reaction centre from *Rhodobacter sphaeroides* at 2.65 Å resolution: Cofactors and protein-cofactor interactions. *Structure* 2: 925-936.
- Feng, D.F. and Doolittle, R.F. (1987) Progressive sequence alignment as a prerequisite to correct phylogenetic trees. *J. Mol. Evol.* 25: 351-360.
- Ghanotakis, D.F. and Yocum, C.F. (1990) Photosystem II and the oxygen-evolving complex. *Annu. Rev. Plant Physiol. Plant Mol. Biol.* 41: 255-276.

- Gilchrist, Jr. M.L., Ball, J.A., Randall, D.W. and Britt, D. (1995) Proximity of the manganese cluster of photosystem II to the redox-active tyrosine Y_Z. *Proc. Natl. Acad. Sci. USA* 92: 9545-9549.
- Giorgi, L.B., Nixon, P.J., Merry, S.A.P., Joseph, D.M., Durrant, J.R., Rivas, J.D., Barber, J., Porter, G. and Klug, D.R. (1996) Comparison of primary charge separation in the photosystem II reaction center complex isolated from wild-type and D1-130 mutants of the cyanobacterium *Synechocystis* PCC 6803. *J. Biol. Chem.* 271: 2093-2101.
- Gounaris, K., Chapman, D.J., Booth, P., Crystall, B., Giorgi, L.B., Klug, D.R., Porter, G. and Barber, J. (1990) Comparison of D1/D2/cytochrome b559 reaction centre complex of photosystem two isolated by two different methods. *FEBS Lett.* 265: 88-92.
- Govindjee. (1993) Bicarbonate-reversible inhibition of plastoquinone reductase in photosystem II. *Z. Naturforsch.* 48c: 251-258.
- Govindjee, van Rensen, J.J.S. (1993) Photosystem II reaction center and bicarbonate. In: Deisenhofer, J. and Norris, J.R. (eds.) *The Photosynthetic reaction center*. Vol. I. pp. 357-389. Academic Press, San Diego.
- Govindjee, Vernotte, C., Peteri, B., Astier, B., Etienne, A.-L. (1990) Differential sensitivity of bicarbonate-reversible formate effects on herbicide-resistant mutants of *Synechocystis* 6714. *FEBS Lett.* 267: 273-276.
- Govindjee, Schwarz, B., Rochaix, J.-D. and Strasser, R.J. (1991) The herbicide-resistant D1 mutants L275F of *Chlamydomonas reinhardtii* fails to show the bicarbonate-reversible formate effect on chlorophyll a fluorescence transients. *Photosyn. Res.* 27: 199-208.
- Govindjee, Eggenberg, P., Pfister, K. and Strasser, R.J. (1992) Chlorophyll a fluorescence decay in herbicide-resistant D1 mutants of *Chlamydomonas reinhardtii* and the formate effect. *Biochim. Biophys. Acta* 1101: 353-358.

- Han, K.F. and Baker, D. (1996) Global properties of the mapping between local amino acid sequence and local structure in proteins. *Proc. Natl. Acad. Sci. USA* 93: 5814-5818.
- Hansson, O. and Wydrzynski, T. (1990) Current perceptions of photosystem II. *Photosyn. Res.* 23: 131-162.
- He, W.-Z., Newell, W.R., Haris, P.I., Chapman, D. and Barber, J. (1991) Protein secondary structure of the isolated photosystem II reaction center and conformational changes studied by Fourier transform infrared spectroscopy. *Biochemistry* 30: 4552-4559.
- Hienerwadel, R. and Berthomieu, C. (1995) Bicarbonate binding to the non-heme iron of photosystem II investigated by Fourier transform infrared difference spectroscopy and ^{13}C -labeled bicarbonate. *Biochemistry* 34: 16288-16297.
- Hirsch, D.J. and Brudvig, G.W. (1993) Long-range electron spin-spin interactions in the bacterial photosynthetic reaction center. *J. Phys. Chem.* 97: 13216-13222.
- Hoganson, C.W. and Babcock, G.T. (1989) Redox cofactor interactions in photosystem II: Electron spin resonance spectrum of P_{680}^+ is broadened in the presence of YZ^+ . *Biochemistry* 28: 1448-1454.
- Holzenburg, A., Bewley, M.C., Wilson, F.H., Nicholson, W.V. and Ford, R.C. (1993) Three-dimensional structure of photosystem II. *Nature* 363: 470-472.
- Hutchison, R.S., Xiong, J., Sayre, R.T. and Govindjee. (1996) Construction and characterization of a D1 mutant (arginine-269-glycine) of *Chlamydomonas reinhardtii*. *Biochim. Biophys. Acta* (in press)
- Jursinic, P.A. and Dennenberg, R.J. (1990) Oxygen release time in leaf discs and thylakoids of peas and photosystem II membrane fragments of spinach. *Biochim. Biophys. Acta* 1020: 195-206.

- Kless, H., Oren-Shamir, M., Ohad, I., Edelman, M. and Vermaas, W.F.J. (1993) Protein modifications in the D2 protein of photosystem II affect properties of the Q_B/herbicide-binding environment. *Z. Naturforsch.* 48c: 185-190.
- Klimov, V.V., Allakhverdiev, S.I., Feyziev, Y.M. and Baranov, S.V. (1995) Bicarbonate requirement for the donor side of photosystem II. *FEBS Lett.* 363: 251-255.
- Kobayashi, M., Maeda, H., Watanabe, T., Nakane, H. and Satoh, K. (1990) Chlorophyll *a* and β -carotene content in the D1/D2/cytochrome *b559* reaction center complex from spinach. *FEBS Lett.* 260: 138-140.
- Kodera, Y., Takura, K. and Kawamori, A. (1992) Distance of P680 from the manganese complex in photosystem II studied by time resolved EPR. *Biochim. Biophys. Acta* 1101: 23-32.
- Kodera, Y., Hara, H., Astashkin, A.V., Kawamori, A., Ono-T.A. (1995) EPR Study of trapped tyrosine Z(+) in Ca-depleted photosystem II. *Biochim. Biophys. Acta* 21: 43-51.
- Koulougliotis, D., Tang, X.S., Diner, B.A. and Brudvig, G.W. (1995) Spectroscopic evidence for the symmetric location of tyrosines D and Z in Photosystem II. *Biochemistry* 34: 2850-2856.
- Kramer, D.M., Roffey, R.A., Govindjee, and Sayre RT. (1994) The At thermoluminescence band from *Chlamydomonas reinhardtii* and the effects of mutagenesis of histidine residues on the donor side of the photosystem II D1 polypeptide. *Biochim. Biophys. Acta* 1185: 228-237.
- Kulkarni, R.D. and Golden, S.S. (1994) Adaptation to high light intensity in *Synechococcus* sp strain PCC 7942 - regulation of three *psbA* genes and two forms of the D1 protein. *J. Bacteriol.* 176: 959-965.
- Kulkarni, R.D., Golden, S.S. (1995) Form II of D1 is important during transition from standard to high light intensity in *Synechococcus* sp. strain PCC 7942. *Photosyn. Res.* 46: 435-443.

- Kwa, S.L.S., Eijkelhoff, C., van Grondelle, R. and Dekker, J.P. (1994) Site-selection spectroscopy of the reaction center complex of photosystem II. 1. Triplet-minus absorption difference: Search for a second exciton band of P-680. *J. Phys. Chem.* 98: 7702-7711.
- Lancaster, C.R. and Michel, H. (1996) Three-dimensional structures of photosynthetic reaction centers. *Photosyn. Res.* 48: 65-74.
- Lancaster, C.R., Ermler, U. and Michel, H. (1995) The structures of photosynthetic reaction centers from purple bacteria as revealed by x-ray crystallography. In: Blankenship RE, Madigan MT and Bauer CE (eds.) *Anoxygenic photosynthetic bacteria*. pp. 503-526. Kluwer Academic Publishers, Dordrecht.
- Lorkovic, Z.J., Schroeder, W.P., Pakrasi, H.B., Irrgang, K.-D., Herrman, R.G. and Oelmueller, R. (1995) Molecular characterization of PsbW, a nuclear-encoded component of the photosystem II reaction center complex in spinach. *Proc. Natl. Acad. Sci. USA* 92: 8930-8934.
- Mackay, S.P., O'Malley, P.J. (1993a) Molecular modelling of the interaction between DCMU and the Q_B-binding site of photosystem II. *Z. Naturforsch.* 48c: 191-198.
- Mackay, S.P. and O'Malley, P.J. (1993b) Molecular modelling of the interactions between optically active triazine herbicide and photosystem II. *Z. Naturforsch.* 48c: 474-481.
- Mackay, S.P. and O'Malley, P.J. (1993c) Molecular modelling of the interactions of cyanoacrylate inhibitors with photosystem II. Part 1. The effects of hydrophobicity of inhibitor binding. *Z. Naturforsch.* 48c: 773-781.
- Mackay, S.P. and O'Malley, P.J. (1993d) Molecular modelling of the interactions of cyanoacrylate inhibitors with photosystem II. Part 2. The effects of stereochemistry of inhibitor binding. *Z. Naturforsch.* 48c: 782-787.
- Mäenpää, P., Miranda, T., Tyystjärvi, E., Tyystjärvi, T., Govindjee, Ducruet, J.-M., Etienne, A.-L. and Kirilovsky, D. (1995) A mutation in the D-de loop of D₁

- modifies the stability of the $S_2Q_A^-$ and $S_2Q_B^-$ states in photosystem II. *Plant Physiol.* 107: 187-197.
- Maróti, P. and Wraight, C.A. (1988) Flash-induced H^+ binding by bacterial photosynthetic reaction centers: Influences of the redox states of the acceptor quinones and primary donor. *Biochim. Biophys. Acta* 934: 329-347.
- McPherson, P.A., Okamura, M.Y. and Feher, G. (1988) Light-induced proton uptake by photosynthetic reaction centers from *Rhodobacter sphaeroides* R-26. I. Protonation of the one-electron states $D^+Q_A^-$, DQ_A^- , $D^+Q_AQ_B^-$ and $DQ_AQ_B^-$. *Biochim. Biophys. Acta* 934: 384-368.
- Metz, J.G., Nixon, P.J., Rogner, M., Brudvig, G.W. and Diner BA. (1989) Directed alteration of the D1 polypeptide of photosystem II: Evidence that tyrosine-161 is the redox component, Z, connecting the oxygen-evolving complex to the primary electron donor, P680. *Biochemistry* 28: 6960-6969.
- Michel, H. and Deisenhofer, J. (1988) Relevance of the photosynthetic reaction center from purple bacteria to the structure of photosystem II. *Biochemistry* 27: 1-7.
- Nanba, O. and Satoh, K. (1987) Isolation of photosystem II reaction center consisting of D1 and D2 polypeptides and cytochrome *b*-559. *Proc. Natl. Acad. Sci. USA* 84: 109-112.
- Nixon, P.J. and Diner BA. (1992) Aspartate 170 of the photosystem II reaction center polypeptide D1 is involved in the assembly of the oxygen-evolving manganese cluster. *Biochemistry* 31: 942-948.
- Nixon, P.J. and Diner, B.A. (1994) Analysis of water-oxidation mutants constructed in the cyanobacterium *Synechocystis* sp. PCC 6803. *Biochem. Soc. Trans.* 22: 338-343.
- Nixon, P.J., Chisholm, D.A. and Diner, B.A. (1992) Isolation and functional analysis of random and site-directed mutants for photosystem II. In: Shewry, P. and Gutteridge, S. (eds.) *Plant protein engineering*. pp. 93-141. Cambridge University Press, Cambridge.

- Noguchi, T., Inoue, Y. and Satoh, K. (1993) FT-IR studies of the triplet state of P680 in the photosystem II reaction center: Triplet equilibrium within a chlorophyll dimer. *Biochemistry* 32: 7186-7195.
- Nugent, J.H.A., Bratt, P.J., Evans, M.C.W., MacLachlan, D.J., Rigby, S.E.J., Ruffle, S.V. and Turconi, S. (1994) Photosystem II electron transfer: The manganese complex to P680. *Biochem. Soc. Trans.* 22: 327-331.
- Ohad, N., Keasar, C. and Hirschberg, J. (1992) Molecular modeling of the plastoquinone (Q_B) binding site in photosystem II. In: Murata, N. (ed.) *Research in photosynthesis*. pp 223-226. Vol. II. Kluwer Academic Publishers, Dordrecht.
- Oettmeier, W. (1992) Herbicides of photosystem II. In: Barber J. (ed.) *The photosystems: Structure, function and molecular biology*. pp 349-408. Elsevier, Amsterdam.
- Okamura, M.Y. and Feher G. (1995) Proton-coupled electron transfer reactions of Q_B in reaction centers from photosynthetic bacteria. In: Blankenship, R.E., Madigan MT, and Bauer, C.E. (eds.) *Anoxygenic photosynthetic bacteria*. pp. 577-594. Kluwer Academic Publishers, Dordrecht.
- Petrouleas, V. and Diner, B. (1990) Formation of NO of nitrosyl adducts of redox components of the photosystem II reaction center. I. NO binds to the acceptor-side non-heme iron. *Biochim. Biophys. Acta* 1015: 131-140.
- Plato, M., Michel-Beyerle, M.E., Bixon, M. and Jortner, J. (1989) On the role of tryptophan as a superexchange mediator for quinone reduction in photosynthetic reaction centers. *FEBS Lett.* 249: 70-74.
- Ramachandran, G.N., Ramakrishnan, C. and Sasisekharan, V. (1963) Stereochemistry of polypeptide chain configurations. *J. Mol. Biol.* 7: 95-99.
- Ravnikar, P., Debus, R., Sevrinck, J., Saetaert, P. and McIntosh, L. (1989) Nucleotide sequence on a second *psbA* gene from the unicellular cyanobacterium *Synechocystis* 6803. *Nucl. Acids. Res.* 17: 3991.

- Renger, G. 1993. Water cleavage by solar radiation-an inspiring challenge of photosynthesis research. *Photosyn. Res.* 38: 229-247.
- Roffey, R.A., Kramer, D.M., Govindjee, and Sayre, R.T. (1994) Lumenal side histidine mutations in the D1 protein of photosystem II affect donor side electron transfer in *Chlamydomonas reinhardtii*. *Biochim. Biophys. Acta* 1185: 257-270.
- Ruffle, S.V., Donnelly, D., Blundell, T.L. and Nugent, J.H.A. (1992) A three-dimensional model of the photosystem II reaction centre of *Pisum sativum*. *Photosyn. Res.* 34: 287-300.
- Santini, C., Tidu, V., Tognon, G., Tognon, G., Magaldi, A. and Bassi, R. (1994) Three-dimensional structure of the higher-plant photosystem II reaction centre and evidence for its dimeric organization *in vivo*. *Eur. J. Biochem.* 221: 307-315.
- Satoh, K. (1993) Isolation and properties of the photosystem II reaction center. In: Deisenhofer, J. and Norris, J.R. (eds.) *The photosynthetic reaction center*. pp. 289-318. Academic Press, New York.
- Sayre, R.T., Anderson, B., Bogorad, L. (1986) The topology of a membrane protein: The orientation of the 32kd Q_B-binding chloroplast thylakoid membrane protein. *Cell* 47: 601-608.
- Schelvis, J.P.M., van Noort, P.I., Aartsma, T.J. and van Gorkom, H.J. (1994) Energy transfer, charge separation and pigment arrangement in the reaction center of photosystem II. *Biochim. Biophys. Acta* 1184: 242-250.
- Semin, B.K., Loviagina, E.R., Aleksandrov, A.Y., Kaurov, Y.N., Novakova, A.A. (1990) Effect of formate on Mössbauer parameters of the non-heme iron of PSII particles of cyanobacteria. *FEBS Lett.* 270: 184-186.
- Shopes, R.J., Blubaugh, D., Wraight, C. and Govindjee. (1989) Absence of a bicarbonate-depletion effect in electron transfer between quinones and reaction centers of *Rhodobacter sphaeroides*. *Biochim. Biophys. Acta* 974: 114-118.

- Shuvalov, V.A., Heber, U., Schreiber, U. (1989) Low temperature photochemistry and spectral properties of a photosystem-2 reaction center complex containing the proteins D1 and D2 and 2 hemes of Cyt *b*-559. *FEBS Lett.* 258: 27-31.
- Sinning, I. (1992) Herbicide binding in the bacterial photosynthetic reaction center. *TIBS* 17: 150-154.
- Sinning, I., Michel, H., Mathis, P., Rutherford, A.W. (1989) Characterization of four herbicide-resistant mutants of *Rhodospseudomonas viridis* by genetic analysis, electron paramagnetic resonance, and optical spectroscopy. *Biochemistry* 28: 5544-5553.
- Sinning, I., Koepke, J. and Michel, H. (1990) Recent advances in the structure analysis of *Rhodospseudomonas viridis* reaction center mutants. In: Michel-Beyerle, M.E. (ed.) *Reaction centres of photosynthetic bacteria*. Vol. 6. pp. 199-208. Springer-Verlag, Berlin.
- Sobolev, V. and Edelman, M. (1995) Modeling the Quinone-B binding site of the photosystem-II reaction center using notions of complementarity and contact-surface between atoms. *Proteins* 21: 214-225.
- Srivastava, A., Strasser, R.J. and Govindjee. (1995) Polyphasic rise of chlorophyll *a* fluorescence in herbicide-resistant D1 mutants of *Chlamydomonas reinhardtii*. *Photosyn. Res.* 43: 131-141.
- Stemler, A. and Jursinic, P. (1993) Oxidation-reduction potential dependence of formate binding to photosystem II in maize thylakoids. *Biochim. Biophys. Acta* 1183: 269-280.
- Strasser, R.J., Eggenberg, P., Pfister, K. and Govindjee. (1992) An equilibrium model for electron transfer in photosystem II acceptor complex: An application to *Chlamydomonas reinhardtii* cells of D1 mutants and those treated with formate. *Arch. Sci. Gen.* 45: 207-224.

- Subramaniam, S., Tchong, D.K. and Fenton, J.M. (1996) A knowledge-based method for protein structure refinement and prediction. In: States, D.J., Agarwal, P., Gaasterland, T., Hunter, L., Smith, R.F. (eds.) Proceedings Fourth International Conference on Intelligent Systems for Molecular Biology. pp. 218-229. AAAI Press, Menlo Park, CA.
- Svensson, B. (1995) The photosystem II reaction centre structure, molecular modelling and experimental verification. Doctoral Thesis, Stockholm University, Sweden.
- Svensson, B., Vass, I., Cedergren, E., Styring, S. (1990) Structure of donor side components in photosystem II predicted by computer modeling. *EMBO J.* 9: 2051-2059.
- Svensson, B., Vass, I. and Styring, S. (1991) Sequence analysis of the D1 and D2 reaction center proteins of photosystem II. *Z. Naturforsch.* 46c: 765-776.
- Svensson, B., Etchebest, C., Tuffery, P., Smith, J., van Kan, P. and Styring, S. (1995a) The structural environment of the tyrosyl radicals in photosystem II. In: Mathis, P. (ed.) *Photosynthesis: From Light to Biosphere*, Vol. I. pp. 647-650. Kluwer Academic Publishers, Dordrecht.
- Svensson, B., van Kan, P.J.M., Styring, S. (1995b) A proposal for the structure of the P680 pigments in photosystem II. In: Mathis, P. (ed.) *Photosynthesis: From light to biosphere*. Vol. I. pp. 425-430. Kluwer Academic Publishers, Dordrecht.
- Tang, X.-S., Peloquin, J.M., Lorigan, G.A. and Diner, B.A. (1995) The binding environment of the reduced primary quinone electron acceptor, Q_A^- , of PSII. In: Mathis, P. (ed.) *Photosynthesis: From Light to Biosphere*. Vol I. pp. 775-778. Kluwer Academic Publishers, Dordrecht.
- Taoka, S. and Crofts, A.R. (1990) Two electron gate in triazine resistant and susceptible *Amaranthus hybridus*. In: Baltscheffsky, M. (ed.) *Current research in photosynthesis*, Vol. 1. pp 547-550. Kluwer Academic Publishers, Dordrecht.

- Telfer, A., Dharni, S., Bishop, S.M., Phillips, D. and Barber, J. (1994) Beta-carotene quenches singlet oxygen formed by isolated photosystem II reactions centers. *Biochemistry* 33: 14469-14474.
- Tietjen, K.G., Kluth, J.F., Andree, R., Haug, M., Lindig, M., Müller, K.H., Wroblowsky, H.J. and Trebst, A. (1991) The herbicide binding niche of photosystem II—a model. *Pest. Sci.* 31: 65-72.
- Trebst, A. (1986) The topology of the plastoquinone and herbicide binding peptides of photosystem II—a model. *Z. Naturforsch.* 41c: 240-245.
- van der Vos, R., van Leeuwen, P.J., Braun, P. and Hoff, A.J. (1992) Analysis of the optical absorbance spectra of D1-D2-cytochrome b-559 complexes by absorbance-detected magnetic resonance. Structural properties of P680. *Biochim. Biophys. Acta* 1140: 184-198.
- van Dorssen, R.J., Breton, J., Plijter, J.J., Satoh, K., van Gorkom, H.J. and Amesz, J. (1987) Spectroscopic properties of the reaction center and of the 47 kDa chlorophyll protein of photosystem II. *Biochim. Biophys. Acta* 893: 267-274.
- van Gorkom, H.J., Schelvis, J.P.M. (1993) Kok's oxygen clock: What makes it tick? The structure of P680 and consequences of oxidizing power. *Photosyn. Res.* 38: 297-301.
- van Leeuwen, P.J., Nieveen, M.C., van de Meent, E.J., Dekker, J.P., van Gorkom, H.J. (1991) Rapid and simple isolation of pure photosystem II core and reaction center particles from spinach. *Photosyn. Res.* 28: 149-153.
- van Miegheem, F.J.E., Satoh, K. and Rutherford, A.W. (1991) A chlorophyll tilted 30° relative the membrane in the photosystem II reaction center. *Biochim. Biophys. Acta* 1058: 379-385.
- van Rensen, J.J.S., Tonk, W.J.M., de Bruijn, S.M. (1988) Involvement of bicarbonate in the protonation of the secondary quinone electron acceptor of photosystem II via the non-heme iron of the quinone-iron acceptor complex. *FEBS Lett.* 226: 347-351.

- Velthuys, B.R. (1981) Electron dependent competition between plastoquinone and inhibitors for binding to photosystem II. *FEBS Lett.* 126: 277-281.
- Vermaas, W. (1993) Molecular-biological approaches to analyze photosystem II structure and function. *Ann. Rev. Plant Physiol. Plant Mol. Biol.* 44: 457-481.
- Vermaas, W.F.J., Rutherford, A.W. (1984) EPR measurements on the effects of bicarbonate and triazine resistance on the acceptor side of photosystem II. *FEBS Lett.* 175: 243-248.
- Vermaas, W.F.J. and Ikeuchi, M. (1991) Photosystem II. In: Bogorad, L., Vasil, I.K. (eds.) *Photosynthetic Apparatus: Molecular Biology and Operation*. pp. 25-111. Academic Press, San Diego.
- Vermaas, W.F.J., Williams, J.G.K. and Arntzen, C.J. (1987) Site-directed mutations of two histidine residues in the D2 protein inactivate and destabilize photosystem II in the cyanobacterium *Synechocystis* 6803. *Z. Naturforsch.* 42c: 762-768.
- Vermaas, W.F.J., Rutherford, A.W. and Hansson, Ö. (1988) Site-directed mutagenesis in photosystem II of the cyanobacterium *Synechocystis* sp. PCC 6803; Donor D is a tyrosyl residue in the D2 protein. *Proc. Natl. Acad. Sci. USA* 85: 8477-8481.
- Vermaas, W.F.J., Charité, J. and Shen, G. (1990) Q_A binding in D2 contributes to the functional and structural stability of photosystem II. *Z. Naturforsch.* 45c: 359-365.
- Vermaas, W.F.J., Styring, S., Schröder, W.P. and Andersson, B. (1993) Photosynthetic water oxidation: The protein framework. *Photosyn. Res.* 38: 249-263.
- Vermaas, W., Vass, I., Eggers, B. and Styring, S. (1994) Mutation of a putative ligand to the non-heme iron in photosystem II: Implications for Q_A reactivity, electron transfer, and herbicide binding. *Biochim. Biophys. Acta* 1184: 263-272.
- Vernotte, C., Briantais, J.-M., Astier, C. and Govindjee. (1995) Differential effects of formate in single and double mutants of D1 in *Synechocystis* sp. PCC 6714. *Biochim. Biophys. Acta* 1229: 296-301.

- Wachtveitl, J., Farchaus, J.W., Das, R., Lutz, M., Robert, B., Mattioli, T.A. (1993) Structure, spectroscopic, and redox properties of *Rhodobacter sphaeroides* reaction centers bearing point mutations near the primary electron donor. *Biochemistry* 32: 12875-12886.
- Wang, X., Cao, J., Maroti, P., Stilz, H.U., Finklele, U., Lauterwasse, C., Zinth, W., Oesterhelt, D., Govindjee and Wraight, C.A. (1992) Is bicarbonate in photosystem II the equivalent of the glutamate ligand to the iron atom in bacterial reaction center? *Biochim. Biophys. Acta* 1100: 1-8.
- Williams, J.G.K. and Chisholm, D.A. (1987) Nucleotide sequence of both *psbD* genes from the cyanobacterium *Synechocystis* 6803. In: Biggins, J. (ed.) *Progress in Photosynthesis Research*. Vol. IV. pp. 809-812. Martinus Nijhoff Publishers, Dordrecht.
- Wincencjusz, H., Allakhverdiev, S.I., Klimov, V.V. and van Gorkom, H.J. (1996) Bicarbonate-reversible formate inhibition at the donor side of photosystem II. *Biochim. Biophys. Acta* 1273: 1-3.
- Wraight, C.A. (1979) Electron acceptors of bacterial photosynthetic reaction centers. II. H^+ binding coupled to secondary electron transfer in the quinone acceptor complex. *Biochim. Biophys. Acta* 548: 309-327.
- Wraight, C.A. (1981) Oxidation-reduction physical chemistry of the acceptor quinone complex in bacterial photosynthetic reaction centers: Evidence for a new model of herbicide activity. *Israel. J. Chem.* 21: 348-354.
- Xiong, J., Hutchison, R.S., Sayre, R. and Govindjee. (1995) Characterization of a site-directed mutant (D1-arginine 269-glycine) of *Chlamydomonas reinhardtii*. In: Mathis, P. (ed.) *Photosynthesis: From Light to Biosphere*. Vol. I. pp. 525-528. Kluwer Academic Publishers, Dordrecht.

- Xiong, J., Subramaniam, S. and Govindjee (1996) Modeling of the D1/D2 proteins and cofactors of the photosystem II reaction center: Implications to herbicide and bicarbonate binding. *Protein Sci.* 5: 2054-2073.
- Xu, C., Taoka, S., Crofts, A.R. and Govindjee. (1991) Kinetic characteristics of formate/formic acid binding at the plastoquinone reductase site in spinach thylakoids. *Biochim. Biophys. Acta* 1098: 32-40.

CHAPTER V. A KNOWLEDGE-BASED THREE DIMENSIONAL MODEL OF D1-D2-CYTOCHROME B559 OF *CHLAMYDOMONAS REINHARDTII*

A. Introduction

Photosystem II (PS II), one of the two protein complexes in plants, algae, and cyanobacteria that perform primary photochemical reactions, is the only protein complex in nature that is able to evolve molecular oxygen by oxidizing water. The reaction center of PSII where the photochemical reactions take place consists of several membrane bound polypeptides, D1, D2, a heterodimer of cytochrome b559, PsbI and PsbW (for reviews, see Renger, 1993; Vermaas et al. 1993; Diner and Babcock 1996; Nugent 1996). The reaction center, utilizing the harvested light energy, undergoes the reaction of charge separation and an electron transfer from water to plastoquinone. Two major polypeptides of the reaction center, D1 and D2, contain a number of inorganic and organic cofactors including a tetra-manganese cluster, two redox active tyrosine residues, six chlorophyll *a* molecules, two pheophytins, and two plastoquinones. A non-heme iron, located between Q_A and Q_B, does not participate directly in the electron transfer but is vital for the transfer process. Bicarbonate anions is crucial for liganding to the non-heme iron and participating in the reduction of plastoquinone in PSII. Two β -carotene molecules are also believed to be embedded in the reaction center and are believed to be involved in the photoprotective process.

Despite the importance of this protein complex to provide the biomass and oxygen on earth, the molecular structure and the functional mechanism of the PSII reaction center are not yet fully understood. A high resolution X-ray crystal structure of the PSII reaction center is not yet available, except low resolution electron microscopy structures (for review, see Rögner et al. 1996; for recent reports, see *e.g.*, Marr et al. 1996; Nakazato et al. 1996). In the absence of the crystal structure of the PSII reaction center, much of the

structural understanding of the PSII reaction center is derived from the significant sequence and functional homology with the non-oxygenic reaction centers of the purple non-sulfur photosynthetic bacteria *Rhodobacter (Rb.) sphaeroides* and *Rhodopseudomonas (Rps.) viridis*, for which high resolution crystal structures are available (for review, see *e.g.* Lancaster et al. 1995). To aid in a more accurate structural understanding of the PSII reaction center, three dimensional computer models have been constructed in the past exclusively based on the homology of D1/D2 polypeptides with the L/M subunits of the bacterial reaction center of *Rhodobacter (Rb.) sphaeroides* and *Rhodopseudomonas (Rps.) viridis* (Bowyer et al. 1990; Svensson et al. 1990; Ruffle et al. 1992; Svensson et al. 1996; Chapter IV).

Though the comparison with the bacterial reaction center is very useful, the PSII reaction center has many unique features and can not be modeled directly by homology. In order to construct a more reasonable and more useful computer model that includes the new structural features of the PSII reaction center, molecular docking techniques in association with other computational tools are employed to model parts of the PSII reaction center that do not have counterparts in the bacterial reaction center, based on the extensive knowledge available through the biochemical, biophysical and molecular biological studies on the structure and function of the PSII reaction center. To this end, various models for the conformation of the P680 chlorophylls responsible for the charge separation and bicarbonate ions have been proposed (see Svensson et al. 1996 and Chapter IV). Two bicarbonate anions and a water molecule was docked in the PSII reaction center for liganding the non-heme iron and facilitating the Q_B protonation (Chapter IV). In a recent review by Nugent (1996), a PSII reaction center model with two extra chlorophylls, the manganese cluster and the heme moiety of cytochrome b559 was also shown. The availability of these models have helped in enhancing our understanding of various issues on the structure of the PSII reaction center, allowing prediction for the testing of various functional questions.

Certain important issues that failed to be adequately addressed in the past, however, are the conformation of cytochrome b559 subunit and β -carotene molecules within the PSII reaction center. By incorporating the available experimental data, we have attempted to model a more complete PSII reaction center of a unicellular green alga *Chlamydomonas reinhardtii*. The reason of choosing this organism is because it is one of most widely used model systems for molecular biological studies of photosynthetic eucaryotes (see review by Rochaix 1995). In this chapter, I present a new three dimensional model of the PSII reaction center of *C. reinhardtii* that includes not only D1, D2, the reaction center chlorophyll P680, two pheophytins, the non-heme iron, two bicarbonate anions and two plastoquinones (Q_A and Q_B), but also four accessory chlorophylls, the alpha and beta subunits of cytochrome b-559 with the heme moiety, and two β -carotene molecules. The constructed model is compared to the major existing PSII models (Ruffles et al. 1992; Svensson et al. 1996; Chapter IV) and is found to be consistent with the majority of the experimental data. The availability of the model is believed to provide a more comprehensive tool for localizing key residues important for the photochemical reactions and will enhance our understanding of this important protein complex.

B. Materials and Methods

The modeling procedure for the D1/D2 proteins of the PSII reaction center of *C. reinhardtii* by homology was similar as described in Chapter IV using the QUANTA/CHARMm (version 4.1) molecular modeling package. The amino acid sequence of D1 of the green alga was according to Erickson et al. (1984); and D2 according to Erickson et al. (1986). The sequence alignment of D1 and D2 proteins with the L or M subunits, respectively, was primarily based on Ruffle et al. (1992) and the one in Chapter IV with minor adjustments done on the Protein Design subprogram of QUANTA. After

alignment, the two bacterial template proteins (1PCR and 1PRC) were matched and superimposed, the coordinates of the aligned sequences were averaged and copied to the modeled sequences. The newly defined coordinates for D1 and D2 were refined with the Structural Regularization algorithm in QUANTA as described in Chapter IV. The sequence variable loop regions of more than four residues (including the C-terminal region of D1) were modeled with a sequence-specific approach by searching for the best matched protein fragments from the protein sequences already having crystal structures available in the Brookhaven Protein Data Bank, using a "basic local alignment search tool" (BLAST, Altschul et al. 1990). For procedural details, see Chapter IV.

The cofactors that are analogous to those in the bacterial reaction center (1PCR) were edited using the Molecular Editor function of QUANTA and incorporated into the D1/D2 protein complex as described in Chapter IV. These corrected structures include two chlorophylls for the special pair, two accessory chlorophylls, two pheophytins, two plastoquinones and a β -carotene (on the D2 side). The structures for the PSII chromophores were based on those reviewed by Cramer and Knaff (1990) and Armstrong (1995).

Further modifications were made on the conformations of certain cofactors based on available experimental suggestions. The two chlorophyll monomers of the chlorophyll special pair (P680) were moved apart to 10 Å away from each other (center to center). Their Q_y excitonic transition moments were rotated to make an angle of 150°. This P680 conformation was suggested to fit all the current data (Svensson et al. 1996). A recent study on the conformation of plastoquinone Q_A indicated that the isoprenyl chain relative to the aromatic head group is rotated by 90° at C β position from that in the bacterial Q_A (Zheng and Dismukes 1996). This correction was also made in our model. Q_B in the structure of 1PCR was not in fully bound state and is displaced by 5 Å when compared with the Q_B in the *Rps. viridis* structure (1PRC, Lancaster et al. 1995). To correct this, the position of plastoquinone Q_B was moved by 5 Å to match the superimposed Q_B of the

1PRC structure. Two bicarbonate anions were also docked into the model at the non-heme iron and the Q_B sites, as described in Chapter IV. Also based on experimental suggestions, two extra accessory chlorophylls liganded on residues D1-H118 and D2-H117 (see *e.g.* Koulougliotis et al. 1994) were included by manually docking them into the sites. An additional β -carotene molecule suggested to exist on the D1 side of the PSII reaction center (Achim Trebst, personal communication) was modeled at the symmetrical position of the D2 β -carotene relative to the central axis of the reaction center.

The D1/D2 protein structure combined with the above cofactors was further energy-minimized using the CHARMM procedure (Brooks et al. 1983). The energy minimization was performed until convergence is reached (rms force < 0.01 kcal/mol-Å²) as described in detail in Chapter IV. During this process, the coordinates of all the cofactors were constrained in place and only the D1 and D2 polypeptides was allowed to move.

Cytochrome b559, an intrinsic transmembrane protein of the PSII reaction center, has no homologous bacterial templates to direct a homology modeling. This protein with two subunits, α and β , was modeled entirely based on existing knowledge in literature (see Results section). We assigned the transmembrane α -helices of the α (residues 18-43) and of the β (residues 18-43) subunits according to Cramer et al. (1993) and Whitmarsh and Pakrasi (1996) and modeled the cytochrome in the α/β heterodimer form. The conformation of the N- and C-terminal regions of the α subunit and the N-terminal region for the β subunit was modeled using the BLAST approach mentioned above. The newly modeled terminal regions were then pasted onto the helical regions and refined by energy minimization. The α and β subunits were then combined with a heme group to allow the histidine residue from each subunit (α -H23 and β -H23) to form a ligand to the heme iron. The coordinates of the heme moiety were derived from cytochrome b562 of *Escherichia coli* (PDB file code, 256B). The α and β subunits together with the heme were docked in the D1/D2 complex on the Q_A side in close association with helix E of the D2 protein. The docking of cytochrome b559 also took consideration of the following experimental

evidence: the estimated distances from the heme to Q_A and P680 are 20 and 35 Å, respectively (Shuvalov 1994); the N terminus of the α subunit is cross-linked to the D1 *de* loop region (D1-F239 to D1-E244) (Barbato et al. 1995). The combined D1/D2/cytochrome b559 was further minimized as above to obtain the final model.

The entire modeling work was performed on UNIX Silicon Graphics Power Series Workstation 4D/440VGXT. Copies of the coordinates of this model in PDB format are available on request from the authors.

C. Results

1. Sequence alignment, loop building and model evaluation

The modeling of the D1/D2 proteins was based on homology with the L/M subunits of both *Rps. viridis* and *Rb. sphaeroides*. The D1 and D2 proteins was aligned with the L and M subunits, respectively. The alignment was primarily based on the PSII modeling of *Synechocystis* 6803 (Chapter IV) with minor adjustment as shown in Fig. 5.1. After alignment, we find 27% sequence identity (92 residues) and 56% sequence similarity (194 residues) for D1 with the L subunit and 24% sequence identity (83 residues) and 63% sequence similarity (217 residues) for D2 with the M subunit. We counted the identify and homology of D1/D2 with L/M either of the bacterial sources, which is a standard protocol followed in family sequence alignments based on structural criteria (see Chapter IV).

As in Chapter IV, the non-homologous loop regions were modeled by searching for highly homologous sequences from amongst all the proteins with known structures, using BLAST (Altschul et al. 1990). The search results are shown in Table 5.1. The searched fragments bear high degrees of similarity to the modeled sequences (the smallest Poisson probability is above 0.95 for all the hits); hence, the sequence homology is significant for all the searched fragments. By combining the loop conformation with the rest of the

Figure 5.1. Sequence alignment of the D1 protein of *C. reinhardtii* with the L subunit of the photosynthetic bacterial reaction center of *Rhodobacter sphaeroides* (SL) and *Rhodopseudomonas viridis* (VL). Sequence alignment of the D2 protein of *C. reinhardtii* with the M subunit of the photosynthetic bacterial reaction center of *Rhodobacter sphaeroides* (SM) and *Rhodopseudomonas viridis* (VM). The D1 and D2 sequences are in lower case and the bacterial sequences are in upper case. The secondary structure profile of the template L and M proteins and the modeled D1 and D2 proteins are also shown. The α -helices are represented in cylinders. Residues that are predicted to be involved in D1/D2 interactions are marked by asterisks. Cytochrome b559 was also modeled as described in Materials and Methods. The predicted α -helices for the α and β subunits are shown in cylinders and the predicted β strands are shown in arrows.

AL 1 --ALLSPK 9 YRFOOTLIG 19 GMLF-DPMVG 28 F---FVOT 24 GVALTIAA 114 GILLANAN 154VAG-THRO 63 LI-----SV 67 -YPPA----- 71
 VL 1 --ALLSPK 9 YRFOOTLIG 19 GMLF-DPMVG 28 F---FVOT 24 GVALTIAA 114 GILLANAN 154VAG-THRO 63 LI-----SV 67 -YPPA----- 71
 DL 1 --ALLSPK 9 YRFOOTLIG 19 GMLF-DPMVG 28 F---FVOT 24 GVALTIAA 114 GILLANAN 154VAG-THRO 63 LI-----SV 67 -YPPA----- 71
 AL 72 E-YOL-QGAP 80 ---LAKOCT 19 YRFOOTLIG 19 GMLF-DPMVG 28 F---FVOT 24 GVALTIAA 114 GILLANAN 154VAG-THRO 63 LI-----SV 67 -YPPA----- 71
 VL 72 E-YOL-QGAP 80 ---LAKOCT 19 YRFOOTLIG 19 GMLF-DPMVG 28 F---FVOT 24 GVALTIAA 114 GILLANAN 154VAG-THRO 63 LI-----SV 67 -YPPA----- 71
 DL 72 E-YOL-QGAP 80 ---LAKOCT 19 YRFOOTLIG 19 GMLF-DPMVG 28 F---FVOT 24 GVALTIAA 114 GILLANAN 154VAG-THRO 63 LI-----SV 67 -YPPA----- 71
 AL 163 YTONYRPA 173 EYALIT 183 EYALIT 193 EYALIT 199 ---NPK-OK 205 EM-R--T-- 209 FORTOTED 213 LV-OK-SIG- 226 TIGIT 226 TIGIT 226
 VL 163 YTONYRPA 173 EYALIT 183 EYALIT 193 EYALIT 199 ---NPK-OK 205 EM-R--T-- 209 FORTOTED 213 LV-OK-SIG- 226 TIGIT 226 TIGIT 226
 DL 163 YTONYRPA 173 EYALIT 183 EYALIT 193 EYALIT 199 ---NPK-OK 205 EM-R--T-- 209 FORTOTED 213 LV-OK-SIG- 226 TIGIT 226 TIGIT 226
 AL 246 LCHITOTI- 255 ---M-FQOMV 261 -DWMOMVCL 270 FPMNIP--G 278 GING
 VL 246 LCHITOTI- 255 ---M-FQOMV 261 -DWMOMVCL 270 FPMNIP--G 278 GING
 DL 246 LCHITOTI- 255 ---M-FQOMV 261 -DWMOMVCL 270 FPMNIP--G 278 GING
 AL 1 AYOQIFSOV 11 QVROPADIG 21 TEDVNAIRS 31 GVOPTSLIG 41 WYMAOQPI 51 YLOCTVLS 61 YLOCTVLS 61 YLOCTVLS 61
 VL 1 AYOQIFSOV 11 QVROPADIG 21 TEDVNAIRS 31 GVOPTSLIG 41 WYMAOQPI 51 YLOCTVLS 61 YLOCTVLS 61 YLOCTVLS 61
 DL 1 AYOQIFSOV 11 QVROPADIG 21 TEDVNAIRS 31 GVOPTSLIG 41 WYMAOQPI 51 YLOCTVLS 61 YLOCTVLS 61 YLOCTVLS 61
 AL 94 LEPPAPE-YO 103 --LSF---AA 108 PL---E 112 --COLLAP 121 FMAVANS 131 GYTLRQ 141 GYTLRQ 141 GYTLRQ 141
 VL 94 LEPPAPE-YO 103 --LSF---AA 108 PL---E 112 --COLLAP 121 FMAVANS 131 GYTLRQ 141 GYTLRQ 141 GYTLRQ 141
 DL 94 LEPPAPE-YO 103 --LSF---AA 108 PL---E 112 --COLLAP 121 FMAVANS 131 GYTLRQ 141 GYTLRQ 141 GYTLRQ 141
 AL 181 BELWYRPA 191 YRFOOTLIG 19 GMLF-DPMVG 28 F---FVOT 24 GVALTIAA 114 GILLANAN 154VAG-THRO 63 LI-----SV 67 -YPPA----- 71
 VL 181 BELWYRPA 191 YRFOOTLIG 19 GMLF-DPMVG 28 F---FVOT 24 GVALTIAA 114 GILLANAN 154VAG-THRO 63 LI-----SV 67 -YPPA----- 71
 DL 181 BELWYRPA 191 YRFOOTLIG 19 GMLF-DPMVG 28 F---FVOT 24 GVALTIAA 114 GILLANAN 154VAG-THRO 63 LI-----SV 67 -YPPA----- 71
 AL 271 MEAVLITIG 281 DIGILLIGOT- 290 ---VDM- 294 ---VDM- 294 ---VDM- 294 ---VDM- 294 ---VDM- 294
 VL 271 MEAVLITIG 281 DIGILLIGOT- 290 ---VDM- 294 ---VDM- 294 ---VDM- 294 ---VDM- 294 ---VDM- 294
 DL 271 MEAVLITIG 281 DIGILLIGOT- 290 ---VDM- 294 ---VDM- 294 ---VDM- 294 ---VDM- 294 ---VDM- 294
 CTB259 1 1 MACKVERFF 11 SDILTSIATN 21 VINSITVAL 31 FIAOHLVST 41 GLANDVOTOP 51 APNEYFTDR 61 QCAPLITDRF 71 MALKOVKLS 81 GN
 CTB259 1 1 MTKKARVL 11 VPIPTVNL 21 AINGIATVI 31 FFLGATIAWQ 41 PIOR

Table 5.1. BLAST search results. Search results by the BLAST program through the Brookhaven Protein Data Bank for the non-conserved loop or terminal sequences of *Chlamydomonas reinhardtii* D1, D2 and cytochrome b559 (Cyt b559) proteins.

SEARCH QUERY		SEARCH RESULTS	
Protein and Residue Range	Sequence	Protein, PDB File Code, and Residue Range	Sequence
D1 (64-69)	REPVSG	Reverse transcriptase, subunit B, 3HVT (311-316)	
D1 (77-90)	IITGAVIPTSNAIG	Mengo encephalomyocarditis virus coat protein, subunit 4, 2MEV (54-67),	LLSGAVNAFSNMLP
D1 (328-344)	MEVMHERNAHNFP LDLA	Myoglobin, 1FCS (112-127)	IHVLHSRHPGNF GADA
D2 (292-297)	NLRAYD	<i>E. coli</i> cytidine deaminase, 1CTT (248-253)	NLKGYP
D2 (302-310)	EIRAAEDPE	Tryptophan synthase, subunit B, 1WSY (32-40)	AVRAQKDPE
D2 (318-326)	NILLNEGIR	Cytochrome P450 (Bm-3), subunit A (315-323)	GMVLNEALR

Table 5.1 (continued)

SEARCH QUERY		SEARCH RESULTS	
Protein and Residue Range	Sequence	Protein, PDB File Code, and Residue Range	Sequence
Cyt b559 α subunit (43-50)	DAFGTPRP	Glactose oxidase, 1GOF (44-51)	GANGDPKP
Cyt b559 α subunit (51-80)	NEYFTEDRQEAPLITDR FNALEQVKKLSGN	Adipocyte lipid- binding protein, 1ALB (71-100)	DEITADDRKVKSITLD GGALVQVQKWDGK
Cyt b559 β subunit (1-16)	TTKKSAEVLVYPIFTV	Chymotrypsin inhibitor, 1COA (41-56)	QDKPEAQIIVLPVGTI

modeled regions, we completed the modeling of the D1/D2 proteins for *C. reinhardtii*. Modeling of cytochrome b559 will be described in detail in a later section.

The constructed D1-D2-Cytochrome b559 model, presented here, was refined using energy minimization methods in CHARMM (Brooks et al. 1983). At the end of the minimization, the energy of the model was -29,670 kcal/mol, compared to 3.82×10^{19} kcal/mol at the beginning of the minimization process (all measured with cofactors constrained). Among various forms of energies, the non-bonded interaction energy (Lennard-Jones energy) was the major form to be reduced from 3.82×10^{19} kcal/mol to -2603 kcal/mol indicating that the minimization process had mainly corrected the bad van der Waals interactions, producing an energetically favorable conformation.

The heavy atoms of the constructed D1/D2 model deviates from their equivalent atoms in the L/M subunits of the *Rb. sphaeroides* reaction center by 1.2 Å root mean square. Our final PSII reaction center model was evaluated using the Protein Health subprogram in QUANTA. The D1 and D2 main chain torsion angles were analyzed using the phi-psi plot (Ramachandran et al. 1963) which shows that 81% of the backbone conformations are within the most favored regions as compared to 88% in the structure of *Rb. sphaeroides* L and M subunits. The modeled cytochrome b559 main chain torsion angles have 91% of the backbone conformation within the most favored regions. We would like to point out that different regions of the modeled PSII reaction center may have different levels of correctness. The D1/D2 transmembrane regions and the quinone binding sites are highly conserved and have been modeled with a high degree of confidence. The stromal and luminal and C-terminal parts of the sequences, which are much less conserved, can only be predicted with a relatively low degree of confidence.

2. General description of the model

As expected, the general topology of the D1/D2 model resembles that of the L/M structure of the bacterial reaction center, each containing five transmembrane α -helices

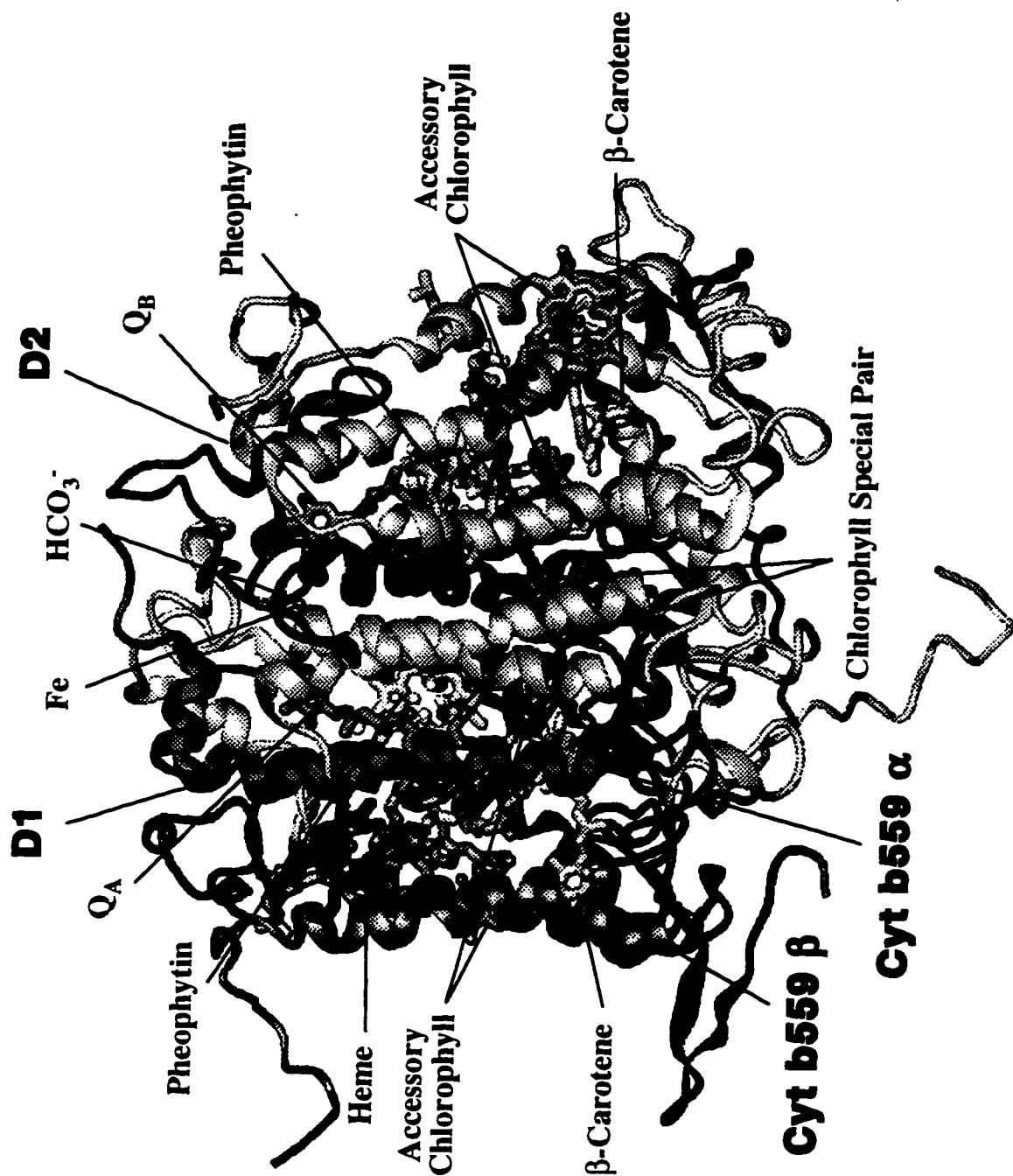
(Figs. 5.1 and 5.2) denoted as A, B, C, D, E. There are also several short non-membrane α -helices between the transmembrane helices on both the luminal and stromal sides, which are denoted as CD, DE, etc. The detailed secondary structure profiles analyzed from the modeled D1, D2 and cytochrome b559 are shown in Fig. 1. The definition for the boundaries of the transmembrane α -helices are slightly different from what was previously reported (*e.g.* Ruffle et al. 1992; Svensson et al. 1996; Chapter IV). The interface between D1 and D2 was also examined which is mostly composed of residues in the N-terminal, transmembrane helices D and E, and the C-terminal regions (marked under the sequences in Fig. 5.1). The contact residues are thought to provide the key protein-protein interactions maintaining the proper conformation of the reaction center complex. Certain contact sites between D1 and D2 has been proposed to be the especially susceptible to proteolytic cleavage in the rapid turnover of the D1 protein during photoinhibition (Trebst 1991).

In the current PSII reaction center model, the modeled cofactors bound to D1/D2 include six chlorophylls, two pheophytins, two β -carotenes, two plastoquinones, one non-heme iron and two bicarbonate ions (Fig. 5.2). The structures for the cofactors are arranged in a two fold symmetry relative to central axis of the reaction center. The stoichiometry and geometry of the above cofactors were modeled according the consensus in the published experimental data as well as the homology principle (see Nanba and Satoh 1987; Gounaris et al. 1990; Kobayashi et al. 1990; van Leeuwen et al. 1991; Chang et al. 1994; Eijkelhoff and Dekker 1995; Pueyo et al. 1995). We will describe the detailed features of the newly modified or added cofactors below.

3. Chlorophylls

In my previous model with D1/D2 and cofactors (see Chapter IV), various possible conformations of P680 were discussed. It was concluded that the P680 conformation for which the special pair is perpendicular to the membrane was the preferred conformation. In this current model, the two monomers of the P680 chlorophyll dimer were further modified

Figure 5.2. The ribbon drawing diagram of the modeled three dimensional structure of the *C. reinhardtii* PSII reaction center including the cofactors. The ribbon form indicates the α -helical structure. D1 and D2 all have five transmembrane helices and several amphipathic helices in the luminal (bottom) and stromal (top) sides. Cytochrome b559 was modeled in α/β form; each subunit has one transmembrane helix. All the bound cofactors are shown in licorice bond forms.

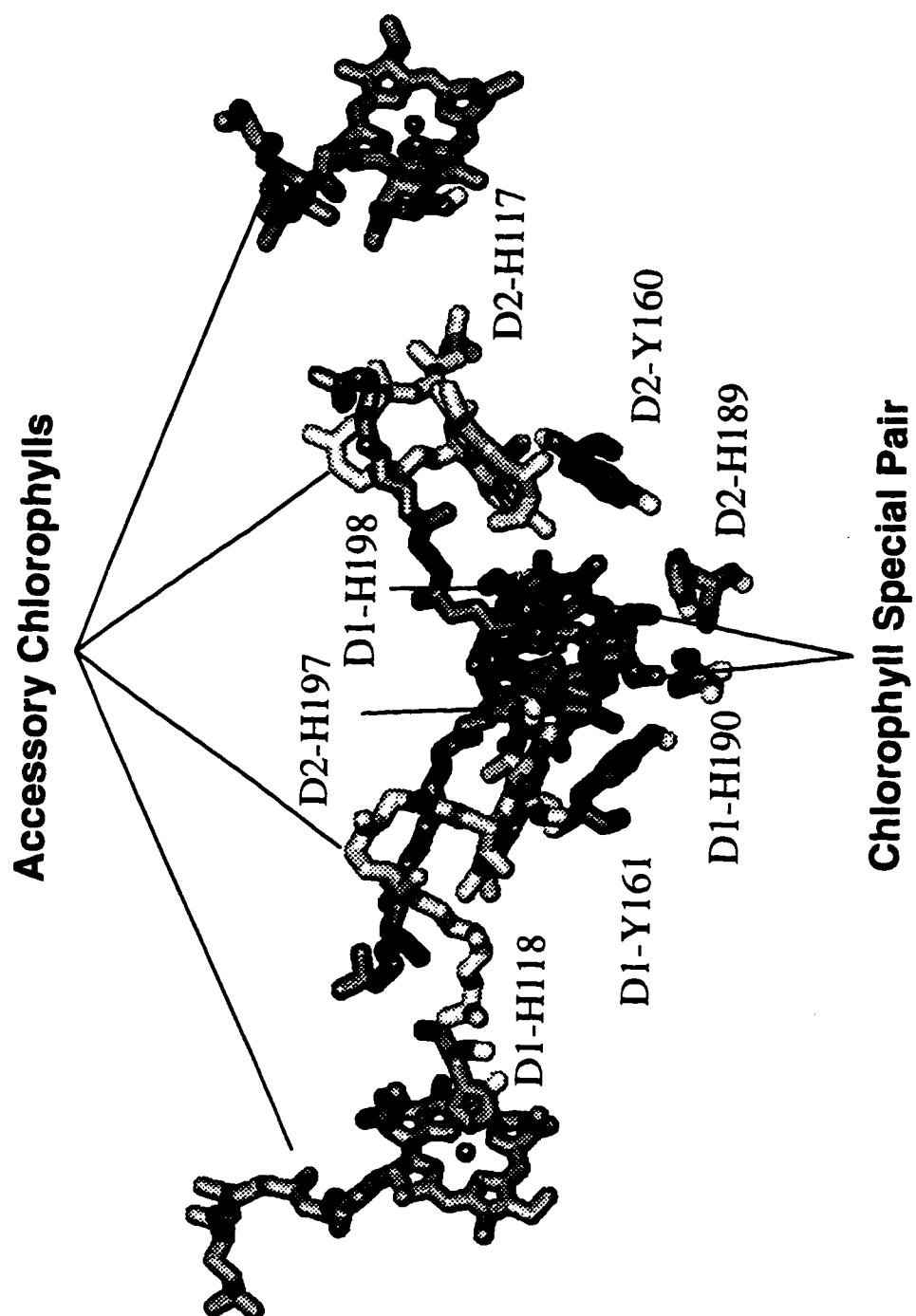


according to Svensson et al. (1996) to allow the center-center distance of the two monomers to be 10.0 Å and their Q_y excitonic transition moments to be at an angle of 150° (Fig. 5.3). Such P680 conformation was suggested to match all existing experimental data on the primary donor (Svensson et al. 1996). Those magnesium ions at the center of the two chlorophyll monomers are liganded by two specific histidine residues, D1-H198 and D2-H197, which, according to sequence comparison, match well with L-H173 and M-H210 (*Rps. viridis* numbering) of the bacterial special pair ligands (Fig. 5.3). Mutations at these two histidine residues have strongly implicated the role of the two residues in coordinating the P680 (see Vermaas et al. 1988; Nixon et al. 1992).

In this current model, two of the accessory chlorophylls were modeled based on their bacterial counterparts (Fig. 5.3). As in previous models (Ruffle et al. 1992; Chapter IV), these two chlorophylls have no conserved histidine ligands in D1 and D2. Svensson et al. (1996) proposed a possibility that water molecules may act as ligands for the chlorophylls. This possibility is supported by the crystal structure of peridinin-chlorophyll-protein of *Amphidinium carterae* (Hofmann et al. 1996) which shows a chlorophyll liganded by a water molecule.

Recent experimental evidence have indicated that two additional accessory chlorophylls may exist and may be liganded by D1-H118 and D2-H117 (D2-H118 in plants) (see e.g. Koulougliotis et al. 1994; Schelvis et al. 1994; Hutchison and Sayre 1995; Mulkidjanian et al. 1996). We have modeled two such accessory chlorophylls (termed chlorophyllz) perpendicular to the membrane and allowed them to be liganded by the above two histidines (Fig. 5.3). In this model, the two docked chlorophylls on D1-H118 and D2-H117 are separated from the non-heme iron by 38.6 Å and 39.4 Å, respectively, which matches well the experimentally determined 39.5 ± 2.5 Å (Koulougliotis et al. 1994). The center-to-center distance of the two accessory chlorophylls to P680 are 30.4 Å and 32.3 Å, for the D1 and D2 chlorophyllzs, respectively, which also match with the experimental determination of 30 Å (Schelvis et al. 1994). Site-directed mutagenesis conducted by

Figure 5.3. The modeled conformation of six chlorophylls in the *C. reinhardtii* PSII reaction center. The center of the chlorophyll special pair (P680) is coordinated by two histidines (D1-H198 and D2-H197). Two accessory chlorophylls on the exterior of the reaction center are liganded by another two histidines (D1-H118 and D2-H117). Two redox active residues D1-Y161 (Z) and D2-Y160 (D) as electron donors to P680 are also shown. Two histidines (D1-H190 and D2-H180) were modeled in close vicinity to the two tyrosines and may modulate the functions of Z and D.



Hutchison and Sayre (1995) on *C. reinhardtii* also indicates the strong possibility of D1-H118 to a chlorophyll liganding residue.

As shown in Figs. 5.2 and 5.3, the two chlorophyll_z molecules are actually located on the exterior of the D1/D2 complex and its binding may involve other PSII core proteins. It is conceivable that in some PSII reaction center preparations the two chlorophylls may be lost when removing the "contaminating" PSII core proteins, resulting in lower number of chlorophylls per reaction center and hence the controversies in experimental determinations (see Nanba and Satoh 1987; Gounaris et al. 1990; Kobayashi et al. 1990; van Leeuwen et al. 1991; Chang et al. 1994; Eijkelhoff and Dekker 1995; Pueyo et al. 1995).

4. Donors to P680⁺

Also shown in Fig. 5.3 are two tyrosine residues, D1-Y161 and D2-Y160, which are electron donors to chlorophyll P680⁺ (known as the donor Z and D). Their role as a donor to P680⁺ were clearly demonstrated by site-directed mutagenesis studies (for review see Vermaas et al. 1993). The two tyrosine residues, both with their hydroxyl groups pointing toward the lumen, are arranged symmetrically around the special pair chlorophylls and in relation to the non-heme iron. The modeled distance from the D1-Y161 phenolic oxygen to the center of the nearest chlorophyll P680 monomer is 12.1 Å, which matches well with the experimentally determined distance of 10-15 Å (Hoganson and Babcock 1989). The measured distance between D1-Y161 and D2-Y160 are 30.0 Å which matches the experimentally measured 29-30 Å distance in spinach samples (Astashkin et al. 1994; Kodera et al. 1995). The modeled distances of the tyrosines Z and D to the non-heme iron is 36.5 Å and 35.0 Å, respectively, which fall in the range of the EPR spectroscopic measurements of 37 ± 5 Å by Kouloughliotis et al. (1995) using spinach samples. The above experimental studies provide strong support to the validity of this PSII three-dimensional model.

Site-directed mutagenesis in *C. reinhardtii* has indicated that one of the crucial residues in the PSII donor side is D1-H190 as it is believed to be involved in the assembly of the manganese cluster (Roffey et al. 1994; Kramer et al. 1994). This residue (Fig. 5.3) was modeled to the close vicinity to donor Z (4.5 Å) consistent with the result of Svensson et al. (1996) who proposed a possible electrostatic interaction between the two residues. D2-H189 is nearly symmetrically located from D1-H190 relative to the P680 chlorophylls (Fig. 5.3). It is modeled at a close distance (3.6 Å) to the donor D (D2-Y160). Spectroscopic studies on the site-directed mutants of D2-H189 in *Synechocystis* 6803 strongly supports its proposed interaction to donor D (Tang et al. 1993). It was suggested that D2-H189 may function to accept the proton from D2-Y160 upon oxidation of D (see Svensson et al. 1996). This close interaction is, however, not observed in my previous model (Chapter IV); I attribute this inconsistency to the slightly different methodology used during the different modeling processes.

5. β -Carotenes

Carotenoids in the PSII reaction center are suggested to function in protecting the complex against photo-oxidation by quenching the triplet state of the primary donor (for review, see Frank and Cogdell 1996). In isolated PSII reaction center preparations, there appears to be two carotene molecules per PSII reaction center (Gounaris et al. 1990; Kobayashi et al. 1990; Montoya et al. 1991; Eijkelhoff and Dekker 1994; Mimuro et al. 1995). Accordingly, I modeled two β -carotene molecules in the D1/D2 protein complex, one which is located on the D2 side was modeled by modifying the structure of dihydro-neurosporene from *Rb. sphaeroides* (1PCR), the other by docking a β -carotene to the symmetrical position of the D2 β -carotene relative to the central axis of the reaction center (personal communication with Achim Trebst). Each of the molecules were modeled to be within the van der Waals contact distance with two accessory chlorophylls, one "proximal" accessory chlorophyll close to the special pair, and the other "distal" accessory chlorophyll

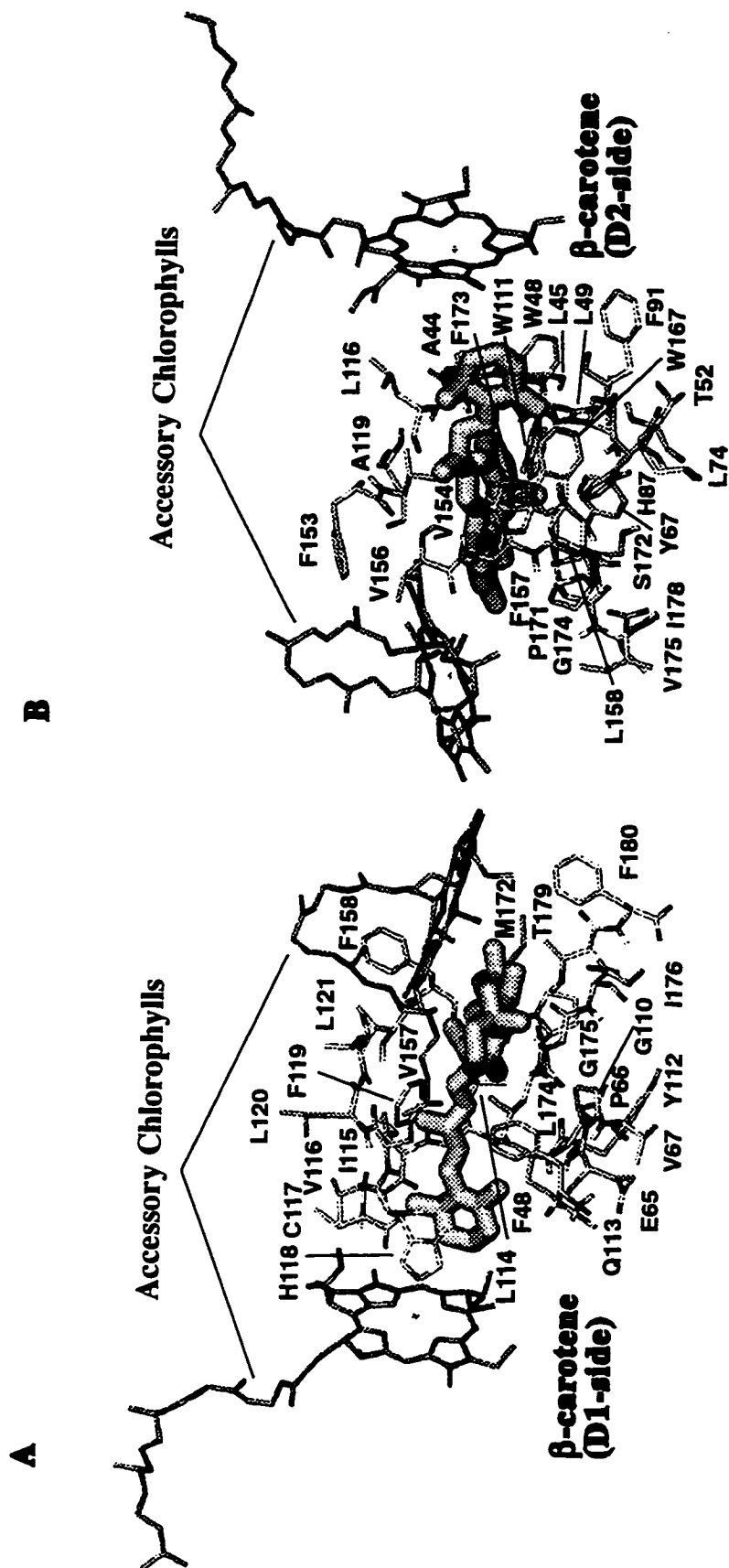
liganding to D1-H118 or D2-H117. The close proximity of β -carotene to the accessory chlorophyll validates the high probability of its function in quenching the triplet state of primary donor P680 via the accessory chlorophyll, analogous to the role of the carotenoid in the bacterial reaction center.

The protein binding environment for the carotenoids was examined. Both β -carotene molecules are located in the middle of the transmembrane region and their surrounding protein binding environment for the β -carotene is exclusively hydrophobic. The protein binding niche for the β -carotene in the D1 side D1-F48, D1-E65, D1-P66, D1-G110, D1-Y112, D1-Q113, D1-L114, D1-I115, D1-V116, D1-C117, D1-H118, D1-F119, D1-L120, D1-L121, D1-V157, D1-F158, D1-M172, D1-L174, D1-G175, D1-I176, D1-T179, and D1-F180 (Fig. 5.4A). The residues that form the binding environment for β -carotene on the D2 side include D2-A44, D2-L45, D2-W48, D2-L49, D2-T52, D2-Y67, D2-L74, D2-H87, D2-F91, D2-W111, D2-A119, D2-L116, D2-F153, D2-V154, D2-V156, D2-F157, D2-L158, D2-W167, D2-P171, D2-S172, D2-F173, D2-G174, D2-V175, and D2-I178 (Fig. 5.4B).

6. Cytochrome b559 and the heme binding region

Cytochrome b559 is an intrinsic and essential component of the PSII reaction center (for reviews, see *e.g.* Cramer et al. 1993; Whitmarsh and Pakrasi 1996). Its presence is critical for the biogenesis and stable assembly of the PSII reaction center. Though the protein is not involved in the primary electron transport in PSII, experimental studies suggest that it may be involved in protecting PSII from photodamage in excess light. However, since this protein has no bacterial homologue to direct its modeling. Thus, it presents a challenge to modeling the structure *de novo* not only at the secondary and tertiary levels, but also at the quaternary level. In this modeling, extensive knowledge on the experimental characterization of this protein is required for constructing the model. The relevant literature will be briefly summarized below.

Figure 5.4. Two β -carotenes were modeled in the *C. reinhardtii* PSII reaction center, one on the D1 side and the other on the D2 side. Each of them is located in between two accessory chlorophylls. The protein binding environment for each of the carotenoids is shown in A and B, respectively. The protein binding environment is exclusively hydrophobic for the β -carotenes.



Cytochrome b559 has two subunits, α and β , each containing one transmembrane α -helical domain (Herrmann et al. 1984; Pakrasi et al. 1988) and one histidine residue which is presumably to be a heme ligand (Babcock et al. 1985). It is proposed that both histidines are required to act as ligands for the heme, which is a common situation in a number of membrane-bound a- and b- type cytochromes (Esposti 1989). Site-directed mutagenesis of the two histidines resulted in a complete loss of PSII (Pakrasi et al. 1991). The number of cytochrome b559 per reaction center determined by spectroscopic and EPR analyses was shown to only one cytochrome b559 in isolated PSII preparations (Buser et al. 1992). Thus, a heterodimer conformation appears to be a preferred one, consistent with the previous work of Herrmann et al. (1984) and Widger et al. (1985). Protease digestion and immuno-gold labeling experiments demonstrate that the amino terminal end of the α subunit is located in the stromal phase and its carboxyl end in the lumenal phase (Tae et al. 1988; Vallon et al. 1989; Marr et al. 1996), and that the amino terminal end of the β subunit is located on the stromal end (Tae and Cramer 1994). If the heme is coordinated by the histidines from each subunit, the above evidence will put the heme on the stromal side of the PSII transmembrane region. The surface-enhanced Raman scattering spectroscopic data further support this suggestion (Picorel et al. 1994). Although the estimate for the number of hemes per reaction center has been a matter of controversy in literature (see review in Whitmarsh and Pakrasi 1996), in isolated reaction center preparations, the stoichiometry for the α and β subunits is 1:1 (Widger et al. 1985), and that for D1, D2, and cytochrome b559 is 1:1:1 (Nanba and Satoh 1987). The heme group can also exist in at least two different interconvertible redox potential forms, a pH-independent high potential form and a pH-dependent low potential form (see review in Whitmarsh and Pakrasi 1996). Shuvalov (1994) has proposed a model that allows a hydroxyl anion binding between the heme iron and the ϵ 2-nitrogen of the histidine of the α subunit in the α/β heterodimer form, making it a low potential (or extra low potential) form of cytochrome b559.

In this modeling, we have proposed a conformation that accommodates the consensus of the above experimental data. We modeled one cytochrome b559 with the α/β form (the amino acid sequences were based on Mor et al. 1995). The cytochrome was positioned with the N-terminal ends of both subunits on the stromal side and C-terminal ends on the luminal side and was placed near the D1/D2 complex fitting into the opening space between the two proteins (Fig. 5.2). This location appears to match the electron projection map of the two dimensional PSII crystal structure (Nakazato et al. 1996). Transmembrane α -helices of the α and β subunits were assigned according to the sequence analyses of Cramer et al. (1993) and Whitmarsh and Pakrasi (1996). The modeling allows the heme to be liganded by the histidine from each subunit (α -H23 and β -H23). The conformation of the N- and C-terminal regions of the α subunit and the N-terminal region for the β subunit was modeled using the BLAST approach. An α -helix was newly generated on the N-terminal region of the α subunit based on one of the searched template fragments (1NHP). Similarly, two short β -strands were newly generated on the C-terminus of the α subunit based on the template structure of 1ALB.

The α and β subunits together with the heme were docked to the D1/D2 complex on the Q_A side in close association with the helix E of the D2 protein. This close association of cytochrome b559 with D2 was based on the experimental suggestion that cytochrome b559 is intimately associated with D2 (Pakrasi et al. 1991; Shukla et al. 1992). However, the cross-linking experiments of Barberto (1995) suggested that the cytochrome is located on the Q_B side. Though we cannot exclude this possibility, we attempted to accommodate the suggestion by modeling the two cross-linked regions, N-terminus of the α subunit and a D1 DE loop region (D1-F239-D1-E244), in close contact. In our docking of the cytochrome protein to the D1/D2 complex, we also took into account of the following experimental evidence: the estimated distances between the heme and Q_A and P680 are 20 and 35 Å, respectively (Shuvalov 1994).

After modeling cytochrome b559, I examined the protein binding region for the heme moiety. As shown in Fig. 5.5, the heme iron is coordinated by the two histidines, α -H23 and β -H23. The bond distances are 1.9 to 2.0 Å. Two tryptophan residues, α -W-20 and β -W19 appear to provide the crucial hydrophobic interactions for stabilizing the heme. The sidechains of β -T16 and β -Y12, provide hydrogen bonds to the two carboxylate groups on the rings III and IV of the heme, respectively. Other residues that are involved in the heme binding are α -V27, α -L30, α -F31, β -P13, β -R18, β -L20, and β -V27. I suggest that site-directed mutagenesis be carried out on these residues to test their actual involvement in the heme binding.

D. Discussion

We have first constructed a three dimensional model of D1-D2-Cytochrome b559 of the PSII reaction center with the inclusion of a complete set of cofactors both based on homology principles and experimental suggestions. We believe this new model will provide a more useful tool for a broad spectrum of research, particularly to test predictions on both the structure and function of PSII.

Compared to the major PSII reaction center models constructed earlier, the current model does share a significant similarities with them. However, due to the procedural differences in the modeling processes, differences do exist among them. A detailed comparison of the key residues associated with the cofactors in several major models (Ruffle et al. 1992; Svensson et al. 1996; Chapter IV; this chapter) is shown in Table 5.2. Through the comparison, a consensus of the modeling results can be drawn and further experiments can be designed to test the validity or resolve inconsistencies between the models.

Figure 5.5. The binding niche for the heme in cytochrome b559. The heme iron is coordinated by α -H23 and β -H23. The two propionate groups on the rings III and IV of heme are hydrogen bonded by β -T16 and β -Y12, respectively. Two tryptophan residues, α -W-20 and β -W19, appear to provide the crucial hydrophobic interactions for stabilizing the heme.

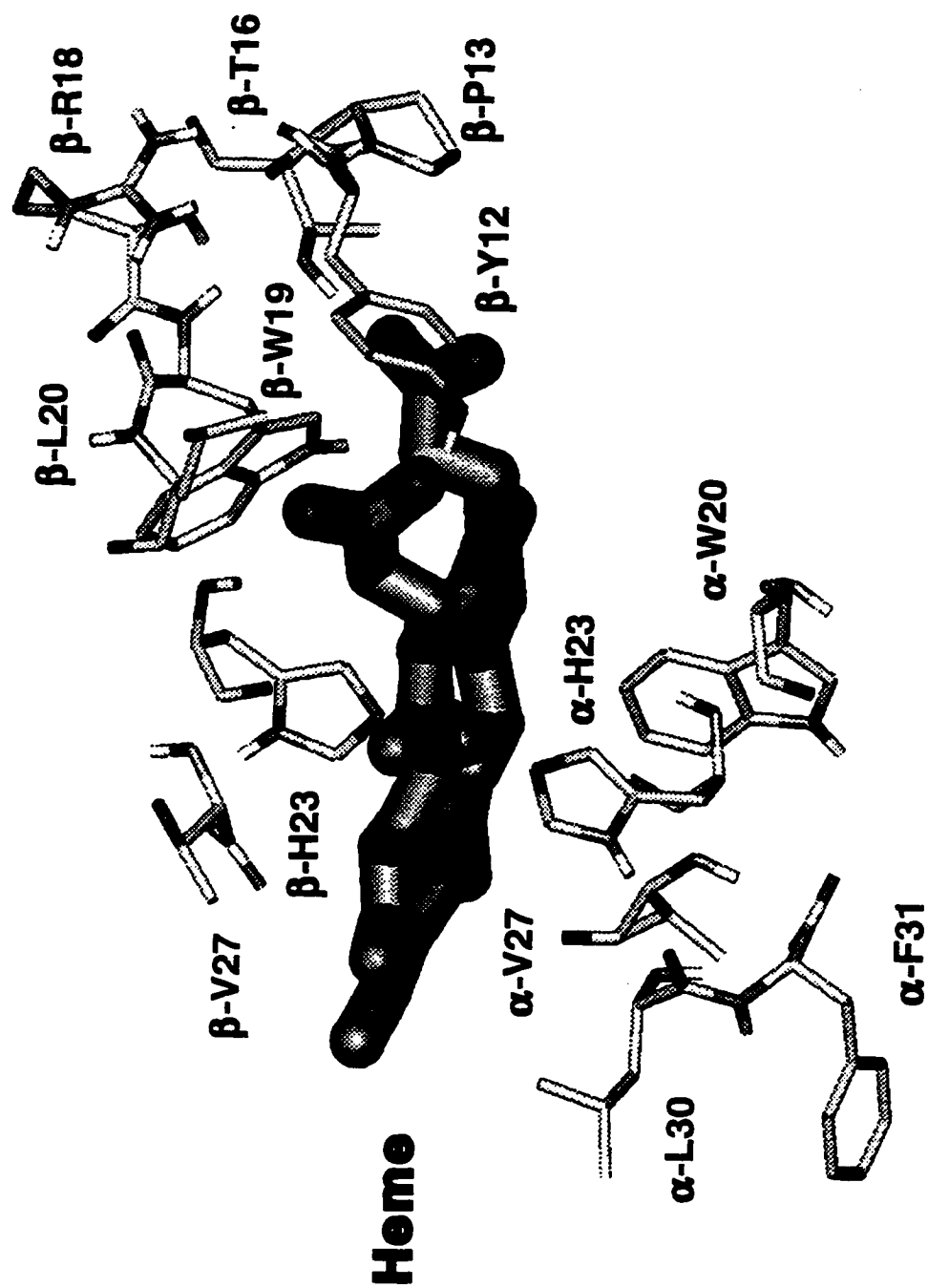


Table 5.2. Comparison of modeling results of the binding niches of PSII cofactors from several existing models of the PSII reaction center. NA: information not available.

Cofactors	Role	Residues (<i>C. reinhardtii</i> model) this chapter	Residues (<i>Synechocystis</i> 6803 model) Chapter IV	Residues (spinach model) Svensson et al. 1996	Residues (pea model) Ruffle et al. 1992
Chlorophyll special pair	Ligand to magnesiums	D1-H198 and D2-H197	D1-H198 and D2-H197	D1-H198 and D2-H198	D1-H198 and D2-H198
	Provide ring stacking forces	D2-W191.	D2-W191.	D2-W192	NA
	H-bond to the ester group on the ring IV of D2 P680 chlorophyll.	NA	NA	D1-T286, D2-W192 and D2-S283	NA
	Electrostatic Interactions	D1-M183	D1-M183	D1-M184	NA
Accessory chlorophyll	Ligands to magnesiums	D1-H118 and D2-H117	NA	NA	NA
	Provide ring stacking forces	D1-F180 and D2-F179	D1-F180 and D2-F179	NA	
	Serve as a conduit for electron transport between the accessory chlorophyll and the active pheophytin on the QA side	D2-L205, D2-G206 and D2-L209	D2-L205	NA	D2-L206

Table 5.2. (continued)

Cofactors	Role	Residues (C. reinhardtii model) this chapter	Residues (Synechocystis 6803 model) Chapter IV	Residues (spinach model) Svensson et al. 1996	Residues (pea model) Ruffle et al. 1992
β -carotenene (D2 side)	Form the binding pocket	D2-A44, D2-L45, D2-W48, D2-L49, D2-T52, D2-Y67, D2-L74, D2-H87, D2-F91, D2-W111, D2-A119, D2-L116, D2-F153, D2-V154, D2-V156, D2-F157, D2-L158, D2-W167, D2-P171, D2-S172, D2-F173, D2-G174, D2-V175, and D2-I178	D2-L45, D2-W48, D2-L49, D2-A71, D2-L74, D2-F91, D2-W111, D2-D112, D2-F113, D2-A115, D2-A119, D2-L116, D2-F153, D2-V154, D2-F157, D2-L158, D2-S172, D2-F173, D2-G174, D2-V175.	NA	NA
β -carotenene (D1 side)	Form the binding pocket	D1-F48, D1-E65, D1-P66, D1-G110, D1-Y112, D1-Q113, D1-L114, D1-I115, D1-V116, D1-C117, D1-H118, D1-F119, D1-L120, D1-L121, D1-V157, D1-F158, D1-M172, D1-L174, D1-G175, D1-I176, D1-T179, and D1-F180	NA	NA	NA

Table 5.2. (continued)

Cofactors	Role	Residues (<i>C. reinhardtii</i> model) this chapter	Residues (<i>Synechocystis</i> 6803 model) Chapter IV	Residues (spinach model) Svensson et al. 1996	Residues (pea model) Rufflé et al. 1992
Pheophytin (active side)	H-bond to the keto group on ring V.	D1-R27 and D1-E130	D1-R27 and D1-Q130	D1-E130	D1-E130
	H-bonds to ester group of the ring IV	D1-Y126	D1-Y147	D1-Y147/D1-Y126	D1-Y126
	Provide ring stacking for pheophytin	NA	D1-Y147	NA	NA
	H-bond to ester oxygen of phytol branch.	NA	D1-Y126	NA	NA
	Important van der Waals interactions	D1-Y147	NA	D1-Y147, D1-P150, D2-L210	NA
	Serve as a conduit for electron transport between the active pheophytin and QA	D2-W253 and D2-I213	D2-W253 and D2-I213	D1-I143 and D2-I214.	D2-W254
Pheophytin on the inactive side	H-bond to the keto group on ring V.	D2-Q-129, D2-N142	D2-Q-129, D2-N142	D2-Q-130, D2-Q143	D2-Q-130
	Provide ring stacking forces	D2-F146	D2-F146	D2-F147	NA
	Located between the inactive pheophytin and QB, function unknown	D1-F255 and D1-M214	D1-F255 and D1-M214	D1-M214	NA

Table 5.2. (continued)

Cofactors	Role	Residues (<i>C. reinhardtii</i> model) this chapter	Residues (<i>Synechocystis</i> 6803 model) Chapter IV	Residues (spinach model) Svensson et al. 1996	Residues (pea model) Ruffle et al. 1992
QA	H-bond to the carbonyl oxygens	D2-H214 and D2-S262	D2-T217, D2-N230, D2-S262 and D2-N263	NA	NA
	Form the binding pocket	D2-T217, D2-V218, D2-A249, D2-N250, D2-W253, D2-N263, D2-K264, D2-L267, D2-L209, D2-L210, D2-I213, D2-Q255, D2-V259, D2-F261, D2-F270, D1-L28, D1-I38, D1-G34, D1-M37, D1-L41, D1-R129, D1-Y126.	D2-H214, D2-T217, D2-T221, D2-N230, D2-A249, D2-N250, D2-W253, D2-S254, D2-S262, D2-N263, D2-K264, D2-L267, D2-L209, D2-L210, D2-I213, D2-Q255, D2-I259, D2-A260, D2-F261, D2-W266.		D2-L211, D2-I214, D2-H215, D2-T218, D2-M247, D2-A250, D2-W254, D2-F262, D2-N264, D2-K265, D2-L268.
Ring stack with QA					
		D2-W252	D2-W252	NA	NA
QB	H-bond to the carbonyl oxygens	D1-H215, D1-H252 and D1-S264.	D1-H215, D1-H252 and D1-S264	NA	D1-S264
	Form the binding pocket	D1-L218, D1-V219, D1-A251, D1-F255, D1-N267, D1-L271, D1-P196, D1-F197, D1-L200, D1-A203, D1-G207, D1-F211, D1-M214, D1-A263, D1-F274, D1-W278, D1-I281, D1-F285, D2-I231, D2-R23	D1-H215, D1-V219, D1-Y246, D1-A251, D1-H252, D1-F255, D1-S264, D1-N266, D1-L271, D2-F232, D1-F211, D1-M214, D1-I259, D1-F260, D1-Y262, D1-A263, D1-F265, D2-I30, D2-L37, D2-F38, D2-F125, D2-R128	NA	D1-F211, D1-M214, D1-H215, D1-L218, D1-V219, D1-A251, D1-H252, D1-F255, D1-I259, D1-Y262, D1-S264, D1-N266, D1-N267, D1-S268, D1-L271.

Table 5.2. (continued)

Cofactors	Role	Residues (<i>C. reinhardtii</i> model) this chapter	Residues (<i>Synechocystis</i> 6803 model) Chapter IV	Residues (spinach model) Svensson et al. 1996	Residues (pea model) Ruffle et al. 1992
Non-heme iron	Ligand to the iron	bicarbonate, D1-H215, D1-H272, D2-H214, and D2-H268	bicarbonate, D1-H215, D1-H272, D2-H214, and D2-H268	D1-H215, D1-H272, D2-H215, D2-H269.	D1-E231, D1-H215, D1-H272, D2-H215, and D2-H269
Bicarbonate ligand	Form the binding pocket	D1-I224, D1-V219, D1-D227, D1-S268, D2-G226, D2-T231, D2-A234, and D2-K264,	D1-V219, D2-F232	NA	NA
Donor Z	Located between Z and P680	D1-A156, D1-V157, D1-F186, D1-G289, D1-L290, D1-T292	D1-A156, D1-F186, D1-A287, D1-M288, D1-G289, D1-V290, D1-S291, D1-T292, D1-M293	NA	D1-V157, D1-V185, D1-I289
	Surrounding protein environment	D1-S155, D1-F158, D1-L159, D1-V160, D1-P162, D1-I163, D1-G164, D1-Q165, D1-G166, D1-S167, D1-D170, D1-F182, D1-H190, D1-M293, and A294.	D1-T155, D1-V157, D1-F158, D1-L159, D1-I160, D1-P162, D1-I163, D1-G164, D1-Q165, D1-G166, D1-N298, D1-G299, D1-N301, D1-N303, and D1-Q304	D1-Q165, D1-D170, D1-F186, D1-Q189, D1-A294,	D1-P162, D1-Q165, D1-D170, D1-G171, D1-F182, D1-F186, D1-H190, D1-I290
	Electrostatic interactions	D1-H190	NA	D1-H190	NA

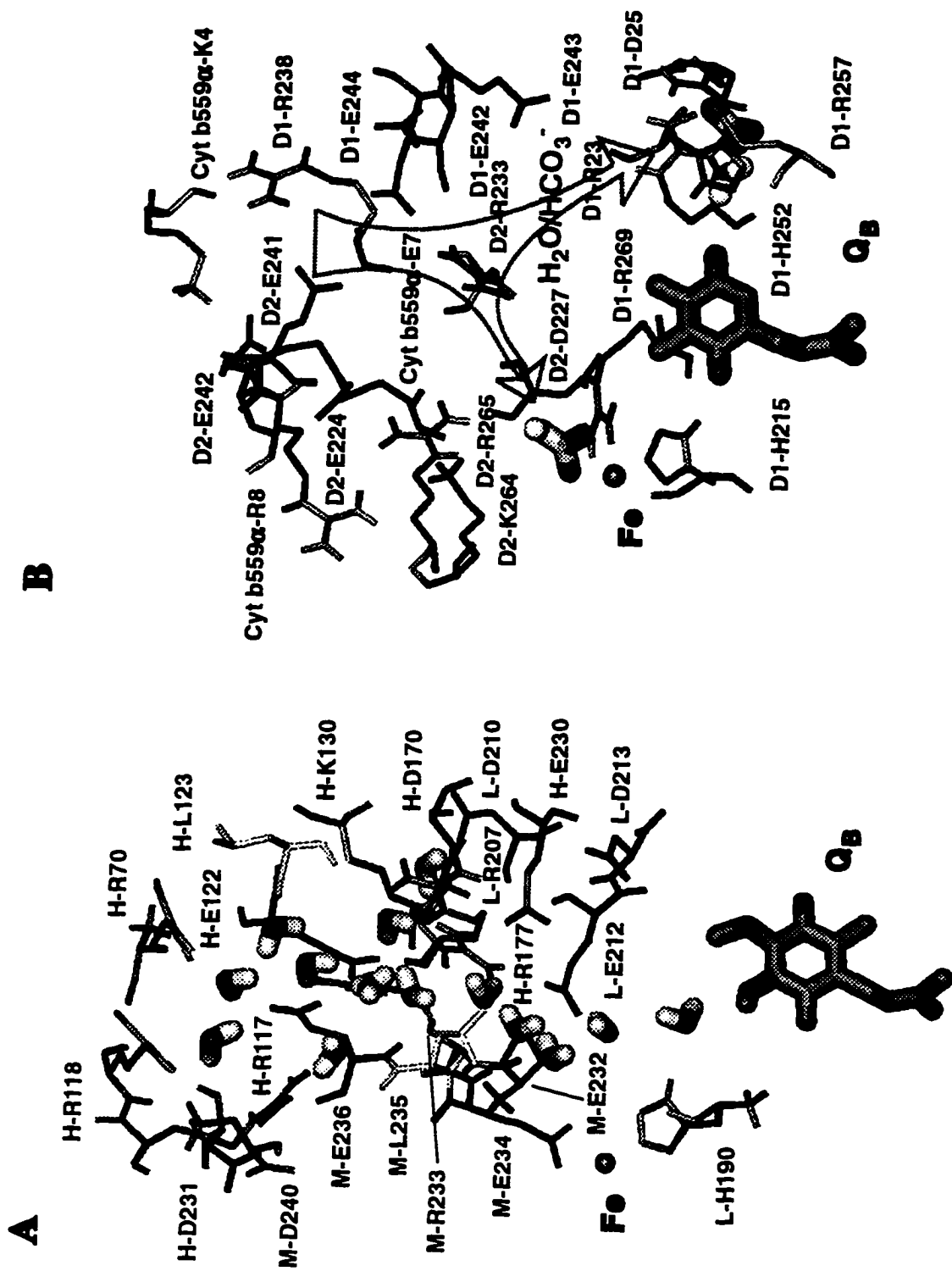
Table 5.2. (continued)

Cofactors	Role	Residues (<i>C. reinhardtii</i> model) this chapter	Residues (<i>Synechocystis</i> 6803 model) Chapter IV	Residues (spinach model) Svensson et al. 1996	Residues (pea model) Ruffle et al. 1992
Donor D	Surrounding protein environment	D2-V154, D2-S155, D2-V156, D2-F157, D2-L158, D2-P161, D2-L162, D2-F169, D2-F185, D2-H189, D2-V287, D2-L289	D2-V154, D2-S155, D2-V156, D2-F157, D2-L158, D2-M159, D2-P161, D2-L162, D2-G163, D2-Q164, D2-F169, D2-A170, D2-P171, D2-F185, D2-A290, D2-L291, D2-N292	D2-F170, D2-F182, D2-F189, D2-L290, D2-A291	D2-P162, D2-Q165, D2-F170, D2-F182, D2-F186, D2-H190, D2-W192, D2-L294
	H-bonding	D2-H189	D2-F169	D2-H190, D2-Q165	D2-H190
	Key van der Waals interactions	NA	NA	D2-A291, D2-P162	NA
Bicarbonate/water	Form the putative transport channel	D1-K238, D1-E242, D1-E243, D1-E244, D1-H252, D1-R257, D1-R269, D2-R23, D2-D25, D2-E224, D2-D227, D2-R233, D2-E242, D2-K264, D2-R26, Cyt α -K3, Cyt α -E6 and Cyt α -R7	D1-H215, D1-K238, D1-E242, D1-E243, D1-E244, D1-H252, D1-R257, D1-R269, D2-K23, D2-D25, D2-E224, D2-R233, D1-E236, D2-E241, D2-E242, D2-K264, and D2-R265	NA	NA

Regarding the physiological role of cytochrome b559, it is worthy to note that the location of the transmembrane helix of the α subunit resemble that of the bacterial H subunit which is involved in the assembly of the bacterial reaction center (Chory et al. 1984; Sockett et al. 1989). It is proposed here that the transmembrane α -helix of the α subunit may assume a similar role by forming a nucleation center for the sequential assembly of the other components of the PSII reaction center, i.e., D1 and D2. The molecular genetic and immunological evidence of Shukla et al. (1992) and Tae and Cramer (1992) may be taken to support the notion that cytochrome b559 may serve a functional homologue of the H subunit in the bacterial system.

Based on discovery from the newly refined crystal structure of the bacterial reaction center (Ermler et al. 1994; Deisenhofer et al. 1995) that multiple water molecules are present to facilitate the protonation of Q_B (Fig. 5.6A), an analogous water/bicarbonate binding niche which may function similarly was first proposed in the D1/D2 model for *Synechocystis* 6803 (Chapter IV). Such a model was constructed by making the assumptions that (1) Q_B molecule in PSII is also buried inside the protein complex; and its protonation is ultimately dependent upon the transport of protons from the outer environment; (2) the direction of the transport in the PSII reaction center is similar to that in the bacterial reaction center; (3) the charged residues form the putative transport channel, as in the bacterial reaction center; (4) the local electrostatic characteristic of the binding region weighs more than the precise geometric match with the bacterial water-binding residues; (5) the channel to be constructed has another end at the non-heme iron site as well. Thus, by superimposing the bacterial structure (1PCR) onto the constructed PSII reaction center model, a series of D1/D2 charged residues were identified as the putative bicarbonate/water binding residues. Interestingly, most of the identified residues had been previously shown in experimental investigations to be related to the "bicarbonate effect". A striking feature was that near the Q_B and non-heme iron sites the residues are predominantly positively charged in contrast to the bacterial reaction center which lacks the bicarbonate effect. In our

Figure 5.6. The water transport channel in the bacterial reaction center (Ermler et al. 1994) and a hypothesis for a similar transport channel for water and bicarbonate in the PSII reaction center of *C. reinhardtii*. (A) Water transport channel to the Q_B site in the bacterial reaction center of *Rb. sphaeroides* (based on Ermler et al. 1994) The water chain and the surrounding amino acids are shown. The water molecules presumably aid in the Q_B protonation. The surrounding residues are color by polarity, the positive in blue and negative in red. The numbering of the residues is according to the released coordinate file (1PCR). For clarity reasons, only the head group of Q_B is shown. (B) A hypothetical water and bicarbonate transport channel in PSII reaction center is proposed to be analogous to the one in the bacterial reaction center based on the assumptions made in the text. Included are the charged residues in the PSII model that are found in close vicinity to the bacterial "channel residues" when the bacterial model and the PSII model were superimposed. In addition to the Q_B site, the non-heme iron is proposed to be another end of the channel. The bicarbonate anion was modeled to provide a bidentate ligand to the iron. Another bicarbonate was modeled to the Q_B site associating with both D1-H252 and D1-R257 in an attempt to explain its role in facilitating the protonation of Q_B (see Xiong et al. 1996). Since our current model contains cytochrome b559, residues with the above geometry in cytochrome b-559 were also included.



current model that includes cytochrome b559, a similar attempt for constructing the channel was made based on the same assumptions (see above). In addition to the charged D1/D2 residues, three residues from the α subunit of cytochrome b559 were also found to fall in the close vicinity of the water channel when the bacterial structure is superimposed on the PSII reaction center model (Fig. 5.6B). Though the inclusion of the residues are considered speculative, site-directed mutagenesis on these residues may provide further clues.

Data presented in this chapter are based on the published work of the author (Xiong et al. 1996).

E. References

- Altschul, S.F., Gish, W., Miller, W., Myers, E.W. and Lipman, D.J. (1990) Basic local alignment search tool. *J. Mol. Biol.* 215: 403-410.
- Armstrong, G.A. (1995) Genetic analysis and regulation of carotenoid biosynthesis. In: Blankenship, R.E., Madigan, M.T., and Bauer, C.E. (eds) *Anoxygenic Photosynthetic Bacteria*, pp 1135-1157. Kluwer Academic Publishers, Dordrecht.
- Astashkin, A.V., Kodera, Y. and Kawamori, A. (1994) Distance between tyrosines Z(+) and D⁺ in plant photosystem II as determined by pulsed EPR. *Biochim. Biophys. Acta* 1187: 89-93.
- Babcock, G.T., Widger, W.R., Cramer, W.A., Oertling, W.A. and Metz, J.G. (1985) Axial ligands of chloroplast cytochrome b-559: Identification and requirement for a heme-cross-linked polypeptide structure. *Biochemistry* 24: 3638-3645.

- Barbato, R., Friso, G., Ponticos, M. and Barber, J. (1995) Characterization of the light-induced cross-linking of the α -subunit of cytochrome b559 and the D1 protein in isolated photosystem II reaction centers. *J. Biol. Chem.* 270: 24032-24037.
- Bowyer, J., Hilton, J.M., Whitelegge, J., Jewess, P., Camilleri, P., Crofts, A. and Robinson, H. (1990) Molecular modelling studies on the binding of phenylurea inhibitors to the D1 protein of photosystem II. *Z. Naturforsch.* 45c: 379-387.
- Brooks, B.R., Bruccoleri, R.E., Olafson, B.D., States, D.J., Swaminathan, S. and Karplus, M. (1983) CHARMM: A program for macromolecular energy, minimization, and dynamics calculations. *J. Computational. Chem.* 4: 187-217.
- Buser, C.A., Diner, B.A. and Brudvig, G.W. (1992) Reevaluation of the stoichiometry of cytochrome b559 in photosystem II and thylakoid membranes. *Biochemistry* 31: 11441-11448.
- Chang, H.C., Jankowiak, R., Reddy, N.R.S., Yocum, C.F., Picorel, R., Seibert, M. and Small, G.J. (1994) On the question of the chlorophyll *a* content of the photosystem II reaction center. *J. Phys. Chem.* 98: 7725-7735.
- Chory, J., Donohue, T.J., Warga, A.R., Staehelin, L.A. and Kaplan, S. (1984) Induction of the photosynthetic membranes of *Rhodospseudomonas sphaeroides*: biochemical and morphological studies. *J. Bacteriol.* 159: 540-554.
- Cramer, W.A. and Knaff, D.B. (1990) *Energy Transduction in Biological Membranes*, A Textbook of Bioenergetics, pp 194-195; 253. Springer-Verlag, New York.
- Cramer, W.A., Tae, G.-S., Furbacher, P.N. and Böttger, M. (1993) The enigmatic cytochrome b-559 of oxygenic photosynthesis. *Physiol. Plant.* 88:705-711.

- Deisenhofer, J., Epp, O., Sinning, I. and Michel, H. (1995) Crystallographic refinement at 2.3-angstrom resolution and refined model of the photosynthetic reaction centre from *Rhodospseudomonas viridis*. *J. Mol. Biol.* 246: 429-457.
- Diner, B.A. and Babcock, G.T. (1996) Structure, dynamics, and energy conversion efficiency in photosystem II. In: Ort, D.R. and Yocum, C.F. (eds.) *Oxygenic Photosynthesis: The light Reactions*. (in press) Kluwer Academic Publishers, Dordrecht.
- Eijkelhoff, C. and Dekker, J.P. (1995) Determination of the pigment stoichiometry of the photochemical reaction center of photosystem II. *Biochim. Biophys. Acta* 1231: 21-28.
- Esposti, M.D. (1989) Prediction and comparison of the haem-binding sites in membrane haemproteins. *Biochim. Biophys. Acta* 977: 249-265.
- Erickson, J.M., Bahire, M. and Rochaix, J.-D. (1984) *Chlamydomonas reinhardtii* gene for the 32,000 mol. wt. protein of photosystem II contains four large introns and is located entirely within the chloroplast inverted repeat. *EMBO J.* 3: 2753-2762.
- Erickson, JM, Rahire, M, Malnoe, P, Girard-Bascou, J, Pierre, Y, Bennoun, P and Rochaix, J.-D. (1986) Lack of the D2 protein in a *Chlamydomonas reinhardtii* *psbD* mutant affect photosystem I stability and D1 protein. *EMBO J.* 5: 1745-1754.
- Ermler, U., Fritsch, G., Buchanan, S.K. and Michel, H. (1994) Structure of the photosynthetic reaction centre from *Rhodobacter sphaeroides* at 2.65 Å resolution: Cofactors and protein-cofactor interactions. *Structure* 2: 925-936.
- Frank, H.A. and Cogdell, R.J. 1996. Carotenoids in photosynthesis. *Photochem. Photobiol.* 63, 257-264.

- Gounaris, K., Chapman, D.J., Booth, P., Crystall, B., Giorgi, L.B., Klug, D.R., Porter, G. and Barber, J. (1990) Comparison of D1/D2/cytochrome b559 reaction centre complex of photosystem two isolated by two different methods. *FEBS Lett.* 265: 88-92.
- Herrmann, R.G., Alt, J., Schiller, B., Widger, W.R. and Cramer, W.A. (1984) Nucleotide sequence of the gene for apocytochrome b559 on the spinach plastid chromosome: Implications for the structure of the membrane proteins. *FEBS Lett.* 176: 239-244.
- Hofmann, E., Wrench, P.M., Sharples, F.P., Hiller, R.G., Welte, W. and Diederichs, K. (1996) Structural basis of light harvesting by carotenoids: Peridinin-chlorophyll-protein from *Amphidinium carterae*. *Science* 272: 1788-1791.
- Hoganson, C.W. and Babcock, G.T. (1989) Redox cofactor interactions in photosystem II: Electron spin resonance spectrum of P_{680}^{+} is broadened in the presence of YZ^{+} . *Biochemistry* 28: 1448-1454.
- Hutchison, R.S. and Sayre, R.T. (1995) Site-specific mutagenesis at histidine 118 of the photosystem II D1 protein of *Chlamydomonas reinhardtii*. In: Mathis, P. (ed.) *Photosynthesis: From Light to Biosphere*, Vol. pp. 471-474. Kluwer Academic Publishers, Dordrecht.
- Kobayashi, M., Maeda, H., Watanabe, T., Nakane, H. and Satoh, K. (1990) Chlorophyll α and β -carotene content in the D1/D2/cytochrome b559 reaction center complex from spinach. *FEBS Lett.* 260: 138-140.
- Kodera, Y., Hara, H., Astashkin, A.V., Kawamori, A. and Ono, T.A. (1995) EPR Study of trapped tyrosine Z^{+} in Ca-depleted photosystem II. *Biochim. Biophys. Acta* 21: 43-51.

- Koulougliotis, D., Innes, J.B. and Brudvig, W. (1994) Location of chlorophyllz in photosystem II. *Biochemistry* 33: 11814-11822.
- Koulougliotis, D., Tang, X.S., Diner, B.A. and Brudvig, G.W. (1995) Spectroscopic evidence for the symmetric location of tyrosines D and Z in Photosystem II. *Biochemistry* 34: 2850-2856.
- Kramer, D.M., Roffey, R.A., Govindjee and Sayre, R.T. (1994) The At thermoluminescence band from *Chlamydomonas reinhardtii* and the effects of mutagenesis of histidine residues on the donor side of the photosystem II D1 polypeptide. *Biochim. Biophys. Acta* 1185: 228-237.
- Lancaster, C.R., Ermler, U. and Michel, H. (1995) The structures of photosynthetic reaction centers from purple bacteria as revealed by x-ray crystallography. In: Blankenship, R.E., Madigan, M.T. and Bauer, C.E. (eds.) *Anoxygenic Photosynthetic Bacteria*. pp. 503-526. Kluwer Academic Publishers, Dordrecht.
- Marr, K.M., Mastronarde, D.N. and Lyon, M.K. (1996) Two dimensional crystals of photosystem II: Biochemical characterization, cryoelectron microscopy and localization of the D1 and cytochrome b559 polypeptides. *J. Cell Biol.* 132: 823-833.
- Mimuro, M., Tomo, T., Nishimura, Y., Yamazaki, I. and Satoh, K. (1995) Identification of a photochemically inactive pheophytin molecule in the spinach D1-D2-cyt b559 complex. *Biochim. Biophys. Acta* 1232: 81-88.
- Montoya, G., Yruela, I. and Picorel, R. (1991) Pigment stoichiometry of a newly isolated D1-D2-Cyt B559 complex from the higher plant *Beta vulgaris*. *FEBS Lett.* 283: 255-258.

- Mor, T.S., Ohad, I., Hirschberg, J. and Pakrasi, H.B. (1995) An unusual organization of the genes encoding cytochrome b₅₅₉ in *Chlamydomonas reinhardtii*: *psbE* and *psbF* genes are separately transcribed from different regions of the plastid chromosome. *Mol. Gen. Genet.* 246: 600-604.
- Mulkidjanian, A.Y., Cherepanov, D.A., Haumann, M. and Junge, W. (1996) Photosystem II of green plants: Topology of core pigments and redox cofactors as inferred from electrochromic difference spectra. *Biochemistry* 35: 3093-3107.
- Nakazato, K., Toyoshima, C., Enami, I. and Inoue, Y. (1996) Two dimensional crystallization and cryo-electron microscopy of photosystem II. *J. Mol. Biol.* 257: 225-232.
- Nanba, O. and Satoh, K. (1987) Isolation of photosystem II reaction center consisting of D1 and D2 polypeptides and cytochrome *b*-559. *Proc. Natl. Acad. Sci. USA* 84: 109-112.
- Nugent, J.H.A. (1996) Oxygenic photosynthesis. Electron transfer in photosystem I and photosystem II. *Eur. J. Biochem.* 237: 519-531.
- Pakrasi, H.B., Williams, J.G.K. and Arntzen, C.J. (1988) Targeted mutagenesis of the *psbE* and *psbF* genes blocks photosynthetic electron transport: Evidence for a functional role of cytochrome b₅₅₉ in photosystem II. *EMBO J.* 7: 325-332.
- Pakrasi, H.B., Ciechi, P.D. and Whitmarsh, J. (1991) Site directed mutagenesis of the heme axial ligands of Cytochrome b₅₅₉ affects the stability of the photosystem II complex. *EMBO J.* 10: 1619-1627.
- Picorel, R., Chumanov, G., Cotton, T.M., Montoya, G., Toon, S. and Sibert, M. (1994) Surface-enhanced resonance Raman scattering spectroscopy of photosystem II pigment-protein complexes. *J. Phys. Chem.* 98: 6017-6022.

- Pueyo, J.J., Moliner, E., Seiber, M. and Picorel, R. (1995) Pigment content of D1-D2-cytochrome b559 reaction center preparations after removal of CP47 contamination: an immunological study. *Biochemistry* 34: 15214-15218.
- Ramachandran, G.N., Ramakrishnan, C. and Sasisekharan, V. (1963) Stereochemistry of polypeptide chain configurations. *J. Mol. Biol.* 7: 95-99.
- Renger, G. (1993) Water cleavage by solar radiation-an inspiring challenge of photosynthesis research. *Photosyn. Res.* 38: 229-247.
- Rochaix, J.-D. (1995) *Chlamydomonas reinhardtii* as the photosynthetic yeast. *Annu. Rev. Genet.* 29: 209-230.
- Roffey, R.A., Kramer, D.M., Govindjee and Sayre, R.T. (1994) Lumenal side histidine mutations in the D1 protein of photosystem II affect donor side electron transfer in *Chlamydomonas reinhardtii*. *Biochim. Biophys. Acta* 1185: 257-270.
- Rögner, M., Boekema, E.J. and Barber, J. (1996) How does photosystem 2 split water? The structural basis of efficient energy conversion. *TIBS* 21: 44-49.
- Ruffle, S.V., Donnelly, D., Blundell, T.L. and Nugent, J.H.A. (1992) A three-dimensional model of the photosystem II reaction centre of *Pisum sativum*. *Photosyn. Res.* 34: 287-300.
- Schelvis, J.P.M., van Noort, P.I., Aartsma, T.J. and van Gorkom, H.J. (1994) Energy transfer, charge separation and pigment arrangement in the reaction center of photosystem II. *Biochim. Biophys. Acta* 1184: 242-250.
- Shukla, V.A., Stanbekova, G.E., Shestakov, S.V. and Pakrasi, H.B. (1992) The D1 protein of the photosystem II reaction center complex accumulates in the absence of

- D2: Analysis of a mutant of the cyanobacterium *Synechocystis* sp. PCC 6803 lacking cytochrome b559. *Mol. Microbiol.* 6: 947-956.
- Shuvalov, V.A. (1994) Composition and function of cytochrome b559 in reaction centers of photosystem II of green plants. *J. Bioenerg. Biomembr.* 26: 619-626.
- Sockett, R.E., Donohue, T.J., Varga, A.R. and Kaplan, S. (1989) Control of photosynthetic membrane assembly in *Rhodobacter sphaeroides* mediated by *puhA* and flanking sequences. *J. Bacteriol.* 171: 436-446.
- Svensson, B., Vass, I., Cedergren, E. and Styring, S. (1990) Structure of donor side components in photosystem II predicted by computer modeling. *EMBO J.* 9: 2051-2059.
- Svensson, B., Etchebest, C., Tuffery, P., van Kan, P., Smith, J. and Styring, S. (1996) A model for the photosystem II reaction centre core including the structure of the primary donor P680. *Biochemistry* (in press)
- Tae, G.-S. and Cramer, W.A. (1994) Topography of the heme prosthetic group of cytochrome b-559 in the photosystem II reaction center. *Biochemistry* 33: 10060-10068.
- Tae, G.-S., Black, M.T., Cramer, W.A., Vallon, O. and Bogorad, L. (1988) Thylakoid membrane protein topography: transmembrane orientation of the chloroplast cytochrome b-559 *psbE* gene product. *Biochemistry* 27: 9075-9080.
- Tang, X.-S., Chisholm, D.A., Dismukes, G.C., Brudvig, G.W. and Diner, B.A. Spectroscopic evidence from site-directed mutants of *Synechocystis* PCC 6803 in favor of a close interaction between histidine 189 and redox-active tyrosine 160, both of polypeptide D2 of the photosystem II reaction center. *Biochemistry* 32: 13742-13748.

- Trebst, A. (1991) A contact site between the two reaction center polypeptides of photosystem II is involved in photoinhibition. *Z. Naturforsch.* 46c: 557-562.
- Vallon, O., Tae, G.-S., Cramer, W.A., Simpson, D., Hoyer-Hanson, G. and Bogorad, L. (1989) Visualization of antibody binding to the photosynthetic membrane: the transmembrane orientation of cytochrome b-559. *Biochim. Biophys. Acta* 975: 132-141.
- van Leeuwen, P.J., Nieveen, M.C., van de Meent, E.J., Dekker, J.P. and van Gorkom, H.J. (1991) Rapid and simple isolation of pure photosystem II core and reaction center particles from spinach. *Photosyn. Res.* 28: 149-153.
- Vermaas, W.F.J., Styring, S., Schröder, W.P. and Andersson, B. (1993) Photosynthetic water oxidation: The protein framework. *Photosyn. Res.* 38: 249-263.
- Whitmarsh, J. and Pakrasi, H.B. (1996) Form and function of cytochrome b559. In: Ort, D.R. and Yocum, C.F. (eds.) *Oxygenic Photosynthesis: The Light Reactions*, Kluwer Academic Publishers, Dordrecht (in press).
- Widger, W.R., Cramer, W.A., Hermodson, M. and Herrmann, R.G. (1985) Evidence for a hetero-oligomeric structure of the chloroplast cytochrome b-559. *FEBS Lett.* 191: 186-190.
- Xiong, J., Subramaniam, S., and Govindjee (1996) A knowledge-based three dimensional model of D1-D2-cytochrome b559 of *Chlamydomonas reinhardtii*. (to be submitted to *Photosyn. Res.*)
- Zheng, M. and Dismukes, G.C. (1996) The conformation of the isoprenyl chain relative to the semiquinone head in the primary electron acceptor (Q_A) of higher plant PSII (plastoquinone) differs from that in bacterial reaction centers (ubiquinone or menaquinone) by ca. 90°. *Biochemistry* 35: 8955-8963.

VITA

Jin Xiong was born on June 12, 1963, in Tianjin, People's Republic of China. In 1984, he received a B.S. degree in botany from Zhongshan University, Guangzhou, China. He then worked in an ecology laboratory at the South China Institute of Botany of the Chinese Academy of Sciences, Guangzhou, China. In 1987, he came to the United States to pursue his graduate education. In 1988, he obtained an M.S. degree in Environmental Biology from Eastern Illinois University, Charleston, IL. He continued his graduate education at Bowling Green State University, Bowling Green, OH, and received an M.S. degree in plant molecular biology in 1991. In the same year, he entered the Ph.D. program in Physiological and Molecular Plant Biology at the University of Illinois at Urbana-Champaign, Urbana, IL, joining the laboratory of Dr. Govindjee in the study of molecular mechanism of photosynthesis. He was a recipient of the University Scholarship of Merit in 1981 while he was an undergraduate student at Zhongshan University. He received Graduate College Conference Travel Awards twice from the University of Illinois (1994 and 1995). He was also awarded the Thomas E. Buetow Memorial Fund from the Carle Development Foundation and a conference travel award from the Genetics Society of America. He was supported by a fellowship from the Integrative Photosynthesis Research Training Grant, as well as by graduate teaching and research assistantships during his studies at the University of Illinois. He is a co-author of the following publications:

1. **Graham, J.S., Xiong, J. and Gillikin, J.W.** (1991) Purification and developmental analysis of a metalloendoproteinase from the leaves of *Glycine max*. *Plant Physiol.* 97: 786-792.
2. **Graham, J.S., Burkhardt, W., Xiong, J. and Gillikin, J.W.** (1992) The complete amino acid sequence of soybean leaf P21: similarity to the thaumatin-like polypeptides. *Plant Physiol.* 98: 163-165.

3. **Cao, J., Ohad, N., Hirschberg, J., Xiong, J. and Govindjee.** (1992) Binding affinity of bicarbonate and formate in herbicide-resistant D1 mutants of *Synechococcus* sp. PCC 7942. *Photosyn. Res.* 34: 397-408.
4. **Xiong, J., Hutchison, R., Sayre, R. and Govindjee.** (1995) Characterization of a site-directed mutant (D1-arginine 269-glycine) of *Chlamydomonas reinhardtii*. In: Mathis, P. (ed), *Photosynthesis: from Light to Biosphere*. Vol. I, pp. 575-578. Dordrecht: Kluwer Academic Publishers.
5. **Hutchison, R. S., Xiong, J., Sayre, R. and Govindjee.** (1996) Construction and characterization of a D1 mutant (arginine-269-glycine) of *Chlamydomonas reinhardtii*. *Biochim. Biophys. Acta* (in press)
6. **Xiong, J., Subramaniam, S. and Govindjee.** (1996) Modeling of the D1/D2 proteins and cofactors of the photosystem II reaction center: Implications for herbicide and bicarbonate binding. *Protein Sci.* 5: 2054-2073.
7. **Xiong, J., Hutchison, R.S., Sayre, R.T. and Govindjee.** (1996) Plastoquinone reductase function of a photosystem II D1 mutant (arginine-269-glycine) of *Chlamydomonas reinhardtii*: Chlorophyll *a* fluorescence and herbicide binding. (submitted to *Biochim. Biophys. Acta*)
8. **Xiong, J., Minagawa, J. Crofts, A.R. and Govindjee.** (1996) Construction and characterization of bicarbonate/formate binding site mutants on arginine-257 in the photosystem II D1 protein of *Chlamydomonas reinhardtii* (to be submitted to *Biochim. Biophys. Acta*)
9. **Xiong, J., Subramaniam, S. and Govindjee.** (1996) A knowledge-based three dimensional model of the D1-D2-Cytochrome b559 of *Chlamydomonas reinhardtii*. (to be submitted to *Photosyn. Res.*)